Second Series *December 1, 1932* *Vol. 42, No. 5*

THE

PHYSICAL REVIEW

The Relative Intensities of the $L\alpha_1$, β_1, β_2, and γ_1 Lines in Tantalum, Tungsten, Iridium, and Platinum

By VICTOR J. ANDREW
Ryerson Physical Laboratory, University of Chicago

(Received October 10, 1932)

The relative intensities of the $L\alpha_1$, β_1, β_2, and γ_1 lines in tantalum, tungsten, iridium, and platinum were measured and corrections were applied for the partial absorption of the beam along its path and within the ionization chamber, for the partial reflection by the crystal, for the effects of voltage and absorption within the target, and for interference from adjacent lines. To verify the method of making the target correction, an experiment was performed which consisted of measuring the relative intensities of $L\alpha_1$, β_1, and γ_1 of platinum at different angles from the face of the target. The following relative intensities were measured at 30 k.v. without correction for reflection by the crystal or absorption within the target:

	α_1	β_1	β_2	γ_1
Tantalum	100	49.5	18.8	9.0
Tungsten	100	49.4	20.2	10.0
Iridium	100	48.0	21.2	10.2
Platinum	100	46.1	21.0	9.7

INTRODUCTION

THE relative intensities of x-ray lines have been investigated with considerable precision where the lines are only slightly separated in wavelength. Where a considerable separation is present, all the corrections to observed intensities become more important. Two of them offer some difficulty. The correction for the fraction of the beam reflected by the crystal can be made only when the dependence of the coefficient of reflection on wavelength has been determined by using the same crystal in a double crystal spectrometer. The correction for the absorption within the target requires a knowledge of the depth distribution of emission of x-rays and is involved with the correction for the tube voltage.

The intensities of the lines in the L series of tantalum, tungsten, and platinum have been measured by Jönsson,[1] Hicks,[2] and Allison and Andrew.[3]

Measurements of the relative intensities were made on the elements tantalum (73), tungsten (74), iridium (77), and platinum (78). The lines α_1, β_1,

[1] Axel Jönsson, Zeits. f. Physik **36**, 426 (1926).
[2] Victor Hicks, Phys. Rev. **36**, 1273 (1930); **38**, 572 (1931).
[3] Allison and Andrew, Phys. Rev. **38**, 441 (1931).

β_2, and γ_1 were chosen because they are widely separated and distributed over a rather broad wave-length range. Particular attention was given to the two more difficult corrections referred to above.

Apparatus and Procedure

The design and adjustment of the apparatus which was used for these experiments has been described by Allison and Andrew.[3] It is a single crystal spectrometer with an ionization chamber. The slits were 25.4 cm apart and 0.013 cm wide. The ionization chamber was filled with methyl bromide to a pressure of 76 cm. The x-ray tube was of a type described by Allison.[4] The target was mounted at 45° to the electron beam, and the x-rays were observed at 45° to its face. The various targets were polished in the vicinity of the focal spot so that they gave a clear mirror-like reflection, and only the slightest scratches were visible to the unaided eye, in order that surface irregularities would produce negligible uncertainty in the thickness of the layer in which the rays were absorbed before leaving the target. The electron current was kept low enough (usually one milliampere) so that the polish was not damaged. The targets were repolished whenever they became seriously coated with tungsten from the filament. Such coating occurred only when the tube was operated without a sufficiently high vacuum.[5] No readings were used in which the intensity of tungsten $L\alpha_1$ was as great as 1 (relative to 100 for the $L\alpha_1$ line of the element being studied), and in most cases it was not measurable (less than 0.3). When it reached 7, the change in intensity of the other lines being studied was approximately 2.

The electrometer sensitivity was about 3 meters per volt. Adjustments were made so that it was found experimentally that the rate of deflection was proportional to the current (with a possible constant correction), and that the rate of deflection for constant current was the same on all parts of the

Table I. *Tantalum (73).*

Trial	Line	i	i_b	$i-i_b$	I_λ	Weight
1	α_1	22.46	0.64	21.82		1
	β_1	16.96	0.64	16.32	74.3	
	β_2	7.70	0.64	7.06	32.1	
	γ_1	4.26	0.64	3.62	16.5	
2	α_1	21.72	0.69	21.03		2
	β_1	14.92	0.69	14.23	67.8	
	β_2	6.45	0.69	5.76	27.6	
	γ_1	3.57	0.69	2.88	13.9	
3	α_1	17.16	0.65	16.51		3
	β_1	12.20	0.65	11.55	69.7	
	β_2	5.76	0.65	5.11	30.9	
	γ_1	3.41	0.65	2.76	16.7	
Weighted averages:		$I(\beta_1)=69.8$		$I(\beta_2)=30.0$		$I(\gamma_1)=15.7$

[4] S. K. Allison, Phys. Rev. **30**, 245 (1927) (Fig. 1).
[5] S. K. Allison, Phys. Rev. **34**, 7 (1929).

TABLE II. *Tungsten* (74).

Trial	Line	i	i_b	$i-i_b$	I_λ	Weight
1	α_1	17.54	0.80	16.74		2
	β_1	11.90	0.80	11.10	68.7	
	β_2	6.80	0.80	6.00	34.4	
	γ_1	4.22	0.80	3.42	19.5	
2	α_1	22.73	0.84	21.89		3
	β_1	15.62	0.84	14.78	67.5	
	β_2	7.30	0.84	6.46	29.5	
	γ_1	4.10	0.84	3.26	14.9	
3	α_1	24.10	0.83	23.27		2
	β_1	16.67	0.83	15.84	68.0	
	β_2	7.87	0.83	7.04	30.2	
	γ_1	4.38	0.83	3.55	15.2	
4	α_1	22.85	0.70	22.15		3
	β_1	15.74	0.70	15.04	67.9	
	β_2	7.49	0.70	6.79	30.7	
	γ_1	4.28	0.70	3.58	16.2	
Weighted averages:						
	$I(\beta_1)=67.9$		$I(\beta_2)=31.0$		$I(\gamma_1)=16.3$	

TABLE III. *Iridium* (77).

Trial	Line	i	i_b	$i-i_b$	I_λ	Weight
1	α_1	25.15	0.75	24.40		2
	β_1	15.73	0.75	14.98	60.7	
	β_2	8.00	0.75	7.25	29.7	
	γ_1	4.18	0.75	3.43	14.1	
2	α_1	25.15	0.76	24.39		3
	β_1	15.38	0.76	14.62	59.9	
	β_2	7.90	0.76	7.14	29.3	
	γ_1	4.07	0.76	3.31	13.6	
3	α_1	23.40	0.69	22.71		2
	β_1	14.56	0.69	13.87	61.2	
	β_2	7.22	0.69	6.53	28.7	
	γ_1	3.81	0.69	3.12	13.7	
Weighted averages:						
	$I(\beta_1)=60.5$		$I(\beta_2)=29.3$		$I(\gamma_1)=13.7$	

scale. The latter condition may be quite different from that of having the deflection proportional to the voltage, and must not be confused with it.[6]

Tables I, II, III, and IV give the experimental data obtained on tantalum, tungsten, iridium, and platinum, respectively. i is the uncorrected electrometer current in mm per second observed at the peak of the line. The tabulated values are not individual readings, but each one is a peak measured on a curve drawn through a group of points (usually five) at intervals of $\frac{1}{4}$ minute of arc, in the vicinity of the peak. i_b, the base line intensity, was observed at angles sufficiently distant from all lines due to the target material or tungsten contamination. The base did not vary perceptibly over the range of the lines

[6] This is due to the charge induced on the quadrant by the moving needle. See J. B. Hoag, *Electron Physics*, p. 142.

involved, and so the same value was used for all of the lines in one trial. Care was taken to measure a value as accurately as possible near the γ_1 line, since this line was the weakest, and therefore required the most accurate base line correction.

TABLE IV. *Platinum* (78).

Trial	Line	i	i_b	$i-i_b$	I_λ	Weight
1	α_1	20.00	0.68	19.32		2
	β_1	11.80	0.68	11.12	57.5	
	β_2	6.80	0.68	6.12	31.7	
	γ_1	3.08	0.68	2.40	12.4	
2	α_1	18.77	0.64	18.13		2
	β_1	10.73	0.64	11.09	55.7	
	β_2	6.22	0.64	5.58	30.8	
	γ_1	2.91	0.64	2.27	12.5	
3	α_1	17.40	0.65	16.75		2
	β_1	10.13	0.65	9.48	56.6	
	β_2	5.83	0.65	5.18	30.9	
	γ_1	2.73	0.65	7.08	12.4	
Weighted averages: $I(\beta_1)=56.6$			$I(\beta_2)=31.1$		$I(\gamma_1)=12.4$	

$$I_\lambda = 100\,\frac{(i-i_b)_\lambda}{(i-i_b)_\alpha}$$

is the intensity of the line λ (representing β_1, β_2, or γ_1) with the base correction, but without the corrections for absorption, etc., relative to the α_1 line as 100. The weights of the different trials were determined by the stability of the x-ray tube during the measurements.

CORRECTIONS TO OBSERVED INTENSITIES

In Table V are shown the observed intensities, the necessary corrections, and the resultant transition probabilities. The corrections for partial absorption in the mica x-ray tube window, in the air, and in the aluminum ionization chamber window are denoted respectively by $F_m=\exp\,[(\mu_{m\lambda}-\mu_{m\alpha})d_m]$, $F_a=\exp\,[(\mu_{a\lambda}-\mu_{a\alpha})d_a]$ and $F_w=\exp\,[(\mu_{w\lambda}-\mu_{w\alpha})d_w]$. μ denotes a linear absorption coefficient and d a thickness in cm. The subscripts m, a, and w refer respectively to mica, air, and aluminum, and the subscripts λ and α, respectively, to the wave-length of the line in question and of the $L\alpha_1$ line.

$$F_i = (1-e^{-\mu_{i\alpha}d_i})/(1-e^{-\mu_{i\lambda}d_i})$$

is the correction for the fraction of each wave-length absorbed in the ionization chamber. The subscript i refers to the methyl bromide in the chamber. In the work of Allison and Andrew[3] it was shown that the relative intensities of certain lines were within experimental error the same when the ionization chamber was filled with air, sulphur dioxide, methyl bromide, methyl iodide, argon, or krypton, and so it is reasonable to suppose that when the proper corrections are made, the relative intensities of any lines are independent of

TABLE V. *Corrections and results.*

Line element at. no.	β_1 Ta 73	W 74	Ir 77	Pt 78	β_2 Ta 73	W 74	Ir 77	Pt 78	γ_1 Ta 73	W 74	Ir 77	Pt 78
I_λ	69.8	67.9	60.5	56.6	30.0	31.0	29.3	31.1	15.7	16.3	13.7	12.4
I					1.7	1.8	1.9	4.0				
I_λ'					28.3	29.2	27.4	27.1				
log I_λ'	1.844	1.832	1.782	1.753	1.452	1.465	1.438	1.433	1.196	1.212	1.137	1.093
log F_m	−0.050	−0.046	−0.036	−0.033	−0.059	−0.053	−0.040	−0.036	−0.084	−0.076	−0.058	−0.053
log F_a	−0.070	−0.066	−0.054	−0.050	−0.082	−0.077	−0.059	−0.055	−0.120	−0.111	−0.088	−0.081
log F_w	−0.032	−0.030	−0.025	−0.023	−0.038	−0.035	−0.027	−0.025	−0.055	−0.051	−0.040	−0.038
log F_t	0.003	0.004	0.014	0.017	0.004	0.006	0.017	0.020	0.018	0.024	0.059	0.068
log F_c	0.040	0.040	0.042	0.044	0.049	0.049	0.049	0.050	0.082	0.084	0.084	0.085
log F_{tR}	0.110	0.110	0.136	0.141	−0.010	−0.020	−0.017	−0.018	0.133	0.132	0.151	0.157
log F_{tW}	0.022	0.022	0.042	0.047	−0.018	−0.030	−0.018	−0.010	0.043	0.042	0.054	0.060
log P'	1.695	1.694	1.681	1.664	1.274	1.305	1.326	1.322	0.955	0.998	1.010	0.989
log P_R	1.845	1.844	1.859	1.849	1.313	1.334	1.358	1.354	1.170	1.214	1.245	1.231
log P_W	1.757	1.756	1.765	1.755	1.305	1.324	1.357	1.362	1.080	1.124	1.148	1.134
P'	49.5	49.4	48.0	46.1	18.9	20.2	21.3	21.7	9.0	10.0	10.2	9.7
P_R	69.9	69.8	72.2	70.6	20.7	21.6	23.0	23.4	14.8	16.4	17.6	17.0
P_W	57.1	57.0	58.2	56.9	20.3	21.1	22.9	23.8	12.0	13.3	14.1	13.6
P'^1		47.4		45.0		20.2				8.3		9.8
P'^2	51.				20.				10.			
P'^3		50.6								10.5		

[1] Jönsson, reference 1. [2] Hicks, reference 2. [3] Allison and Andrew, reference 3.

the gas in the ionization chamber. The wave-lengths measured were all long enough so that no bromine K fluorescent radiation was excited, and all other fluorescent radiation was so soft that it was practically all absorbed before it reached the walls of the ionization chamber. The dimensions of the ionization chamber and the gas pressure within it were such that practically all of the β-rays came to the end of their ionizing range within it. F_c is the ratio of the coefficient of reflection of the calcite crystal for α_1 and for λ. As pointed out by Allison,[7] the coefficient of reflection of a single crystal cannot be measured experimentally. However, the coefficient of reflection defined as the area under the rocking curve of crystal B of a double-crystal spectrometer is approximately proportional to the coefficient of reflection from a single crystal, and, since we use only ratios of the coefficient of reflection, the proportionality constant will drop out. The values of F_c are derived from graphical interpolation of data obtained by Professor Allison on a double-crystal spectrometer, when using the same crystal, which is numbered V-B in his paper. F_t is the correction for the effects of the tube voltage and the absorption within the target. The derivation of this correction is discussed in the next section.

In Table VI are shown the various constants used in the calculation of the corrections. The absorption coefficients of mica, air, and methyl bromide were taken from Allison and Andrew.[3] Those of aluminum were taken from Comp-

TABLE VI. *Constants.*

Element	Line	$\lambda(A)$	μ_m	μ_a	μ_w	μ_i	V_0(k.v.)
Ta	α_1	1.519	136.4	0.0109	132.6	0.266	9.87
	β_1	1.324	86.0	0.0072	88.0	0.174	11.11
	β_2	1.282	77.4	0.00655	80.0	0.160	9.87
	γ_1	1.136	52.6	0.00455	56.3	0.112	11.11
W	α_1	1.473	123.0	0.0100	121.2	0.201	10.18
	β_1	1.279	76.8	0.0065	79.4	0.158	11.52
	β_2	1.242	69.8	0.00595	72.7	0.144	10.18
	γ_1	1.096	47.0	0.0041	50.8	0.102	11.52
Ir	α_1	1.348	91.7	0.00765	93.6	0.185	11.17
	β_1	1.155	55.4	0.0048	59.2	0.116	12.80
	β_2	1.133	52.2	0.0045	55.7	0.110	11.17
	γ_1	0.989	34.0	0.0030	37.0	0.072	12.80
Pt	α_1	1.310	83.2	0.0070	85.4	0.171	11.53
	β_1	1.118	50.1	0.00435	53.8	0.108	13.24
	β_2	1.100	47.5	0.0041	51.4	0.105	11.53
	γ_1	0.956	30.6	0.0027	29.6	0.067	13.24

$d_m=0.0023$ $d_a=43.5$ $d_w=0.00165$ $d_i=28.1$ $V=30$

μ_a and μ_i were calculated for 76 cm pressure and 20°C.

ton.[8] For mica, air, aluminum, and methyl bromide, curves were drawn for μ versus λ^3, which were nearly linear, and then μ was read from the curves for the desired wave-lengths. For the four target materials, the absorption coefficients were calculated from the equation[9]

[7] S. K. Allison, Phys. Rev. **41**, 1 (1932).
[8] A. H. Compton, *X-Rays and Electrons*, p. 180.
[9] Ivor Backhurst, Phil. Mag. **7**, 353 (1929).

$$\log \mu/\rho = C + m \log \lambda + 4 \log Z.$$

From the experimental measurements of μ by Allen[10] for tungsten, platinum, gold, and lead, by Kellström[11] for silver, by Backhurst[9] for platinum and gold, and by Uber[12] for mercury, average values of the contants were chosen as $C = -5.750$ and $m = 2.63$ for the lines α_1, β_1, and β_2 (above the L_{III} absorption limit), and $C = -5.356$ and $m = 2.61$ for the line γ_1 (between the L_{II} and the L_{III} absorption limits). The constant b/ρ of the Thomson-Whiddington equation does not vary rapidly with Z. The value 4.55×10^5 for all of the elements used as targets was chosen by interpolation between values obtained for various elements by Terrill.[13] ρ appears in both the factor μ/ρ and the factor b/ρ, but it cancels out in the calculations.

In several instances the lines measured lie close to other lines. In all such cases, the amount of error in the observed intensity of the principal line was calculated, and when it exceeded 0.2 a correction was made. Table VII shows the derivation of such corrections. $\delta\lambda$ and $\delta\theta$ are the separation between the principal line and the interfering line, in angstroms and in minutes of arc,

TABLE VII. *Interfering lines.*

Element	Line	Interfering line	$\delta\lambda$[14]	$\delta\theta$	f	I_i'	I_λ'	I_i
Ta	β_2	β_{15}	0.0016	0.92	0.6	0.1[15]	28.3	1.7
W	β_2	β_{15}	0.0016	0.92	0.6	0.1[15]	29.2	1.8
Ir	β_2	β_{15}	0.0016	0.92	0.6	0.1[15]	27.4	1.6
Ir	β_2	β_3	0.0055	3.2	0.04	0.23[16]	27.4	0.3
Pt	β_2	β_{15}	0.0016	0.92	0.6	0.1[15]	27.1	1.6
Pt	β_2	β_3	0.0019	1.1	0.44	0.20[16]	27.1	2.4

respectively. Since the peak of intensity *vs.* angle which is found experimentally is approximately identical with the peak of the principal line, and is in general considerably off the peak of the interfering line, a factor f is introduced by which the intensity of the interfering line must be multiplied to de-

[10] S. J. M. Allen, Phys. Rev. **28**, 907 (1926).

[11] G. Kellström, Zeits. f. Physik **44**, 269 (1927).

[12] F. M. Uber, Phys. Rev. **38**, 217 (1931).

[13] H. M. Terrill, Phys. Rev. **22**, 107 (1923).

[14] From S. K. Allison, Phys. Rev **34**, 176 (1929) and Manne Siegbahn, *Spektroskopie der Röntgenstrahlen*, Ed. II, p. 208.

[15] S. K. Allison, Phys. Rev. **34**, 176 (1929).

[16] The following sources of data were used for the relative intensities of β_2 and β_3. All of the data were taken at, or corrected to, 30 k.v. Since the lines are very close together, all corrections other than for the tube voltage disappear. A curve for I_i' *vs.* Z was drawn from these data, and the values used above were read from the curve.

I_i'	Element	Source
0.34	Ta	Victor Hicks, Phys. Rev. **38**, 572 (1931).
0.33	W	Allison and Armstrong, Phys. Rev. **26**, 714 (1925).
0.26	Os	S. K. Allison, Phys. Rev. **34**, 7 (1929).
0.35	W	Axel Jönsson, Zeits. f. Physik **36**, 426 (1926).
0.23	Ir	Fig. 2 of this paper.

termine the amount of interference present at the peak of the principal line. f varies from unity to zero with increasing $\delta\theta$. It is assumed that the apparent shape of all lines is the same (and is due to the width of the slits). Fig. 1 shows an experimental curve of the iridium β_2 and β_3 lines. The values of f were measured on the left side of the curve. I_i' is the ratio of the intensity of the interfering line to the intensity I_λ' of the principal line. The final correction for interference $I_i = fI_i'I_\lambda'$ is substracted from the intensity I_λ in Table V to obtain the intensity I_λ' of the principal line alone.

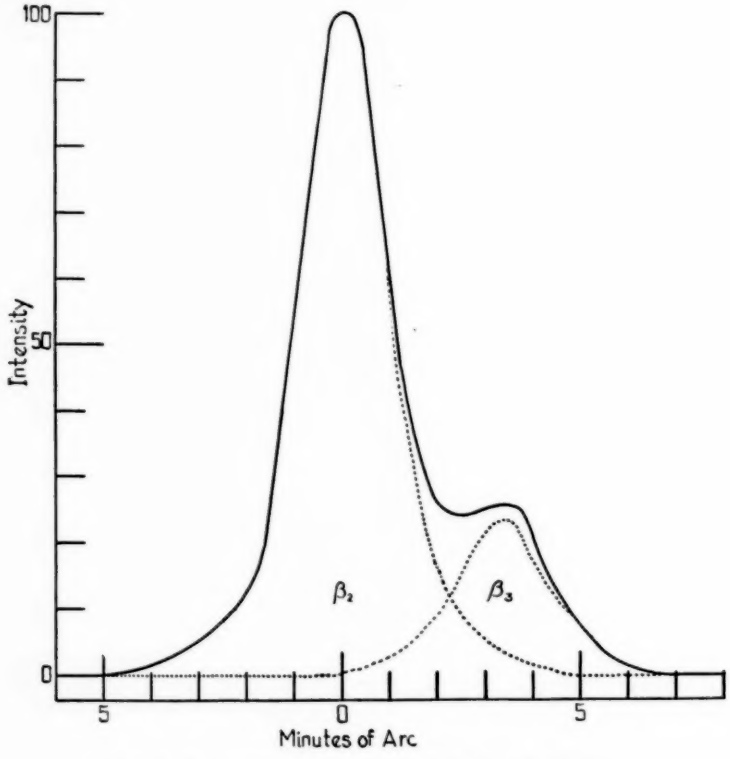

Fig. 1. Separation of the $L\beta_2$ and β_3 lines in iridium.

Theory of the Correction within the Target

In most intensity measurements heretofore the effect of absorption within the target has been neglected. Kulenkampff[17] and Wisshak[18] have used such a correction, but it was based on the assumption that electrons falling on the target maintain their initial velocity until they are suddenly stopped, rather than losing velocity according to the now accepted Thomson-Whiddington law, and that the number of electrons decreases exponentially with depth within the target. It has been customary to express intensities extrapolated to infinite voltage. The expression for transition probability developed here-

[17] H. Kulenkampff, Ann. d. Physik **69**, 548 (1922).
[18] F. Wisshak, Ann. d. Physik **5**, 507 (1930).

after does not agree with this convention. It follows an expression developed by Jönsson.[19] An experiment was then performed to test certain aspects of the calculations.

The intensity dJ_λ of a given spectrum line λ, due to the increment of depth dx within the target is

$$dJ_\lambda = c_\lambda F(x)dx e^{-\mu_\lambda x/\sin\theta}. \tag{1}$$

c_λ is a constant which includes the geometry of the spectrometer, the power into the x-ray tube, etc., and of particular interest, the probability of a transition which will produce the line λ after an electron has been removed from the proper inner shell. $F(x)$ is the ionization function or the probability of ejection of an electron from a particular shell by an incident electron with the velocity which it retains after penetrating the target to the depth x. $e^{-\mu_\lambda x/\sin\theta}$ is the correction for the absorption of the x-rays between the depth x of their emission and the surface of the target, when they are measured at an angle θ with the surface. μ_λ is the absorption coefficient of the target material.

The total intensity J_λ observed for the line is the integral of Eq. (1) from the surface of the target to the depth x_0 where the velocity of the impinging electrons has been reduced so much that they are no longer able to remove electrons from the proper inner shells.

$$J_\lambda = c_\lambda \int_0^{x_0} F(x)e^{-\mu_\lambda x/\sin\theta}dx. \tag{2}$$

It is more convenient to use as the variable V_x, the velocity of electrons in electron kilovolts at the depth x. The relation between V_x and x is taken from the Thomson-Whiddington equation $V_x^2 = V^2 - bx$ or $x = (V^2 - V_x^2)/b$. Eq. (2) now becomes

$$J_\lambda = \frac{2c_\lambda}{b} e^{-\mu_\lambda V^2/b\sin\theta} \int_{V_0}^{V} F(x)e^{\mu_\lambda V_x^2/b\sin\theta} V_x dV_x. \tag{3}$$

The integration is between the limits V, which is the velocity of the impinging electrons at the surface of the target, or the voltage across the x-ray tube, and V_0, which is the critical excitation voltage for the line λ.

Before Eq. (3) can be integrated, an expression for $F(x)$ must be found. Rosseland[20] has found from theoretical considerations

$$F_R(x) = k_\lambda(1/V_x)(1/V_0 - 1/V_x). \tag{4$_R$}$$

Webster, Clark, Yeatman, and Hansen[21] have an empirical

$$F_W(x) = k_\lambda(1 - V_0/V_x)/(3 + V_x/V_0). \tag{4$_W$}$$

which they find fits experimental curves of intensity *vs.* tube voltage with a thin target better than Rosseland's expression does. k_λ in Eq. (4) represents

[19] Axel Jönsson, Zeits. f. Physik **43**, 845 (1927).
[20] S. Rosseland, Phil. Mag. **45**, 65 (1923).
[21] Webster, Clark, Yeatman, and Hansen, Proc. Nat. Acad. Sci. **14**, 679 (1928).

the relative probability of a particular inner shell being ionized, and the remainder of the equation gives the variation of this probability with the velocity of the impinging electrons. The subscripts R and W are used to denote the results dependent on each of the two preceding expressions.

Inserting Eq. (4) in Eq. (3), we obtain

$$J_{\lambda R} = \frac{2c_\lambda k_\lambda}{b} e^{-\mu_\lambda V^2/b\sin\theta} A_{\lambda R}$$

$$J_{\lambda W} = \frac{2c_\lambda k_\lambda}{b} V_0 e^{-\mu_\lambda V^2/b\sin\theta} A_{\lambda W}$$

where

$$A_{\lambda R} = \int_{V_0}^{V} \left(\frac{1}{V_0} - \frac{1}{V_x}\right) e^{\mu_\lambda V_x^2/b\sin\theta} dV_x \tag{5$_R$}$$

$$A_{\lambda W} = \int_{V_0}^{V} \frac{V - V_0 + V_x}{3V_0 + V_x} e^{\mu_\lambda V_x^2/b\sin\theta} dV_x. \tag{5$_W$}$$

Taking the ratio J_λ/J_α which was defined as I_λ' in the preceding experimental data,

$$I'_{\lambda R} = P_\lambda e^{(\mu_\alpha - \mu_\lambda)V^2/b\sin\theta}(A_{\lambda R}/A_{\alpha R}) \tag{6$_R$}$$

$$I'_{\lambda W} = P_\lambda (V_{0\lambda}/V_{0\alpha}) e^{(\mu_\alpha - \mu_\lambda)V^2/b\sin\theta}(A_{\lambda W}/A_{\alpha W}) \tag{6$_W$}$$

where

$$P_\lambda = c_\lambda k_\lambda / c_\alpha k_\alpha.$$

Geometric, etc., factors in c_λ and c_α cancel, so there remains in P_λ only the ratio of probabilities of transitions which will produce particular lines when electrons have been removed from the proper inner shells, times the probabilities of these particular electrons being removed. The purpose of the preceding intensity measurements and the subsequent calculations was to evaluate P_λ, called the transition probability.

For numerical evaluation it is more convenient to have Eq. (6) in logarithmic form.

$$\log I'_{\lambda R} = \log P_\lambda + 0.4343(\mu_\alpha - \mu_\lambda)V^2/b\sin\theta + \log A_{\lambda R} + \log A_{\alpha R}$$

$$\log I'_{\lambda W} \quad \log P_\lambda + \log V_{0\lambda} - \log V_{0\alpha} + 0.4343(\mu_\alpha - \mu_\lambda)V^2/b\sin\theta + \log A_{\lambda W} - \log A_{\alpha W}.$$

The factor 0.4343 changes from a logarithm to the base e to a logarithm to the base 10. The correction factor F_t is the expression which must be multiplied by, or in the logarithmic form, added to, I_λ' in order to obtain P_λ.

$$\log F_{tR} = 0.4343(\mu_\lambda - \mu_\alpha)V^2/b\sin\theta + \log A_{\alpha R} - \log A_{\lambda R} \tag{7$_R$}$$

$$\log F_{tW} = \log V_{0\alpha} - \log V_{0\lambda} + 0.4343(\mu_\lambda - \mu_\alpha)V^2/b\sin\theta + \log A_{\alpha W} - \log A_{\lambda W}. \tag{7$_W$}$$

The definite integrals in Eq. (5) are not readily obtained. It is sometimes more convenient to divide log F_t into two parts, such that

$$\log F_t = \log F_v + \log F_u. \tag{8}$$

Log F_v is defined as the value of log F_t when $1/\sin\theta = 0$ (an imaginary value of θ). Log F_u is then defined by Eq. (8). The advantage of this separation is that log F_v can be evaluated by integration, and log F_u is so small that an approximate estimate of its magnitude is sufficient. By calculation, F_u was found to vary not more than 0.003 per unit of atomic number, for the elements from tantalum to platinum, with $V = 30$ and $1/\sin\theta = 1$.

Setting $1/\sin\theta = 0$ in Eq. (5) and integrating, we get

$$A_{\lambda R0} = V/V_0 - (1/0.4343)(\log V - \log V_0) - 1 \tag{9$_R$}$$

$$A_{\lambda W0} = V - V_0 - (4V_0/0.4343)\log(V/4V_0 + \tfrac{3}{4}). \tag{9$_W$}$$

Using Eqs. (7) and (9), we find that

$$\log F_{vR} = \log\left\{\frac{V}{V_{0\alpha}} - \frac{1}{0.4343}(\log V - \log V_{0\alpha}) - 1\right\} - \log\left\{\frac{V}{V_{0\lambda}} - \frac{1}{0.4343}(\log V - \log V_{0\lambda}) - 1\right\} \tag{10$_R$}$$

$$\log F_{vW} = \log V_{0\alpha} - \log V_{0\lambda} + \log\left\{V - V_{0\alpha} - \frac{4V_0}{0.4343}\log(V/4V_{0\alpha} + \tfrac{3}{4})\right\} - \log\left\{V - V_{0\lambda} - \frac{4V_{0\lambda}}{0.4343}\log(V/4V_{0\lambda} + \tfrac{3}{4})\right\}. \tag{10$_W$}$$

At least qualitatively we may call F_v the correction for tube voltage (replacing the correction to infinite voltage which has been used heretofore). Then F_u may be called the correction for absorption within the target (which has usually been neglected heretofore). As log F_u approaches zero the application of the foregoing names to F_v and F_u becomes more nearly correct. When log F_u becomes numerically large, due to considerable absorption within the target, the effects of tube voltage and of absorption within the target become interrelated due to the greater absorption of x-rays from greater depth, and thus the fraction of the beam produced by electrons of one velocity is not the same as the fraction which escapes from the target.

Experimental Verification of the Correction within the Target

In order to test the validity of the preceding theory, experimental measurements pertaining to the correction within the target were made with a platinum target and are shown in comparison with the theoretical calculations in Fig. 2. The curves represent the theoretical values of log F_u and the points show experimental values. The theoretical values were obtained by

evaluating Eq. (7). The integration was accomplished graphically, by drawing the curve of the function and measuring the area below it. $1/\sin\theta$ is used instead of θ as the abscissa since the thickness through which the x-rays from a given point are absorbed before leaving the target is proportional to $1/\sin\theta$, and the curves with this abscissa are more nearly linear. Table VIII gives the data for the theoretical curves.

TABLE VIII. *Calculated values of F_u for platinum at different angles.*

$1/\sin\theta$	$\log F_{uR\beta_1}$	$\log F_{uW\beta_1}$	$\log F_{uR\gamma_1}$	$\log F_{uW\gamma_1}$
1	−0.020	−0.013	−0.004	0
4	−0.071	−0.056	−0.006	0
8	−0.120	−0.102	−0.010	0
16	−0.183	−0.161	−0.008	−0.025
32	−0.254	−0.225	−0.026	−0.018

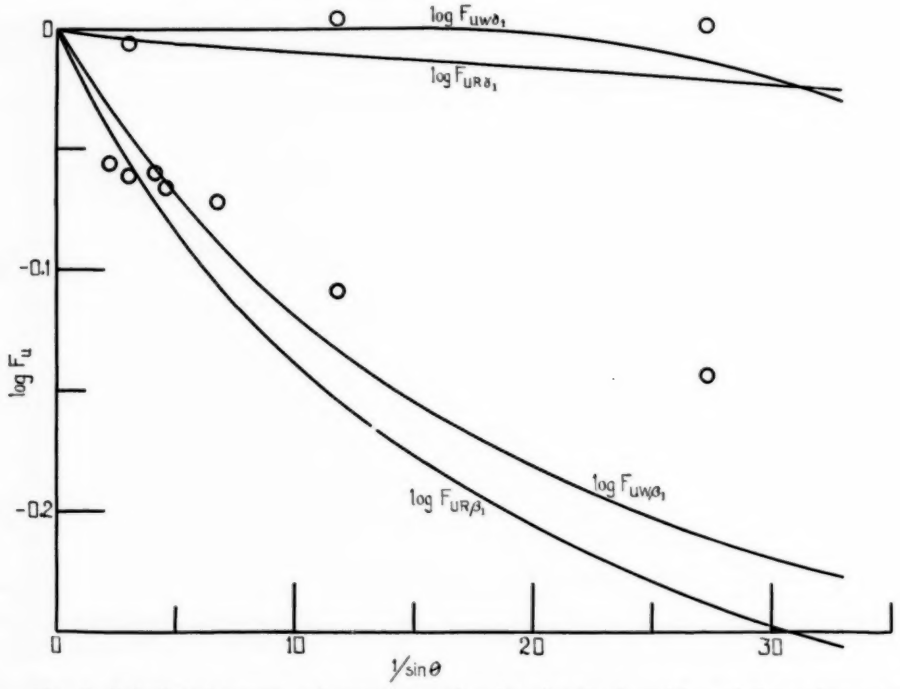

Fig. 2. Calculated curves and experimental points for the logarithm of the reciprocal of the relative intensity as observed at different angles from the surface of a polished platinum target.

The apparatus used for the experimental measurements was the same as described previously for relative intensity measurements, with the exception of the x-ray tube and its mounting. The electron beam was perpendicular to the face of the target. The tube was mounted so that it could be rotated about a vertical axis through its focal spot, and the window of the tube was made large enough to permit the beam to be observed at angles from 0 to 30° with the surface of the target.

TABLE IX. *Experimental data for* $I(\beta_1)$.

	Trial	$I(\beta_1)$	$I(W\alpha_1)$
$\theta=28°08'$	1	37.0	10
$1/\sin\theta=2.19$	2	36.8	10
$I'(\beta_1)=37.6$	3	38.2	15
$\log I'(\beta_1)=1.575$	4	36.0	40
	5	36.0	39
	6	37.0	13
	7	37.0	15
	8	37.5	3
$\theta=19°22'$	1	37.0	3
$1/\sin\theta=3.02$	2	38.9	3
$I'(\beta_1)=38.0$	3	38.0	3
$\log I'(\beta_1)=1.580$			
$\theta=14°13'$	1	37.9	3
$1/\sin\theta=4.07$	2	37.9	3
$I'(\beta_1)=37.9$			
$\log I'(\beta_1)=1.579$			
$\theta=12°40'$	1	35.7	37
$1/\sin\theta=4.56$	2	39.9	3
$I'(\beta_1)=38.5$	3	39.5	3
$\log I'(\beta_1)=1.585$	4	38.8	7
	5	38.8	8
	6	38.3	8
$\theta=8°31'$	1	38.6	16
$1/\sin\theta=6.75$	2	39.8[22]	3
$I'(\beta_1)=39.0$	3	38.8[22]	3
$\log I'(\beta_1)=1.591$			
$\theta=4°52'$	1	43.4[22]	5
$1/\sin\theta=11.78$	2	42.6[22]	5
$I'(\beta_1)=42.5$	3	42.4[22]	5
$\log I'(\beta_1)=1.628$			
$\theta=2°06'$	1	48.5[22]	8
$1/\sin\theta=27.3$	2	46.2[22]	8
$I'(\beta_1)=46.0$	3	46.6[22]	9
$\log I'(\beta_1)=1.663$	4	46.6[22]	10

TABLE X. *Experimental data for* $I(\gamma_1)$.

	Trial	$I(\gamma_1)$	$I(W\alpha_1)$	Weight
$\theta=19°22'$	1	11.9	6	3
$1/\sin\theta=3.02$	2	11.9	8	1
$I'=12.6$	3	12.0	8	2
$\log I'=1.100$	4	11.6	8	2
	5	12.0	8	2
$\theta=4°52'$	1	10.7	15	2
$1/\sin\theta=11.78$	2	10.9	15	1
$I'=12.3$	3	10.8	16	2
$\log I'=1.090$	4	11.8	6	2
	5	11.7	6	3
$\theta=2°06'$	1	12.1	10	1
$1/\sin\theta=27.3$	2	11.3	10	3
$I'=12.4$	3	11.0	12	3
$\log I'=1.093$	4	11.4	13	3

[22] A 0.0033 cm mica window was used on the x-ray tube. The observed $I(\beta_1)$ has been corrected to be comparable with the values observed with the 0.0020 cm window used elsewhere.

TABLE XI. *Experimental values for F_u of platinum at different angles.*

$1/\sin\theta$	$\log I'(\beta_1)$	$\log F_{u\beta_1}$	$\log I'(\gamma_1^*)$	$\log F_{u\gamma_1}$
2.19	1.575	−0.056		
3.02	1.580	−0.061	1.100	−0.006
4.07	1.579	−0.060		
4.56	1.585	−0.066		
6.75	1.591	−0.072		
11.78	1.628	−0.109	1.090	0.004
27.3	1.663	−0.144	1.093	0.001

The measurement procedure and base corrections were the same as those used in the intensity measurements. In Tables IX and X are shown measurements of I_λ at different angles, and Table XI summarizes these data. The $I(\beta_1)$ and $I(\gamma_1)$ measurements were made under different conditions of the tube window and ionization chamber pressure. They were not corrected to the same conditions, since it is unnecessary. Since many of the measurements were made with an appreciable tungsten film on the target, the corrected average I_λ' is obtained by plotting I_λ versus $I(W\alpha_1)$, the intensity of tungsten $L\alpha_1$, and extrapolating to $I(W\alpha_1)=0$.

When θ is varied the transition probability and the corrections other than F_u do not vary, so the observed variation in I_λ' must be inversely proportional to the variation in F_u. Since the transition probability is an unknown factor in the proportionality constant, the experimental points are adjusted (by an arbitrary additive constant when expressed in logarithmic form) to fit the calculated curves as well as possible.

It is seen in Fig. 2 that there is a qualitative agreement between the two different theoretical and the experimental results. In each of the three cases $F_{u\beta_1}$ decreases sharply and $F_{u\gamma_1}$ remains nearly constant with $1/\sin\theta$.

The difference between the Rosseland and the Webster calculations consists of a slight separation of the curves. The difference between the shape of the two theoretical curves is less than the separation between them and the experimental points. Consequently no information is gained concerning the relative accuracy of the Rosseland and the Webster functions. In the calculations it is assumed that the surface of the target is a perfect plane. The average depth of production is approximately 4000A. It is believed that the irregularities on the surface of the target were small compared to this depth. The calculations do not take any account of ionization in the target produced by indirect means, such as reabsorption of x-rays. Presuming that one of the theories is correct, both irregularities on the surface and indirect ionization may contribute to the disagreement of the experimental points.

The approximate average depth of production is determined by observing that when $1/\sin\theta=1$ all the curves of Eq. (5) (the curves which were drawn for graphical integration) were roughly linear, touching zero at $V_x=V_0$. The abscissa is V_x and the ordinate is the intensity contributed at the depth x corresponding to V_x. Therefore the center of gravity has the V_x of the average depth of production. The center of gravity of the triangle is $\frac{1}{3}$ of the way from $V=30$ to $V_0\doteq 12$, or $V_x\doteq 24$. With the use of the Thomson-Whiddington equation, the corresponding $x\doteq 4\times 10^{-5}=4000$A.

Application of the Correction within the Target

Log F_{tR} and log F_{tW} were calculated for the preceding intensity measurements, with graphical integration, and are shown in Table V. Since the incident beam of electrons and the emergent x-ray beam each make a 45° angle with the face of the target, the depth of the penetration of an electron before ionizing an atom is equal to the thickness of target material which the x-rays must pass through to reach the surface. This is the same condition as $1/\sin\theta = 1$ when the electron beam is perpendicular to the face of the target.

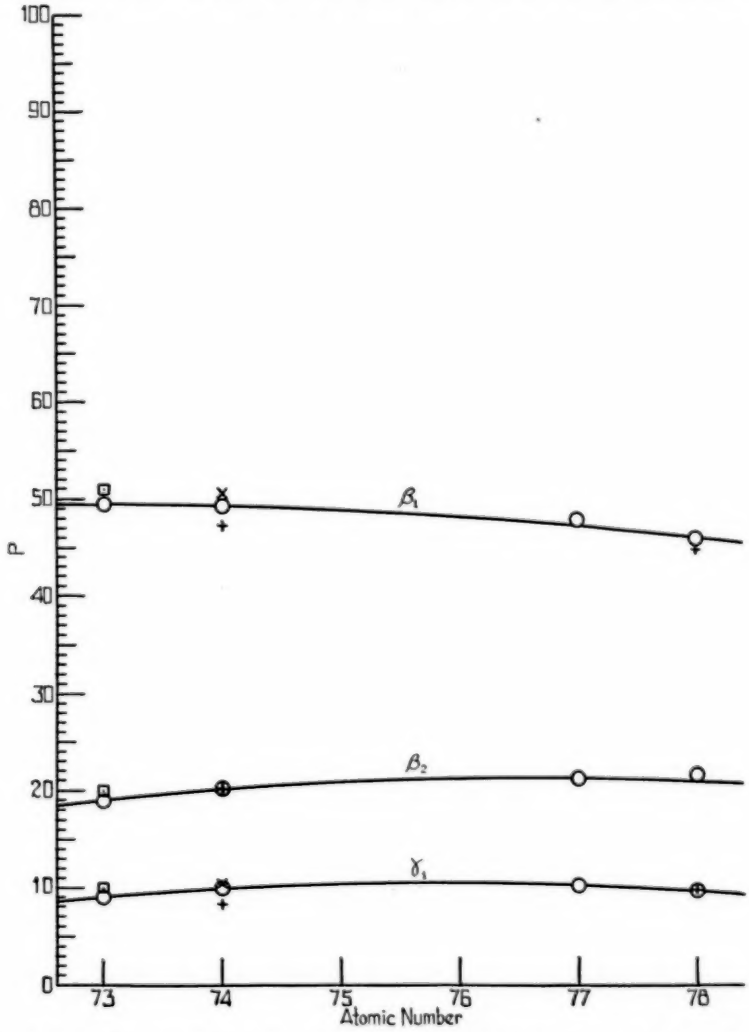

Fig. 3. Intensity relative to $L\alpha_1 = 100$ at 30 k.v. without correction for partial reflection by the crystal. Plus signs, Jönsson; squares with dots, Hicks; crosses, Allison and Andrew; circles, Andrew.

Conclusion

In Table V the corrected intensities are given in three forms, P', P_R, and P_W. The first is the intensity with all corrections except for partial reflection

at the crystal and for effects within the target. In this form the data are comparable to those of previous investigators, which are also shown in Table V. The published data of Jönsson at 20 k.v. werecorrected to 30 k v. by the assumption that the intensity of a line is proportional to $(V-V_0)^2$. The published data of Allison and Andrew were corrected for absorption in air and in the tube and ionization chamber windows. P_R and P_W are the transition

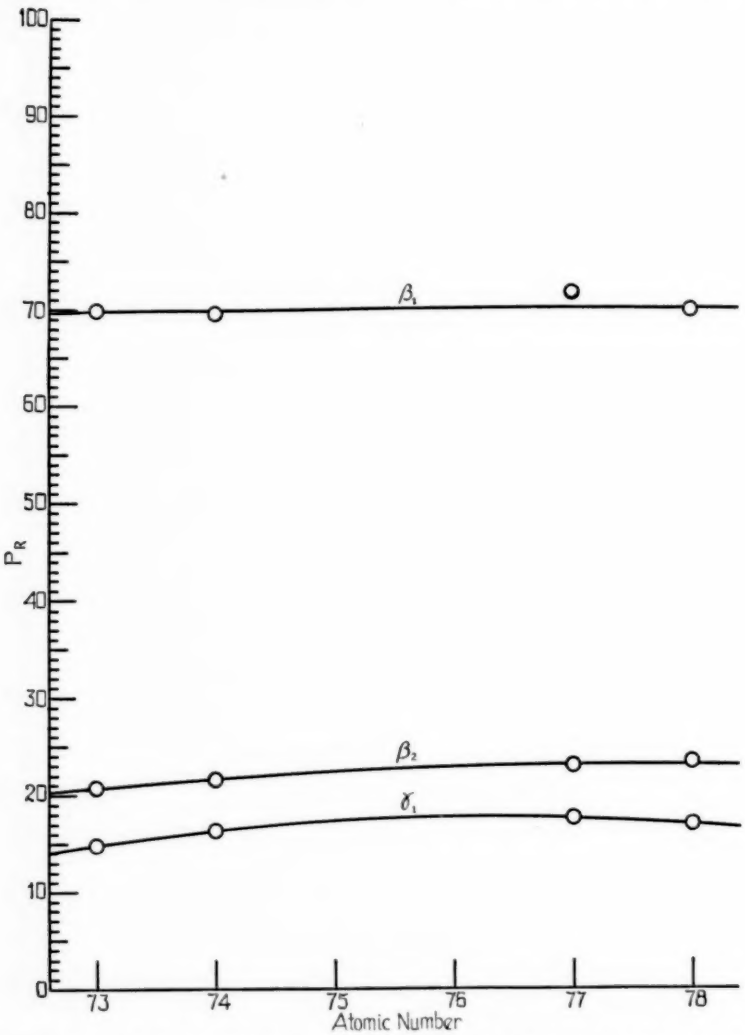

Fig. 4. Transition probability relative to $L\alpha_1 = 100$ calculated with the Rosseland function.

probabilities according to the Rosseland expression and according to the Webster expression, respectively. In Figs. 3, 4 and 5 the results in the three forms mentioned are plotted against the atomic number. In Fig. 3 the measurements of other investigators are shown for comparison. It is seen that the results reported here are in good agreement with former work, and are quite consistent from element to element.

The Webster expression gives transition probability ratios which agree much better than those from the Rosseland expression with the theoretical predictions of the sum rule of Burger and Dorgelo.[23] The predictions are

$$P(\alpha_1):P(\beta_1) = P(\beta_2):P(\gamma_1) = 9:5.$$

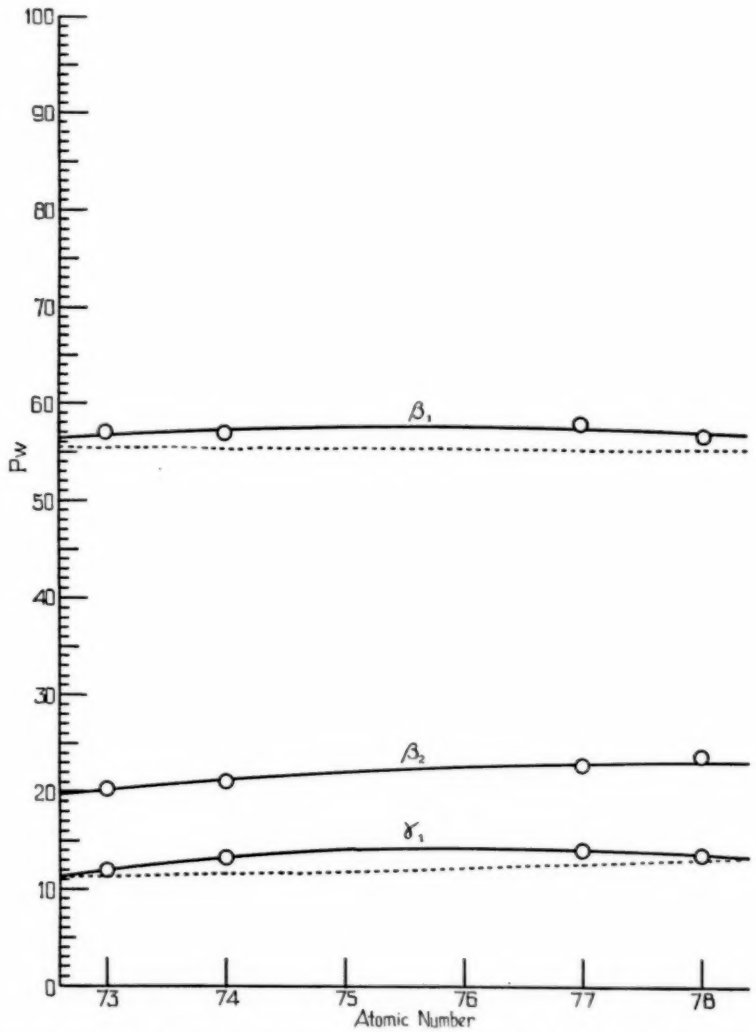

Fig. 5. Transition probability relative to $L\alpha_1 = 100$ calculated with the Webster, Clark, Yeatman, and Hansen function. Full curve, experimental; broken curve, sum rule.

The dotted curves in Fig. 5 show the predictions for $P(\beta_1)$ $((5/9)P(\alpha_1)$, $P(\alpha_1) = 100)$ and $P(\gamma_1)$ $((5/9)P(\beta_2)$, experimental values of $P(\beta_2))$.

It should be observed that the empirical origin of Eq. (4_W), which may be written

[23] Burger and Dorgelo, Zeits. f. Physik **23**, 258 (1924).

$$F_W(x) = k_\lambda V_0 \frac{1}{V_x} \frac{V_x - V_0}{V_x + 3V_0} \qquad (4_W')$$

permits changing V_0 in the coefficient to any other power without invalidating the agreement of the function with the experimental data for which it was originated (the variation of intensity of one line with V_x, hence V_0 was a constant). The first power of V_0 is apparently a fortuitous circumstance which results in making the observed intensities agree so closely with the sum rule. Inserting a V_0 in the coefficient of the Rosseland function would make the observed intensities with the corresponding correction fall much closer to the sum rule predictions. However, the theoretical derivation of the Rosseland function shows that such a constant cannot be arbitrarily inserted.

The writer wishes to take this opportunity to express his thanks for the use of the x-ray spectrometer and his appreciation to Professor S. K. Allison for the suggestion of the problem and guidance during the investigation.

The Band Spectra of MgO, CaO and SrO

By P. C. MAHANTI
University College of Science and Technology, Calcutta

(Received September 9, 1932)

New measurements of the wave-lengths of the band heads attributed to the oxides of Mg, Ca and Sr have been made from moderate dispersion spectrograms. For each of these molecules the bands have been classified into two systems. The equations of the band heads in terms of half-quantum numbers for the different systems are as follows:

MgO, red bands:

$$\nu = 16{,}418.06 + \{821.95(v' + \tfrac{1}{2}) - 4.05(v' + \tfrac{1}{2})^2\} - \{665.74(v'' + \tfrac{1}{2}) - 4.41(v'' + \tfrac{1}{2})^2\}$$

MgO, green bands:

$$\nu = 19{,}944.82 + \{811.67(v' + \tfrac{1}{2}) - 3.74(v' + \tfrac{1}{2})^2\} - \{771.42(v'' + \tfrac{1}{2}) - 4.81(v'' + \tfrac{1}{2})^2\}$$

CaO, blue bands:

$$\nu = 23{,}817.62 + \{726.53(v' + \tfrac{1}{2}) - 11.66(v' + \tfrac{1}{2})^2\} - \{811.28(v'' + \tfrac{1}{2}) - 6.60(v'' + \tfrac{1}{2})^2\}$$

CaO, ultraviolet bands:

$$\nu = 28{,}849.13 + \{565.06(v' + \tfrac{1}{2}) - 4.48(v' + \tfrac{1}{2})^2\} - \{725.37(v'' + \tfrac{1}{2}) - 3.56(v'' + \tfrac{1}{2})^2\}$$

SrO, blue bands:

$$\nu = 24{,}702.81 + \{519.09(v' + \tfrac{1}{2}) - 3.50(v' + \tfrac{1}{2})^2\} - \{653.47(v'' + \tfrac{1}{2}) - 4.02(v'' + \tfrac{1}{2})^2\}$$

SrO, ultraviolet bands:

$$\nu = 28{,}622.18 + \{497.81(v' + \tfrac{1}{2}) - 5.97(v' + \tfrac{1}{2})^2\} - \{679.13(v'' + \tfrac{1}{2}) - 9.13(v'' + \tfrac{1}{2})^2\}.$$

INTRODUCTION

THE earliest spectroscopic workers[1] noticed in the spectrum of Mg, Ca and Sr or their salts subjected to a variety of conditions of excitation, a class of bands, which were ascribed by them either to the metals or to their oxides. Kayser was, however, of opinion that both types of bands are present in the spectrum. He has collected the old measurements of wave-lengths of the band heads but no satisfactory agreement is to be found among the various data. With the improvement of the experimental technique, it has however been found that some of these bands, although they appear in the ordinary arc or flame spectrum of Mg, Ca and Sr or their salts, fail to show themselves if the arcing is conducted in vacuum or in a dry hydrogen or nitrogen atmosphere

[1] Kayser, Handbuch der Spectroscopie **5**, 252, 717 (1910); **7**, 172 (1924); **6**, 551 (1912).

but increase in their intensity depending on the amount of oxygen present. It is these bands which have been ascribed to the oxides and they form the subject of the present investigation.

In 1927, Mecke and Guillery[2] analyzed one system in the case of CaO and SrO from the old data then available. The present analysis however discloses that they have used parts of two different systems for CaO. For SrO they have not published any data of band heads analyzed by them. More recently a vibrational quantum analysis[3] of the well-known green bands of MgO from measurements on low dispersion spectrograms (about 23A/mm at λ5000) has been published.

The present paper deals with the vibrational quantum analysis of the bands of MgO, CaO and SrO from new measurements of the wave-lengths of band heads, believed to be more accurate than existing data. For each of these molecules, the spectrum has been investigated between the region λ7500–λ2300, and the bands have been found to form two different systems. Only the bands of MgO lying in the red region appear to offer the best possibilities for a fine structure analysis. Such an analysis is being undertaken and will be reported in a subsequent paper.

Experimental

The spectra herein described, except that of magnesium, were produced in electric arcs between carbon electrodes with some salt of the element under investigation. In the case of magnesium the lower electrode (+) was drilled to hold magnesium rods about $\frac{1}{8}$ inch in diameter. During a single exposure several rods had to be used. The salts employed were pure anhydrous calcium chloride and strontium chloride. The arc was operated on a 220 volt d.c. circuit with the current varying from six to seven amperes but in the case of magnesium, the current was about an ampere.

Spectrograms were taken with the Hilger-Littrow-mounted E.1 prism spectrograph, having a dispersion with the glass optical system of approximately 35A/mm at λ7500 to 6A/mm at λ4400, and with the quartz system of 17A/mm at λ4500 to 2A/mm at λ2300 as well as in the first and second orders of a 15 ft. Rowland concave grating set up in a Paschen mounting. The dispersion in the first order is about 3.52A per mm. Ilford Empress and green sensitive orthochromatic plates as well as special rapid panchromatic plates freshly dyed with pinacyanol were used.

The heads are apparently single and fairly sharp except where they are greatly superposed by the structure lines of the preceding bands. With a Gaertner comparator (MI201a), the intense band heads were measured on grating plates while prism spectrograms of moderate dispersion were used for the measurement of the weaker ones. For standards, iron and neon lines were taken.

Eye estimates of the intensities of the heads were made from the plates taken with the prism spectrographs.

[2] Mecke and Guillery, Phys. Zeits. **28,** 514 (1927).
[3] Ghosh, Mahanti and Mukherjee, Phys. Rev. **35,** 1491 (1930).

The band head data and their vibrational quantum assignments are given in Tables I–VI. λ is the wave-length in air in international angstroms, I the visual estimate of the relative photographic intensity of the band heads, and ν the vacuum wave-number in cm^{-1}. O-C is the difference between the wave-number observed and that calculated from the empirical equation for each system.

Magnified reproductions of typical sequences in the band systems of MgO, CaO and SrO are given in Figs. 1, 2 and 3.

Magnesium Oxide

In the spectrum of magnesium arc in air the band groups lying between λ7000–λ5250 and also extending as far as λ4700 as well as those at λ5205 and λ5007, which are given in the excellent reproduction of Eder and Valenta,[4] have been attributed to the oxide of magnesium while the ultraviolet bands and a number of visible bands at λ5125 and λ4819 have been ascribed to the metal. The bands at λ5007 were observed by each one of the earliest spectroscopic workers[5] in the spectrum of magnesium or its salts under various modes of excitation. Lockeyer[6] found them also present in the spectrum of nebulae. The band group at λ5205 was obtained only by Eder[7] in the flame and spark spectra of magnesium and by Brooks[8] in the anode spectrum in oxygen when a high voltage unidirectional but pulsating discharge was passed between magnesium electrodes. In addition to the above two groups of bands, the latter also observed a number of bands at the red end of the same spectrum and gave approximate measurements of seven band heads between λ6600–λ5250. In the present investigation as many as twenty-five heads have been measured in this region and the measurements extended on both sides thus bringing the total number of heads measured to forty-seven for the red bands. Spectrograms taken with the glass spectrograph as well as in the first order of the 15 ft concave grating were used for measurements which are correct to ±0.05A. The two band groups at λ5205 and λ5007 were also measured from the glass prism spectrograms as well as from those taken in the second order of the same grating. They form, respectively, $\Delta\nu = +1$, and 0 sequences of the green system, which includes twenty-three band heads.

The red bands are not of perceptible intensity in the usual flame surrounding the magnesium arc in air. But they are fairly intense if the arc bursts out into a vigorous flame. With an exposure for about an hour with this type of flame, they are well developed on the plates taken with the glass spectrograph, but the band heads lying below λ5210 are very much superposed by the green bands.

So far as the writer is aware, no new measurements or vibrational quantum analysis of the red bands have yet been published, while for the green

[4] Eder and Valenta, *Atlas Typischer Spektren*, Wien (1924).
[5] Kayser, Handbuch der Spectroscopie **5,** 717 (1910).
[6] Lockeyer, Proc. Roy. Soc. **48,** 167 (1890).
[7] Eder, Denkschr. Wien. Akad. **74,** 45 (1903).
[8] Brooks, Astrophys. J. **29,** 177 (1909).

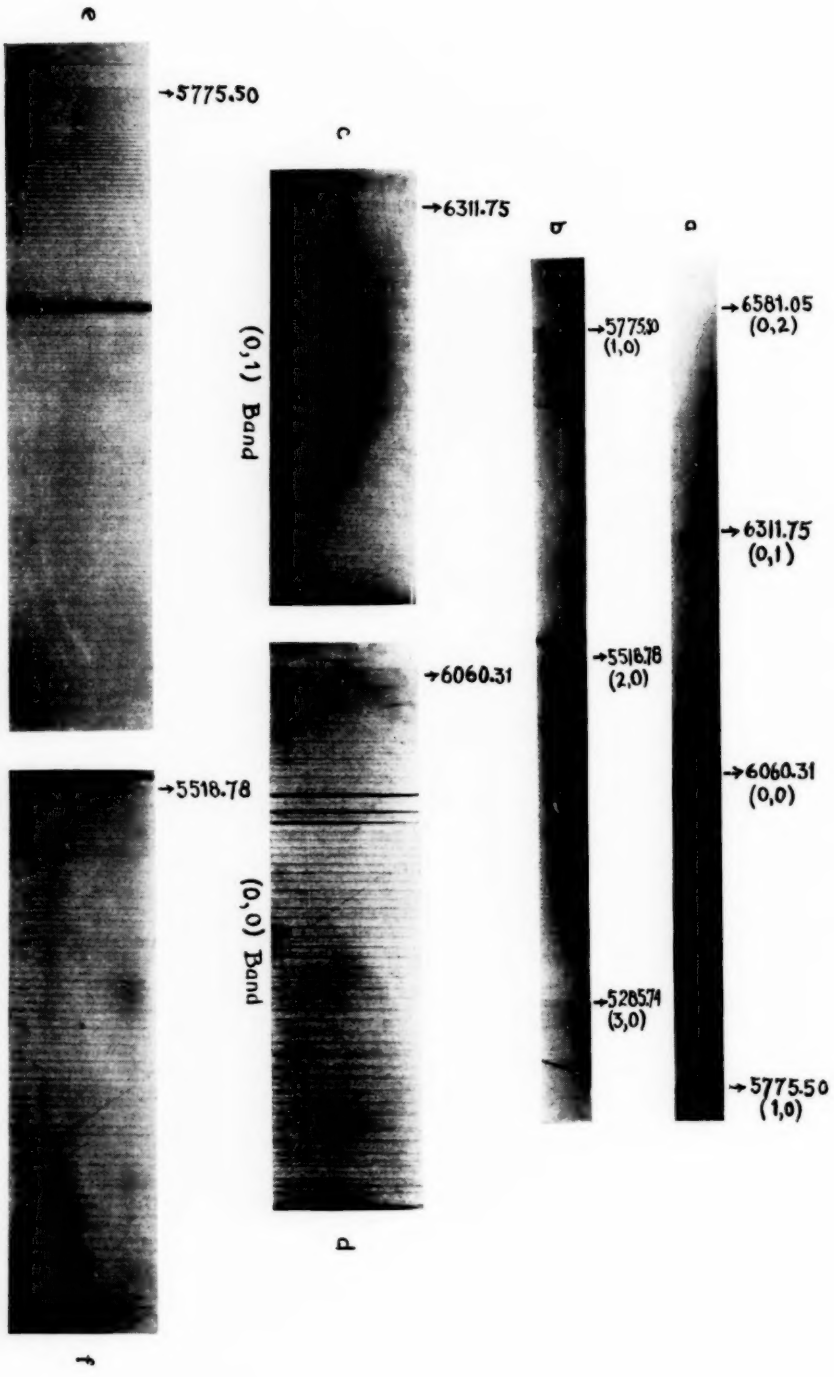

Fig. 1 Red bands of MgO: a, b, Hilger E. 52, glass spectrograph; c, d, e, f, 15 ft. grating first order.

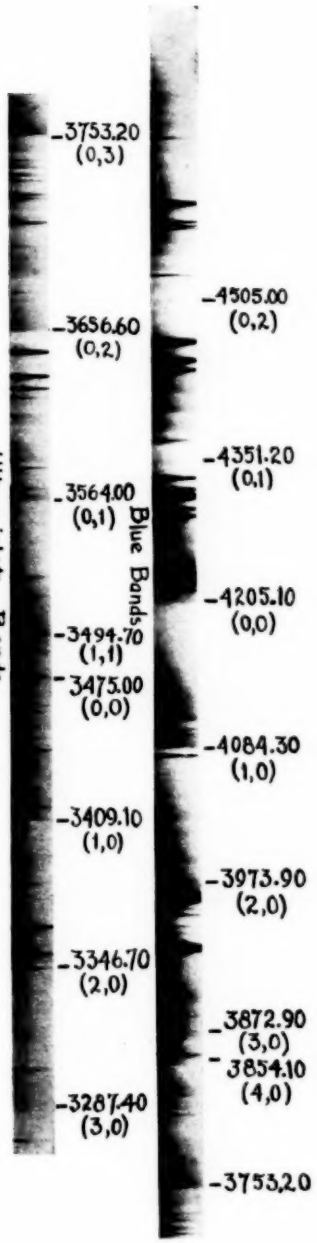

Fig. 2. Ultraviolet bands of CaO (Hilger E.1. quartz spectrograph).

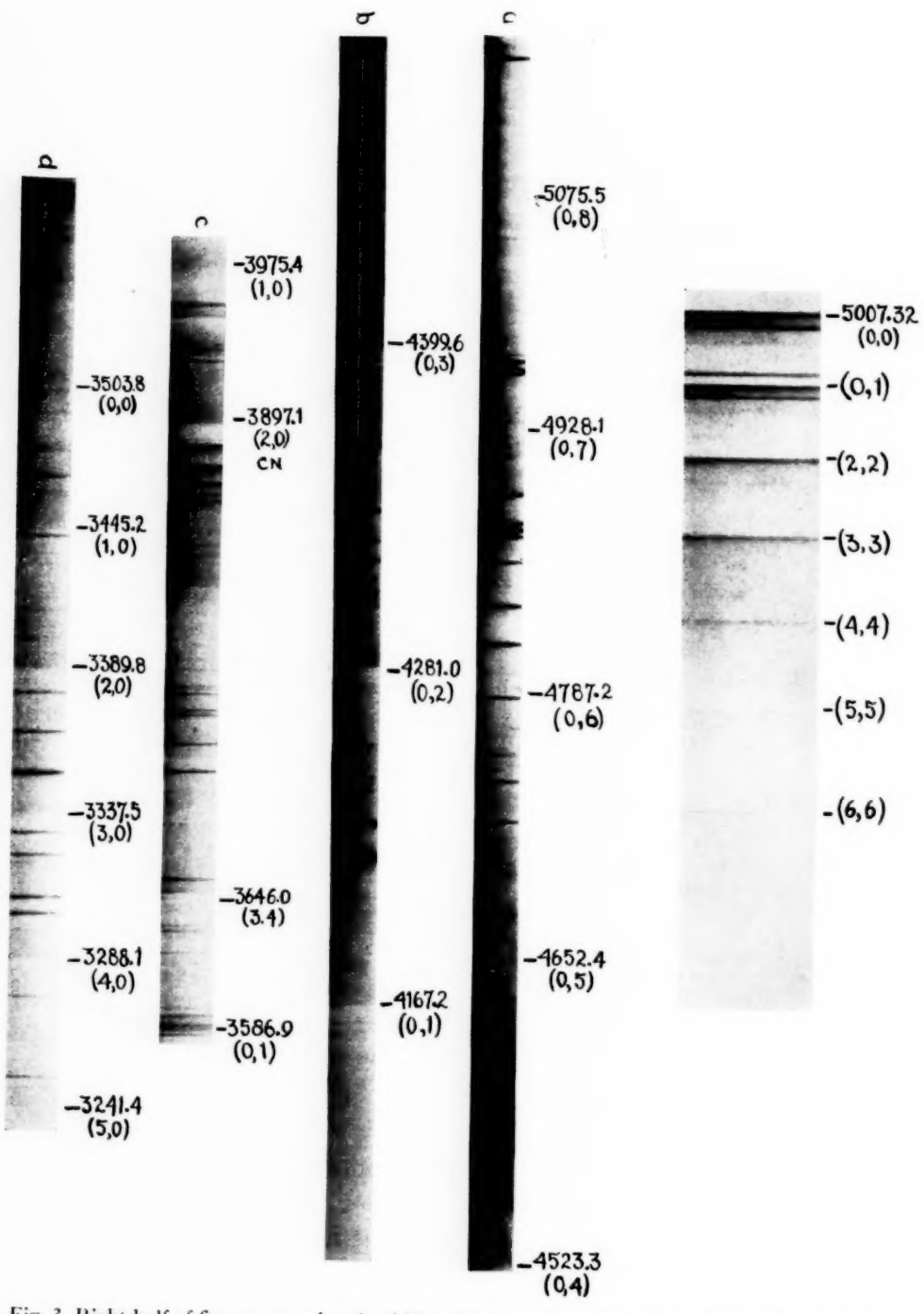

Fig 3. Right half of figure, green bands of MgO (15 ft. grating second order). Left half, bands of SrO; a, b, Hilger E. 52. glass spectrograph; c, d, Hilger E.1. quartz spectrograph.

bands the analysis has only been done from measurements on low dispersion spectrograms. New measurements of band heads as well as their vibrational assignments are given in Tables I and II.

TABLE I. *The red bands. New data and vibrational quantum analysis.*

v'	v''	$\lambda_{Hd.}$(I.A.)	I	ν (cm^{-1})	$O-C$ (cm^{-1})
0	3	6870.19	2	14,551.63	−0.35
1	4	6783.61	1	14,737.35	+1.97
2	5	6699.97	1	14,921.33	+1.83
3	6	6617.78	0	15,106.64	+2.29
0	2	6581.05	3	15,190.95	−0.29
4	7	6537.37	0	15,292.46	+2.56
1	3	6506.26	2	15,365.58	−0.25
2	4	6432.12	1	15,542.69	+1.57
3	5	6359.64	1	15,719.82	+2.68
0	1	6311.75	4	15,839.35	+0.01
4	6	6289.93	0	15,894.04	+0.16
1	2	6246.38	3	16,004.95	−0.14
5	7	6220.59	0	16,071.21	+0.12
2	3	6181.84	2	16,171.95	+0.38
3	4	6118.47	1	16,339.45	+0.69
0	0	6060.31	6	16,496.25	+0.00
1	1	6003.26	2	16,552.99	−0.20
2	2	5947.18	1	16,810.05	−0.78
1	0	5775.50	5	17,309.73	−0.37
2	1	5726.34	3	17,458.33	−0.60
3	2	5677.03	2	17,609.97	+1.50
4	3	5629.06	1	17,760.04	+1.30
2	0	5518.78	4	18,114.93	−0.91
3	1	5475.94	3	18,256.65	+0.08
4	2	5433.39	2	18,399.61	+1.61
5	3	5391.74	1	18,541.74	+1.57
6	4	5349.78	0	18,687.17	+4.12
3	0	5285.74	3	18,913.58	+0.10
4	1	5249.58	2	19,043.86	−2.24
5	2	5212.44	1	19,179.55	+0.12
4	0	5073.95	2	19,703.03	+0.02
5	1	5041.44	1	19,830.09	+2.56
10	7	5034.12	0	19,858.92	+2.00
6	2	5010.39	1	19,952.98	+0.22
10	6	4887.09	1	20,456.38	−4.52
11	7	4855.54	1	20,589.30	−0.43
6	1	4851.49	1	20,606.49	+5.63
7	2	4825.94	1	20,715.58	−2.40
12	8	4824.39	1	20,722.23	+2.94
8	3	4797.98	0	20,836.30	+0.46
13	9	4794.59	1	20,851.03	+1.47
9	4	4772.07	1	20,949.42	−4.98
14	10	4764.61	1	20,982.23	+1.68
10	5	4744.02	1	21,073.06	−0.63
15	11	4736.21	1	21,108.04	−4.22
11	6	4717.73	1	21,190.72	−2.99

The equations of the band heads in terms of half-quantum numbers for the two systems are as follows.
For the red system:

$$\nu = 16{,}418.06 + \{821.95(v' + \tfrac{1}{2}) - 4.05(v' + \tfrac{1}{2})^2\} - \{665.74(v'' + \tfrac{1}{2}) - 4.41(v'' + \tfrac{1}{2})^2\} \quad (1)$$

TABLE II. *The green bands. New data and vibrational quantum analysis.*

v'	v''	$\lambda_{Hd.}$(I.A.)	I	ν (cm^{-1})	$O-C$ (cm^{-1})
0	1	5205.96	4	19,203.42	+0.03
1	2	5191.98	4	19,255.13	+0.00
2	3	5177.37	3	19,309.46	+0.01
3	4	5162.50	3	19,365.50	−0.16
4	5	5146.85	3	19,423.96	−0.03
5	6	5130.58	2	19,485.56	+1.12
6	7	5113.75	1	19,549.69	+2.68
7	8	5097.04	1	19,613.74	+2.04
8	9	5081.45	0	19,673.95	−4.56
0	0	5007.32	10	19,965.21	0.00
1	1	4996.71	9	20,007.60	+0.02
2	2	4985.92	8	20,050.90	−1.17
3	3	4974.47	7	20,097.06	−1.62
4	4	4962.10	6	20,147.15	−0.26
5	5	4949.53	5	20,198.32	+0.06
6	6	4935.30	4	20,256.56	+5.53
7	7	4923.87	3	20,303.58	−2.74
8	8	4908.61	2	20,366.70	+3.17
9	9	4895.20	2	20,422.49	−0.37
10	10	4880.69	2	20,483.20	−1.11
11	11	4865.41	1	20,547.53	−0.35
12	12	4849.63	0	20,614.39	+0.82
13	13	4834.05	0	20,680.82	−0.56

and for the green system:

$$\nu = 19{,}944.82 + \{811.67(v' + \tfrac{1}{2}) - 3.74(v' + \tfrac{1}{2})^2\} - \{771.42(v'' + \tfrac{1}{2}) - 4.81(v'' + \tfrac{1}{2})^2\}. \quad (2)$$

The intensity distribution among the band heads of the red system follows a typical wide Condon[9] parabola as is usual for high temperature emission spectra. The bands associated with either $v'=0$ or $v''=0$ are developed strongly but those associated with $v'=0$ are more intense than those with $v''=0$. On the other hand, for the green system, the intensity distribution lies on a very narrow Condon parabola. The distribution of the bands in a $\Delta v=0$ sequence with only weaker $\Delta v=+1$ sequence is in theoretical accordance with the very small change in vibrational frequency as is indicated by Eq. (2), and with correspondingly small change in moment of inertia which it accompanies. In fact, in the extreme case, the small percentage change in moment of inertia is indicative of a very narrow Condon parabola in the v', v'' array of bands and only the $\Delta v=0$ sequence is to be expected. Probably for the green bands, the sequence $\Delta v=-1$ is present but the bands are too weak to be measured under the high magnification of the comparator.

It is evident from Eqs. (1) and (2) that while $\omega_e' > \omega_e''$, $\omega_e'\chi_e' < \omega_e''\chi_e''$. As a result of this, the successive heads in a sequence diverge with increasing quantum number. The heats of dissociation calculated for the lower levels of the two systems are, respectively, 3.06 and 3.76 volts.

CALCIUM OXIDE

In 1906 Olmsted,[10] during the course of his investigation of the spectra of the flame of the oxy-hydrogen blow-pipe fed with calcium salts, measured

[9] Condon, Phys. Rev. **28**, 1182 (1926).

[10] Olmsted, Zeits. f. Wiss. Photo. **4**, 255 (1906).

thirty-two heads between the region λ4400–λ3300 and attributed them to the metal. Later on Eder and Valenta[11] photographed the spectra of the flame of the arc as also of the oxy-coal gas with different salts of calcium introduced into it and published measurements of a number of band heads lying between λ6650–5300 and also between λ4600–λ3400. They, however, ascribed all these bands to the oxide. In 1914 Harnack[12] was led to the same view from a systematic investigation into the spectra of the flame arc in the atmosphere of oxygen and hydrogen as also of the flame formed by spraying finely powdered salts of calcium across an uncondensed spark. In the present investigation only the bands lying between λ4600–λ3200 have been definitely ascribed to the oxide while those between λ6750–λ5300 are probably emitted by the metal. They are very much superposed by the well-known CaCl bands lying in this region. Seventy-seven heads have been measured on prism spectrograms for the oxide bands and the wave-lengths are correct to ±0.1A. Their analysis is presented in Tables III and IV. In 1927, Mecke and Guillery[2] classified twenty-eight heads from the measurements of Olmsted into a single system but it now appears that they used parts of two different systems.

TABLE III. *The blue bands. New data and vibrational quantum analysis.*

v'	v''	$\lambda_{Hd.}$ (I.A.)	I	ν (cm^{-1})	$O-C$ (cm^{-1})
5	7	4597.0	0	21,747.24	−0.23
4	6	4573.9	0	21,857.07	+0.65
3	5	4553.4	1	21,955.48	+0.23
2	4	4535.1	2	22,044.07	+0.10
1	3	4519.1	3	22,122.12	−0.43
0	2	4505.0	4	22,191.35	+0.33
5	6	4449.9	2	22,466.13	−0.22
4	5	4425.8	3	22,588.46	−0.04
3	4	4403.9	6	22,700.79	+0.26
2	3	4384.3	6	22,802.27	−0.17
1	2	4366.7	5	22,894.18	−0.05
0	1	4351.2	5	22,975.73	−0.17
6	6	4336.7	0	23,052.55	−0.41
5	5	4309.5	1	23,198.04	−0.39
4	4	4284.6	1	23,332.86	−0.92
3	3	4261.8	2	23,457.68	−1.33
2	2	4240.8	3	23,573.84	−0.28
1	1	4221.9	5	23,679.37	+0.26
0	0	4205.1	6	23,773.97	−0.01
5	4	4175.4	1	23,943.08	−0.63
4	3	4149.8	2	24,090.77	−1.49
3	2	4126.0	3	24,229.74	−0.95
2	1	4104.1	4	24,359.03	+0.03
1	0	4084.3	5	24,477.11	−0.08
6	4	4075.5	0	24,529.96	−0.36
5	3	4047.3	1	24,700.88	−1.31
4	2	4020.9	1	24,863.05	−0.89
3	1	3996.5	2	25,014.85	−0.72
2	0	3973.9	3	25,157.11	+0.03
6	3	3953.4	0	25,287.55	−1.25
5	2	3924.6	1	25,473.12	−0.75
4	1	3897.8	1	25,648.26	−0.56
3	0	3872.9	2	25,813.15	−0.50

[11] Eder and Valenta, *Atlas typischer Spektren*, Wien (1924).
[12] Harnack, Phys. Zeits. **15**, 578 (1914).

TABLE IV. *The ultraviolet bands. New data and vibrational quantum analysis.*

v'	v''	$\lambda_{Hd.}$(I.A.)	I	ν (cm^{-1})	$O-C$ (cm^{-1})
2	7	4000.0	1	24,992.96	−0.79
1	6	3979.5	1	25,121.71	−0.44
0	5	3959.4	2	25,249.23	+0.53
4	8	3937.3	0	25,390.95	−1.80
3	7	3915.7	1	25,531.01	−0.93
2	6	3894.7	2	25,668.67	−0.62
1	5	3874.2	2	25,804.49	−0.31
5	8	3858.3	1	25,910.83	−2.18
0	4	3854.1	2	25,939.07	+0.60
4	7	3836.2	1	26,060.10	−1.06
3	6	3814.7	1	26,206.97	−0.49
2	5	3793.7	2	26,352.04	+0.11
1	4	3773.2	2	26,495.20	+0.64
5	7	3761.2	0	26,579.73	−1.68
0	3	3753.2	3	26,636.39	+1.04
4	6	3739.2	1	26,736.12	−0.56
3	5	3717.8	1	26,890.01	−0.10
2	4	3696.9	2	27,042.02	+0.32
1	3	3676.5	3	27,192.07	+0.62
5	6	3667.9	0	27,255.82	−1.12
0	2	3656.6	4	27,340.05	+0.69
4	5	3646.1	1	27,418.78	−0.55
3	4	3624.8	2	27,579.90	+0.02
2	3	3604.0	2	27,739.06	+0.47
1	2	3583.7	3	27,996.19	+0.73
0	1	3564.0	5	28,050.38	−0.11
4	4	3556.6	0	28,108.74	−0.36
3	3	3535.4	1	28,277.29	+0.52
2	2	3514.8	2	28,443.02	+0.42
1	1	3494.7	3	28,606.60	+0.01
0	0	3475.0	6	28,768.77	+0.03
4	3	3470.5	0	28,806.07	+0.08
3	2	3449.6	1	28,980.59	−0.19
2	1	3429.1	2	29,153.84	+0.11
1	0	3409.1	4	29,324.87	+0.03
4	2	3387.7	0	29,510.11	+0.11
3	1	3366.9	1	29,692.41	+0.50
2	0	3346.7	3	29,872.52	+0.53
5	2	3329.0	1	30,030.44	+0.18
4	1	3308.0	2	30,221.08	−0.05
3	0	3287.4	3	30,410.45	+0.29
6	2	3273.3	0	30,541.44	−0.12
5	1	3252.0	1	30,741.47	+0.08
4	0	3231.2	2	30,939.35	−0.03

The equations of the band heads in terms of half-quantum numbers for the two systems are as follows. Blue bands:

$$\nu = 23{,}817.62 + \{726.53(v' + \tfrac{1}{2}) - 11.66(v' + \tfrac{1}{2})^2\} - \{811.28(v'' + \tfrac{1}{2}) - 6.60(v'' + \tfrac{1}{2})^2\} \quad (3)$$

and ultraviolet bands:

$$\nu = 28{,}849.13 + \{565.06(v' + \tfrac{1}{2}) - 4.48(v' + \tfrac{1}{2})^2\} - \{725.37(v'' + \tfrac{1}{2}) - 3.56(v'' + \tfrac{1}{2})^2\}. \quad (4)$$

As in the case of MgO band systems, the bands of CaO forming a sequence diverge with increasing quantum number. This is evident from Eqs. (3) and (4) that while $\omega_e' < \omega_e''$, $\omega_e'\chi_e' > \omega_e''\chi_e''$.

The relative intensities of the bands in each system lie on a wide Condon parabola as in the case of the red bands of MgO.

The heats of dissociation calculated for the lower levels of the two systems are respectively 3.03 and 4.56 volts.

Strontium Oxide

The earliest spectroscopists[13] noticed a class of bands between λ7000–λ5800 in the flame and spark spectra of strontium salts and attributed them to the oxide. In 1905 Hagenbach and Konen,[14] in addition to these, measured another class of bands between λ4500–λ3600 and attributed them both to the metal as their emitter. Later on, Olmsted[15] pointed out that the bands lying below λ3800 were due to the oxide. He photographed the spectrum of the oxy-coal gas flame fed with different salts of strontium and published measurements of sixty-six heads between λ4800–λ3600 with a concave grating of one meter radius. Afterwards Hartley[16] noticed these bands in the spark spectrum of $Sr(NO_3)_2$ in solution as well as in that of oxy-hydrogen flame fed with $SrCl_2$ and ascribed a part of the spectrum to the oxide. The bands were also measured by Auerbach,[17] Eder and Valenta,[18] and by Harnack,[19] who extended the measurements up to λ3200. These authors ascribed all the bands to the oxide. Kayser[20] was, however, of opinion that the bands in the long wave-length region might be due to the metal. In the present investigation the bands lying between λ7100–λ5300 have been definitely attributed to the metal and those between λ5300–λ3200 to the oxide. In the latter region as many as 108 heads have been measured from prism spectrograms and analyzed into two systems (Tables V and VI). The analysis of Mecke and Guillery[2] is essentially correct for the blue system. It may here be pointed out that the metal bands in the long wave-length region are very much superposed by the well-known SrCl band systems as in the case of calcium.

Table V. *The blue bands. New data and vibrational quantum analysis.*

v'	v''	$\lambda_{Hd.}$ (I.A.)	I	ν (cm^{-1})	$O-C$ (cm^{-1})
3	12	5279.5	0	18,935.93	−0.57
2	11	5263.0	0	18,995.30	−0.10
1	10	5246.5	1	19,055.04	−0.30
0	9	5229.8	1	19,115.88	−0.44
4	12	5146.0	0	19,427.17	−0.42
3	11	5128.6	0	19,493.08	−0.41
2	10	5111.0	1	19,560.21	−0.22
1	9	5093.3	1	19,628.18	−0.23
0	8	5075.5	1	19,697.02	−0.41
5	12	5021.0	0	19,910.81	−0.87
4	11	5002.6	0	19,984.05	−0.53

[13] Kayser, Handbuch der Spectroscopie **6**, 544 (1912).
[14] Hagenbach and Konen, *Atlas der Emission Spectra*, Jena, bei Fischer (1905).
[15] Olmsted, Zeits. f. Wiss. Photo. **4**, 255 (1906).
[16] Hartley, Trans. Roy. Soc. Dublin **9**, (2), 85 (1908).
[17] Averbach, Zeits. f. Wiss. Photo. **7**, 30 (1909).
[18] Eder and Valenta, *Atlas Typischer Spektren*, Wien (1924).
[19] Harnack, Zeits. f. Wiss. Photo. **10**, 281 (1912).
[20] Kayser, Handbuch der Spectroscopie **6**, 551 (1912).

TABLE V. (*Continued*).

v'	v''	$\lambda_{Hd.}$(I.A.)	I	ν (cm^{-1})	$O-C$ (cm^{-1})
3	10	4983.9	0	20,059.03	+0.51
2	9	4965.6	0	20,132.95	−1.55
1	8	4946.9	1	20,209.06	−0.46
0	7	4928.1	1	20,286.15	−0.43
6	12	4903.5	0	20,387.92	+0.15
5	11	4884.3	0	20,468.06	−0.61
4	10	4864.8	0	20,550.11	+0.50
3	9	4845.5	1	20,631.96	+0.37
2	8	4826.1	1	20,714.89	+0.28
1	7	4806.7	1	20,798.50	−0.17
0	6	4787.2	2	20,883.22	−0.55
6	11	4773.1	0	20,944.91	−0.85
5	10	4752.8	0	21,034.36	+0.66
4	9	4732.9	1	21,122.81	+0.13
3	8	4712.8	2	21,212.89	+0.19
2	7	4692.7	5	21,303.75	−0.01
1	6	4672.6	4	21,395.39	−0.47
0	5	4652.4	3	21,488.28	−0.72
6	10	4647.4	0	21,511.40	+0.61
5	9	4626.9	1	21,606.71	−0.06
4	8	4606.2	2	21,703.81	+0.02
3	7	4585.5	3	21,801.78	−0.07
2	6	4564.8	5	21,900.65	−0.30
1	5	4544.1	5	22,000.41	−0.68
6	9	4526.9	1	22,084.00	+0.14
0	4	4523.3	4	22,101.58	−0.69
5	8	4505.7	1	22,187.91	+0.03
4	7	4484.5	3	22,292.80	−0.14
3	6	4463.3	4	22,398.68	−0.36
2	5	4442.1	3	22,505.58	−0.60
1	4	4420.9	5	22,613.50	−0.86
6	8	4410.9	0	22,664.77	−0.20
0	3	4399.6	6	22,722.98	−0.60
5	7	4389.2	1	22,776.72	−0.31
4	6	4367.6	2	22,889.46	−0.67
3	5	4345.9	3	23,003.75	−0.52
2	4	4324.3	3	23,118.65	−0.80
1	3	4302.7	4	23,234.71	−0.96
6	7	4299.2	0	23,253.62	−0.50
0	2	4281.0	5	23,352.48	−0.45
5	6	4277.2	0	23,373.23	−0.99
4	5	4255.1	1	23,494.62	+0.26
3	4	4233.2	2	23,616.16	−1.38
2	3	4211.2	3	23,739.54	−1.22
1	2	4189.1	4	23,864.77	−0.25
0	1	4167.2	5	23,990.19	−0.13
4	4	4147.0	1	24,107.04	−1.59
3	3	4124.7	2	24,237.37	−1.48
7	6	4110.6	0	24,320.51	+0.11
2	2	4102.3	2	24,369.72	−0.39
6	5	4087.9	0	24,455.56	+0.02
1	1	4080.1	2	24,502.31	−0.10
5	4	4065.4	0	24,590.91	−1.81
0	0	4058.0	3	24,635.75	0.00
4	3	4042.8	1	24,728.37	−1.57
3	2	4020.1	2	24,868.00	−0.20
7	5	4010.8	0	24,925.66	−0.97
2	1	3997.7	2	25,007.34	−0.16
6	4	3988.0	0	25,068.16	−0.65
1	0	3975.4	3	25,147.61	−0.23
5	3	3965.2	1	25,212.30	−0.73
4	2	3942.3	1	25,358.75	−0.54
3	1	3919.6	2	25,505.61	+0.02
7	4	3914.6	0	25,538.19	−1.71

TABLE V. (*Continued*).

v'	v''	$\lambda_{Hd.}$ (I.A.)	I	ν (cm^{-1})	$O-C$ (cm^{-1})
2	0	3897.1	3	25,652.86	−0.07
6	3	3891.6	0	25,689.12	−2.00
5	2	3868.5	0	25,842.51	−0.87
4	1	3845.6	1	25,996.40	−0.28
3	0	3822.4	2	26,150.76	−0.26
6	2	3798.4	0	26,319.43	−1.04
5	1	3775.3	0	26,480.47	−0.30
4	0	3752.4	1	26,642.07	−0.04

TABLE VI. *The ultraviolet bands. New data and vibrational quantum analysis.*

v'	v''	λ_{Hd} (I.A.)	I	ν (cm^{-1})	$O-C$ (cm^{-1})
2	4	3708.5	0	26,957.44	−0.72
1	3	3690.2	1	27,091.12	+0.79
0	2	3671.5	2	27,229.10	+0.28
3	4	3646.0	2	27,419.53	−0.63
2	3	3627.0	1	27,563.17	−1.10
1	2	3607.1	2	27,715.22	+0.53
0	1	3586.9	3	27,871.30	−0.14
3	3	3567.1	1	28,026.00	−0.27
2	2	3546.6	2	28,187.99	−0.64
1	1	3525.4	3	28,357.50	+0.19
0	0	3503.8	6	28,532.31	0.00
3	2	3489.3	1	28,650.87	−0.39
2	1	3467.5	2	28,830.99	−0.89
1	0	3445.2	4	29,017.61	−1.20
4	2	3435.3	1	29,101.23	−0.10
3	1	3412.8	2	29,293.08	−0.85
2	0	3389.8	4	29,491.83	−0.92
4	1	3361.2	1	29,742.76	−0.56
3	0	3337.5	3	29,953.96	−0.16
5	1	3312.4	0	30,180.93	−0.52
4	0	3288.1	2	30,403.97	−0.22
5	0	3241.4	1	30,842.00	−0.32

Besides the bands included in the two systems, there are a few unidentified heads. These were also measured by Olmsted and others, strongest of these are λ4135.0 (4), 4113.6 (5) and 4092.6 (4).

The equations representing the band heads of the two systems are as follows.

For the blue bands:

$$\nu = 24{,}702.81 + \{519.09(v' + \tfrac{1}{2}) - 3.50(v' + \tfrac{1}{2})^2\} - \{653.47(v'' + \tfrac{1}{2}) - 4.02(v'' + \tfrac{1}{2})^2\} \quad (5)$$

and for the ultraviolet bands:

$$\nu = 28{,}622.18 + \{497.81(v' + \tfrac{1}{2}) - 5.97(v'' + \tfrac{1}{2})^2\} - \{679.13(v'' + \tfrac{1}{2}) - 9.13(v'' + \tfrac{1}{2})^2\}. \quad (6)$$

Unlike the band systems of MgO and CaO, the bands of SrO in a sequence converge with increasing quantum number as is to be expected from the coefficients of ω_e', $\omega_e'\chi_e'$, ω_e'' and $\omega_e''\chi_e''$ in Eqs. (5) and (6). On the other hand, the distribution of intensity among the various heads of the two band systems is very much similar to that of CaO. The heats of dissociation calculated for the lower levels of the two systems are, respectively, 3.24 and 1.52 volts.

My best thanks are due to Professor P. N. Ghosh for offering me all the facilities to carry out this investigation.

The Infrared Absorption Spectrum and the Molecular Structure of Ozone

By SHERMAN L. GERHARD
University of Michigan

(Received October 13, 1932)

Of the seven known infrared absorption bands of ozone, four (4.7μ, 7.39μ, 9.6μ, and 11.38μ) have been investigated for the first time with a grating spectrometer. The band at 4.7μ shows three branches, not very sharply defined, while the one at 7.39μ shows only a single peak. The strongest band, at 9.6μ, has been resolved into two main branches which probably belong to two different vibrations. The band at 11.38μ has been tentatively ascribed to nitrogen pentoxide, which often occurs as an impurity in ozone. Three fundamental vibrational frequencies, *viz.*, 528 cm^{-1}, 1033 cm^{-1}, and 1355 cm^{-1}, have been selected from the observational data. The rotational fine structure could not be completely resolved; it appears to have the irregularity characteristic of an asymmetrical rotator. The envelopes of the four observed bands have been completely mapped out. The infrared absorption spectrum of ozone is discussed and it is shown that the molecule cannot have the form of a straight line nor an equilateral triangle but it is probably represented by an isosceles triangle where the angle at the apex is less than 60°. By making use of these assumptions it was possible to order the observed frequencies in a fashion consistent with their envelopes. This general shape of isosceles triangle is the only one allowed by the observational data; the other shape of isosceles triangle, with apex angle greater than 60°, is ruled out.

DURING the past ten years ozone has attracted considerable interest and many attempts have been made to determine its structure. It is one of the few triatomic molecules whose infrared absorption spectrum has not heretofore been investigated with the high dispersion of a grating spectrometer. It is true that very many data have been collected on its absorption bands in the photographic region of the spectrum, but from these it has not been possible as yet to give a satisfactory description of its molecular structure.

John Tyndall[1] in 1872 discovered that ozone absorbs infrared radiation and, in 1904, K. Angstrom[2] first measured its infrared absorption spectrum. With low concentrations of ozone he found bands at 4.8μ, 5.8μ, 6.7μ and 9.6μ.

A more thorough investigation of the ozone absorption in this region was carried out by E. Ladenburg and E. Lehmann[3] in 1906. By using a more efficient method of preparation they were able to observe it in higher concentrations and consequently found some weaker bands which Angstrom had missed. They found bands at 1.1μ, 3.7μ, 4.8μ, 5.9μ, 6.6μ, 7.6μ, 9.9μ and 11.35μ. Of these, the one at 5.9μ was later shown by E. Warburg and G. Leithauser[4] to be due to nitrogen pentoxide.

[1] John Tyndall, *Contributions to Physics in the Domain of Radiant Heat*, London (1872).
[2] K. Angstrom, Arch. f. Mat., Astron., och Physik **1**, 347, 395 (1904).
[3] E. Ladenburg and E. Lehmann, Ann. d. Physik **21**, 305 (1906).
[4] E. Warburg and G. Leithauser, Ann. d. Physik **23**, 209 (1907). See also another paper by these same two investigators, Ann. d. Physik **28**, 313 (1909).

Quite recently A. Jakowlewa and V. Kondratjew[5] made measurements on some of the ultraviolet electronic bands of ozone. They concluded from the results of their own measurements and those of others that ozone is a linear molecule, but this is not in agreement with our conclusions, as will be shown later.

Experimental

The classical and most common method of preparing ozone is one using a Siemens' ozonizer, in which a silent electric discharge is passed through air or oxygen. This gives only a low yield; the exit gases contain at best only about 10 percent of ozone.

A more efficient method of preparing ozone, described by A. K. Brewer and J. W. Westhaver[6] was used in the present investigation. In this method a glow discharge is maintained in oxygen while the discharge tube is immersed in liquid air. Under these conditions liquid ozone condenses out on the walls of the discharge tube. Practically pure ozone gas may be obtained by distilling the liquid ozone thus formed. This last procedure, the distillation of the liquid ozone, was a hazardous one in spite of the fact that all organic matter was excluded from the entire system. On four different occasions the discharge tube exploded violently during the course of the distillation.

The absorption cells were glass tubes 4.5 cm in internal diameter and 25 cm and 1 m in length, respectively. Rocksalt windows were fastened on the ends by means of a thin, quick-drying lacquer. This method of fastening the windows had the advantage of enabling one to remove them when necessary by merely soaking in acetone or wood alcohol, thus avoiding the application of heat. The ozone was kept in the cells at atmospheric pressure by means of traps filled with phosphoric acid.

The spectrometer was of the usual type employing a rocksalt prism as a monochromator for the radiation falling on the grating. The thermocouples were very kindly supplied by Dr. J. D. Hardy. They were of the Pfund design and were connected to the familiar type of Moll relay, where the deflections of the first galvanometer were amplified. The aperture throughout the spectrometer was f5. A 25 cm parabolic mirror of 120 cm focal length was used in front of the grating. The slit widths used for each band are indicated in Fig. 1. With 0.88 ampere passing through the Nernst glower, which was used as a source, and the lamp in the Moll relay operating at 2.83 volts a deflection of about 70 mm was obtained at 9.6μ through the empty cell, and with a slit width of 0.3 cm^{-1}. Two gratings were used, with 1440 and 1200 lines per inch, respectively. The calibrations were obtained from charts previously prepared for them by means of standard infrared lines.

On account of the difficulty and hazard involved in handling highly concentrated ozone no attempt was made to perform a quantitative analysis of the contents of the absorption cell. It was, however, possible to make a

[5] A. Jakowlewa and V. Kondratjew, Phys. Zeits. d. Sowjetunion **1**, 471 (1932).
[6] A. K. Brewer and J. W. Westhaver, J. Phys. Chem. **34**, 1280 (1930).

rough estimate of the amount of ozone in the cell from considerations of the general behavior of the preparation.

The results of the investigation are shown in Fig. 1 as a group of curves giving the envelopes of the four different absorption bands studied. Most of the envelopes shows persistent irregularities, which indicate that the resolving power of the spectrometer was almost great enough to reveal the fine structure. It seems probable not only that the fine structure lines observed are real but also that they are distributed in the irregular manner which is characteristic of the asymmetrical rotator. This point will be discussed later.

The 9.6μ band was investigated with both the meter cell and the 25 cm cell. Curve I was taken with practically pure ozone gas at atmospheric pres-

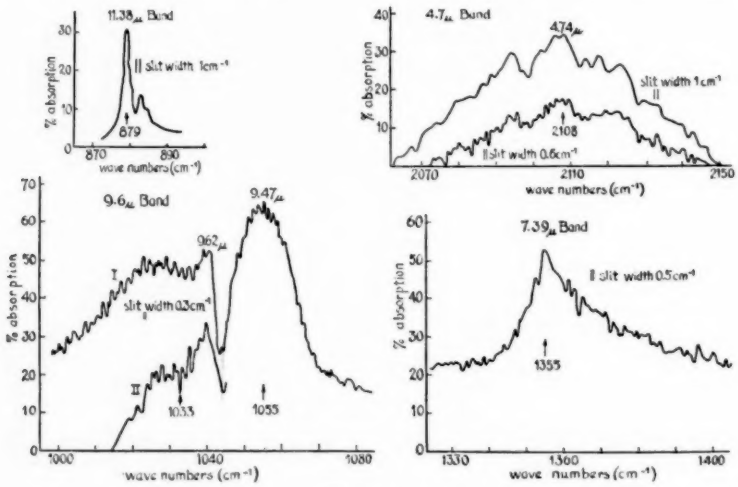

Fig. 1.

sure in the shorter cell, and curve II with a very low concentration in the meter cell. This band has apparently three branches. The one on the high-frequency side of the center (9.62μ) is the strongest, and the one on the low-frequency is the weakest of the three. The low-frequency branch becomes weaker than the other two at low concentration. The high-frequency branch was not studied in detail at low concentrations but a few readings taken at 9.47μ at the same time curve II was taken showed an absorption of about 48 percent, showing that this branch remained the strongest of the three. This behavior indicates that the high-frequency branch may be associated with one fundamental frequency, and the rest of the band with another.

The 7.39μ band lies in a region where the absorption due to water vapor is very noticeable. It also was observed with the same high concentration of ozone in the 25 cm cell that was used in obtaining curve I for the 9.6μ band. The curve shown for this 7.39μ band represents the average of two separate and consistent sets of data taken under the same conditions. The high background on each side of the strong single branch might be fictitious on account of the uncertainty in calculating the percentage absorption in a region where

water vapor absorbs as strongly as it does here. However, it is stronger than the 4.7μ band, which could not be detected under the same conditions.

The bands at 9.6μ and at 7.39μ are the two strongest ones; the others were looked for but could not be detected with the same concentration of ozone in the 25 cm cell.

The two curves shown for the 4.7μ band were obtained with two slightly different ozone concentrations in the meter cell, and also with different slit widths, as indicated in Fig. 1.

The small single peak of absorption at 11.38μ was observable only with very high concentrations of ozone in the meter cell. The curve shown for it was obtained with a higher concentration of ozone in the meter cell than was used to obtain the 4.7μ band, in fact it was not observable under the conditions which yielded the curves for the 4.7μ band.

In the first two columns of Table I is a summary of the wave-lengths and relative intensities of the absorption maxima of ozone obtained in this in-

TABLE I.

		Ladenburg and Lehmann	
Wave-lengths	Relative intensities	Wave-lengths	Relative intensities
—	—	1.1μ	1
—	—	3.7	2
4.74μ	5	4.7	5
—	—	6.6	2
7.39	7	7.7	3
9.47	10		
9.62	8	9.9	10
11.38	2	11.3	3

vestigation. In the last two columns are given the values reported by Ladenburg and Lehmann,[3] it is seen that there is very satisfactory agreement between these two sets of results, considering the fact that Ladenburg and Lehmann used a prism spectrometer.

The weak band at 11.38μ does not fit with the other observed bands into any scheme of frequencies. It may possibly be due to nitrogen pentoxide, which has a very strong band at 5.75μ, for the band at 5.75μ may be the first overtone of a fundamental at 11.38μ.

Several attempts were made to find the Raman spectrum of liquid ozone, using pure ozone as well as solutions of ozone in liquid oxygen. The details of these attempts have already been published.[7] The extreme faintness of the doublet observed, corresponding to a mean frequency shift of 1280 cm^{-1} (7.81μ), and the fact that this frequency does not fit in with the infrared frequencies makes it doubtful whether it is real.

THEORETICAL

§1

The data obtained in this investigation of the infrared absorption bands of ozone are not as complete as might be desired. In the first place its insta-

[7] G. B. B. M. Sutherland and S. L. Gerhard, Nature **130**, 241 (1932).

bility caused several explosions and made the gathering of data expensive and difficult, and in the second place the rotational fine structure is so closely spaced that it was not possible to resolve it. It is therefore necessary in the interpretation of the data to approach the subject from a rather general point of view and this requires the discussion of all the possible models for its structure. It will be shown that the data are consistent with only one model, and that furthermore this model has certain other properties similar to the known properties of ozone.

The frequencies observed for ozone have been satisfactorily correlated in the following way. The single band at 1355 cm^{-1} is taken as the first fundamental frequency, ν_1, then the band at 2710 cm^{-1}, reported by Ladenburg and Lehmann, is its first harmonic, $2\nu_1$. The strong band at 1055 cm^{-1} is assigned to the first overtone of a fundamental ν_2, at 528 cm^{-1}, which could not be observed because of the high absorption of the rocksalt windows in this region. The minimum at 1033 cm^{-1} is taken as the center of a doublet type band representing the third fundamental frequency, ν_3. The 2108 cm^{-1} band may be called $2\nu_3$; it is apparently multiple and contains other combinations as well. The weak band reported by Ladenburg and Lehmann at 1515 cm^{-1} may very well be the combination $\nu_2+\nu_3$. Except for the 11.38μ band, which is ascribed to nitrogen pentoxide, all the known bands of ozone are thus accounted for. There are three fundamental frequencies represented. The fundamental of two of them and the first harmonics of all three have been observed, as well as several combinations.

These bands display different kinds of envelopes. The fundamental, ν_1 at 1355 cm^{-1}, has certainly a zero branch type of envelope, with the zero branch very strong in comparison with the positive and negative branches. The $2\nu_2$ band, at 1055 cm^{-1}, has also a zero branch type of envelope, while that for ν_3, at 1033 cm^{-1}, is of the doublet type. The envelope for $2\nu_3$, at 2108 cm^{-1}, is apparently of the zero branch type. Unfortunately the envelopes of the remaining bands of ozone have not been observed, however, it will be possible to gather from the data in hand sufficient information to decide on the shape of the molecule.

For a triatomic molecule, such as ozone, there are three plausible shapes, *viz.*, linear, equilateral triangle and isosceles triangle. The three atoms of oxygen making up the ozone molecule need not all be alike; the force fields and electron configurations may not be the same for all the atoms. The possibilities of these three types of structure will now be discussed in connection with the data obtained and with the aid of the results of the wave mechanical analysis of infrared spectra given in a recent paper by D. M. Dennison.[8]

§2

There are two possible linear models for ozone, a symmetrical one, with the three atoms symmetrically arranged along a line, as is the case in carbon

[8] D. M. Dennison, Rev. Mod. Phys. **3**, 280 (1931).

dioxide, and an unsymmetrical one. The symmetrical type of linear molecule would display absorption bands resembling those of carbon dioxide. It would have similar vibrational properties and would obey the same selection rules, namely, that combinations or overtone frequencies which are the sum of any two observed frequencies cannot occur.[8] These conditions are not met by the frequencies observed for ozone, *viz.*, the band at 2108 cm^{-1} has twice the frequency of the 1033 cm^{-1} band, and the one reported at 2710 cm^{-1} has twice the frequency of the 1355 cm^{-1} band. With 528 cm^{-1} as a fundamental the band reported at 1515 cm^{-1} is assigned to the combination 1033 +528. The occurrence of these overtones and combinations is definitely in disagreement with the requirements for a linear symmetrical model and is sufficient to rule it out as a possible structure for ozone.

The other possible linear model would resemble the molecule of nitrous oxide, NNO. The selection rules for this model allow three active fundamental frequencies and all possible combinations and overtones. The vibration-rotation bands consist of fine structure lines regularly spaced in frequency.[9] There are two types of bands, both having essentially similar positive and negative branches, the one having a strong zero branch and the other none. When the ozone bands are examined it is found that none of them have regularly spaced fine structure lines. The positive and negative branches of the several bands do not stand out distinctly as they do in the case of nitrous oxide. There is no similarity between even the general outlines of the envelopes of any two bands. If ozone were this unsymmetrical linear type of molecule, then the positive and negative branches of the 1033 cm^{-1} and 1355 cm^{-1} (fundamental) bands should be similar and should have almost equal doublet spacings, but this is obviously not the case. These fundamental differences between the observed bands of ozone and those to be expected from linear molecules make it evident that the ozone molecule cannot be a linear one.

§3

In the isosceles triangle model for ozone the oxygen atom at the apex is taken to be different from the two at the base. The general solution of the vibrational problem has already been given by several investigators.[10,11] Three fundamental frequencies are to be expected for the general isosceles triangle. According to the conventions adopted in labelling these frequencies the electric moment vibrates along the Y axis (i.e., the bisector of the apex angle) for the frequencies ν_1 and ν_2, where $\nu_1 \geqq \nu_2$, and along the X axis (which is perpendicular to the Y axis) for the frequency ν_3.

In specializing to the equilateral triangle all three atoms become identical. In this case the frequency ν_1 is certainly inactive, since it corresponds to a motion in which all the atoms vibrate along the bisectors of their respective (apex) angles with the same amplitude and in the same phase with respect

[9] E. K. Plyler and E. F. Barker, Phys. Rev. **38**, 1827 (1931).
[10] N. Bjerrum, Verh. d. Deut. Phys. Ges. **16**, 640, 737 (1914).
[11] D. M. Dennison, Phil. Mag. **1**, 195 (1926).

to the center of gravity of the molecule. The two frequencies ν_2 and ν_3 become equal, thus forming degenerate states. Whether or not the frequency ν_2 would also be inactive depends upon the interaction of the electron clouds surrounding the three nuclei when they execute this normal vibration. It is conceivable that at one extreme displacement in this vibration the electrons surrounding the two lower nulcei could so repel those surrounding the upper nucleus that the center of the negative charges would lie above the center of the positive charges, thus producing a change in the electric moment of the molecule. Even if it were active it is very likely that it would be comparatively weak because of the relatively small amplitude of the oscillating electric doublet.

If ozone were this type of molecule it should be possible to correlate all the observed bands with only two fundamental frequencies, and one of these should be inactive. On the contrary the bands observed for ozone cannot be arranged in any scheme with only two fundamental frequencies unless very low frequencies are chosen and the observed bands ascribed to combinations and high multiples of them. This sort of procedure is evidently unreasonable in view of the simple relations existing between the frequencies observed for substances heretofore investigated. It takes three fundamental frequencies to account for all the ozone bands, and these three all appear to be active. This is very strong evidence against the equilateral triangle as the correct model for ozone.

Another source of evidence which is equally important is the almost complete absence of the Raman spectrum of ozone. Up to the present it has been observed that molecules possessing a highly symmetrical configuration, which results in an inactive vibrational frequency, have fairly strong Raman spectra, as in the cases of carbon dioxide and carbon tetrachloride. On the other hand it has also been found true that molecules lacking an inactive frequency, such as water, have a weak Raman spectrum.[12]

§4

The solution of the vibration problem for the isosceles triangle model has already been described. There are three different and active fundamental frequencies. The question of the overtones of these frequencies has been discussed by Dennison,[8] who showed that in general they would all be active. If the overtone is represented by $\nu = n_1\nu_1 + n_2\nu_2 + n_3\nu_3$ the change of the electric moment is along the Y axis for even values of n_3 and along the X axis for odd values.

The shapes of the envelopes of the bands at these various vibrational frequencies will depend upon the direction of the change of the electric moment with respect to the principal axes of inertia. If in the case of ozone the apex angle is less than 60°, then the axis of least moment of inertia, A, will be along the Y axis, and the axis of middle moment of inertia, B, will be along the X axis.

[12] These results have recently been justified and explained on a theoretical basis by Placzek, Zeits. f. Physik **70**, 84 (1931).

The axis of greatest moment of inertia, C, is perpendicular to the plane of the figure. No changes of electric moment can ever lie along this axis because no vibrations can take place outside the plane of the triangle. Thus in the general overtone $n_1\nu_1+n_2\nu_2+n_3\nu_3$ the change of electric moment will lie along the A axis for even values of n_3 and along the B axis for odd values.

On the other hand, if the apex angle in the case of ozone were greater than 60° the inertial axes A and B would be interchanged, and then in the general overtone the change of electric moment would be along the B axis for even values of n_3 and along the A axis for odd values.

According to Dennison[8] the envelopes of the bands produced by vibrations of the electric moment along the least axis of inertia should show a decided zero branch, while those produced by vibrations along the middle axis of inertia should show a doublet structure.

Whatever the disposition of the axes of inertia may be in the molecule the two frequencies ν_1 and ν_2 will have the same kind of envelopes, and ν_3 will have a different kind. If only one fundamental frequency displays the doublet type of envelope, then the apex angle is less than 60°, whereas if only one of the fundamental frequencies displays a zero branch, then the apex angle is greater than 60°.

When the envelopes of the ozone bands are examined it becomes evident that they can be very nicely arranged to fit the requirements for an isosceles triangle with the apex angle less than 60°. In Table II is given a comparison

TABLE II.

Wave-lengths	ν_i	Frequencies observed	Calculated	Type of envelope Observed	Predicted
(18.9μ)*	ν_2	—	528 cm^{-1}	—	Z
9.67	ν_3	1033 cm^{-1}	—	D	D
9.47	$2\nu_2$	1055	—	Z	Z
7.39	ν_1	1355	—	Z	Z
6.6†	$\nu_2+\nu_3$	1515	1561	—	D
	$3\nu_2$		1584		Z
	$2\nu_3$		2066		Z
4.7	$2\nu_2+\nu_3$	2108	2088	Z	D
	$4\nu_2$		2110		Z
3.7†	$2\nu_1$	2710	2710	—	Z

* This band was not looked for, because it is in a region where the absorption due to the rocksalt windows on the cell made observations impossible.

† Reported by Ladenburg and Lehmann. The wave-lengths are not known as accurately as those of the other bands and nothing is known about the envelopes.

of the observed envelopes and those predicated for ozone on the basis of the isosceles triangle model. In the last two columns D stands for doublet type and Z for zero branch type of envelope.

The fundamental ν_1 displays a zero branch type of envelope, with very weak positive and negative branches; the same holds true for $2\nu_2$. The envelope for ν_3 is of the doublet type, while that for $2\nu_3$ is of the zero branch type, as it should be for even values of n_3 if the apex angle is less than 60°. The observed envelope for the combination $2\nu_2+\nu_3$ is somewhat obscured by the envelopes of the overtone bands in its immediate vicinity, but the shape

of the whole envelope does not rule out the possibility of a doublet type envelope for this particular combination frequency.

The types of the envelopes of the bands observed show that ozone has the shape of an isosceles triangle with the apex angle less than 60°. This is proven by the occurrence of the zero branch type of envelope for ν_1 and $2\nu_2$. If the molecule were to be represented by an isosceles triangle with an apex angle greater than 60°, then ν_1 and $2\nu_2$ would have the doublet type of envelope and ν_3 would have the zero branch type of envelope. The preponderance of zero branch type over doublet type envelopes in the bands observed for ozone indicates that it has the shape of an isosceles triangle with the apex angle less than 60°. Except for the unknown envelopes of other combinations and overtones the observed data for ozone agree very well with the predictions for this model. The ordering of the ozone data under this scheme may not be unique, but it is a self-consistent one. Other ways of allotting the observed frequencies are possible, but they must all fulfill the requirements of the types of envelopes for the various frequencies.[13]

Conclusions

The experimental data for ozone have been critically compared with the theoretical predictions for various possible models and also with the data for certain molecules of known structure.

The combination and overtone frequencies observed in the ozone spectrum do not obey the selection rules for a linear symmetrical molecule. The envelopes of the bands and the lack of regularly spaced rotational fine structure lines are not in agreement with those to be expected of a linear unsymmetrical molecule. The equilateral triangle is very definitely ruled out because the frequencies observed for ozone do not obey the requirements that for an equilateral triangle there should be only one active fundamental frequency, and only two fundamental frequencies in all. In addition to this, ozone displays a very weak Raman spectrum, while a highly symmetrical molecule in the form of an equilateral triangle should certainly have a strong Raman spectrum.

The data for ozone do meet the requirements for the isosceles triangle model. There is the correct number of active fundamental frequencies, *viz.*, ν_1 at 1355 cm^{-1}, ν_2 at 528 cm^{-1}, and ν_3 at 1033 cm^{-1}. Overtones and combinations of these fundamental frequencies are also observed. Each fundamental shows its first overtone, and ν_2 apparently displays its second and third overtones. The assignments given the fundamental frequencies thus form a self-consistent scheme, and the calculated frequencies are in fairly good agreement with the observed frequencies. The types of envelopes, zero branch or doublet type, predicted for the fundamental frequencies and the various combinations and overtones appear in the observed bands for the proper fre-

[13] The case of the oblique triangle has not been discussed since it appears to be so improbable on general grounds. Such a model would, however, have much the same vibrational and rotational properties as an isosceles triangle, except that the direction of change of electric moment would no longer be so simply related to the orientation of the principal axes of inertia.

quencies. On the whole, the observed data for ozone fulfill the requirements for an isosceles triangle with the apex angle less than 60°.

The writer gratefully acknowledges Professor D. M. Dennison's many helpful suggestions in the interpretation of the experimental data, and the generous cooperation of the various members of the Physics Department who made possible the completion of this work.

The Dispersion and Absorption of Helium

By J. P. VINTI
Massachusetts Institute of Technology

(Received September 29, 1932)

An investigation is made of the relative importance of singly-excited, doubly-excited, and continuous states in the dispersion and absorption spectrum of helium. The f-values of the lines due to singly-excited and doubly-excited states are calculated by using wave functions of a screening-constant type, the most important of them having been obtained by variational methods. The f-sum of the continuous spectrum is then obtained by difference, from the Kuhn-Reiche sum rule. It is shown that the role of the singly-excited states is moderate, of the doubly-excited states small, and of the continuous spectrum very large. A table is given of relative intensities in the principal series absorption spectrum. Incidentally, a variational calculation of a wave function for the doubly-excited state $(2s)(2p)^1P$ places this level 302,000 cm^{-1} above the limit of single ionization. The corresponding absorption line comes out about one-thirtieth as strong as the first absorption line of the principal series or about as strong as the fifth line of this series.

IT IS our purpose to investigate the relative importance of the discrete and continuous energy states of atomic helium in dispersion and absorption.

The refractive index of a gas is given by $\mu^2=1+4\pi L\alpha$, where μ is the refractive index, L the number of atoms per unit volume, and α the polarizability of the atom. The polarizability of an N-electron atom is given by an expression of the form:

$$\alpha = \frac{2}{3}\frac{e^2}{h}\sum_{k\neq 0}\frac{\nu_{k0}(|x_{0k}|^2+|y_{0k}|^2+|z_{0k}|^2)}{\nu_{k0}^2-\nu^2}.$$

Here e and h have their usual meanings, ν_{k0} is the frequency difference between the excited state k and the normal state 0, ν is the frequency of the incident radiation, and ez_{0k}, e.g., is the matrix element between the states 0 and k of the z-component of electric moment, so that:

$$z_{0k}=\int\bar{\psi}_0\Big(\sum_{\mu=1}^{N}z_\mu\Big)\psi_k d\tau_1\cdots d\tau_N,$$

where ψ_0 and ψ_k are the wave functions of the state 0 and k. The summation is to be extended over all the excited states of the atom, continuous included, which have dipole combinations with the normal state.

We can most easily investigate the role of the various parts of the energy spectrum by writing the above formula for α in atomic units, expressing lengths in terms of a_0 (Bohr radius) as unit, and energies in terms of $e^2/(2a_0)$:

$$\alpha = 4a_0^3\sum_{k\neq 0}\frac{(\frac{1}{3})(W_k-W_0)(|x_{0k}|^2+|y_{0k}|^2+|z_{0k}|^2)}{(W_k-W_0)^2-W_\nu^2}.$$

Here W_ν is the energy in atomic units of a quantum of the incident radiation. If the applied frequency ν is not too large (not greater than that correspond-

ing to 600A), we have $W_r \leqq 1.5$. For any state beyond the limit of single ionization (i.e., any doubly-excited or continuous state), $W_k \geqq -4$. Then, since $W_0 = -5.81$, we have $W_k - W_0 \geqq 1.81$, and $(W_k - W_0)^2 - W_r^2 \geqq 1$. Thus the numerator for such a state gives an upper limit to its contribution to the dispersion formula; this numerator is called an f-value. The sum of the f-values of all the doubly-excited and continuous states thus gives an upper limit to their dispersion contribution.

The only singly-excited states which have dipole combinations with the normal state are the "principal series" $(1s)\ (np)^1P$. One can show that their f-sum gives a lower limit to their dispersion contribution, since for most of them (the lower and thus more important ones) the denominator is less than unity.

These f-values satisfy a simple sum rule by means of which we can estimate the role of the continuous spectrum without handling any continuous spectrum wave functions. Using atomic units, let

$$z = \sum_{\mu=1}^{N} z_\mu, \quad z_{0k} = \int \bar{\psi}_0 z \psi_k d\tau_1 \cdots d\tau_N, \text{ etc.},$$

and

$$f_{k0} = (\tfrac{1}{3})(W_k - W_0)(|x_{0k}|^2 + |y_{0k}|^2 + |z_{0k}|^2).$$

Then

$$\sum_k f_{k0} = N.$$

For atomic helium, $N = 2$, so that

$$\sum_k f_{k0} = 2. \tag{1}$$

(The summation sign is used for all the states, but is understood to include an integral over the continuous spectrum.) We obtain the form pertinent to our problem by splitting the sum into the parts: f', referring to the states $(1s)\ (np)^1P$; f'', referring to doubly excited states arising from the configurations sp, pd, df, etc.;[1] and f_c, referring to the mixed and purely continuous states lumped together.
Then

$$f' + f'' + f_c = 2. \tag{2}$$

We proceed to calculate f'. Now

$$z_{n0} = \int \bar{\psi}_n (r_1 \cos\theta_1 + r_2 \cos\theta_2) \psi_0 d\tau_1 d\tau_2,$$

where ψ_0 refers to the normal state, ψ_n to the state $(1s)\ (np)^1P$, and the in-

[1] By the Laporte rule no other configurations have dipole combinations with the normal state.

tegration is extended over the coordinates of both electrons. For ψ_0 we use a function due to Eckart:[2]

$$\psi_0 = [u(\gamma 1)u(\delta 2) + u(\gamma 2)u(\delta 1)]/[2(1 + c^2)]^{1/2} \tag{3}$$

where the u's are hydrogenic functions for $1s$, with parameters $\gamma = 2.14$ and $\delta = 1.19$ in place of $Z = 2$.

This function has the property of giving slightly too large a value for the diamagnetic susceptibility $|\chi|$; the calculation of $|\chi|$, involving as it does $(\Sigma_i r_i^2)_{00}$, weights comparatively heavily the values of the wave function for large values of r. This means that ψ_0 is likely to be too large rather than too small at large distances; any error in $|z_{n0}|^2$ due to ψ_0 is thus likely to be positive (since z_{n0} contains r_1, r_2 in the integrand). The error in ψ_0 is thus such as to make the calculated f' slightly too large, so that if in spite of this, we find a large value for f_c from the sum rule, we know that such a result is not due to error in ψ_0.

Letting ψ_2 refer to $(1s)\ (2p)^1P$, we use the function of Eckart:[3]

$$\psi_2 = [u(\alpha 1)v(\beta 2) + u(\alpha 2)v(\beta 1)]/2^{1/2}, \tag{4}$$

where u and v are hydrogenic functions of $1s$ and $2p$, and $\alpha = 2.003$, $\beta = 0.965$, are parameters replacing $Z = 2$. For ψ_n we take the hint from ψ_2 and use a function with zero screening for $1s$, and unit screening for np, since the p electron is now at least two shells farther out than the s-electron:

$$\psi_n = [u(Z1)v_n(\beta 2) + u(Z2)v_n(\beta 1)]/2^{1/2}, \tag{5}$$

where u and v_n refer to the hydrogenic functions for $1s$ and np, Z now replacing α, which in ψ_2 differed negligibly from Z, and $\beta = Z - 1 = 1$. Because of this slight difference we treat z_{20} and z_{n0} separately. By integration,

$$|z_{20}|^2 = [A(\delta)B(\gamma) + A(\gamma)B(\delta)]^2/(1 + c^2),$$

where

$$c^2 = 64(\gamma\delta)^3(\gamma + \delta)^{-6} = 0.775$$
$$A(\epsilon) = 4(2\beta^5\epsilon^3)^{1/2}(\epsilon + \beta/2)^{-5}$$
$$B(\epsilon) = 8(\alpha\epsilon)^{3/2}(\alpha + \epsilon)^{-3}.$$

Inserting the values of α, β, γ, and δ, $|z_{20}|^2 = 0.224$. Similarly, for $n > 2$:

$$|z_{n0}|^2 = [E(\delta)F(\gamma) + E(\gamma)F(\delta)]^2/1.775 \tag{6}$$

where

$$E(\epsilon) = \int u(Z1)u(\epsilon 1)d\tau_1 = 8(Z\epsilon)^{3/2}(Z + \epsilon)^{-3}$$

$$F(\epsilon) = \int r_1 \cos\theta_1 u(\epsilon 1)\bar{v}(\beta 1)d\tau_1$$

[2] C. Eckart, Phys. Rev. **36**, 883, Eq. (17) (1930).
[3] C. Eckart, Phys. Rev. **36**, 883, Eq. (18) (1930).

$$= 16\beta^{-4}(\epsilon^3\beta^3/3)^{1/2}(2\epsilon/\beta-1)n^3[(n+1)n(n-1)]^{1/2} \\ (\epsilon n/\beta-1)^{n-3}(\epsilon n/\beta+1)^{-(n+3)}. \tag{7}$$

By using $E(\gamma)=0.998$, $E(\delta)=0.905$, we get the Table I:

TABLE I. (*Energies and lengths are in atomic units.*)

n	$\lvert z_{n0}\rvert^2$	(W_n-W_0) obs.	$f_{n0}=(W_n-W_0)\lvert z_{n0}\rvert^2$
2	0.224	1.5593	0.349
3	0.0547	1.6966	0.0928
4	0.0204	1.7448	0.0357
5	0.0100	1.7671	0.0177
6	0.00588	1.7792	0.0105
7	0.00351	1.7866	0.0063

We find $\sum_{n=2}^{7} f_{n0}=0.512$, and we get an upper limit to $f_{8,0}+f_{9,0}+f_{10,0}$ by taking $3f_{7,0}=3\times0.0063=0.0189$. Thus $\sum_{2}^{10} f_{n0}=0.53$, and by using asymptotic values of W_n-W_0 and $F(\epsilon, n)$ for large n, we find that the sum from 11 to ∞ is of the order 0.0095. Thus essentially,

$$f' \equiv \sum_{n=2}^{\infty} f_{n0} = 0.54. \tag{8}$$

Since $h\nu_{0n}B_{0n}$ (where B_{0n} is the usual probability of induced transition) is proportional to f_{0n}, the relative intensities of the lines of the absorption spectrum are given by the last column of Table I. Taking the intensity of the first absorption line $(1s)^2\ {}^1S\rightarrow(1s)\ (2p)^1P$ arbitrarily as 100, the relative intensities of absorption are given by Table II.

TABLE II. *Relative intensities of absorption per unit intensity of incident radiation.*

2^1P	3^1P	4^1P	5^1P	6^1P	7^1P
100	26.6	10.2	5.07	3.01	1.80

Table II can be continued by means of formulas (6) and (7). For $n>10$, the asymptotic calculations previously referred to show that $\lvert z_{0n}\rvert^2$ and thus f_{0n} and the entries in Table II fall off inversely as n^3.

We now consider the doubly-excited states. From the Laporte rule,[4] or directly from the angular parts of the wave functions, we see that such states as $(2s)^2\ {}^1S$, etc., do not combine with the normal state, and that the only doubly-excited states which do so are the singlet states arising from the configurations $(ms)\ (np)$, $(mp)\ (nd)$, $(md)\ (nf)$, etc. In order to obtain an idea of the order of magnitude of the transition probabilities involved, we next investigate in detail that state from this group which is expected to be the most important, namely $(2s)\ (2p)^1P$.

If u_2 and v are hydrogenic functions of $2s$ and $2p$, respectively, the "unperturbed" wave function of $(2s)\ (2p)^1P$ is:

$$[u_2(Z1)v(Z2)+u_2(Z2)v(Z1)]/2^{1/2}.$$

[4] L. Pauling and S. Goudsmit, *Structure of Line Spectra*, McGraw-Hill, 1930, p. 94.

Suppose we should introduce a parameter β in place of Z in the function v, leaving u_2 unchanged. Then

$$\phi = [u_2(Z1)v(\beta 2) + u_2(Z2)v(\beta 1)]/2^{1/2}. \tag{9}$$

Now Eckart's function for $(1s)\ (2p)^1P$, which is presumably good because of the close check which it gives for the energy, has the form (4), where α is very closely equal to Z, and $\beta = 0.965$. For $(1s)\ (np)^1P$, where $n > 2$, we have used (5). We see then that the above trial function ϕ for $(2s)\ (2p)^1P$ is orthogonal to the wave functions of all the states $(1s)\ (np)^1P$; this statement follows from the presence of the function $u_2\ (Z)$ *without* parameters. Because of the angle functions it is orthogonal to the wave functions of all singly-excited singlet states not included in $(1s)\ (np)^1P$, and to the wave function of $(2s)^2\ ^1S$. Finally, because of its symmetry in electrons 1 and 2, it is orthogonal to the functions of all the triplet states. It is thus a function with the proper symmetry to represent $(2s)\ (2p)^1P$, possessing the property of orthogonality to the wave functions of all lower states. The minimum of the integral $E \equiv \int \bar{\phi} H \phi d\tau$ with respect to the parameter β is thus expected to furnish a value of the energy better than the usual first approximation, and higher than the true energy.[5]

This trial function leads to the variational integral: $-E = Z^2/4 + [2(Z-\sigma)-\beta]\beta/4$, where $\sigma = 1+J$, and $I = (4/\beta) \int (u^2(Z1)\,|v(\beta 2)|^2/r_{12}) d\tau_1 d\tau_2$

$$\text{or } I = \frac{x}{(1+x)^5}\left[1 + \frac{5x}{1+x} - \frac{15x^2}{(1+x)^2} + \frac{105x^3}{(1+x)^3}\right]$$
$$+ \frac{x^3}{(1+x)^3}\left[1 + \frac{3(1-x)}{1+x} + \frac{3(x^2-4x+2)}{(1+x)^2}\right.$$
$$\left. + \frac{5(3x^2-6x+2)}{(1+x)^3} + \frac{15x(3x-4)}{(1+x)^4} + \frac{105x^2}{(1+x)^5}\right]$$

$$J = (4/\beta) \int u(Z1)u(Z2)v(\beta 1)\bar{v}(\beta 2)/r_{12} d\tau_1 d\tau_2$$
$$= \frac{4x^3}{3(1+x)^7}\left[14 - \frac{98x}{1+x} + \frac{185x^2}{(1+x)^2}\right], \quad x = Z/\beta.$$

The minimum of E occurs at $\beta = 1.58$ and has the value -1.25 atomic units, thus placing the level 3.02×10^5 cm^{-1} above the limit of single ionization. This value can be checked against the value of 2^1P extrapolated from BII. The nucleus of boron plus its K shell we take as equivalent to a nucleus of charge Z^*, and treat BII as a helium-like atom of nuclear charge Z^*. Expressing the term value in atomic units as $(Z^*-s)^2/2^2$, the assumption of perfect shielding by the K shell leads to $Z^* = 3$ and $s = 0.90$; the assumption of 85 percent shielding by each K electron (from Slater's rules) leads to $Z^* = 3.30$ and $s = 1.20$. These values of s applied to $(2s)\ (2p)^1P$ of helium lead

[5] C. Eckart, Phys. Rev. **36**, 880, 881 (1930).

to -1.30 and -1.16, respectively, for the total energy, so that our value -1.25 lies in the correct range.

A direct application of Slater's[6] shielding rules to $(2s)$ $(2p)$ of helium gives the value -1.36. Majorana[7] also has computed this energy, using a variational method due to Fock,[8] and obtains the value -1.31; this value, however, is apt to be lower than the correct value, because the variational method of Fock does not make the trial function orthogonal to the wave functions of the lower states.

With our wave function for $j \equiv (2s)$ $(2p)^1P$ and Eq. (1) for the normal state 0, we find:

$$|z_{0j}|^2 = [M(\delta)N(\gamma) + M(\gamma)N(\delta)]^2/1.775,$$

where

$$M(\epsilon) = 4(2\beta^5\epsilon^3)^{1/2}(\epsilon + \beta/2)^{-5}$$
$$N(\epsilon) = 2(2Z^3\epsilon^3)^{1/2}(\epsilon - Z)(\epsilon + Z/2)^{-4}.$$

By inserting $\gamma = 2.14$, $\delta = 1.19$, $\beta = 1.58$, $Z = 2$, we find that $|z_{0j}|^2 = 0.00251$. Since $W_j - W_0 = 4.56$, we obtain $f_{0j} = 4.56 \times 0.00251 = 0.0114$. By comparing with Table I, we see that the absorption line due to $(2s)$ $(2p)^1P$ comes out about one-thirtieth as strong as the first absorption line of the principal series, or about as strong as the fifth line of the principal series.

We have now the problem of finding a wave function valid in the general case (ms) $(np)^1P$, where $m \geqq 2$, $n \geqq 2$, computing the matrix elements, and summing f_{0j} over the whole square array of such states. We picture the array as follows:

$$\begin{array}{llll}
(2s)(2p) & (2s)(3p) \cdots & (2s)(10p) \cdots & (2s)(np) \cdots \\
(3s)(2p) & (3s)(3p) \cdots & (3s)(10p) \cdots & (3s)(np) \cdots \\
\cdots\cdots & \cdots\cdots & \cdots\cdots & \cdots\cdots \\
(10s)(2p) \cdots & \cdots\cdots & (10s)(10p) \cdots & (10s)(np) \cdots \\
\cdots\cdots & \cdots\cdots & \cdots\cdots & \cdots\cdots \\
(ms)(2p) \cdots & \cdots\cdots & (ms)(10p) \cdots & (ms)(np) \cdots \\
\cdots\cdots & \cdots\cdots & \cdots\cdots & \cdots\cdots
\end{array}$$

We must consider separately the upper right half, the lower left half, and the main diagonal of this array. To treat the upper right half, we can write the unperturbed wave function for (ms) $(np)^1P$:

$$[u_{ms}(Z1)v_{np}(\beta 2) + u_{ms}(Z2)v_{np}(\beta 1)]/2^{1/2} \tag{10}$$

replacing in v_{np}, however, Z by the parameter $\beta = Z - 1 = 1$. That is, we consider the ms electron to be a perfect shield when $n > m$; this procedure is suggested by the similar one for $(1s)$ $(np)^1P$.

[6] J. C. Slater, Phys. Rev. **36**, 57 (1930).
[7] E. Majorana, Nuovo Cimento **VIII**, (2) 78 (1931).
[8] V. Fock, Zeits. f. Physik **63**, 855 (1930).

To treat the main diagonal $(ns)\ (np)^1P$, we use the same form of wave function, taking for β the value 1.58 found by actual calculation in the case $(2s)\ (2p)^1P$ (justification later).

The lower left half is not amenable to treatment in this way, since we cannot expect a p electron to be as complete a shield as an s electron, because of the non-spherical symmetry. Since, however, we have no reason to believe that its f-sum would be greater than that of the upper right half, we take its f-sum equal to that of the upper right half. This procedure gives us an upper limit, which is all that we need.

The total f-sum of all the doubly-excited sp states can then be expressed as $2R+D$, where R is the f-sum of the upper right half and D that of the main diagonal.

To obtain R, we first calculate $|z_{0j}|^2$ between the normal state 0 and the excited state j, using Eq. (1) for ψ_0 and Eq. (9) for ψ_j. We find:

$$|z_{0j}|^2 = [F(\delta)G(\gamma) + F(\gamma)G(\delta)]^2/1.775, \tag{11}$$

where $F(\epsilon)$ is given by Eq. (7) with $\beta=1$, and

$$G(\epsilon) = 8(m/Z)^3(Z\epsilon)^{3/2}m^{-1/2}[(\epsilon m/Z-1)/(\epsilon m/Z+1)]^{m-2}(\epsilon/Z-1)(1+\epsilon m/Z)^{-4}. \tag{12}$$

By using the asymptotic values of $F(\epsilon)$ and $G(\epsilon)$ for large m and n, and replacing the double summation by a double integral which can be shown to be larger, one can show that $\sum^{\infty}\sum_{n>m>10} f_{0j}$ is of the order 10^{-7}, so that the infinite "tail" of R is negligible.

R thus consists essentially of the sum of the f-values of the finite half-array:

$$\begin{array}{llll} (2s)(3p) & (2s)(4p) & \cdots\cdots & (2s)(10p) \\ & (3s)(4p) & \cdots\cdots & (3s)(10p) \\ & (4s)(5p) & \cdots & (4s)(10p) \\ & & \cdots\cdots & \\ & & \cdots\cdot & \\ & & \cdots & (9s)(10p) \end{array}$$

Using formulas (11) and (12), we obtain for the sum of $|z_{0j}|^2$ for the first row the value 0.000568/1.775, and since W_j-W_0 is of the order $5.807-1-1/n^2$, we have $W_j-W_0<4.807$; thus the f-sum of the first row is less than $4.807\times 0.000568/1.775$ or 0.00154. There are eight rows in all, each row containing one less member than the preceding, and each member lies higher in the diagram of energy levels than the one immediately above, so that its f-value must be less. We thus arrive at an upper limit for R by multiplying 0.00154 by the factor 8, so that $R<0.0123$, and $2R<0.0246$. That is, *0.0246* is an upper limit to the f-sum of all the doubly-excited sp states in which the two electrons have different principal quantum numbers.

We now turn to D, the diagonal f-sum. We must obtain a wave function for $(ns)\ (np)^1P$. We have already found a function for $(2s)\ (2p)^1P$ of the form (9), where $\beta=1.58$. As the best improvement that we can make over the

unperturbed zeroth approximation (without encountering prohibitive labor), we can write down such a function for $(ns)\ (np)^1P$, where u and v now refer to the states ns and np; we take $\beta = 1.58$. The argument for such a procedure is this: Such a function with $\beta = 2$ is the zeroth approximation, in which the interaction of the electrons is entirely neglected; we know, however, that the deviation from "hydrogenness" can be expressed in most cases sufficiently well by considering that the interaction of the electrons results in a screening effect. If the screening were perfect, we should have $\beta = 1$; no screening means $\beta = 2$. β thus lies between 1 and 2, and since it equals 1.58 for $n = 2$, 1.58 is our only possible estimate for the general case $(ns)\ (np)^1P$.

With this function, the squared matrix element $|z_{n0}|^2$ is given by Eq. (11), where now $G(\epsilon)$ is given by Eq. (12) with m replaced by n, and $F(\epsilon)$ is given by Eq. (7) with $\beta = 1.58$.

By using the asymptotic values of $F(\epsilon)$ and $G(\epsilon)$ for large n, we can then show that the diagonal f-sum from $n = 11$ to $n = \infty$ is less than an integral of the order 2×10^{-7}, so that it is negligible.

To obtain the diagonal f-sum from $n = 3$ to $n = 10$, we use the formula just found for $|z_{n0}|^2$ and estimate W_n by means of Slater's shielding rules, obtaining $W_n \sim -2(Z-0.35)^2/n^2 = -5.44/n^2$. Thus $W_n - W_0 \sim 5.807 - 5.44/n^2$. The f-value of $(3s)\ (3p)^1P$ turns out to be 7.55×10^{-4}, and we can obtain an upper limit to the f-sum from $n = 3$ to $n = 10$ by applying to this the factor 8; this limit is 0.006. On adding 0.0114, the f-value of $(2s)\ (2p)^1P$, the diagonal f-sum D becomes $\leqq 0.017$. Since

$$2R \leqq 0.0025, \text{ and } D \leqq 0.017, \text{ we have } f'' \equiv 2R + D \leqq 0.042. \quad (13)$$

Using Eqs. (2), (8) and (13), we have:

$$f_c = 2 - 0.54 - 0.04 = 1.42. \quad (14)$$

We wish now to investigate the question as to whether allowance for all the other doubly-excited states which combine with the normal state would affect appreciably the value of f''. We have to consider the states $(ml_1)\ (nl_2)^1P$, where $l_1 + l_2$ is odd (by the Laporte rule). In our screening constant functions, the function of $(ml_1)\ (nl_2)$ differs from that of $(ms)\ (np)^1P$ only in the angle functions. Since the latter contribute a factor to $|z_{n0}|^2$ which is less than unity, we can obtain an upper limit for each $(ml_1)\ (nl_2)$ by taking it to be equal to that of $(ms)\ (np)$. $W_n - W_0$ for a state $(ml_1)\ (nl_2)$ is of the same order as for the state $(ms)\ (np)$, since the principal quantum numbers play the principal role in the determination of the energy. We can thus obtain an upper limit to the f-contribution of a given part of the array which gives f'', when all these other states are included, by applying to the f-value of each $(ms)\ (np)$ a factor g_{mn} denoting the number of configurations which have values of m and n in common. Neglect of the Laporte rule leads to $g_{mn} \leqq mn$; recognition of the rule leads to a smaller value. If, accordingly, a portion of f which was negligible before is found still to be so when the factor mn is applied to each part, we know that it will still be negligible when the Laporte rule is used. In this way it is found that the infinite tails that we met before

are still negligible. On applying the factor mn to the other parts, we find that $f'' \leqq 0.043$. Thus Eqs. (13) and (14) remain essentially unchanged by this correction.

It is interesting to compare these figures with some obtained by Margenau.[9] He finds by a semi-empirical method $f' = 0.18$, and $f'' + f_c = 1.82$. From the large value of the latter he concludes that the neglect of "double jumps" is responsible for the inaccurate value found in the simple theory of London for van der Waals forces in helium. The present work makes it appear very probable that the inclusion of states beyond the ordinary series limit is essential, but it indicates that of these states, the continuous ones are by far the most important; namely, that part of the continuous spectrum which lies at the limit of the principal series. Stated in another way, the principal series lines in the absorption spectrum of helium are of moderate intensity, the lines due to jumps from the normal state to doubly-excited states are very weak, and the continuous absorption spectrum is very strong. These results are certainly in qualitative agreement with experiment, as evidenced by the measurements of Herzfeld and Wolf on the dispersion of helium.[10] Quantitative comparison can be made only after the absorption spectrum, which lies in the far ultraviolet (around 700A) has been photographed and measured.

The author wishes to acknowledge his indebtedness to Professors J. C. Slater and P. M. Morse for interesting discussions and suggestions during the course of this work.

[9] H. Margenau, Phys. Rev. **37**, 1425 (1931).
[10] K. F. Herzfeld and K. L. Wolf, Ann. d. Physik **76**, 71 (1925); **76**, 567 (1925).

Radiation from Slow Electrons

By LEO NEDELSKY
University of California

(Received October 4, 1932)

We have developed expressions describing radiation emitted by an electron in the field of a neutral atom, using as a model for the latter a point charge Ze surrounded by a spherical shell of radius a carrying a charge $-Ze$. In the introduction we formulate the physical foundations of the problem. In section I we set up expressions for the matrix components of acceleration and give methods for evaluating the integrals involved. In section II we use results of section I to compute the intensity of radiation J_ν and the polarization P. For low velocity electrons ($Va^2<1$, where V is the energy in volt-electrons and a is in angstrom units) we give simple formulas for both J_ν and P. For heavier elements J_ν is independent of Z and is nearly proportional to Va^2, while for lighter elements J_ν as a function of Za exhibits a series of striking maxima and minima. For higher velocities we give our results for the most part graphically. We find that the criterion of applicability of bare nucleus model to neutral atoms is $(Z^2/2v)^2 \ll 1$. Except for high voltages however Z should be less than the nuclear charge of the actual atom. We also show that the radiation from protons in the field of our model is simply related to the radiation from electrons in the field of an unscreened nucleus. In section III we discuss how Z and a should be chosen in order that our model, or a nuclear model, may represent an actual atom, and make comparison with experiment finding agreement in the order of magnitude. The last part of the paper is a summary containing all the formulas of importance.

INTRODUCTION

THE first quantum-theoretical treatment of the problem of continuous radiation emitted by an accelerated electron was done by Kramers.[1] On the basis of the correspondence principle Kramers computed the intensity of radiation from an electron which passes through the coulomb field of a point charge Ze. He obtained the following well-known formula

$$J_{kr}' = J_{kr} g'(\gamma_0)$$

with

$$J_{kr} = 32\pi^2 Z^2 e^6 / 3^{3/2} c^3 m^2 v^2 \text{ and } \gamma_0 = 2\pi\nu Ze^2/mv^3 \qquad (1)$$

where v is the initial velocity of the electron. The value of the factor $g'(\gamma_0)$ does not differ greatly from unity except for small values of γ_0 where it becomes logarithmically infinite. Kramer extended this result to the case of a thick target by using the Thomson-Whiddington law for the loss of velocity of a charged particle in its passage through matter. The resulting expression for J has been found in very good agreement with experimental values for Bremsstrahlung generated by electrons with energies corresponding to several kilovolts.

[1] Kramers, Phil. Mag. **46**, 836 (1923).

The more recent quantum-mechanical investigations of the same problem by Oppenheimer,[2] Gaunt,[3] Sugiura,[4] and finally by Sommerfeld,[5] confirmed substantially Kramers' formula. The agreement between the results obtained by the two methods has been shown by Gaunt to be especially good for the cases in which the energy of the electrons is not too great. However, even for fast electrons, Oppenheimer and Sommerfeld obtained formulas which confirm Kramers' results in the region of relatively soft radiation.

Agreement between the results predicted by Eq. (1) and the experimental values in the x-ray region is indicative of the fact that for the range of voltages there used the neutral atoms of the target are sufficiently well represented by the nuclear model. This representation fails, however, in the following two cases: (1) low voltages; (2) long wave-length end of the spectrum. In the first place, we notice that the total amount of radiation

$$R = \int_0^{\nu_0} J_\nu d\nu$$

is independent of the voltage and therefore remains finite and large as the voltage goes to zero. In the second place, the intensity of radiation is infinite for vanishing frequencies; i.e., $J_\nu \to \infty$ as $\nu \to 0$.

Both the finiteness of the total amount of radiation for zero voltages and the infinite value of the intensity for zero frequency are explainable by the fact that the field of an unscreened nucleus falls off very slowly. We therefore thought it desirable to investigate the effect on the intensity and on the amount of radiation of the screening by the electrons of the atom. We shall give later a criterion for the approximate validity of calculations based on the nuclear model; but we know on physical grounds that screening becomes important chiefly for slow electrons. The case of fast electrons and low frequencies is of no physical interest since the soft radiation emitted is of finite total intensity, hard to observe and of small practical importance.

Of several simple approximate models of the atom we have chosen that of a positive point charge surrounded by a negatively charged spherical shell, the whole system being neutral. We have also made a few computations with a model having two charged concentric shells and obtained results of the same order of magnitude as those for the single shell model. We believe that this qualitative agreement indicates that our model with its sharply defined boundaries is not unsuitable for representing an actual atom.

I

We first consider a system of an electron and an atom—in our case an electron moving in the screened field of force of a nucleus—and find the stationary states of this system with the neclect of radiative forces. Transitions between these states will occur in which the energy of the system diminishes

[2] Oppenheimer, Zeits. f. Physik **41**, 268 (1927); **55**, 725 (1929).
[3] Gaunt, Proc. Roy. Soc. **A126**, 654 (1930).
[4] Sugiura, Phys. Rev. **34**, 858 (1929).
[5] Sommerfeld, Ann. d. Physik **11**, 257 (1931).

by an amount $E-E'$ and appears in the form of radiation of frequency $\nu=(E-E')/h$. The intensity per unit frequency range of this radiation is given by the well-known formula

$$J_\nu = (4e^2/3c^3)\,|\,\alpha_{E,E'}\,|^2$$

where $\alpha_{E,E'}$ is the matrix component of acceleration of the radiating electron corresponding to the transition $E\rightarrow E'$. This classical formula may of course be justified quantum-mechanically on Dirac's radiation theory. In order to find $\alpha_{E,E'}$ we must know the wave functions corresponding to the initial and to the final states of the system. We shall suppose the former to consist of a uniform stream of electrons incident on the atom together with electrons moving radially away from the atom with velocities equal to those of the incident beam. Since with our model of the atom but a few discrete states are allowable we shall carry out calculations for the continuous radiation only. Then to a transition involving emission of radiation of frequency ν we have an infinite multitude of possible final states corresponding to various directions of ejection of the electron. Various choices of orthogonal functions to represent the final states have been made by different authors. In our case we shall choose those final states which are characterized by the values of the energy, the angular momentum, and the component of the angular momentum in the direction of the incident beam, i.e., by the quantum numbers n, l, and m. These final states present themselves when we separate the wave equation in polar coordinates.

We have chosen polar coordinates because due to the spherical symmetry of our model it is only in these coordinates that the boundary conditions are simple. A further advantage of this choice can be seen as follows. In order to obtain the total transition probability of emission of radiation of a given frequency we must perform a summation over l and m. Now, classically, an electron possessing an angular momentum greater than the product of its linear momentum and the radius of the screening shell would not enter the field of our model and therefore would not radiate. By analogy, we should expect that in quantum mechanics most of the radiation from a slow electron would be produced in transitions between states characterized by small values of l, and that the sum over l would therefore be strongly convergent.

1–1. Wave functions

The wave functions are the solutions of the Schrödinger equation

$$\Delta\psi + (8\pi^2m/h^2)(E - V)\psi = 0. \tag{2}$$

If we call the screening radius, i.e., the radius of the negatively charged shell, a, we must take for our potential function

$$V = Ze^2/a - Ze^2/r \text{ for } r \leqq a, \tag{3a}$$

$$V = 0 \qquad \text{for } r \geqq a. \tag{3b}$$

In polar coordinates the Eq. (2) is separable, and the normalized solution can be written in the form

$$\Psi = \xi_l{}^m P_l{}^m(\theta, \phi) u(E, l, r) \tag{4}$$

where

$$P_l{}^m(\theta, \phi) = (l - m)! \sin^m \theta \left(\frac{d}{d \cos \theta}\right)^{l+m} \frac{(\cos^2 \theta - 1)^l}{2^l l!} e^{im\phi}$$

$$(\xi_l{}^m)^{-2} = \frac{4\pi}{2l + 1}(l - m)!(l + m)!$$

$\xi_l{}^m$ is the normalizing factor for the angular function $P_l{}^m$. $u(E, l, r)$ is the normalized radial function; for the two cases (3a) and (3b) it is known to be

$$\begin{aligned} u(E, l, r) = \psi(n, l, r) &= 4(mb/h)^{1/2} \left| \delta_l \right| x^l e^{-x/2} F(\alpha, \rho, x) \\ &= 4(mb/h)^{1/2} \left| \delta_l \right| (M_{n,l}(x)/x) \end{aligned} \quad (r \leqq a) \tag{4a}$$

$$u(E, l, r) = \phi(b, l, r) = (\left| N \right| /(br)^{1/2}) \{J_{l+1/2}(br) + \beta_l J_{-l-1/2}(br)\} \quad (r \geqq a) \tag{4b}$$

with the following notation.

$$\left.\begin{array}{ll} J_p(br) \text{ is the Bessel function of the order } p & \\ F(\alpha, \rho, x) \text{ is the confluent hypergeometric function}^6 & \\ \alpha = l + 1 - n & k = (2\pi/h)[2m(Ze^2/a - E)]^{1/2} \\ \rho = 2l + 2 & b = (2\pi/h)mv \\ x = 2kr & n = 4\pi^2 mZe^2/h^2 k \end{array}\right\} \tag{5}$$

$\left|N\right|$, $\left|\delta_l\right|$ and β_l are constants which are to be determined by the requirement that the radial function $u(E, l, r)$ be normalized with respect to the frequency E/h and be continuous and possess continuous derivatives at the boundary $r = a$.

Following Oppenheimer we normalize $u(E, l, r)$ by the condition

$$\int_0^\infty r^2 dr \left\{ u^*(E', l, r) \int_E^{E+\Delta E} u(E, l, r) dE/h \right\} \to 1 \text{ as } \Delta E \to 0$$

$$\text{and } E < E' < E + \Delta E.$$

The integral with respect to r, if taken over a finite range, vanishes as $\Delta E \to 0$. We shall therefore use the asymptotic expansion of $\phi(b, l, r)$ in place of $u(E, l, r)$. This condition determines the value of N

$$\left| N \right|^2 = 4\pi^2 mb/h(1 + \beta_l{}^2). \tag{6}$$

We determine the remaining two constant δ_l and β_l by imposing the boundary conditions

$$\left.\begin{array}{l} \phi(b, l, a) = \psi(n, l, a) \\ (d/dr)\phi(b, l, a) = (d/dr)\psi(n, l, a) \end{array}\right\}. \tag{7}$$

We thus obtain

[6] A very complete account of the properties of this function is given by Barnes, Cambr. Phil. Soc. Trans. **20**, 253 (1907). He uses the notation ${}_1F_1(\alpha, \rho, x)$.

$$\left.\begin{aligned}\beta_l &= \frac{y^{1/2}J_{l+1/2}(y)M'_{n,l}(z) - (y/z)M_{n,l}(z)(y^{1/2}J_{l+1/2}(y))'}{(y/z)M_{n,l}(z)(y^{1/2}J_{-l-1/2}(y))' - y^{1/2}J_{-l-1/2}(y)M'_{n,l}(z)}\\ \delta_l &= (-1)^{l+1}/[M'_{n,l}(z)H_l(y) - (y/z)M_{n,l}(z)H_l'(y)]\end{aligned}\right\} \quad (8)$$

where[7]

$$\begin{aligned}H_l(y) &= \{y^{1/2}e^{(l+1/2)\pi i}J_{l+1/2}(y) - J_{-l-1/2}(y)\}\\ &= \left(\frac{2}{\pi}\right)^{1/2}e^{-iy}\sum_{\nu=0}^{l}\frac{(-i)^{l+\nu}(l+\nu)!}{\nu!(l-\nu)!(2y)^\nu} \quad (9)\end{aligned}$$

$$y = ba \text{ and } z = 2ka.$$

1–2. Form of solution

We shall now proceed to form the wave functions corresponding to the initial and to the final states of our system. The wave functions for the final states are given by the complete orthogonal normalized set (4). According to our plan we wish the wave function for the initial state to represent a uniform stream of electrons together with a stream moving radially away from the atom with velocity equal to that of the incident beam. Following Gordon[8] we take as the wave function for the initial state

$$\Phi_0 = \left(\frac{\pi}{2v}\right)^{1/2}\sum_{l=0}^{\infty}i^l(2l+1)P_l(\cos\theta)\alpha_l\left(\frac{J_{l+1/2}(br)}{(br)^{1/2}} + \beta_l\frac{J_{-l-1/2}(br)}{(br)^{1/2}}\right)$$

$$(r \geqq a). \quad (10)$$

α_l is the normalizing factor to be used for determining the intensity of the electronic beam. It can be found in the following way. At large distances from the atom Φ_0 should be a plane wave; its amplitude is determined by the requirement that it represent a stream of one electron crossing unit area per unit time. The expression for such a plane wave is known to be

$$(\pi/2v)^{1/2}\sum_{l=v}^{\infty}i^l(2l+1)P_l(\cos\theta)[J_{l+1/2}(br)/(br)^{1/2}]. \quad (11)$$

Asymptotically we have

$$\frac{J_{l+1/2}(br)}{(br)^{1/2}} = \left(\frac{2}{\pi}\right)^{1/2}\frac{1}{br}\{e^{-\pi i(l+1)/2}e^{ibr} + e^{\pi i(l+1)/2}e^{-ibr}\}$$

$$\frac{J_{-l-1/2}(br)}{(br)^{1/2}} = \left(\frac{2}{\pi}\right)^{1/2}\frac{1}{br}\{e^{\pi il/2}e^{ibr} + e^{-\pi il/2}e^{-ibr}\}.$$

Substituting these values in the expressions for Φ_0(10) and for the plane wave (11) and equating the coefficients of e^{-ibr}/br (representing the ingoing wave) we arrive at the desired result of having a plane wave of the correct amplitude as a part of the wave function for the initial state. We thus obtain

[7] $H_l(y) = i \sin(l+\frac{1}{2})\pi \cdot y^{1/2}H_{l+1/2}^{(2)}(y)$, where $H_{l+1/2}^{(2)}(y)$ is Hankel's function of the second kind. See Jahnke-Emde, *Funktiontafeln*, p. 95.

[8] Gordon, Zeits. f. Physik **48**, 180 (1928).

$$\alpha_l = [1 + \beta_l e^{\pi i(l+1/2)}]^{-1}. \tag{12}$$

The remainder of Φ_0, namely the terms containing e^{ibr}/br, when we have subtracted from it the similar terms of the plane wave (11) can be shown for any field of force which vanishes faster than $1/r^2$ as $r \to \infty$, to give a spherical scattered wave.

To obtain the wave function for the initial state for $r<a$ we apply the boundary conditions (7) to (10). Our result is

$$\Psi_0 = (2/\pi v)^{1/2} \sum_{l=0}^{\infty} i^l (2l+1) P_l(\cos\theta) \delta_l \frac{M_{n,l}(x)}{x} \quad (r \leqq a). \tag{13}$$

1–3. Matrix components of acceleration

The matrix component of acceleration corresponding to the transition

$$E \to E' \quad l \to l' \quad m \to m'$$

is defined by the integral

$$(E, l, m \,|\, \boldsymbol{\alpha} \,|\, E', l', m') = \int \Psi^*(E', l', m', r, \theta, \phi) \boldsymbol{\alpha} \Psi(E, l, m, r, \theta, \phi) d\tau \tag{14}$$

the integration being over all space. $\boldsymbol{\alpha}$ is the vector acceleration which in our case is given by

$$\left.\begin{aligned} \boldsymbol{\alpha} &= -(ze^2/r^2)(1/m)j \quad (r < a) \\ \boldsymbol{\alpha} &= 0 \qquad\qquad\qquad\quad (r > a) \end{aligned}\right\} \tag{15}$$

where j is a unit vector with components $(\sin\theta\cos\phi, \sin\theta\sin\phi, \cos\theta)$. Consequently, the integration with respect to r is from 0 to a. We notice further that the initial state of our system (13) is characterized by a single parameter n, l being absent, and m being equal to zero. The final state (4), on the other hand, is specified by n', l', m'. We shall accordingly denote the matrix component of acceleration corresponding to the transition from the initial to the final state by $(n \,|\boldsymbol{\alpha}|\, n'l'm')$. We find its value by substituting for $\Psi(Elmr\theta\phi)$ and $\Psi(E'l'm'r\theta\phi)$ in (14) the wave functions given by (13) and (4), respectively, and for $\boldsymbol{\alpha}$ expression (15).

$$(n \,|\, \boldsymbol{\alpha} \,|\, n'l'm') = -\frac{4ze^2}{hk}\left(\frac{v'}{v}\right)^{1/2} \sum_{l=0}^{\infty} i^l (2l+1) \delta_l \,|\, \delta_{l'} \,|\, (l0 \,|\, j \,|\, l'm') I_{l,l'}(n,n') \tag{16}$$

with the abbreviations

$$(l0 \,|\, j \,|\, l'm') = \int_0^{\pi} \int_0^{2\pi} \xi_{l'}{}^{m'*} P_{l'}{}^{m'*} j P_l \sin\theta d\theta d\phi \tag{17}$$

$$I_{l,l'}(n,n') = \int_0^{z} \frac{M^*{}_{n'l'}(x') M_{n,l}(x)}{x^2} dx. \tag{18}$$

Finally, in order to obtain the total transition probability corresponding to the emission of radiation of a given frequency ν, i.e., corresponding to a

transition in which only the initial and the final energies are specified, we must square the matrix components (16) and sum over all the possible values of l' and m'. We thus obtain

$$J_\nu = (4e^2/3c^3)\,|\,\alpha_{n,n'}\,|^2 \text{ where } |\,\alpha_{n,n'}\,|^2 = \sum_{l'} \sum_{m'} |\,(n\,|\,\boldsymbol{\alpha}\,|\,n'l'm')\,|^2. \quad (19)$$

1–4. Evaluation of $(lo\,|\,j\,|\,l'm')$ and summation with respect to m'

We first observe that the integrals (17) vanish unless

$$l = l' \pm 1 \quad m' = \pm 1 \text{ or } 0. \quad (20)$$

Consequently the summation in (16) reduces to two terms $l = l' \pm 1$.

The transition corresponding to $m' = 0$ gives rise to radiation with its electric vector polarized in the direction of the incident beam of electrons; we shall call the intensity of this radiation $J_\parallel$. The other two transitions, i.e., to $m' = \pm 1$ give rise to radiation polarized in the plane at right angles to the direction of the incident beam; we shall denote the corresponding intensity by $J_\perp$. We thus have

$$\begin{aligned} J_\parallel &= (4e^2/3c^3) \sum_{l'} |\,(n\,|\,\boldsymbol{\alpha}\,|\,n', l', 0)\,|^2 \\ J_\perp &= (4e^2/3c^3) \sum_{l'} \sum_{m'=\pm 1} |\,(n\,|\,\boldsymbol{\alpha}\,|\,n', l', m')\,|^2. \end{aligned} \quad (21)$$

We shall define the degree of polarization of the emitted radiation as observed in the direction at right angles to the incident beam by the usual formula

$$P = (J_\parallel - \tfrac{1}{2}J_\perp)/(J_\parallel + \tfrac{1}{2}J_\perp). \quad (22)$$

When the selection rules (20) are satisfied the integration in (17) can be carried out giving the following easily verifiable results

$$\begin{aligned} |\,(l-1,0\,|\,j\,|\,l,0)\,|^2 &= 4\pi l^2/(2l+1)(2l-1)^2 \\ |\,(l-1,0\,|\,j\,|\,l,\pm 1)\,|^2 &= 2\pi l(l+1)/(2l+1)(2l-1)^2 \\ |\,(l+1,0\,|\,j\,|\,l,0)\,|^2 &= 4\pi(l+1)^2/(2l+1)(2l+3)^2 \\ |\,(l+1,0\,|\,j\,|\,l,\pm 1)\,|^2 &= 2\pi l(l+1)/(2l+1)(2l+3)^2 \\ (l-1,0\,|\,j\,|\,l,0)(l+1,0\,|\,j\,|\,l,0)^* &= 4\pi l(l+1)/(2l-1)(2l+3)(2l+1) \\ (l-1,0\,|\,j\,|\,l,\pm 1)(l+1,0\,|\,j\,|\,l_1\pm 1)^* &= -2\pi l(l+1)/(2l-1)(2l+1)(2l+3). \end{aligned} \quad (23a)$$

It follows immediately that

$$\begin{aligned} \sum_{m'=0,\pm 1} |\,(l-1,0\,|\,j\,|\,l,m')\,|^2 &= 4\pi l/(2l-1)^2 \\ \sum_{m'=0,\pm 1} |\,(l+1,0\,|\,j\,|\,l,m')\,|^2 &= 4\pi(l+1)/(2l+3)^2 \\ \sum_{m'=0,\pm 1} (l-1,0\,|\,j\,|\,l,m')(l+1,0\,|\,j\,|\,l,m')^* &= 0. \end{aligned} \quad (23b)$$

Substituting (23b) into (16) and (19) we obtain an expression for J_ν in which only δ_l and $I_{l,l'}(n, n')$ remain to be evaluated.

$$J_\nu = \frac{16e^2h^2n'^2}{3c^3\pi^3m^2}\frac{y'}{y}\sum_{l=0}^{\infty}|\delta_l'|^2\{l|\delta_{l-1}|^2|I_{l-1,l}(n, n')|^2 + (l+1)|\delta_{l+1}|^2|I_{l+1,l}(n, n')|^2\}. \tag{24}$$

1–5. Evaluation of $I_{l,l'}(n, n')$

We must now evaluate the radial integrals

$$I_{l,l'}(n, n') = \int_0^z M^*_{n'l'}(x')M_{n,l}(x)/x^2dx.$$

First we express $M_{n,l}(x)$ in terms of the confluent hypergeometric functions $F(\alpha, \rho, x)$ by (4a)

$$M_{n,l}(x) = x^{l+1}e^{-x/2}F(\alpha, \rho, x).$$

From (5) we see that either both x and n are real or both purely imaginary. Using the identity

$$F(\alpha, \rho, x) = e^xF(\rho-\alpha, \rho, -x) \tag{25}$$

or in our case $F(l+1-n, 2l+2, x) = e^xF(l+1+n, 2l+2, -x)$ we conclude that $e^{-x/2}F(\alpha, \rho, x)$ is always real since it is equal to its own complex conjugate. Except for a constant factor, which is unity if x is real and $(-1)^{l+1}$ if x is imaginary, we may thus write

$$I_{l,l'}(n, n') = \epsilon^{l'+1}\int_0^z x^{l+l'}e^{-bx}F(\alpha, \rho, x)F(\alpha', \rho', \epsilon x)dx \tag{26}$$

where

$$\epsilon = x'/x \quad b = (x'+x)/2x = (\epsilon+1)/2. \tag{27}$$

Definite integrals of the type (26) and with the upper limit $\pm i\infty$ occur whenever one deals with wave functions in a Coulomb field of force. In our case, however, the integral is indefinite and requires different methods of treatment. The evaluation of this integral is much more difficult than that of the definite one and we have not been able to obtain a closed form except in certain special cases. Thus we have computed numerical values of I only for real values of the parameters involved. Fortunately it is for the real parameters that our results differ appreciably from those obtained with the nuclear model.

Since in most cases which we shall treat, the value of z is not very large, the most convenient method is to use expansions in small powers of x

$$F(\alpha, \rho, x) = \frac{\Gamma(\rho)}{\Gamma(\alpha)}\sum_{n=0}^{\infty}\frac{\Gamma(\alpha+n)x^n}{\Gamma(\rho+n)\Gamma(n+1)}$$
$$F(\alpha', \rho', \epsilon x) = \frac{\Gamma(\rho')}{\Gamma(\alpha')}\sum_{\nu=0}^{\infty}\frac{\Gamma(\alpha'+\nu)(\epsilon x)^\nu}{\Gamma(\rho'+\nu)\Gamma(\nu+1)}. \tag{28}$$

Integrating term by term and using symbol $\gamma(\mu, z)$ for the incomplete gamma-function defined by

$$\gamma(\mu, z) = \int_0^z x^{\mu-1}e^{-x}dx \tag{29}$$

we obtain

$$I_{l,l'}(n, n') = \frac{\Gamma(\rho)\Gamma(\rho')}{\Gamma(\alpha)\Gamma(\alpha')} \frac{\epsilon^{l'+1}}{b^{l+l'+1}} \sum_{\nu=0}^{\infty} \frac{\Gamma(\alpha'+\nu)(\epsilon/b)^{\nu}}{\Gamma(\rho'+\nu)\Gamma(\nu+1)} \sum_{n=0}^{\infty} \frac{b^{-n}\Gamma(\alpha+n)\gamma(l+l'+1+\nu+n, bz)}{\Gamma(\rho+n)\Gamma(n+1)}. \tag{30}$$

The value of $\gamma(\mu, z)$, since μ is always an integer can be computed from the terminating series

$$\gamma(\mu, z) = \Gamma(\mu)\left\{1 - e^{-z}z^{\mu-1}\sum_{s=0}^{\mu-1} \frac{z^{-s}}{\Gamma(\mu-s)}\right\}. \tag{31}$$

Substituting (31) into (30) we obtain $I = I' + I''$, where

$$I' = \frac{\Gamma(\rho')}{\Gamma(\alpha')} \frac{\epsilon^{l'+1}}{b^{l+l'+1}} \sum_{\nu=0}^{\infty} \frac{\Gamma(\alpha'+\nu)\Gamma(l+l'+1+\nu)(\epsilon/b)^{\nu}F(\alpha, l+l'+1+\nu; \rho; b^{-1})}{\Gamma(\rho'+\nu)\Gamma(\nu+1)} \tag{32a}$$

and

$$\begin{aligned} I'' &= \frac{\Gamma(\rho)\Gamma(\rho')\epsilon^{l'+1}e^{-bz}}{\Gamma(\alpha)\Gamma(\alpha')b} \sum_{s=0}^{\infty}(bz)^{-s} \sum_{\nu=0}^{\infty} \frac{\Gamma(\alpha'+\nu)(\epsilon z)^{\nu}}{\Gamma(\rho'+\nu)\Gamma(\nu+1)} \\ &\quad \sum_{n=0}^{\infty} \frac{\Gamma(\alpha+n)\Gamma(l+l'+1+\nu+n)z^n}{\Gamma(\rho+n)\Gamma(l+l'+1+\nu-s+n)\Gamma(n+1)} \\ &= \frac{\epsilon^{l'+1}}{b} e^{-bz} \sum_{s=0}^{\infty} \binom{d}{} \left(\frac{d}{db\,z}\right)^{s} \left\{z^{l+l'}F(\alpha, \rho, z)F(\alpha', \rho', \epsilon z)\right\}. \end{aligned} \tag{32b}$$

The above method is especially convenient in two special cases. (1) α and α' are negative integers. In this case both series of (30) terminate. (2) z is large and imaginary. This case corresponds to very high voltages, or large radii of the model. ($z \to +\infty$ corresponds to infinite nuclear charge and the integral diverges.) We can now use the asymptotic expansions

$$F(\alpha, \rho, z) \sim \Gamma(\rho)\left\{\frac{e^z z^{\alpha-\rho}}{\Gamma(\alpha)} + \frac{(-z)^{-\alpha}}{\Gamma(\rho-\alpha)}\right\} \tag{33}$$

and conclude that all the terms in the summation of I'' are small of the order $1/z^2$, remembering that $\alpha = (\rho/2) + n$ where n is now imaginary.

Another simple case is that of very small z. Provided $\alpha z/\rho$ and $\alpha' z\epsilon/\rho'$ are much smaller than unity, we can take only the first term in the expansion (28). Hence

$$F(\alpha, \rho, x) = F(\alpha', \rho', \epsilon x) \leqq 1$$

and the integral (26) becomes

$$I_{l,l'}(n, n') = \frac{\epsilon^{l'+1}}{b^{l+l'+1}} \gamma(l + l' + 1, bz). \tag{34}$$

For certain values of the parameters the integral (26) can be evaluated in terms of Bessel functions. Thus for $n = n' = \frac{1}{2}$ we have

$$e^{-x/2}F(\alpha, \rho, x) = e^{-x/2}F(l + \tfrac{1}{2}, 2l + 2, x) = \frac{2^l\Gamma(l + 1)}{y^l}\{J_l(y) + iJ_{l+1}(y)\}$$

where $y = ix/2$. We now have

$$I_{l,l+1}(\tfrac{1}{2}, \tfrac{1}{2}) = 2^{4l+3}\Gamma(l + 1)\Gamma(l + 2)(-1)^{l+1} \int_0^{iz/2} \{J_l + iJ_{l+1}\}\{J_{l+1} + iJ_{l+2}\}dy$$

which with the aid of

$$\int_0^y \{J_lJ_{l+2} + J_{l+1}^2\}dy = y\{J_{l+1}^2 - J_lJ_{l+2}\}$$

and

$$\int_0^y J_{l+1}\{J_l - J_{l+2}\}dy = \int_0^y 2J_{l+1}J'_{l+1}dy = J_{l+1}^2(y)$$

becomes

$$I_{l,l+1}(\tfrac{1}{2}, \tfrac{1}{2}) = 2^{4l+3}\Gamma(l + 1)\Gamma(l + 2)(-1)^{l+1}\{(z/2)[J_l(iz/2)J_{l+2}(iz/2) - J_{l+1}^2(iz/2)] + J_{l+1}^2(iz/2)\}. \tag{35}$$

II

2–1. Parametric analysis of J_ν

In the preceding section we have given methods for evaluating $I_{l,l'}(n, n')$. J_ν could now be computed by assigning definite values to the parameters involved; namely Z, a, v and v'. Before doing this, however, we shall find out in what combinations these parameters enter, for the purpose of reducing, if possible, the number of cases to be considered. On inspecting the expressions (24), (8), and (26) we notice that J_ν is a function of

$$z, z', n, n', y, y'$$

if we neglect for the moment the factor e^2/m^2. Now

$$\begin{aligned} z &= 2ka = 4\pi(2mZae^2/h^2 - m^2v^2a^2/h^2)^{1/2} &&= z(mZae^2/h^2, mva/h) \\ n &= 4\pi^2mZe^2/h^2k = 8\pi^2mZae^2/h^2z &&= n(mZae^2/h^2, mva/h) \\ y &= (2\pi/h)mva &&= y(mva/h). \end{aligned}$$

It follows therefore that

$$J_\nu = \frac{h^2e^2}{c^3m^2} f(mZae^2/h^2, mva/h, mv'a/h). \tag{36}$$

We notice that (1) m enters only in the form of the product ma except for the factor $1/m^2$; (2) Z enters only in the form of the product Za.

The first of these conditions we shall utilize in estimating the radiation emitted by a particle of large mass in the field of a screened nucleus. The second condition will allow us to limit our investigations to the relevant range of values of the product Za without specifying the values of the two factors Z and a. We shall use throughout the parameters Za, Va^2 and ν/ν_0.

2–2. Low voltages

2–21. Intensity of radiation. We shall consider the case of low voltages first. As is seen from (9) $|\delta_l|^2$ given by (8) diminishes roughly as y^{2l} for small value of y, i.e., for slow electrons. Hence provided $y \ll 1$ we need consider only two transitions $l0 \to 1$ and $1 \to 0$, contribution to the sum (24) from higher values of l being negligible. Further if y is sufficiently small for the inequality, $mv^2/2 \ll Ze^2/a$, to be true, we have approximately $n = n'$, $Z = Z' = 4n$, and therefore $I_{l',l}(n, n') = I_{l,l'}(n, n')$. (24) now simplifies to

$$J_\nu = \frac{16e^2h^2n'^2}{3c^3\pi^3m^2} \frac{y}{y'} |I_{0,1}(n, n)|^2 \{|\delta_0|^2 |\delta_1'|^2 + |\delta_1|^2 |\delta_0'|^2\}.$$

Substituting for δ_l their values and neglecting y^2 in comparison with unity we further reduce (24)

$$J_\nu = \frac{4e^2h^2n^2}{3c^3\pi m^2} \frac{|I_{0,1}(n, n)|^2}{|M'_{n,0}|^2 |M'_{n,1} + M_{n,1}/z|^2} \frac{y'}{y} (y^2 + y'^2).$$

We can write J_ν in terms of the frequency ν of radiation emitted and the energy V of the incident electron in electron-volts. Thus defining ν_0 by $h\nu_0 = \frac{1}{2}mv^2$ and using $Va^2 = 300h^2y^2/8\pi^2em = 3.8y^2$, we obtain the following expression

$$J_\nu = \frac{4e^2}{3c^3} f(n) Va^2 (1 - \nu/\nu_0)^{1/2} (2 - \nu/\nu_0) \quad (Va^2 < 1) \tag{37}$$

where

$$f(n) = \frac{8\pi e}{300m} n^2 \frac{|I_{0,1}(n, n)|^2}{|M'_{n,0}|^2 |M'_{n,1} + M_{n,1}/z|^2} \times 10^{-16} \tag{38}$$

and is a function of the parameters of the model only. We have also found by numerical computation that the two inequalities limiting the region of applicability of (37) can be replaced by a single one $Va^2 < 1$, where V is in volts and a in angstrom units. In its dependence on the frequency, J_ν of (37) is a monotonically decreasing function of ν having a negatively infinite derivative at the Duane-Hunt limit.

2–22. The total amount of radiation. To obtain the total amount of radiation R we integrate (37) with respect to the frequency

$$R = \int_0^{\nu_0} J_\nu d\nu = (64e/45c^3)(e/300h)V^2a^2f(n). \tag{39}$$

We notice especially that R vanishes rapidly as the voltage goes to zero instead of remaining constant as was the case with the nuclear model.

2–23. Dependence on the parameters of the model. The dependence of J_ν and R on the central charge Z and the screening radius a is given by $a^2f(n)$. For

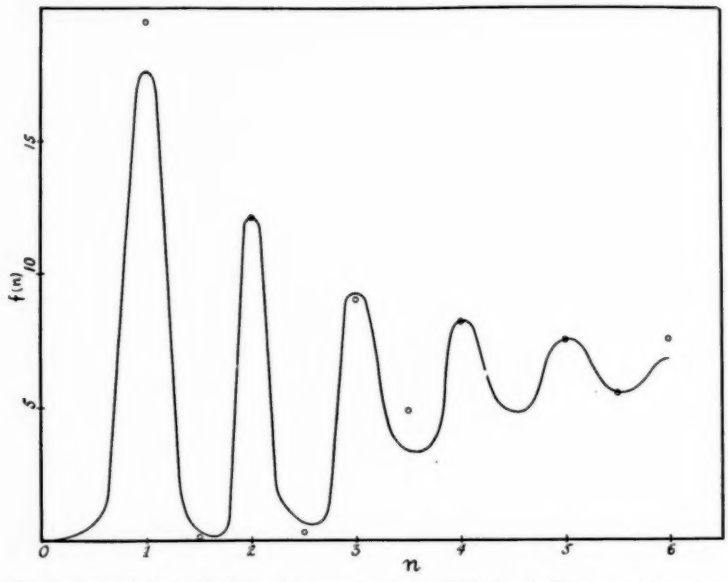

Fig. 1. Variation of $f(n)$ with respect to n. (Circles indicate points computed from the approximate Eq. (38b).)

very small values of n we can use (34) to evaluate $I_{0,1}(n, n)$; to the same approximation we obtain

$$f(n) = (8\pi en^4/300m)10^{-16}. \quad (n \ll 1). \tag{38a}$$

For larger values of n we have used Eq. (38) to calculate $f(n)$ and found that for the range $1 < n < 6$ the calculated points lie rather accurately on the curve represented by an "empirical-theoretical" formula

$$f(n) = 6.5\,|\,1 + (2/n^{3/2})\cos 2\pi n\,|\,, \quad (1 < n < 6). \tag{38b}$$

In Fig. 1 we show $f(n)$ as a function of n indicating by means of circles values computed from (38b). We observe that $f(n)$ exhibits a series of maxima corresponding to integral values of n. For large values of n, $f(n)$ has a nearly constant value of about 7. In this region therefore J_ν is independent of the central charge and is proportional to the cross-sectional area of the atom.

In order to find a physical explanation of the oscillatory character of $f(n)$ we have computed the values of the integral $I_{n,l} = \int_0^a |\psi_{n,l}|^2 dr$ for several

values of n. We have found that $I_{n,l}$ exhibits even more pronounced maxima for integral values of n than does $f(n)$. Now, since $|\psi(r_1)|^2$ is equal to the probability of finding the electron at $r=r_1$, the integral $I_{n,l}$ is a measure of the time spent by the electron in the region $0<r<a$, i.e., inside the screening shell. We may suppose therefore that for certain values of Za the electron stays in the field of the model for a very long time, executing several revolutions about the nucleus before escaping.

A similar phenomenon has been found by Allis and Morse[9] in their study of the cross section for elastic scattering. These authors used a model which is identical with ours. The variation of the cross section q_0 for slow electrons with respect to parameters n and y is shown in their Fig. 3. Their β is our n and their x is our y. For small values of x, i.e., for slow electrons, q_0 exhibits maxima near integral values of n.

2–24. Polarization. Using relations

$$I_{0,1}(n, n) = I_{1,0}(n, n)$$

$$|\delta_0'|^2|\delta_1|^2/|\delta_0|^2|\delta_1'|^2 = y'^2/y^2 = 1 - v/v_0$$

and considering as before only the two transitions $l1\rightarrow 0$ and $l0\rightarrow 1$, we obtain for the degree of polarization P defined by (22)

$$P = 3/(5 - 2v/v_0). \tag{40}$$

2–3. Moderate voltages

In this section we shall consider radiation from electrons whose velocity is limited by the relation

$$mv^2/2 < Ze^2/a. \tag{41}$$

For this range of velocities both z and n are real with the result that the evaluation of the radial integrals (18) is simplified.

In contradistinction to the analysis of the preceding sections, now we may no longer assume that $y\ll 1$ and must therefore take into consideration contribution from several values of l. In carrying out the summation over l we have noticed some interesting analogies to classical mechanics. Just as was the case for low voltages the contributions from terms with $(h/2\pi)\cdot l > mva$, i.e., $l>y$ is negligible. Further, for a given voltage, the most important values of l are $l \leqq y$ for relatively soft radiation, and smaller values for higher frequencies. As we increase the voltage, thus increasing y, the value of l contributing the most also increases but not as rapidly as does y. These facts seem to indicate that—as was to be expected—most of the radiation from fast electrons and relatively hard radiation from all electrons is emitted in the intense field in the neighborhood of the nucleus, while softer radiation is more likely to be produced with weaker fields and larger paths, the time spent in the field being here the dominant factor. We have also noticed that for the important values of l the transitions $l\rightarrow l-1$ are much more probable than the transitions $l\rightarrow l+1$.

[9] Allis and Morse, Zeits. f. Physik **20**, 567 (1931).

We have carried out calculations for three different values of Za, namely 37, 25.7, 12.6. The range of the parameter Va^2 was from 140 to 350, where V is in volts and a in angstroms. Except for a few control computations, we have chosen the values of Va^2 and ν/ν_0 in such a way as to make both α and α' negative integers. For these values of α and α' formula (30) takes an especially simple form. The range of ν for which this is possible is $\nu/\nu_0<0.6$ and $\nu/\nu_0=1$ for $Za=37$ or 25.7, and $\nu/\nu_0<0.7$ for $Za=12.6$. For frequencies other than these we have estimated the values of $I_{l,l'}(n, n')$ by interpolation. Although $I_{l,l'}(n, n')$ is in most cases a monotonic function of ν, because of rapid changes of the slope of this function the interpolation is extremely difficult and therefore the values of $I_{l,l'}(n, n')$ unreliable. In this region the more exact methods such as direct application of the formula (30) proved to be exceedingly laborious, and we have not used them in view of the doubtful importance of precise values of J_ν.

The results of these calculations in their dependence on the various parameters involved are given below.

2–31. Duane-Hunt limit. Near the Duane-Hunt limit $y'\ll 1$ and practically all of the radiation is emitted during the transition $l1\to 0$. Proceeding as in section 2–21 we obtain

$$J_\nu = G(Va^2, Za)(1-\nu/\nu_0)^{1/2} \quad (1-\nu/\nu_0 \ll 1) \tag{42}$$

valid for all voltages, where

$$G(Va^2, Za) = \frac{8e^2h^2n'^2}{3c^3\pi^2m^2}\,\frac{|\delta_1|^2}{|M'_{n',0}|^2}\,|I_{1,0}(n, n')|^2. \tag{43}$$

Of special interest is the behavior of J_ν with respect to the frequency ν, given by $(1-\nu/\nu_0)^{1/2}$. We see that at the high-frequency limit J_ν vanishes for all finite values of V and a, and that $dJ_\nu/d\nu=-\infty$. The physical reason for the vanishing of J_ν can be seen as follows. On the one hand J_ν is known to be continuous at the limit $\nu=\nu_0$; on the other hand a spectral line of frequency $\nu=\nu_0$ would correspond to an orbit of infinite radius and is therefore disallowed as long as we keep the value of a finite.

We shall now investigate the case of $a=\infty$, i.e., the case of an unscreened nucleus. In this case we can use formula (32). We now have $|z|=\infty$ and therefore $I''=0$. Limiting ourselves to high voltages and hard radiation, i.e., $|n|\ll 1$ and $|n/n'|\ll 1$, we shall take only the first two terms in the summation of I'. We thus obtain on neglecting $|n|^2$ and $|n/n'|^2$ in comparison with unity $|I_{1,0}|^2=144\,|n/n'|^2$ and $|I_{0,1}|^2=16\,|n/n'|^2$. The normalizing factors δ_l can be easily evaluated by using the asymptotic expansions (33) and (9).

$$|\delta_0|^2 = \pi^2|n|/(1-e^{-2\pi|n|})$$
$$|\delta_1|^2 = \pi^2|n|/36(1-e^{-2\pi|n|}).$$

Contribution from values of l and l' greater than unity can be safely neglected to the approximations which we are using. Substituting the above values of δ_l and I into (24) we finally obtain

$$J_\nu = \frac{2^8\pi^3 Z^2 e^6}{3c^3 m^2 v} |n|^2 \frac{1 + |n/n'|^2(1 + |n'|^2)/9}{(1 - e^{-2\pi|n|})(1 - e^{-2\pi|n'|})}$$
$$\leqq \frac{2^8\pi^3 Z^2 e^6}{3c^3 m^2 v^2} \frac{|n|^2}{(1 - e^{-2\pi|n|})(1 - e^{-2\pi|n'|})}. \quad (44)$$

In the limit of small $|n|$ and $|n/n'|$ Eq. (44) agrees both with the Sommerfeld's[5] Eq. (99b) and with Oppenheimer's[2] equation for I^2 on p. 733.

Since in either formula, (42) or (44), only one transition $l1 \to 0$ is important the radiation at the Duane-Hunt limit is always plane polarized in the direction of the incident beam of electrons; i.e., $P = 1$.

2–32. J_ν as a function of the frequency. Fig. 2 below shows the variation of J_ν with respect to ν/ν_0 for various values of parameters Va^2 and Za. In each

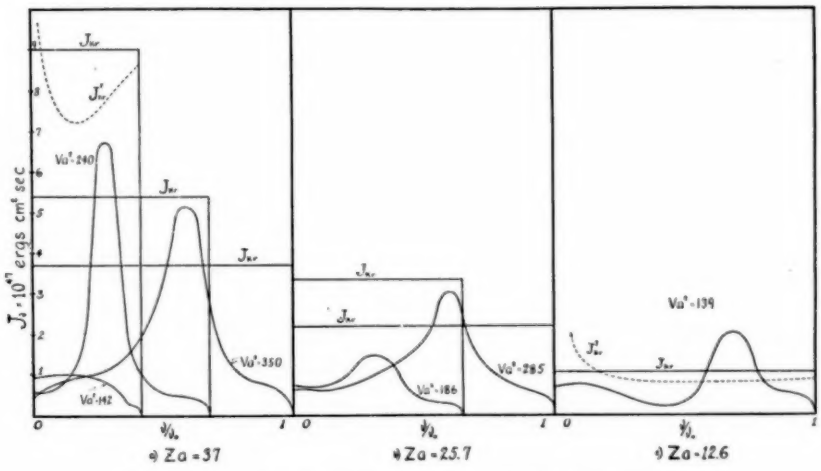

Fig. 2. Intensity of radiation as a function of the frequency.
(V is in volts and a in angstroms.)

of the three parts a, b and c of the figure, ν_0 represents the frequency of the Duane-Hunt limit for the highest value of Va^2 indicated. The straight line curves give the values of J_{kr} and the dotted curves values of J_{kr}' computed from Eq. (1) for the appropriate values of the ratio Z^2a^2/Va^2.

We notice that the general shape of the curves is approximately the same for all the values of Za and Va^2. At $\nu = 0$ all the curves start with a small slope from a value of J_ν near 0.6×10^{-47} ergs cm² sec.; they reach a maximum near the middle of the spectrum and come to zero at the Duane-Hunt limit with an infinite slope. The maximum corresponds approximately to the smallest integral value of n'. As stated in the beginning of section 2–3, *beyond the maximum the curves are definitely unreliable.* They have been determined from the known fact that the slope is infinite at the Duane-Hunt limit and by the use of a few points obtained by difficult graphical interpolation.

2–33. Dependence of average intensity or V, Z, a. Despite the uncertainties in values of J_ν for the high-frequency range we can obtain the average values

of J_ν fairly accurately by computing the areas under the curves of Fig. 2. For convenience of interpolation and extrapolation we shall give a "theoretical-empirical" formula which gives within 10 percent the six values of $\bar{J}$ computable from Fig. 2 and which agrees with Kramers' value J_{kr} as either V or a becomes large, or Z becomes small.

$$\bar{J} = \frac{J_{kr}(Z, V)}{\left[1 + \left(\frac{Z^2}{2V}\right)^2 \frac{1}{1 + (Za/22)^4}\right]^2}. \tag{45}$$

As always, V is in volts and a in angstrom units. It must be remembered that this formula can be relied upon only within the range of values investigated. We know that it is wrong in the region of very small V or a where Eq. (37) should be used. We feel, however, that (45) could be safely used for large V or a, for then it differs from $J_{Kr}(Z, V)$ only by a small quantity the exact value of which is not very important.

The region in which $\bar{J}$ is nearly equal to $J_{Kr}(Z, V)$ is defined for all values of a by the inequality

$$(Z^2/2V)^2 \ll 1. \tag{46}$$

This inequality may thus be used to define the region of applicability of a nuclear model to a neutral atom. We must remember, however, that even in the region (46) the equality $\bar{J} \cong J_{Kr}(Z, V)$ is true only provided the central charge Z is the same for either model. It is clear that Z should always be less than the nuclear charge of the actual atom. We shall discuss the choice of Z in section III.

2–4. Double shell model

Since the model consisting of a point charge surrounded by a negatively charged shell is but a crude approximation to the actual atom it is of interest to find what changes are introduced when the model is varied. For this purpose we modified our model by adding a second negatively charged shell concentric with the first one, the whole system as before being neutral; and carried out calculations only as far as it was necessary in order to ascertain the order of magnitude of J_ν.

The procedure for setting up an expression for J_ν is essentially the same as in the case of a single shell. We shall consider a point charge Ze, surrounded by an inner shell of radius a and an outer shell of radius R, the latter carrying a charge $-Z_1e$. In order to make the whole system neutral the charge on the inner shell must be $-(Z-Z_1)e$. The potential V in the Schrödinger Eq. (2) must now have 3 different values

$$V = 0 \qquad (r \geqq R)$$

$$V = Z_1e^2/R - Z_1e^2/r \qquad (a \leqq r \leqq R)$$

$$V = Ze^2/a - Ze^2/r + Z_1e^2/R - Z_1e^2/a. \qquad (r \leqq a)$$

Proceeding as before it is easy to show that

$$J_\nu = \frac{16e^2h^2p^2}{3c^3\pi^3m^2}\,\frac{y'}{y}\sum_{l=0}^{\infty}|\delta_l'|^2\left\{l\,|\delta_{l-1}|^2\left|\epsilon_l'^*\epsilon_{l-1}\frac{k}{s}\frac{Z}{Z_1}I^{(1)}_{l-1,l}+I^{(2)}_{l-1,l}\right|^2+(l+1)\,|\delta_{l+1}|^2\left|\epsilon_l'^*\epsilon_{l+1}\frac{k}{s}\frac{Z}{Z_1}I^{(1)}_{l+1,l}+I^{(2)}_{l+1,l}\right|^2\right\}$$

where

$$I^{(1)}_{l,l'} = \int_0^a \frac{M^*_{n'l'}(2k'r)M_{n,l}(2kr)}{(2kr)^2}\,2kdr$$

$$I^{(2)}_{l,l'} = \int_a^R \frac{\psi^*_{p'l'}(2s'r)\psi_{p,l}(2sr)}{(2sr)^2}\,2sdr$$

$$\psi_{p,l}(2sr) = \frac{1}{2sr}\{W_{p,l+1/2}(2sr)+\lambda_l W_{-p,l+1/2}(-2sr)\}\ ^{10}$$

$$\lambda_l = \frac{M_{n,l}(2ka)W'_{p,l}(2sa)-(k/s)M'_{n,l}(2ka)W_{p,l}(2sa)}{(k/s)M'_{n,l}(2ka)W_{-p,l+1/2}(2sa)-M_{n,l}(2ka)W'_{-p,l+1/2}(2sa)}$$

$$\delta_l = \frac{(-1)^{l+1}}{\psi'_{p,l}(2kR)H_l(y)-(b/2s)\psi_{p,l}(2kR)H_l'(y)}$$

$$\epsilon_l = \psi_{p,l}(2sa)/M_{n,l}(2ka)$$

$$s = (2\pi/h)[2m\{Z_1e^2/R-E\}]^{1/2}$$

$$k = (2\pi/h)[2m\{Z_1e^2/R+(Z-Z_1)e^2/a-E]^{1/2}$$

$$p = 4\pi^2mZ_1e^2/h^2s.$$

The result of the few calculations carried out seems to show that J_ν has the same order of magnitude whether we represent an atomic field as given by Slater[11] by a single shell model or by a double-shell one. This is very satisfactory, for since a charged shell model is not very sensitive even to such radical changes as increasing the number of shells, we may hope that our crude model represents fairly accurately the actual atom with its diffuse boundaries.

2–5. Radiation from protons

In this section we shall use the results of the parametric analysis of section 2–1 to estimate the intensity of radiation emitted by a proton in the field of our model. In section 2–1 we have shown that the mass of the incident particle, m, and the radius of the shell, a, enter only in the form of the product ma, except for the factor $1/m^2$. Let us now consider two particles of equal initial velocities, v, and of masses M and m passing through fields limited by radii a and R, respectively. Further, let the values of the radii and masses be so chosen as to satisfy the relation $Ma=mR$. We shall consider transitions in which the final velocity, v', has the same value for both particles. The frequency ν_1 of radiation emitted by the particle of mass M is then given by

[10] See *Modern Analysis*, Whittaker and Watson, section 16.12 of the 4th edition.

[11] Slater, Phys. Rev. **36**, 57 (1930).

$$h\nu_1 = \tfrac{1}{2}(v^2 - v'^2)M.$$

The other particle emits radiation of frequency ν_2

$$h\nu_2 = \tfrac{1}{2}(v^2 - v'^2)m.$$

It therefore follows from (36) that the intensities of radiation for the two particles per unit ranges of the respective frequencies are connected by the relation

$$J_{\nu_1}(M, a) = (m^2/M^2)J_{\nu_2}(m, R) \tag{47}$$

where $\nu_1/\nu_2 = R/a = M/m$.

We shall apply (47) to the case of a proton of mass M in the field of an atom whose field may be considered limited by a radius, a, of the order of magnitude of $1A$. We shall compare the intensity of radiation emitted by the proton to that of an electron of mass m in the field limited by the radius $R = (M/m)a$. From the known ratio of the masses $M/m = 1850$ we conclude that R is of the order of magnitude of 2000A. Now it is obvious that a model with a radius of 2000A is very nearly equivalent to an unscreened nucleus. We therefore obtain quite generally, provided the velocities of the two particles are equal

$$J_{\nu_1}(\text{proton, atom}) = (m^2/M^2)J_{\nu_2}(\text{electron, nucleus}) \tag{48}$$

where as before $\nu_1/\nu_2 = M/m = 1850$.

If we use Kramers' formula (1) for $J\nu_2$ in (48), the resulting expression for J_{ν_1} is identical with Kramers' formula for a proton radiating in the field of an unscreened nucleus. It is perhaps not surprising, however, that a proton radiates nearly as much in a limited field as it does in the field of an unscreened nucleus, for the mass of the proton is so large that its acceleration is negligible except in very intense fields.

III.

3–1. Choice of Z and a

In the preceding section we have given formulas describing the radiation emitted by an electron in the field of a model consisting of a central charge Z surrounded by a negatively charged shell of radius a. Before comparing our results with experimental data we must give methods for the proper choice of Z and a in order that our model may correctly represent an actual atom. We shall see that this choice can be made unambiguously in two limiting cases: (1) high voltages and (2) low voltages. In the intermediate region Z and a must be found by interpolation.

3–11. High voltages. In section 2–33 we saw that there exists a region, $(Z^2/2V)^2 \ll 1$, in which the radiation is independent of a and depends only on Z. In this region therefore the nuclear model should give correct results provided Z is properly chosen. In order to determine Z we shall proceed as follows. We shall assume that in the actual atom the effective charge Z at a distance r from the nucleus is given by an expression

$$Z = N(1 - r/R)^s \tag{49}$$

where N is the nuclear charge, and R and s are constants at our disposal to be determined for each atom by investigating its field, for example by Slater's[11] method. We shall now determine the region of the field, say near $r = r_{\text{eff}}$, in which most of the radiation is produced when a stream of electrons is incident upon the atom, and take the corresponding charge $Z_{\text{eff}} = N(1 - r_{\text{eff}}/R)^s$ for the central charge of our model. Now for each electron of the incident beam characterized by the distance p of the original path from the nucleus there is a region of the field say about $r = r_p$ in which this particular electron radiates most. We shall assume further then that the radiation of this electron does not differ greatly from that emitted in a coulomb field of central charge $Z_p = N(1 - r_p/R)^s$. The difference is the smaller, the closer the path of the electron approaches a circular orbit of radius r_p.

We may now use Kramers'[1] expression (Eq. (70)) for the intensity of radiation

$$i_\nu d\rho d\nu = \frac{8\pi^3 Z_p^2 e^6}{c^3 m^2 v^2} \frac{P(\gamma)}{p} d\rho d\nu \tag{50}$$

where

$$\left.\begin{aligned} P(\gamma) &= \tfrac{1}{3}\left\{[\gamma i^{4/3} 3^{-1/2} H^{(1)}_{1/3}(i\gamma/3)]^2 + [\gamma i^{5/3} 3^{-1/2} H^{(1)}_{2/3}(i\gamma/3)]^2\right\} \\ \text{and} \qquad \gamma &= 2\pi\nu p^3 v^3 m^2 / Z_p^2 e^4, \end{aligned}\right\} \tag{51}$$

and find the value of p corresponding to the maximum of i_ν. This will give us r_p of the electron which radiates more than any other electron of the beam, i.e., it will give us the value of r_{eff}. Before doing this however we must postulate some functional relation between r_p and p. We shall take it to be

$$r_p = kp \tag{52}$$

where k is independent of p.

Letting

$$\gamma = x^3;\ kp/R = w;\ s = 3m/2;\ \epsilon^3 = N^2 e^4 k^3 / 2\pi\nu v^3 m^2 R^3 \tag{53}$$

we obtain

$$\epsilon x = w/(1 - w)^m \tag{54}$$

and

$$i_\nu = cv^2 P(x^3)/x^3. \tag{55}$$

Since we have to deal only with small values of $i\gamma/3$ we have used expansions about the origin of the Hankel's functions in the expression (51) for $P(x^3)$ and retained only the first two terms for each $H^{(1)}$. The maximum of i_ν can now be found in the usual way by equating the derivative of i_ν to zero.

We carried out our calculations for three special cases: (a) small ϵ; (b) large ϵ; (c) $s = 3/2$.

(a) When ϵ is small, ϵx and hence w are also small. Thus to the first approximation we have from (54) $\epsilon x = w$. Going to the second approximation we let $w = \epsilon x + g$ where g is small of the order w^2. Putting this value of w into (54) we obtain

$$\epsilon x = \frac{\epsilon x + g}{(1 - \epsilon x)^m} \frac{1}{(1 - g/1 - \epsilon x)^m} = \frac{\epsilon x + g}{(1 - \epsilon x)^m} \left\{ 1 + \frac{mg}{1 - \epsilon x} + \cdots \right\}$$

whence on neglecting g^2

$$w = \frac{\epsilon x}{1 + \epsilon x(m - 1)} [(1 - \epsilon x)^{m+1} + m\epsilon x]. \tag{56}$$

Substituting (56) into $di_\nu/dx = 0$ we obtain an equation in x. By using special values for m we found that the maximum lies near $x = 0.7$. We have therefore introduced a new variable $y = x - 0.7$ and neglecting y^3 we have obtained a quadratic equation in y which we have solved. Our result is

$$\left.\begin{aligned} Z_{\text{eff}} &= \frac{N}{(1 + 0.75\epsilon)^s} \\ \text{and} \qquad r_{\text{eff}}/R &= \frac{0.75\epsilon}{(1 + 0.75\epsilon)^{2s/3}} \end{aligned}\right\} \begin{array}{l} \text{provided } \epsilon^2 \ll \left| \dfrac{8}{s(2s - 3)} \right| \\ \text{or if } s = 3/2,\ 0.75\epsilon < 1 \end{array} \Bigg\}. \tag{57}$$

(b) When $\epsilon \gg 1$, we have $\gamma \ll 1$, and may take only the lowest power of γ in the expansion of $P(\gamma)$, namely $\gamma^{2/3}$. We thus have

$$i_\nu = C_1 Z_p^{2/3} p$$

and without further approximations

$$Z_{\text{eff}} = N/(1 + 3/2s)^s; \quad r_{\text{eff}}/R = 3/(3 + 2s). \tag{58}$$

(c) $s = 3/2$.

Locating the maximum of i_ν is especially easy when $s = 3/2$, for then $w = \epsilon x/(1 + \epsilon x)$. Using the method outlined in (a) we have determined the maxima for all values of ϵ. The resulting ratios Z_{eff}/N and r_{eff}/R are plotted against ϵ in Fig. 3.

In all the above formulas we have three adjustable parameters s, R and k. The first two are determined by the field of the atom; the third parameter, k, is some function of N, V, ν and R. The following considerations seem to show, however, that k should not differ greatly from unity; i.e., $r_p \cong p$.

In the first place the path of the incident electron is certain to traverse both regions $r > p$ and $r < p$. For very fast electrons the closest distance of approach to the nucleus, r_m, which is certainly the most important region for these electrons, is nearly equal to p. As we go to slower electrons r_m becomes smaller than p but at the same time the strength of the field becomes less important in comparison with the time spent in the field with the result that the relation between r_p and p tends to remain constant.

We may also arrive at a rough estimate of r_p in the following way. We shall assume that the total radiation from an electron which is deflected through an angle less than 90° is equal to the radiation which would be emitted if the path of the electron consisted of a quarter of a circle of radius r_p. For the latter case we have

$$R = \frac{2e^2}{3c^3}\int\left(\frac{Ne^2}{mr_p}\right)^2 dt = \frac{\pi N^2 e^6}{3c^3 m^2 v r_p}.$$

On the other hand for such deflections, Kramers[1] gives a formula

$$R = \pi N^2 e^6/3c^3 m^2 v p.$$

Hence if the two R's are to be equal we must have $r_p = p$.

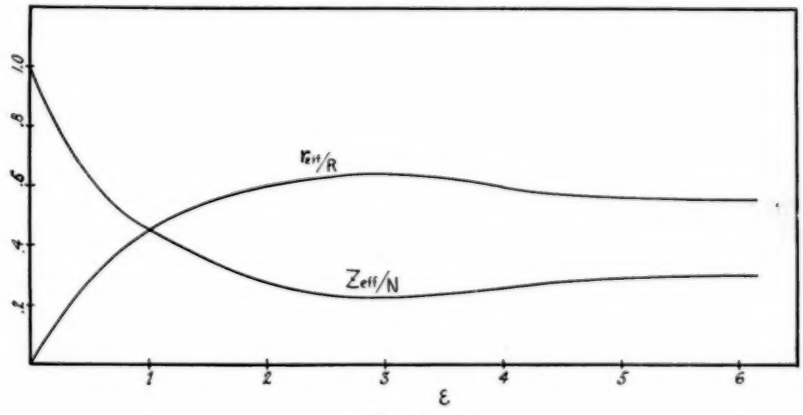

Fig. 3.

Having obtained an estimate of k we may now determine the regions of applicability of Eqs. (57) and (58). For this purpose we shall take $s=3/2$, and $R=2A$, i.e., equal roughly to the radius of an atom. Eq. (57) then becomes:

$$Z_{eff} = N/[1 + 4.4(N^{2/3}/V^{5/6})(\nu_0/\nu)^{1/3}]^{3/2} \tag{57a}$$

with the condition for its validity

$$(4.4N^{2/3}/V^{5/6})(\nu_0/\nu)^{1/3} < 1. \tag{59}$$

It is clear that (59) is satisfied in all cases of physical interest, especially in the region in which the nuclear model could be used, i.e., in the region defined by $(Z^2/2V)^2 \ll 1$. Hence Eq. (58) need be used only for the long wave-length end of the spectrum.

3–12. Low voltages. We have seen that in the region $Va^2 < 1$ where our Eq. (37) should be used J_r is nearly independent of Z (at least for larger values of n) and is proportional to a^2. Hence in this region a must be taken somewhat larger than the radius of the atom while Z may be equated to some sort of average of the effective charge inside the atom, the exact value of Z being of little importance.

3–13. Moderate voltages. In the region intermediate between the two discussed above, i.e., where Eq. (45) is to be used, the proper choice of Z and a is difficult to determine. For want of better criterion we may suggest that provided $(Z^2/2V)^2$ is not too large or Va^2 too small, Eq. (57) be used, and Z taken to be equal to Z_{eff} and a equal to, say, twice the value of r_{eff}. In the other limiting case the method of section 3–12 may be used with the modification that a should be given a value which is the smaller (and therefore the average value of Z the larger) the harder the radiation.

3–2. Comparison with experiment

Perhaps the greatest applicability of our results and the test of their correctness should be sought in the field of astro-physics, for it is known that certain portions of stellar atmospheres contain a great many neutral atoms. Comparison with terrestrial experiments is made difficult by the fact that our calculations apply only to infinitely thin targets, while the only available data, for the region of voltages in which we are interested, are on radiation from thick targets. On the other hand, we cannot use the Thomson-Whiddington law—as was done by Kramers—to extend our results to the case of thick targets for the following reasons. As we have seen, for slow electrons the cross section for radiation of an atom is small in comparison to its gas-kinetic cross section; as a consequence only a small part of the energy lost by the incident electron appears as radiation, the rest being consumed in increasing the thermal agitations of the lattice. Further it is known that for such electrons the cross section of an atom for inelastic collisions and its gas-kinetic cross section are of the same order of magnitude. Thus only a very few atomic layers contribute appreciably to the radiation since the range in matter of low velocity electrons is extremely short. It is clear therefore that the Thomson-Whiddington which implies continuous loss of energy while applicable to fast electrons with their longer paths and small losses in a single collision, must be replaced in our case by much more detailed and less general calculation. Moreover in the case of metal targets it is questionable whether our spherically symmetrical model is a good approximation to the field about each lattice point of the metal crystal. The problem is simpler in its astrophysical applications since there we have to deal with a gas and the velocity distribution of electrons may be supposed known.

In view of these difficulties and the further difficulty that in the case of thick targets and soft radiation a large part of the radiation may fail to escape due to internal reflection and to absorption we can hope to obtain agreement with experimental results in the order of magnitude only. The only available data in the region of low voltages are to be found in the work of Mohler and Boeckner.[12] These authors, using a small metal probe, measured the absolute intensity of continuous radiation emitted by electrons of energies below 30 volts.

We have made the comparison with their values on the assumption that the amount of radiation emitted by an electron is proportional to the number

[12] Mohler and Boeckner, Bur. Standards J. Research **6,** 673 (1931); **7,** 751 (1931).

of atoms it encounters. Knowing the number of atoms per unit volume of target and calling the depth of penetration of the electron l we can compute the intensity J of radiation per atom per unit intensity of the electronic beam. Thus for the case of a copper probe, 9.1 volts and 3700A we have

$$J = (3.87 \times 10^{-56})/l \text{ ergs cm}^2 \text{ sec.} \tag{60}$$

We may now evaluate l by equating the experimental and the theoretical values of J. Thus if we use Kramers' formula (1) we obtain $l_{Kr} = 0.0045$A. This absurdly small value of l indicates that the nuclear model cannot be used for very low voltages.

Mohler and Boeckner tentatively used a formula, which Kramers derived for the case of a thick target by using the Thomson-Whiddington law, and found agreement within a factor of 2. We have seen however that neither the nuclear model nor the Thomson-Whiddington law can be applied to the case of very slow electrons; the agreement must therefore be considered accidental.

Before comparing (60) with the equations derived with the aid of our model we must decide upon the values of Z and a corresponding to a neutral copper atom. Using methods of section 3–12 and Slater's atomic fields we obtain $a = 1.73$A and $Z = 9$. We notice that (58) with $s = 3/2$ gives nearly identical results; namely $Z_{\text{eff}} = 10.3$ and $A = 2r_{\text{eff}} = R = 1.73A$. By using the former values of a and Z in Eq. (45) we obtain in conjunction with (60), $l = 18A$, a value which corresponds to the penetration of 7 or 8 atomic layers. This value of l seems altogether reasonable for very slow electrons and thus provides us with a partial experimental verification of the validity of our formulas at least as to the order to magnitude.

Summary

We have developed expressions describing the radiation emitted by a stream of electrons in the field of a model consisting of a point charge Ze surrounded by a negatively charged spherical shell of radius a, the whole system being neutral. In all the formulas below, a is in angstrom units and V, the energy content of the incident electrons, in electron-volts. We have labeled (emp) formulas which have not been theoretically derived but merely set up to give approximately the same values as those obtained from exact expressions.

We have divided our field of investigation into three regions: (1) low voltages, (2) moderate voltages and (3) high voltages.

(1) Low voltages ($Va^2 < 1$)

$$J_\nu = \frac{4e^2}{3c^3} f(n) V a^2 (1 - \nu/\nu_0)^{1/2}(2 - \nu/\nu_0) \tag{37}$$

where $f(n)$ is given by the graph of Fig. 1, or approximately by

$$f(n) = \frac{8\pi e n^4}{300m}\,10^{-16} \qquad (n \ll 1) \tag{38a}$$

$$f(n) = 6.5\left|1 + \frac{2}{n^{3/2}}\cos 2\pi n\right| \quad (n > 1)(\text{emp}) \tag{38b}$$

$$P = 3/(5 - 2\nu/\nu_0). \tag{40}$$

(2) Moderate voltages ($Va^2 < 3\times 10^{10} eZa$)

$$\bar{J} = \frac{J_{kr}(Z, V)}{\left[1 + \left(\frac{Z^2}{2V}\right)^2 \frac{1}{1 + (Za/22)^4}\right]^2} \text{(emp)} \tag{45}$$

where

$$J_{kr}(Z, V) = (1600\pi^2 e^5/3^{1/2}c^3 m)(Z^2/V). \tag{1}$$

(3) High voltages ($(Z^2/2V)^2 \ll 1$)

$$J_\nu = J_{kr}(Z_{\text{eff}}, V)$$

where

$$Z_{\text{eff}} = N/(1 + 0.75\epsilon)^s \quad \left(\begin{array}{c} \epsilon^2 \ll |\,8/s(2s-3)\,| \\ \text{or if } s = 3/2,\ 0.75\epsilon < 1 \end{array}\right) \tag{57}$$

$$Z_{\text{eff}} = N/(1 + 3/2s)^s \quad (\epsilon \gg 1) \tag{58}$$

and

$$\epsilon^3 = N^2 e^4/2\pi\nu m^2 v^3 R^3 \tag{53}$$

$$P = 1 \text{ for } \nu = \nu_0.$$

We have also carried out a few calculations using a model having two concentric spherical shells of different radii and obtained results of the same order of magnitude with those for the single shell model.

From the fact that the mass of the particle m and the radius of the screening shell a enter into the expression for J_ν only in the form of the product ma we have derived an expression connecting the intensities of radiation from a proton in the field of our model and from an electron of the same velocity in the field of an unscreened nucleus.

$$J_{\nu_1}(\text{proton, atom}) = (m/M^2)J_{\nu_2}(\text{electron, nucleus}) \tag{48}$$

where

$$\nu_1/\nu_2 = M/m \cong 1850$$

and J's are the intensities per unit range of the respective frequencies.

In section III we have discussed the proper choice of Z and a in order that our model may represent an actual atom. There we have also compared our results with the experimental data of Mohler and Boeckner[12] and found agreement in the order of magnitude.

The writer wishes to thank Dr. H. A. Kramers for suggesting the problem and Dr. J. R. Oppenheimer for his friendly and helpful supervision of this work.

Influence of Crystalline Fields on the Susceptibilities of Salts of Paramagnetic Ions. II. The Iron Group, Especially Ni, Cr and Co

By Robert Schlapp and William G. Penney*
Department of Physics, University of Wisconsin

(Received October 13, 1932)

The present paper is concerned with the calculation of the paramagnetic susceptibility of highly hydrated crystals of the iron group elements Ni, Cr and Co. On the assumption that the metallic ion is subject to a crystalline electric field, predominantly cubic but also with a smaller rhombic term, the Hamiltonian function in a magnetic field $\boldsymbol{H}$ is given by

$$D(x^4+y^4+z^4)+Ax^2+By^2-(A+B)z^2+\lambda(\boldsymbol{L}\cdot\boldsymbol{S})+\beta\boldsymbol{H}\cdot(\boldsymbol{L}+2\boldsymbol{S})$$

the numerical value of λ being known from the work of Laporte but the other constants yet to be determined. It actually proves possible to formulate and solve approximately the resulting secular equations and so obtain the first and second order Zeeman effects and hence the susceptibility. For all three ions $L=3$, so that the orbital problem is the same for all. This problem is exactly soluble, the energy levels consisting of two triplets and a singlet, the singlet not lying between the triplets. The effect of the introduction of the spin and its coupling to the orbit then leads to a determinant of order 21 for Ni and of order 28 for Cr and Co. That for Ni factors into one of order 10 and one of order 11, while those for Cr and Co factor into two determinants, identical except for the sign of the coefficient of H. On the assumption of a cubic field of the same sign and of approximately the same magnitude for all three ions the orbit-spin, together with the rhombic field, is able to remove the degeneracy of the lowest level in Ni and Cr only in a high approximation, while with Co the degeneracy is removed in first approximation. This difference accounts for the isotropy of Ni and Cr compared with the anisotropy of Co. In order to obtain agreement with experiment it is necessary to assume that in Ni the singlet of the orbital problem lies lowest. It then follows from the work of Van Vleck that the singlet also lies lowest for Cr but that for Co the singlet lies highest. When the singlet lies lowest, the square of the magneton number is given by the "spin only" value $4S(S+1)$, together with a small orbital contribution of order λ/D, whose sign can be either positive or negative. Actually it is positive for Ni and negative for Cr. In order to fit the results on the principal susceptibilities of Ni, it is necessary to take $D=1260$ cm^{-1}, $A=176$ cm^{-1}, $B=352$ cm^{-1}, the magnitude of λ being -335 cm^{-1}. For Ni and Cr the theory requires that for the mean susceptibility $\chi=Q+P/T$, where P and Q are constants, Q being uniquely determined when P is fixed. Choosing P so that χT passes through the experimental point at 170°K we find that good agreement is obtained over the whole temperature range. For Cr $\lambda=87$ cm^{-1} and we find $D=3730$ cm^{-1}, but we cannot determine A or B since there are no data on the principal susceptibilities.

Computational difficulties prevent the accurate solution of the Co problem. The situation is complicated by the experimental data not being complete. It proves necessary to consider a sextet which is soluble only numerically in the general case but perturbation theory can be applied when either the orbit-spin is large compared with the rhombic field or *vice-versa*. We obtain fair agreement with experiment and our calculations indicate that good agreement would be obtained in an intermediate case.

* Commonwealth Fund Fellow.

Introduction

IN THE following paper the idea of crystal fields of definite symmetry, developed by Van Vleck and others,[1] and already used in a previous article by the authors,[2] is applied to calculate the susceptibilities of salts of the elements Ni, Co and Cr. There are two respects in which the present problem differs from that of susceptibilities in the rare earth group. In the first place, the incomplete shell which is responsible for the paramagnetism of the iron elements consists of $3d$ electrons, which are much more strongly affected by the crystal fields than the more sheltered $4f$ shell of the rare earths. In the second place the orbit-spin coupling, which determines the multiplet width, is usually smaller in the iron group than in the rare earths. For the latter it was allowable to suppose that each multiplet component underwent a "Stark effect" due to the crystal field, without distortion on account of the other multiplet components. In the iron group, however, the electric field of the crystal is able to break down the relatively weak coupling between orbit and spin, producing an electric Paschen-Back effect; the orbit-spin coupling may be treated hence as a perturbation on an unperturbed problem which neglects the spin. This unperturbed, or orbital problem, as we shall call it, is the same for all three ions Ni^{++} Co^{++} Cr^{++}, since they all have an F state ($L=3$) as ground state.

We assume that the crystal field has no more than rhombic symmetry.[3] The high degree of isotropy of Ni salts suggests that in this case the departure from cubic symmetry is small. Now it is known that a field which is nearly cubic decomposes the seven coincident levels of the F state (without spin) into a single level and two triplets, the single level lying outside the triplets and the triplet widths being small compared with the singlet-triplet or the triplet-triplet separations. If the spin and its coupling to the orbit be included, further decompositions of these levels occur. The general theory of susceptibilities shows that Curie's law will cease to be obeyed at low temperatures if kT becomes comparable with the separation of the lowest group of levels. The close conformity of Ni salts to Curie's law over a range of temperature from 300°K down to 14°K thus requires that a very narrow group of levels must lie considerably below all others. These conditions are satisfied if the single level of the orbital problem lies below the others, and on this assumption it is possible to account qualitatively for both the small anisotropy and the conformity to Curie's law. This arrangement of levels, however, appears to preclude an explanation on the same lines of the much greater anisotropy of the very similar and sometimes isomorphous salts of Co, and of the considerable departures from Curie's law which they exhibit. To ac-

[1] J. H. Van Vleck, *Theory of Electric and Magnetic Susceptibilities*, Oxford (1932).

[2] W. G. Penney and R. Schlapp, Phys. Rev. **41**, 194 (1932). Attention may be called here to a printers error in this paper. Minus signs were omitted in Eqs. (8) and (9) which should read $q=-I/10395$ for (8) and $q=-I/32670$ for (9). Moreover, in the secular determinant for Pr $a=\frac{1}{2}pD$ (not pD) and similarly for Nd $A=6ap(14)^{1/2}$.

[3] The assumption of a rhombic field not predominantly cubic was found to lead to very large asymmetry, in contradiction with experiment.

count for the behavior of Co salts it is necessary to suppose that the levels of the orbital problem in Co are inverted relatively to those in Ni. That such an inversion is actually to be expected in passing from Ni and Cr to Co has been neatly demonstrated by Van Vleck.[4]

Experimental Data

It is useful at this stage to review the experimental data available on the hydrated salts of Ni, Cr and Co. We restrict ourselves to salts of large magnetic dilution, so that exchange effects may be neglected. Determinations of the three principal susceptibilities of the double sulphates of Co with ammonium, potassium and rubidium, have been made by Rabi[5] at 300°K. Jackson[6] has measured the susceptibility of powdered $Ni(NH_4)_2(SO_4)_2 \cdot 6H_2O$ and Gorter, de Haas and v. d. Handel[7] that of powdered $NiSO_4 \cdot 7H_2O$ over a range of temperature between 14°K and 290°K. The graph of $1/\chi$ against T is approximately a straight line through the origin in both cases. Jackson[6] has measured the three principal susceptibilities of $Co(NH_4)_2(SO_4)_2 \cdot 6H_2O$ at various temperatures down to 14°K. His values of the susceptibility extrapolated to a temperature of 300°K differ considerably from Rabi's, and there is only one determination between 20° and 290°K. As far as one can judge, however, the graph of $1/\chi$ against T is a straight line for each of the three principal susceptibilities, down to a temperature of about 50°K, below which the curve bends downwards slightly, so that the susceptibilities are higher than those predicted by the relation $\chi = C/(T+\Delta)$ of Weiss.

Very recently determinations over a temperature range from 250°K to 360°K have been made by Bartlett[8] for crystalline cobalt ammonium sulphate and certain other crystals. They seem to be the most reliable measurements yet taken, being consistent and in agreement with Rabi's at the single temperature used by him. We are indebted to Dr. Bartlett for communicating these results to us in advance of publication.

The susceptibility of potassium chrome alum in powder form has been measured by de Haas and Gorter[9] at various temperatures between 290°K and 14°K. They find that the law $\chi = C/T$ is closely obeyed over the whole range. Chrome alum forms crystals in the cubic system so that it may be expected to be magnetically isotropic.[10]

[4] J. H. Van Vleck, Phys. Rev. **41**, 208 (1932).

[5] I. I. Rabi, Phys. Rev. **29**, 184 (1927).

[6] L. C. Jackson, Phil. Trans. Roy. Soc. London, **224**, 1 (1922), Leiden Com. 163.

[7] C. J. Gorter, W. J. de Haas and v. d. Handel, Proc. Amst. Acad. **34**, 1 (1931), Leiden Com. 218d.

[8] B. W. Bartlett, Phys. Rev. **41**, 818 (1932).

[9] W. J. de Haas and C. J. Gorter, Leiden Com. 208d.

[10] Measurements of the susceptibilities of the paramagnetic cubic crystal pyrite were made long ago by Voigt and Kinoshita (Ann. d. Physik **24**, 492 (1907)) who found it to be magnetically isotropic. There does not, however, seem to be any reason why magnetic dissymmetry should not exist in cubic crystals, as the electric field acting on the ion may have a lower symmetry than the lattice. See also reference **18**.

The Ion in a Perfectly Cubic Field

Before considering the secular determinant explicitly, it is instructive to look at the problem from a more general point of view. The analysis of Bethe[11] shows that the cubic field breaks up the F level into three, corresponding to the irreducible representations Γ_2, Γ_4, Γ_5, of the cubic group, in his notation. The level Γ_5 lies between Γ_2 and Γ_4; Γ_2 is single, while Γ_4 and Γ_5 are each triply degenerate. We shall see later that the intervals between Γ_2, Γ_4, Γ_5 are of the order 10^4 cm^{-1}. The reader is referred to Van Vleck's[4] paper for the demonstration of the fact that in Ni and Cr Γ_2 lies lowest and in Co Γ_4 lies lowest, for a given sign of D in the Hamiltonian. The level Γ_2 is non-magnetic; that is to say an atom in this state has no average orbital magnetic moment. The level Γ_4 is magnetic. Hence if Γ_2 is lowest the orbit is "quenched", i.e., contributes nothing to the susceptibility except a term independent of temperature. If, however, Γ_4 is lowest a certain portion survives.

We have now to consider the influence of the spin. Inclusion of the spin S ($=1$ for Ni and $3/2$ for Co and Cr) without interaction with the orbit makes each level of the orbital problem have an additional $(2S+1)$-fold degeneracy, which is partially removed by the interaction. By the methods of Bethe's paper the decomposition of the levels is found by reducing the six direct products $\Gamma_i D_k$, ($i=2, 4, 5$; $k=1, 3/2$) to represent the cubic group. Here D_k is the representation group for the rotation of the spin k alone. The result is, in Bethe's notation,

$$\begin{aligned} \Gamma_2 D_1 &= \Gamma_5, & \Gamma_2 D_{3/2} &= \Gamma_8 \\ \Gamma_4 D_1 &= \Gamma_2 + \Gamma_3 + \Gamma_4 + \Gamma_5, & \Gamma_4 D_{3/2} &= \Gamma_6 + \Gamma_7 + 2\Gamma_8, \\ \Gamma_5 D_1 &= \Gamma_1 + \Gamma_3 + \Gamma_4 + \Gamma_5, & \Gamma_5 D_{3/2} &= \Gamma_6 + \Gamma_7 + 2\Gamma_8. \end{aligned} \tag{1}$$

Here Γ_6, Γ_7, Γ_8 are the "zweideutig" representations of the cubic group, of dimensions 2, 2, 4, respectively, which always arise with half-integral quantum numbers. These equations state that for Ni, Cr and Co the orbit-spin-interaction does not split the cubic level Γ_2 but splits each of the levels Γ_4, Γ_5 into four components.

Let us suppose that the level Γ_2 of the orbital problem lies lowest. The above reductions show that under the orbit-spin interaction this level does not break up, but remains triply degenerate (in Ni) or quadruply degenerate (in Co and Cr); no energy differences arise in consequence of different orientations of the spin, which therefore remains entirely free at all temperatures to orientate itself along the magnetic field. If the orbital contribution to the moment be neglected, the magneton number would be the Bose-Stoner or "spin only" value $[4S(S+1)]^{1/2}$. A further deduction is that the orbit-spin interaction causes the state Γ_2 to interact with components of Γ_4 and Γ_5 as is seen from the threefold occurrence of Γ_5 or Γ_8 on the right-hand side of (1). This produces a sharing of properties, and in particular gives rise to an orbital contribution to the magnetic moment in the state Γ_2 which is of order

[11] H. Bethe, Ann. d. Physik **3**, 133 (1929).

λ/D. Thus the orbit-spin coupling produces, in an ion in a cubic field, departures from the Bose-Stoner value which may be either positive or negative according to the sign of λ/D.

The circumstances are not quite so simple if the state Γ_4 lies lowest. Here the orbit-spin coupling partially removes the degeneracy, so that different orientations of the spin have different energies, although, of course, it is not possible to associate a definite axial quantization of the spin with each of the levels. Thus the spin is only partially free and the orbital contribution will also be modified.

The Constant Δ

In a cubic field the quantity Δ of the Curie-Weiss formula $\chi = C/(T+\Delta)$ is given to a first approximation by the ratio of the coefficients of $1/T$ and $1/T^2$ in the expansion of the susceptibility in inverse powers of T. If we make the usual assumption that the magnetic moment in the absence of the magnetic field contains, besides low-frequency elements $M(n, n')$, only high-frequency elements, and none of intermediate frequency, it is easily shown[12] that

$$k\Delta = \left\{ \sum_{nn'} W_n \left| M(n, n') \right|^2 / \sum \left| M(n, n') \right|^2 \right\} - \overline{W}$$

the summation being over the group of levels connected by low-frequency elements, and $\overline{W}$ being their mean energy. When the level Γ_2 of the orbital problem, which is not split up by the orbit-spin interaction, lies lowest, the magnetic mean center and the energetic mean center, whose difference gives $k\Delta$ according to the last equation, necessarily coincide. Hence in this case the susceptibility is of the form $\chi = C/T$, correct to terms in $1/T^2$. To this approximation the ion in a cubic field behaves as if it were in the gaseous state.

If the level Γ_4 lies lowest, the magnetic mean center and the energetic mean center do not necessarily coincide, so that the susceptibility will in general have a term in $1/T^2$. Thus leaving aside the question of asymmetry produced by a rhombic field, which is considered in the next section, we should expect Ni and Cr to conform much more closely to Curie's law than Co, as is indeed found to be the case.

Asymmetry Due to a Rhombic Field

Let us for the moment neglect the spin. The effect of superposing a rhombic field on the cubic field is, as shown by Bethe,[11] to remove all the degeneracy in the orbital problem, the appropriate reduction being

$$\Gamma_2 = G_1, \quad \Gamma_4 = G_2 + G_3 + G_4, \quad \Gamma_5 = G_2 + G_3 + G_4, \tag{2}$$

where G_1, G_2, G_3, G_4 are the four one-dimensional representations of the rhombic group. Fig. 1 shows diagrammatically the decomposition of the levels under the various fields. The level Γ_2 is seen to be completely isolated

[12] C. J. Gorter, Arch. Musee Teyler, 7 (3), 183 (1932). This formula can readily be obtained from the equation for $k\Delta$ on page 197, reference 2, $\overline{W}$ in this case having been chosen to be zero,

from the others. The rhombic field alone, unlike the orbit-spin coupling, does not lead to a sharing of properties between Γ_2 and the other states. If Γ_2 is lowest the rhombic field does not give rise to any orbital contribution to the part of the susceptibility depending on the temperature. The part independent of the temperature is rendered slightly asymmetrical. Although no asymmetry is introduced directly by the rhombic field, the orbit-spin interaction, as we have seen, evokes an orbital contribution to the susceptibility, and this will be rendered anisotropic by the rhombic field. The anisotropy is thus a second order effect; the rhombic field may be comparatively large without producing much anisotropy. Neither the rhombic field alone nor the orbit-

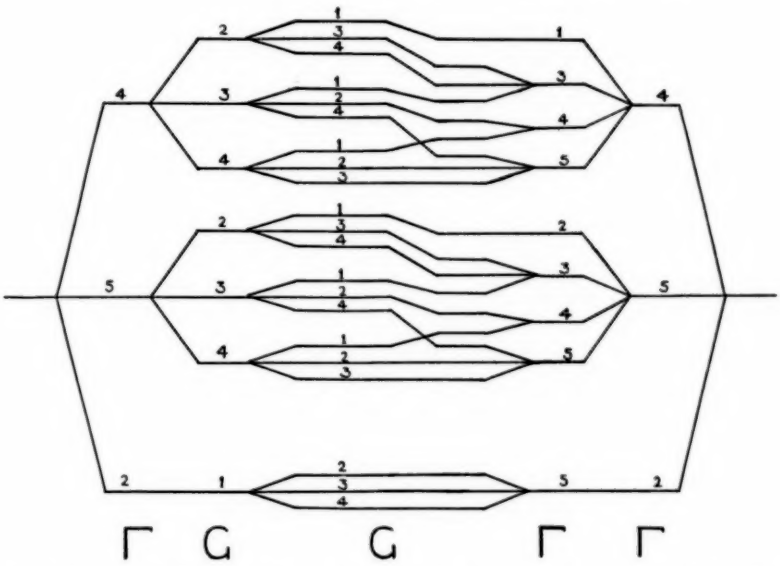

Fig. 1. Fig. 1 shows how the ^3F state in nickel is affected by the cubic field, the rhombic field and the orbit-spin coupling. By starting at the left with the free ion, the cubic field splits the single level into three, the numbers and symbols underneath denoting to which representation, in Bethe's notation, the levels belong. The application of the rhombic field splits Γ_4 and Γ_5 each into three, leaving Γ_2 single. The addition of the orbit-spin then removes all the remaining degeneracy. Making the rhombic field zero leaves only orbit-spin and cubic, the way the levels come together being shown. Removal of the orbit-spin leaves only the cubic field, and making this shrink to zero gives once again the free ion.

spin interaction alone can split the level Γ_2 of the cubic field. Both acting together will remove all degeneracy, but the separation produced will depend on a cross term and in addition is a second order effect in λ owing to the vanishing of the mean orbital angular momentum. If the level Γ_4 is lowest, these conclusions do not hold, both the anisotropy and Δ being first order effects of the rhombic field.

If Γ_2 lies lowest, as in Ni and Cr, it is possible to prove a result very similar to that which was shown to hold for the rare earths, namely that the expansion of χ for a crystal powder should contain no term in $1/T^2$. The Hamiltonian inclusive of the magnetic field is invariant for a half turn about the magnetic field. The group consisting of this operation and the identical

operation has two one-dimensional (eindeutig) representations, associated respectively with the odd and even series of values of the quantum number M. (M is not a good quantum number when the electric field and $(\boldsymbol{L}\cdot\boldsymbol{S})$ are diagonalized.) It is clear that of the three constituent levels ϵ_1, ϵ_2, ϵ_3 of Γ_2, two, (ϵ_1, ϵ_2) belong to one representation, and the third (ϵ_3) to the other. The third level has therefore no magnetic or other connection with the other two, which are linked to each other. In the presence of the magnetic field, the level ϵ_3 is unaltered, while ϵ_1, ϵ_2 undergo equal and opposite displacements away from each other. This neglects the high-frequency shift, which is practically the same for all three levels. The value of $k\Delta$ is therefore $(\epsilon_1+\epsilon_2+\epsilon_3)/3-(\epsilon_1+\epsilon_2)/2=(2\epsilon_3-\epsilon_1-\epsilon_2)/6$, an expression which is of course invariant of the origin of energy. On permuting the axes the "field free" levels ϵ_1, ϵ_2, ϵ_3 undergo a corresponding permutation; if we average the above expressions for $k\Delta$ over three cyclic permutations, which corresponds to finding the value of $k\Delta$ for a crystal powder, the result is seen to vanish.

We now turn our attention to the secular determinant of the problem in order to give the considerations of the foregoing sections a more quantitative form.

The Secular Determinant

The Hamiltonian

We assume a Hamiltonian function

$$\sum_i [D(x_i^4 + y_i^4 + z_i^4) + Ax_i^2 + By_i^2 - (A+B)z_i^2] + \lambda(\boldsymbol{L}\cdot\boldsymbol{S}) + \beta\boldsymbol{H}\cdot(\boldsymbol{L}+2\boldsymbol{S}) \quad (3)$$

where A, B, D are constants specifying the crystal field, λ is the constant of the orbit-spin interaction, β is the Bohr magneton $eh/4\pi mc$ and $\boldsymbol{H}$ is the magnetic field.

In the Hamiltonian (3) the dominant term is the term in D. The most general field of rhombic symmetry which is nearly cubic would give a Hamiltonian containing other terms in addition to those written down. These would be of higher order and no greater generality would be obtained by their inclusion. The rhombic term and the orbit-spin coupling are of comparable magnitude. The magnetic energy may always be regarded as a small perturbation in calculating the susceptibility, even though the field is strong enough to produce a Paschen-Back effect, always provided that the magnetic separations do not become comparable with kT so that saturation effects occur. This follows from an application of the principle of spectroscopic stability due to Van Vleck.[13]

The matrix elements

The following matrix elements in the (M_L, M_S) system of quantization are required. They have been obtained by the method used in the previous paper.[2]

$$D\sum_i (x_i^4 + y_i^4 + z_i^4)(M_L, M_L) = \text{const.} + q'DM_L^2[7M_L^2 + 5 - 6L(L+1)],$$

$$D\sum (x_i^4 + y_i^4 + z_i^4)(M_L, M_L \pm 4) = \tfrac{1}{2}q'D[(L \mp M_L)!(L \pm M_L + 4)!/(L \pm M_L)!(L \mp M_L - 4)!]^{1/2},$$

[13] Reference 1, page 231.

$$\sum[Ax_i^2 + By_i^2 - (A+B)z_i^2](M_L, M_L)$$
$$= \text{const.} + \tfrac{1}{2}a(A+B)[3M_L^2 - L(L+1)],$$
$$\sum[Ax_i^2 + By_i^2 - (A+B)z_i^2](M_L, M_L \pm 2)$$
$$= -a(A-B)[(L \mp M_L)!(L \pm M_L + 2)!/(L \mp M_L - 2)!(L \pm M_L)!]^{1/2}/4.$$

Here q and a are the ratios of the matrix elements calculated for a system of n electrons to those for a one-electron system; the sign of q has been discussed by Van Vleck.[4] The summation is over all the electrons of the incomplete group. The two additive constants, as well as q and a, are independent of M_L. These matrix elements are all diagonal in L. The elements non-diagonal in L are not required, since the crystal field is assumed not to destroy the Russell-Saunders coupling of the vectors $\boldsymbol{l}_i$, $\boldsymbol{s}_i$. Since the elements do not involve the spin, they may be regarded as diagonal in M_S. We also require

$$(\boldsymbol{L}\cdot\boldsymbol{S})(M_L, M_S; M_L, M_S) = M_L M_S,$$
$$(\boldsymbol{L}\cdot\boldsymbol{S})(M_L, M_S; M_L \pm 1, M_S \mp 1)$$
$$= \tfrac{1}{2}[(S \pm M_S)(S \mp M_S + 1)(L \mp M_L)(L \pm M_L + 1)]^{1/2}.$$

The secular determinant

The orbital problem, being common to all three ions Ni, Co, Cr, may be treated first. The orbital terms of the Hamiltonian are all of type $\Delta M_L = 0, \pm 2, \pm 4$, so that the secular determinant

$$\mathfrak{IC}(M_L, M_S; M_L', M_S') - \delta(M_L, M_S; M_L', M_S')W = 0,$$

breaks up into two factors, one of the fourth order involving $M_L = \pm 3, \pm 1$, and one of the third order involving $M_L = 0, \pm 2$. These factors are symmetrical about the principal and secondary diagonals, so that it is necessary to write down only the first row and central elements of the second row of each

$$\begin{vmatrix} -3Dq + 15\sigma & -15^{1/2}\delta & 15^{1/2}Dq & 0 \\ & -5Dq - 9\sigma & -6\delta & \end{vmatrix}, \quad \begin{vmatrix} -13Dq & -30^{1/2}\delta & 5Dq \\ & -12\sigma & \end{vmatrix}$$

Here σ, δ have been written for $a(A \pm B)/2$ and $q = 12q'$. The terms in D can be diagonalized[14] by means of unitary transformations SS^{-1}, TT^{-1} with

$$S = (\tfrac{1}{4})\begin{pmatrix} h & k & -k & -h \\ -k & h & -h & k \\ k & h & h & k \\ h & -k & -k & h \end{pmatrix} \quad h = 5^{1/2} \quad k = 3^{1/2} \qquad T = (\tfrac{1}{2})^{1/2}\begin{pmatrix} 1 & 0 & 1 \\ 0 & 2^{1/2} & 0 \\ -1 & 0 & 1 \end{pmatrix}$$

We may denote the matrices S, T by $S(N, M_L)$, $T(N, M_L)$. The columns are numbered by M_L having values $-3, -1, 1, 3$, for S and $-2, 0, 2$ for T. The

[14] The wave functions $S\psi$, $T\psi$ which the transformations S, T introduce are precisely those given by Bethe (reference 11, page 166). They diagonalize the cubic and rhombic fields except for matrix elements of the rhombic field between different cubic levels.

rows are numbered by a new "cubic" quantum number N which may be supposed to take on the same set of values as M_L. N has no obvious physical meaning, but served to identify the roots W_N in the cubic field according to the scheme

$$W_{-3} = W_0 = W_3 = 0,\ W_{-2} = W_{-1} = W_1 = -8Dq,\ W_2 = -18Dq.$$

The relations (2) show that the transformation which diagonalizes the terms in D will factorize the orbital problem into three quadratics and a singlet. These are

$$\begin{vmatrix} 6(\sigma-\delta) & -(15)^{1/2}(3\sigma+\delta) \\ -(15)^{1/2}(3\sigma+\delta) & -8Dq \end{vmatrix} \quad \begin{vmatrix} -8Dq & (15)^{1/2}(3\sigma-\delta) \\ (15)^{1/2}(3\sigma-\delta) & 6(\sigma+\delta) \end{vmatrix}$$

$$\begin{vmatrix} -8Dq & -2(15)^{1/2}\delta \\ -2(15)^{1/2}\delta & -12\sigma \end{vmatrix} \qquad -18Dq$$

We denote the roots of these by (r_{-3}, r_{-1}), (r_1, r_3), (r_{-2}, r_0) and r_2, where the suffix is a new "rhombic" quantum number taking on the same values as N or M_L. This set of roots is, of course, invariant if the coefficients of the rhombic field be permuted cyclically, $A \to B \to -(A+B)$ but they undergo the cyclic permutation $r_{-1} \to r_{-2} \to r_1$, $r_{-3} \to r_0 \to r_3$, while r_2 is invariant. Let the transformation matrices which diagonalize these quadratics for given values of D, A and B be

$$\begin{array}{c|cc} & -3 & -1 \\ \hline -3 & r & s \\ -1 & -s & r \end{array} \qquad \begin{array}{c|cc} & 1 & 3 \\ \hline 1 & t & u \\ 3 & -u & t \end{array} \qquad \begin{array}{c|cc} & -2 & 0 \\ \hline -2 & p & q \\ 0 & -q & p \end{array} \qquad \begin{array}{c|c} & 2 \\ \hline 2 & 1 \end{array} \tag{4}$$

The values of the elements can be calculated for any given values of D, A and B. The columns are numbered by the "cubic" quantum number N and the rows by the "rhombic" quantum number Q. We now introduce the spin and have to differentiate between Ni, Cr and Co.

Nickel

Mathematical theory

For nickel $S=1$, so that $M_S = -1, 0, 1$. The secular determinant, of order 21, breaks up into one of the tenth and one of the eleventh order, involving, respectively, even and odd values of $M = M_L + M_S$. This follows since the complete Hamiltonian contains only terms of the type $\Delta M = 0, \pm 2, \pm 4$. We are interested primarily in the root $-18Dq$ which lies below the others. It occurs once (with $M_S=0$) in the eleventh order determinant, and twice ($M_S = \pm 1$) in the tenth order determinant. Transforming the eleventh order determinant to the (N, M_S) representation, we require the element

$$\mathfrak{H}(2, 0; N', M_S') = T(2, 0; M_L, 0)\,\mathfrak{H}(M_L, 0; M_L', M_S')R^{-1}(M_L', M_S'; N', M_S'),$$

where R stands for S if $M_S' = \pm 1$, and for T if $M_S' = 0$. We have included the quantum number M_S in T and R as though they were diagonal in M_S. They are indeed independent of M_S. In the N, M_S representation the only nonvanishing elements of the orbit-spin and magnetic energies are found to be

$$\mathcal{H}(2,0;1,1) = \mathcal{H}(2,0;-1,1) = \mathcal{H}(2,0;1,-1) = -\mathcal{H}(2,0;-1,-1) = (2)^{1/2}\lambda$$
$$\mathcal{H}(2,0;-2,0) = 2\omega.$$

We know from (1) that the diagonalization of the orbit-spin terms involves the solution of cubic equations, so that it is simpler to diagonalize rhombic field terms instead. This is accomplished by the matrices (4). The relevant matrix elements in the (Q, M_S) system of representation are

$$\mathcal{H}(2,0;-3,-1) = \mathcal{H}(2,0;-3,1) = (2)^{1/2}\lambda S,$$
$$\mathcal{H}(2,0;-1,-1) = \mathcal{H}(2,0;-1,1) = (2)^{1/2}\lambda r,$$
$$\mathcal{H}(2,0;1,-1) = \mathcal{H}(2,0;1,1) = (2)^{1/2}\lambda t,$$
$$\mathcal{H}(2,0;3,-1) = \mathcal{H}(2,0;3,1) = -(2)^{1/2}\lambda\omega,$$
$$\mathcal{H}(2,0;-2,0) = 2\omega p, \mathcal{H}(2,0;0,0) = -2\omega q,$$

from which the first approximation to the energy can be found. The tenth order determinant is not quite so simple, for the root $-18Dq$ occurs twice, with $M_S = \pm 1$, the degeneracy not being removed by the rhombic field. Suppose the Hamiltonian has been transformed to the (Q, M_S) system, i.e., to the form $\mathcal{H}_0+\lambda_0\mathcal{H}_1+\omega_0\mathcal{H}_2$, where $\mathcal{H}_0$ is diagonal and $\mathcal{H}_1$ has no diagonal terms. Apply the transformation

$$(1 + \lambda S)(\mathcal{H}_0 + \lambda\mathcal{H}_1 + \omega\mathcal{H}_2)(1 - \lambda S + \lambda^2 S^2 + \cdots)$$

and choose S so as to make the coefficient of λ vanish in this expression. Then the Hamiltonian becomes

$$\mathcal{H}(n,m) = \mathcal{H}_0(n,m) + \lambda^2 \sum \mathcal{H}_1(n,i)\,\mathcal{H}_1(i,m)/h\nu(n,i) + \omega\mathcal{H}_2(n,m)$$
$$+ \lambda\omega \sum [\mathcal{H}_1(n,i)\,\mathcal{H}_2(i,m)/h\nu(n,i) - \mathcal{H}_2(n,i)\,\mathcal{H}_1(i,m)/h\nu(i,m)]$$
$$+ \cdots.$$

There are now terms in λ^2 on the diagonal which remove the degeneracy[15] and the coefficient of ω is altered by a term of order $\lambda|D$. We can now set up the quadratic secular problem connected with the two coincident roots, and solve it on the assumption that the magnetic field is small. The two resulting values of W,[16] together with that obtained from the eleventh order determinant, are given below.

$$-18Dq + 4\lambda^2(\alpha_1+\alpha_2) + \omega^2(1+8\lambda\alpha_1)/\lambda^2(\alpha_2-\alpha_3) + 4\omega^2\alpha_1,$$
$$-18Dq + 4\lambda^2(\alpha_1+\alpha_3) - \omega^2(1+8\lambda\alpha_1)/\lambda^2(\alpha_2-\alpha_3) + 4\omega^2\alpha_1,$$
$$-18Dq + 4\lambda^2(\alpha_2+\alpha_3) + 4\omega^2\alpha_1.$$

Here

$$\alpha_1 = p^2/(r_2 - r_{-2}) + q^2/(r_2 - r_0),$$
$$\alpha_2 = r^2/(r_2 - r_{-1}) + s^2/(r_2 - r_3),$$
$$\alpha_3 = t^2/(r_2 - r_1) + u^2/(r_2 - r_3).$$

[15] J. H. Van Vleck, Phys. Rev. **33**, 467 (1929).

[16] There are actually first order terms in the magnetic field of order $(\lambda^2/\text{cubic sepn.})^2$ but the contribution of these to the susceptibility is so small that they can be completely neglected.

If the axes undergo a permutation represented by $A \rightarrow B \rightarrow -(A+B)$ it is readily verified that the roots r undergo a corresponding permutation, and $\alpha_1 \rightarrow \alpha_2 \rightarrow \alpha_3$. The susceptibility along the z axis is found from the general formula

$$\chi = -(N/H) \sum(\partial W/\partial H) e^{-W/kT} / \sum e^{-W/kT}.$$

On the assumption that the exponentials can be expanded, this gives

$$\chi_1 = (8N\beta^2/3kT)[1 + 8\lambda\alpha_1 + \theta_1/kT + \cdots] - 8N\beta^2\alpha_1, \qquad (5A)$$

where terms in $1/T^3$ and above have been discarded, and

$$\theta_1 = 2\lambda^2(\alpha_2 + \alpha_3 - 2\alpha_1)/3.$$

The term independent of temperature arises as usual from the term in H^2 in the energy. The other two principal susceptibilities are obtained by permuting the axes cyclically, so that the mean of the three principal susceptibilities is

$$\bar{\chi} = (8N\beta^2/3kT)[1 + (8\lambda/3 - kT)(\alpha_1 + \alpha_2 + \alpha_3)], \qquad (5B)$$

in which there is rigorously no term in $1/T^2$.

If the crystal field is assumed to have cubic symmetry, the lowest level has a first order effect, and the susceptibility is

$$\chi = (8N\beta^2/3kT)(1 - 4\lambda/5D) + 4N\beta^2/5D. \qquad (5C)$$

Comparison with experiment

In the Hamiltonian the constant λ of the orbit-spin coupling is known, while Aa, Ba, Dq are to be determined from the observed susceptibilities. A measurement of the mean susceptibility at one temperature will enable us to determine the one parameter D if we assume as an approximation that Aa and Ba vanish. The assumption of a purely cubic field is a convenient approximation in estimating the order of magnitude of D. We shall consider later the effect of the rhombic field.

In Ni the multiplet is inverted; its over-all width is given by $|\Delta\nu| = \lambda S(2L+1)$. By using the value 2347 cm^{-1} given by Laporte[17] for $\Delta\nu$ we obtain $\lambda = -335$ cm^{-1}. The observed value 26.56×10^{-6} of the susceptibility at 170°K,[7] giving $\chi T = 45.15 \times 10^{-4}$, then leads to a value of Dq from Eq. (5) equal to 1485 cm^{-1}, which corresponds to an over-all separation due to the cubic field of the order of 3 volts. Thus according to (5) the graph of χT against T is a straight line which we have chosen to pass through the experimental point at 170°K, and which cuts the χT axis at $\chi T = 43.64 \times 10^{-4}$. If we had calculated Dq from experimental points at different temperatures, slightly different values would have been obtained. In Fig. 2 we have plotted the experimental values of χT obtained by Gorter, de Haas, and van den Handel,[7] using T as abscissa. It is seen that the experimental points, with the

[17] O. Laporte, Zeits. f. Physik **47**, 761 (1928).

exception of those at low temperatures, lie fairly close to the theoretical curve. The relation proposed by Gorter, de Haas, and van den Handel is $\chi(T+3)=\text{const.}$ In Fig. 2 we have also plotted the experimental values of $\Delta(T+3)$ as a function of T; the approximation of this function to a constant is seen to be very poor indeed. We conclude that the observations are represented much more closely by $\chi T=\text{const.}$ than by $\chi(T+3)=\text{const.}$ It should be remembered that this method of plotting the experimental data, which is equivalent to plotting the square of the effective magneton number as a function of T, is a much more severe test than plotting $1/\chi$ against T, as is usually done.

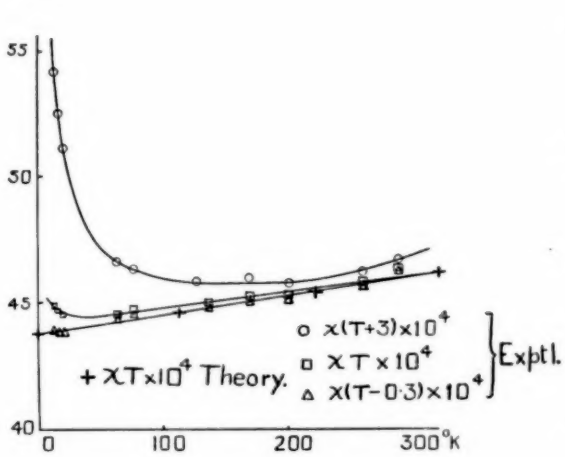

Fig. 2A.

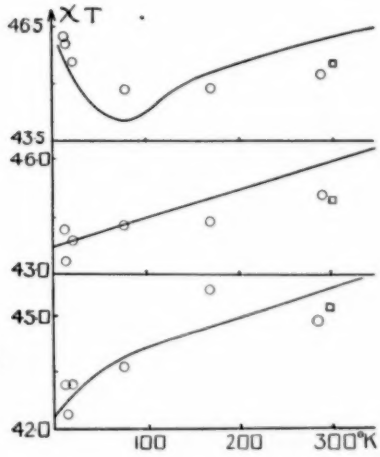

Fig. 2B.

Fig. 2. The curves in Fig. 2A serve a double purpose. In the first place they show that a formula of the type $\chi T=A+BT$ demanded by theory for Ni, represents the experimental points better than the curve $\chi(T+3{\cdot}0)=\text{const.}$ given by Gorter, de Haas and v. d. Handel.[7] In the second place it is seen that the experimental values of $\chi(T-0{\cdot}3)=\text{const.}$ fit the theoretical curve for χT exactly. The addition of -0.3 to T is a minor effect and perhaps represents the result of exchange forces not envisaged in the crystalline potential we have assumed. The one arbitrary parameter in the theory has been chosen to fit the observed magneton number at 170°K. The slope of the χT curve is then uniquely determined and its agreement with experiment is a good confirmation of the theory. Fig. 2B shows the theoretical principal susceptibilities χT of Ni plotted against T, and the experimental points of Jackson corrected by Gorter, de Haas and v. d. Handel,[7] which are marked in circles (see text).

There still remains the deviation of the three low temperature points from the theoretical curve. The present calculation takes no account of intermolecular actions, such as exchange effects, which are not describable by an electric field of definite symmetry. These effects are known to be capable of giving rise to a term Δ which will however be small on account of the high dilution of the salt. This correction will be important at low temperatures. If we plot $\chi(T-0.3)$ against T, the experimental points are brought to lie much more nearly on a straight line. It may be that the term $\Delta=0.3°$ is a measure of inter-molecular actions other than the crystal fields here contemplated,

We must now consider the effect of the rhombic field in producing asymmetry in the principal susceptibilities. Using Rabi's[5] values for $NiSO_4(NH_4)_2SO_4 \cdot 6H_2O$ and equating them to the three expressions obtained by permuting cyclically the indices in (5A), we obtain three simultaneous equations for α_1, α_2, α_3, whose solution is

$$\alpha_1 = -7.94 \times 10^{-5},\ \alpha_2 = -8.12 \times 10^{-5},\ \alpha_3 = -8.29 \times 10^{-5}.$$

From these we have to determine the three parameters Dq, Aa and Ba which specify the crystal field. To set up and solve the algebraic equations connecting these parameters with the α's would be very lengthy, so we have to recourse to the method of trial and error. Thus we find that a crystal field having the Hamiltonian

$$1260(x^4 + y^4 + z^4) + 176(x^2 + 2y^2 - 3z^2)$$

gives

$$\alpha_1 = -7.96 \times 10^{-5},\ \alpha_2 = -8.13 \times 10^{-5},\ \alpha_3 = -8.24 \times 10^{-5}.$$

Better agreement could be obtained by using a slightly larger value of the constant of the rhombic field and by changing the ratios of the coefficients of the rhombic field, but it is not, perhaps, worth while pursuing numerical accuracy when the experimental precision is not very high. It is instructive, particularly for comparison with cobalt, to observe how little dissymmetry is produced by a comparatively large rhombic term. Thus the field given above produces an over-all separation of the cubic level Γ_4 amounting to about one-half the interval separating this cubic level from the level Γ_5. The separation produced in the level Γ_2 has an over-all width of 1.5 cm^{-1} so that the individual values of Δ for the three axes are almost negligible, and the expansions of the exponentials which we have used is legitimate even at liquid hydrogen temperatures. At extremely low temperatures Δ is relatively important and it is this fact that accounts for the different behavior of the principal χT for small values of T, shown in Fig. 2B.

Gorter, de Haas and v. d. Handel[7] have given values of the principal susceptibilities of $Ni(SO_4) \cdot 7H_2O$ using their own values of the mean susceptibility together with the differences in the principal susceptibilities found by Jackson.[6] The exactitude of these values is open to question, but to illustrate how they check with the theory we have plotted the experimental values (shown by circles) and the theoretical curves *using for the constants of the crystal field those values found for* $Ni(SO_4)_2(NH_4)_2 \cdot 6H_2O$. The agreement is very good, considering the sensitivity of the method of plotting the results, and the experimental results confirm the existence of a $1/T^2$ term for the individual axes although there is none in the mean. The values found by Rabi[5] on the ammonium salt are marked by squares. Since, as far as we can tell, the constants of the crystal field acting on the Ni ion are exactly equal in the two salts, it seems likely that the ions surrounding the Ni ions are the same and in the same relative positions in the two salts.

Chromium

Chrome alum, whose susceptibility at temperatures down to that of liquid helium has been measured by de Haas and Gorter,[9] forms cubic crystals, so that no differences in the principal susceptibilities are to be expected.[18] It will be sufficient to suppose the crystal field to have cubic symmetry. Van Vleck[14] has shown that for Cr, whose ground state is ${}^4F$, the matrix elements of $\sum_i (x_i^4 + y_i^4 + z_i^4)$ have the same sign as those of $(x^4 + y^4 + z^4)$ calculated for a single electron system; that is the coefficient q is positive. The root $-18Dq$ (Γ_2) is accordingly lowest. The secular problem inclusive of spin is of order 28; but on account of the selection rule $\Delta M = 0, \pm 2, \pm 4$, obeyed by the Hamiltonian ($\Delta M = 0, \pm 4$ if the rhombic field is absent) the secular determinant breaks up into the product of two, which are identical except as regards the sign of the terms in H. This is, of course, an example of the Kramers degeneracy.[19] Reference to the diagram in Bethe[11] shows that the orbit-spin interaction is incapable of removing the degeneracy of Γ_2 in any approximation, so that we need consider only the terms in H, which give rise to first and second order Zeeman effects. Fixing our attention on one of the two secular determinants of order 14, we observe first of all that the root Γ_2 occurs twice ($N = 2$, with $M_S = -\frac{1}{2}, \frac{3}{2}$, say). In passing from the original M_L, M_S representation to that in which the cubic field is diagonal, the spin terms $2M_S$ will of course remain on the diagonal, so that the two occurrences of the root Γ_2 have first order moments 3ω and $-\omega$ from this determinant and -3ω and ω from the other. If this were all, the magneton number would have the "spin only" value $(15)^{1/2}$, verifying that the spin is free. But we have still to consider the off-diagonal terms involving ω, which represent the contribution of the orbit, and which are diagonal in M_S. We readily find for the elements satisfying this condition

$$\mathfrak{H}(2, -\tfrac{1}{2}; -2, -\tfrac{1}{2}) = -\lambda + 2\omega$$

$$\mathfrak{H}(2, 3/2; -2, 3/2) = 3\lambda + 2\omega$$

which gives for the levels in the presence of the field

$$-\omega(1 - 2\lambda/5Dq) - 2\omega^2/5Dq,$$

$$\pm 3\omega(1 - 2\lambda/5Dq) - 2\omega^2/5Dq.$$

Disregarding the high-frequency term for the moment, we obtain for the susceptibility

$$\chi = (15N\beta^2/3kT)(1 - 2\lambda/5Dq)^2.$$

[18] The chrome alum $KCr(SeO_4)_2 \cdot 12H_2O$, which forms cubic crystals has in its absorption spectrum a narrow doublet whose separation is roughly 4 cm^{-1} (cf. K. Schnetzler, Ann. d. Physik **10**, 373 (1931)). If this doublet is due to the doubling of the basic level Γ_2, the Hamiltonian must contain non-cubic terms, besides the predominant cubic terms. This follows since the orbit-spin coupling does not decompose Γ_2. If this is so, this alum should exhibit slight asymmetry in its principal susceptibilities.

[19] H. A. Kramers, Proc. Amst. Acad. **33**, 959 (1930).

Here λ is positive, so that the magneton number should be less than the "spin-only" value, which is actually found to be the case. From the value 912 cm^{-1} given by Laporte[17] for the over-all separation of the ^4F multiplet in chromium, we deduce $\lambda = 87$ cm^{-1} and taking de Haas and Gorter's[9] value 19.02 for the Weiss magneton number of Cr, we obtain $Dq = 3730$ cm^{-1}. This justifies our neglect of the high-frequency term, which is proportional to λ/D. The experimental results do not show any trace of high-frequency effects. It is not possible to place much reliance on the above estimate of the magnitude of the separation due to the cubic field, since a small change in the experimental magneton number would produce a very considerable change in the calculated value of Dq. It need scarcely be pointed out that for Cr, as for Ni, the introduction of even a large rhombic field will not appreciably affect the isotropy of the susceptibility. As yet, however, no measurements have been made on the principal susceptibilities of Cr salts.

Cobalt

Mathematical theory

It may be stated here that our calculations on Co are not as complete as those on Ni and Cr, but the difficulties are only in the numerical computation. There seems to be no doubt, however, that good agreement with experiment could be obtained by a more exhaustive trial-and-error procedure. The ground state of cobalt is ^4F, and the secular determinant is of order 28. On account of the Kramer's degeneracy, it breaks up into two determinants of order 14, identical except for the sign of the terms in the magnetic field. The orbital part of the problem is the same as for nickel, where the ground state was also an F state, so that in a cubic field the roots are 0, $-8Dq$, $-18Dq$. On account of the inversion discussed above, the level 0 (denoted Γ_4 above) is now lowest, and occurs six times in each secular determinant of order 14, namely, with $N = -3$, 0, 3 and $M_S = \frac{3}{2}$, $\frac{1}{2}$ or $-\frac{3}{2}$, $-\frac{1}{2}$. The portion of the determinant involving these roots, which coincide in the absence of a rhombic field and orbit-spin coupling, is

$$\begin{vmatrix} 6B - 3l\omega & -3m + 3\omega/2 & 0 & 0 & n & 0 \\ -3m + 3\omega/2 & 6A - 3l\omega & 0 & 0 & -n & 0 \\ 0 & 0 & 6B + l\omega & m + 3\omega/2 & 2m & n \\ 0 & 0 & m + 3\omega/2 & 6A + l\omega & 2m & -n \\ n & -n & 2m & 2m & 6C - \omega & 0 \\ 0 & 0 & n & -n & 0 & 6C + 3\omega \end{vmatrix} \tag{6}$$

Here $l = 1 + 15\lambda/32D$, $m = 3\lambda/4$, $n = 3(3)^{1/2}\lambda/4$. Interaction between the levels $0, -8Dq, -18Dq$ has been taken account of with sufficient accuracy by the diagonal terms in $\omega\lambda/D$. This amounts to discarding the high-frequency part of the susceptibility; if we do this we may restrict ourselves to this sixth order determinant in calculating the levels. As the sextic secular equation is not soluble when the rhombic field is comparable with the orbit-spin coupling,

we must assume that the former is much smaller than the latter or *vice-versa*. Our calculations indicate that the two influences are in fact of comparable magnitude, which makes close numerical agreement difficult to obtain without more elaborate computations. Here we deal with the two extreme cases only.

Orbit-spin greater than rhombic field

Consider first the case where the orbit-spin coupling is greater than the rhombic field. The orbit-spin interaction alone is capable of partially removing the degeneracy in (6). When we do not restrict ourselves to interactions within the sextet the degeneracy which survives the cubic field and the orbit-spin interaction is given by the resolution $\Gamma_4 D_{3/2} = \Gamma_6 + \Gamma_7 + 2\Gamma_8$, i.e., two singlets and a quadratic occurring twice. When we restrict ourselves to interactions within the sextet the degeneracy must at least be as great as this, which ensures that the sextet will have simple roots when σ, δ, ω all vanish. These are readily found to be $15\lambda/4$, $3\lambda/2$ (twice), $-9\lambda/4$ (three times), and the corresponding form of the sextet, with these roots on the diagonal, can easily be written down. The energy levels in the presence of the magnetic field have now to be found on the assumption that the rhombic field is small compared with the orbit-spin interaction. In cobalt $\lambda = -180$ cm^{-1} so that the triply degenerate level $-9\lambda/4$ will have such a small Boltzmann factor that its contribution to the susceptibility may be neglected even at room temperatures; this level does not affect the moment of the level $15\lambda/4$, and in calculating its influence on the moment of the levels $3\lambda/2$, which is relatively less important in any case, we may suppose it to remain undecomposed by the rhombic field. But in obtaining the moments of the two levels $3\lambda/2$, it is necessary to allow the rhombic field to remove this degeneracy. We have calculated the level $15\lambda/4$ correct to a third order approximation and the two levels $3\lambda/2$ to a second order approximation.[20] The calculation is straightforward but too elaborate to be given here. To illustrate the type of result obtained, we give the energy levels in the presence of the magnetic field only for the lowest level, correct to a second order perturbation calculation. For brevity the third order terms have been omitted. We find

$$W = 15\lambda/4 - \omega(13/6 + 5\lambda/8D) + [(36\sigma - 35\omega - 165\lambda\omega/16D)^2 + 432\delta^2]/405\lambda + \cdots.$$

The expressions for the other levels are of the same type.

At sufficiently low temperatures the square of the effective Bohr magneton number $n_B^2 = 3\chi kT/N\beta^2$ is given by three times the square of the coefficient of the term in H. Hence, if we extrapolate the experimental values of χT to $T=0$, we obtain three equations which theoretically enable us to determine σ, δ and D. The values obtained in this way are however so sensitive to variations in χT at $T=0$ within the range of possible error that it is

[20] The details of the inclusion of the third order terms in the perturbation problem will be considered by Mr. Jordahl in his paper on Cu.

preferable to proceed differently. The argument of Van Vleck[4] shows that if the cubic field acting on the metallic ion be the same in nickel ammonium sulphate as in cobalt ammonium sulphate the constant Dq has the same value numerically. We accordingly assume $Dq = -1200\ \text{cm}^{-1}$, thereby giving up the possibility of obtaining values of σ and δ for arbitrarily given values of $(\chi T)_0$; instead we assume values for σ and δ and calculate the susceptibilities at various temperatures. The values which have been chosen for illustration are $\sigma = \delta = 20$, corresponding to a term $40(x^2 - z^2)$ in the Hamiltonian, which gives roughly the right degree of asymmetry. It is of course possible to choose different values for the individual coefficients of x^2, y^2, z^2, but the computations are laborious and do not give any new information. Two points deserve mention. In the first place, a much smaller rhombic field is required in cobalt salts to produce the observed asymmetry than is needed for nickel salts despite the much greater isotropy of the latter. In the second place the calculated mean susceptibility for the three orientations is consistently greater than that observed. Fig. 3A shows the calculated values of $n_B^2 = 3kT\chi/N\beta^2$ plotted against T for the three magnetic axes of $Co(NH_4)_2(SO_4)_2 \cdot 6H_2O$. The trend of these curves may readily be understood in a qualitative way. At low temperatures the only level contributing to the susceptibility is the lowest. Since this has both a first and a second order Zeeman effect $\chi T = a + bT$, a and b being constants. At higher temperatures the two states $3\lambda/2$ begin to contribute to the susceptibility, but this is counteracted by the depopulation of the lowest level; these higher levels have smaller Zeeman effects than the levels $15\lambda/4$ so that the curve of χT against T rises less steeply and tends to an almost constant value. At still higher temperatures the three levels $-9\lambda/4$ would also contribute to the susceptibility but these temperatures are not reached experimentally.

The value of n_B^2 is plotted also for the case where there is no rhombic field and this curve is shown dotted in Fig. 3A. It should be noticed that the effect of the rhombic field is to produce asymmetry and also to lower the mean value of the three principal susceptibilities.[21] Unfortunately, it is not within the limits of the present approximation to make the rhombic field sufficiently large to give agreement with experiment, as then the convergence would be poor. It is very reasonable, however, to suppose that a larger

[21] Let us imagine the magnitude of the rhombic field is varied from a very large value down to zero. The behavior of the three principal susceptibilities is as follows. Orientation (3) starts at the "spin only" value, decreases and then starts to increase again, finally ending on the curve for zero rhombic field shown in Fig. 3A. Orientation (2) starts slightly above the "spin only" value due to the introduction by the orbit spin coupling of small diagonal elements in the orbital angular momentum, representing the contribution of the higher cubic levels, and then decreases at low temperatures but increases at higher temperatures, ending finally with (3). Orientation (1) is rather complicated. It starts with (2) but the susceptibility increases rapidly with decreasing rhombic field, and develops a hump at low temperatures. This is because for this orientation the lowest level has a large first order Zeeman effect. The susceptibility then begins to fall again, passing through a representative curve shown in Fig. 3B. The hump fades out, the susceptibility decreasing at low and increasing at high temperatures, finally ending with (2) and (3).

rhombic field would give good agreement with experiment, except possibly at low temperatures. Since the only measurements at low temperatures are those of Jackson,[6] made as long ago as 1922, and which at other temperatures are known to be greatly in error, this discrepancy is not worth considering. When better experimental data are available another effort will be made to obtain a better solution of this troublesome sextet.

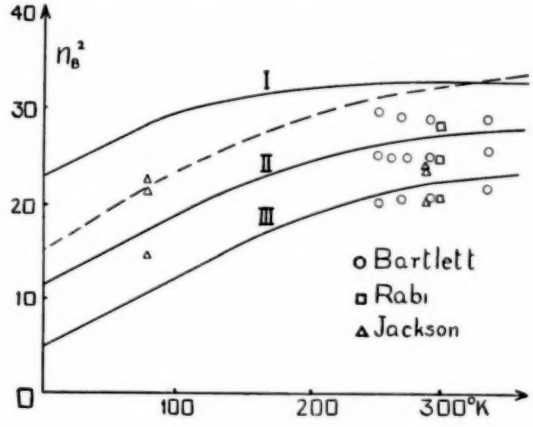

Fig. 3A.

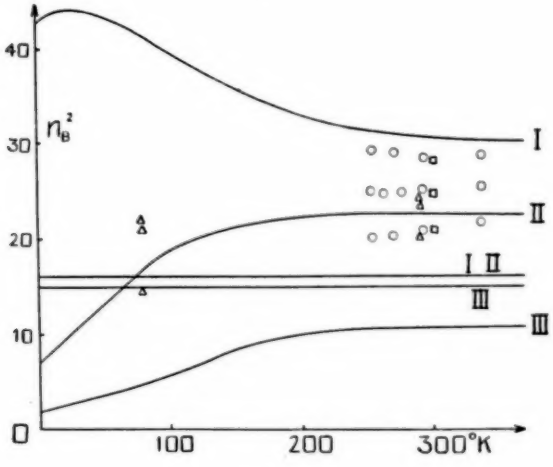

Fig. 3B.

Fig. 3. The heavy lines in Figs. 3 show the calculated values of nB^2 for Co $(NH_4)_2(SO_4)_2 \cdot 6H_2O$ for the two rhombic fields (3A) $40(x^2-z^2)$ (3B) $200(x^2-z^2)$, while for comparison, the experimental points obtained by different observers are given. The numbers on the curves denote the axes to which the curves refer. The dotted lines in Fig. 3A is for zero rhombic field; the horizontal straight lines in Fig. 3B are for extremely large rhombic fields. It is reasonable to suppose that a rhombic field intermediate to the values we have taken would give agreement with experiment. It is significant that the results of Bartlett[8] along axis (1) do actually seem to be falling with increasing T, as would be the case for an intermediate field. The agreement at low temperatures is not good but the experimental values are those of Jackson[6] and may easily be in error.

Rhombic field greater than orbit-spin

In the hope that a perturbation calculation from the other limiting case would be more effective, calculations were also made from this end. Here the orbit spin is subsidiary to the rhombic field. The rhombic field can be seen to decompose the sextuply degenerate level into three doubly degenerate ones, with separations proportional to the coefficients of the rhombic field. The orbit-spin interaction does not remove the remaining degeneracy in the first approximation, but only in the second. Expressions for the energy levels and their first and second order Zeeman effects can be written down, and the susceptibility calculated for given values of the constants D, A, B, C of the crystal field, such that the rhombic field alone produces a separation which is small compared with that due to the orbit-spin alone. In the absence of the spin the energy levels are $6Aa$, $6Ba$, $-6a(A+B)$. We suppose that $-6a(A+B)$ lies below $6Aa$ and $6Ba$ and calculate the Zeeman effects of the two lowest roots correct to a third approximation, retaining terms in the magnetic field up to H^2, in the usual way. The Zeeman effects are different according as the magnetic field acts along the x, y, or z axes. The exact expressions are long, but for illustration we give the two lowest roots, when the magnetic field acts along the x, y and z axes, correct only up to a second order perturbation calculation. For brevity the third order terms have been omitted.

$$\left.\begin{aligned} W_{\pm}(x) &= W_{\pm} - \omega_{+}[1 \pm (\alpha + 2\beta)\theta] \pm 2\omega_{+}{}^{2}\alpha^{2}\theta^{3}/3\lambda^{2}, \\ W_{\pm}(y) &= W_{\pm} - \omega_{-}[1 \mp (2\alpha + \beta)\theta] \pm 2\omega_{-}{}^{2}\beta^{2}\theta^{3}/3\lambda^{2}, \\ W_{\pm}(z) &= W_{\pm} + \omega[1 \pm (\alpha - \beta)\theta] \pm 2\omega^{2}\theta^{3}(\alpha + \beta)^{2}/3\lambda^{2} \end{aligned}\right\}$$

where

$$\begin{aligned} W_{\pm} &= -6a(A + B) + 45\lambda^{2}(\beta - \alpha)/16 \pm 9\lambda^{2}\theta/4, \\ \theta &= (\alpha^{2} + \beta^{2} + \alpha\beta), \ \omega_{+} = \omega(1 + 9\lambda/128D + 9\lambda\beta/4), \\ \omega_{-} &= \omega(1 + 9\lambda/128D - 9\lambda\alpha/4). \end{aligned}$$

We have written $\alpha = 1/6a(B-C)$ and β, γ for the cyclic permutations. From these expressions the principal susceptibilities may be calculated. For illustration, a rhombic field represented by $200(x^2-z^2)$ in the Hamiltonian has been taken. The result is shown by the curves in Fig. 3B. It is readily verified that the curves correspond with those in Fig. 3A as shown by the numbering. The values of $n_B{}^2$ for a very large rhombic field are also shown by the horizontal straight lines. These are only limiting curves, however, since we have assumed the cubic field to predominate and therefore we cannot make the rhombic field as large as we please.

We have now calculated the susceptibilities (*i*) for a rhombic field $40(x^2-z^2)$ (*ii*) for a rhombic field $200(x^2-z^2)$, inclusive of orbit-spin coupling in both cases. The latter alone produces an over-all splitting of the level Γ_4 of the cubic field amounting to roughly 1000 cm^{-1}, while the separations produced by fields (*i*) and (*ii*) are respectively 480 cm^{-1} and 2400 cm^{-1}. The principal susceptibilities calculated on the basis of field (*i*) show roughly the

right degree of asymmetry, but are too high. Interpolating between (*i*) and (*ii*), it seems that a rhombic field of magnitude intermediate between (*i*) and (*ii*), but much nearer (*i*), will give good agreement with experimental values, except possibly at low temperatures, where however, the experimental values are in considerable doubt. Neither of the two methods of approximation used above are applicable in this intermediate region and the calculation would consist in the numerical solution of the original sextic secular equation.

It is interesting to notice that there would have been no gain in generality if we had added to the Hamiltonian terms representing a field of tetragonal symmetry or terms of rhombic symmetry of higher degree, provided the field of cubic symmetry always predominates. In order to see this we need only observe that in the orbital problem the lowest level Γ_4 of the cubic field is split by the rhombic field into the three levels G_2, G_3, G_4, no two of which belong to the same representation of the rhombic group. Consequently it is not possibly to change the moments of these levels by changing the type of rhombic field nor can this be accomplished even by the superposition of a tetragonal field, since this is only a particular form of rhombic field. Because the moments are fixed, the susceptibility can be changed only through the relative position of the energy levels and as there are three levels, it needs only two parameters to specify them. The two parameters A and B are capable of doing this.

Conclusion

In the present paper no account has been taken of the variation with temperature of the constants of the crystal field. The very small changes in interatomic distances caused by thermal expansion may possibly affect these constants quite appreciably because the force between ions in a crystal is known to vary very rapidly with the distance. We have moreover assumed that the principal axes of the various types of crystalline fields all coincide. Perhaps a better approximation to the actual state of affairs would be to assume fields of different symmetry, whose principal axes were inclined to each other, the relative orientations depending on temperature in some complicated way. There would then arise the possibility of an explanation of the results of Bartlett,[8] who finds that the orientation of the principal susceptibilities relative to the crystallographic axes depend on temperature, the total variation being of the order of 5 degrees in a range of temperature 100°C.

From the considerations developed in this and the preceding paper, it should be evident that it is only rarely that the constant Δ of the experimenters has any theoretical interpretation. In order that it may have, it is necessary that the expansion $\chi = C/T - C\Delta/T^2 + \cdots$, should converge very rapidly. This condition may be expressed in another form, that the Stark separations of the levels contributing to the susceptibility should be small compared with kT. This is not satisfied in the rare earths nor with Co but our calculations have shown that it is satisfied with Ni and Cr. That the susceptibility of the rare earths can be represented by the Curie-Weiss law

is merely fortuitous. Even here the value of Δ obtained depends on the temperature at which the measurements are made and in this sense Δ has no theoretical significance.

One of the most surprising facts revealed by our calculations of the susceptibilities in crystals is that a field of cubic symmetry should be capable of allowing such excellent agreement to be obtained with experiment. At first sight there seems to be no reason whatever for the field to possess cubic, or even nearly cubic, symmetry. In the case of Ni it was definitely established that a field predominantly rhombic and of the form $Ax^2+By^2-(A+B)z^2$, was incapable of giving the observed principal susceptibilities. The next assumption is naturally a field of cubic symmetry together with a much smaller rhombic term, an assumption which has proved completely successful with Ni, Cr and Co. For the rare earths, where measurements of the principal susceptibilities are lacking, and only the variation with temperature of the mean susceptibility has been observed, good agreement with experiment is obtained on the assumption of a cubic field alone. Without understanding why complicated crystals should have such simple crystalline fields, it must at least be conceded that the evidence in favor of a predominant field of cubic symmetry is strong. Whether or not there are other types of field which will give equally as good agreement with experiment remains to be seen.

In our calculations of paramagnetic susceptibilities, both of the rare earths and of the elements of the iron group, the sign of D in Eq. (3) has been consistently positive. In a Letter to the Editor[22] Gorter finds that this choice of the sign of D agrees with there being water molecules (or else oxygen ions) arranged at the corners of an octahedron around the paramagnetic ion.

The writers wish to place on record their thanks to Professor J. H. Van Vleck, to whose constructive and stimulating criticisms the present work owes a great deal.

[22] C J Gorter, Phys. Rev. **42**, 437 (1932).

Diamagnetism of Water at Different Temperatures

By A. P. WILLS AND G. F. BOEKER
Department of Physics, Columbia University

(Received October 10, 1932)

Attention is called to the discordant results found by different observers for the diamagnetism of water at different temperatures. A new and very sensitive device called a manometric balance is described. The device was designed for the purpose of investigating the variation of the specific susceptibility of water with varying temperature. Experiments with water which had just been boiled in order to get rid of dissolved air indicated less diamagnetism at temperatures higher than 23.5°C; and experiments upon water which was boiled and left standing for several days in contact with helium gas indicated greater diamagnetism at temperatures higher than 23.5°C; the change in the specific susceptiblity was less than one percent in each case.

THE subject of the present communication has already received considerable attention from various experimentalists. The results obtained by different investigators,[1] using different methods, are not in agreement; in fact, the variations found for the specific susceptibility of water do not always agree as regards sign; for example, Piccard, using a modified Quincke method, found that the diamagnetism of water is greater at higher temperatures, while Cabrera and Duperier, using a torsion method, found it to be less. The magnitudes of the variations found were in all cases less than 3 percent of the specific susceptibility (susceptibility per unit mass) of water at 20°C, which from previous absolute measurements is known to have a numerical value of -0.72×10^{-6}, approximately, in c.g.s. units.

At a recent meeting[2] of the French Academy a summary of the results obtained by the various investigators referred to above was presented in the form of a diagram. This diagram on a somewhat different scale is reproduced in Fig. 1, a curve representing the results of Mathur, obtained in 1931, being added. The lack of agreement in the results obtained by these investigators for the diamagnetism of water at different temperatures is very remarkable, and the reasons therefore seem very obscure.

The purpose of the present paper is to describe a new method for the investigation of the phenomena in question, and to present the results of some preliminary experiments which may serve to throw some light upon the anomalous results previously obtained.

The device which we employ is called a manometric balance and operates on the principle of balancing the actions of two magnetic fields, one acting upon water at some specified temperature and the other upon water at a

[1] Du Bois, Wied. Ann. **95**, 167 (1888); Jager and Meyer, Wied. Ann. **67**, 427, 707 (1899); Piaggesi, Phys. Zeits. **4**, 347 (1905); Piccard, C. R. **155**, 1497 (1912); Marke, Bull. Acad. Danemark p. 395 (1916); Cabrera and Duperier, Jour. d. Physique et le Radium **6**, 121 (1925); Mathur, Ind. Jour. Phys. **15**, part 3, 207 (1931).

[2] See Comptes Rendus **191**, 589 (1930).

standard temperature. The theory of the balance will be given after the apparatus itself has been described.

The Manometric Balance

In Fig. 2 the letter M designates one of the two coaxial cores of an electromagnet, each core being about 10 cm in diameter, and M_1, M_2 designate two of four equal pole-tips in the forms of truncated cones, cemented on M; the smaller circular faces of these pole-tips were about 1.5 cm in diameter. The second core M' (not shown in the figure) is also provided with two pole tips M_1', M_2' (not shown in the figure) facing M_1, M_2; the gaps between M_1, M_1' and M_2, M_2' were approximately 1 cm in length.

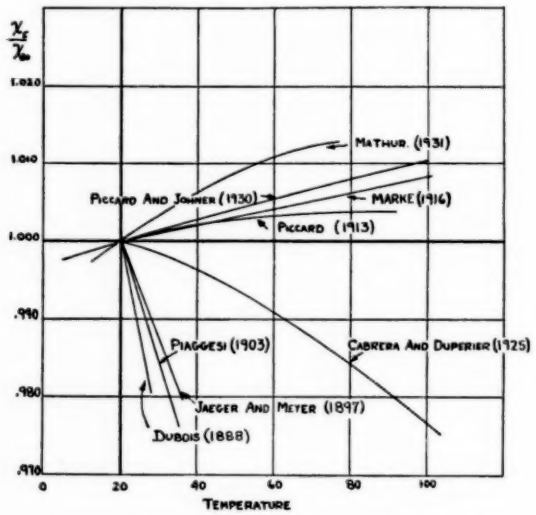

Fig. 1. Summary of results obtained for χ_t/χ_{20}.

The manometric balance itself is made of Pyrex glass throughout, and consists of two branches, a left branch and a right branch. Its essential features are represented in Fig. 2 with designations whose significance is given in the legend below the figure.

The procedure of filling and adjusting the balance is as follows. After mercury has been introduced to the same level in the bulbs E_1, E_2, the stopcock connecting these bulbs is closed, and liquids are then admitted to the two branches through the filling-funnels A_1, A_2. After the liquids have reached the tubes t_1, t_2 at the bottom, the 3-way stopcocks B_1, B_2 are so set as to connect each branch with a corresponding mercury cup which, by a vertical adjusting screw C_1, or C_2, can be raised or lowered so as to bring the corresponding meniscus m_1, or m_2, to approximately the desired position in the meniscus tube t_1, or t_2, between the pole-tips M_1, M_1', or M_2, M_2'. The stopcocks B_1, B_2 are then closed and further adjustments of the menisci m_1, m_2 are made by varying the currents through the resistance coils designated in the figure as coil 1 and coil 2, whereby expansion or contraction of the portions of the liquid columns which they enclose is produced.

The liquid used in the right branch was water at the standard temperature T_0, (23.5°C), and in the left branch water at some temperature T, or a calibrating solution of nickel chloride at the standard temperature.

The positions of the menisci with respect to their respective pole-tips are determined by two telescopes (not shown in the figure) provided with micrometer eyepieces.

The right branch of the balance is connected with a funnel F through which water containing suspended particles of anise oil can be admitted when desired, the motion of which in the capillary tube designated *Cap*

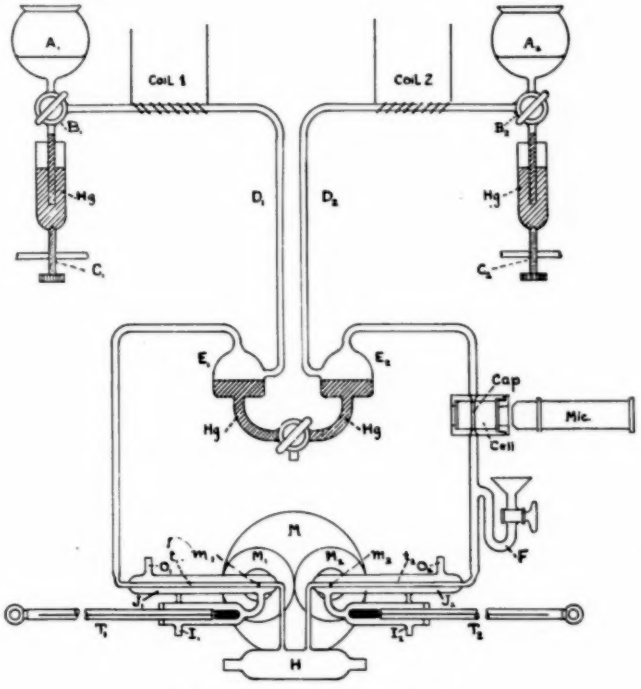

Fig. 2. Manometric balance.

A_1, A_2—Filling funnels	H —Helium container
B_1, B_2—3-way stopcocks	Hg —Mercury
C_1, C_2—Adjusting screws	I_1, I_2 —Inlets for water jackets
Cap —Capillary tube	J_1, J_2 —Water jackets
Cell —Canada balsam container	M —Core of electromagnet
Coil 1 —Resistance coil	M_1, M_2—Pole tips of electromagnet
Coil 2 —Resistance coil	m_1, m_2 —Menisci of liquids
D_1, D_2—Auxiliary tubes	O_1, O_2 —Outlets for water jackets
E_1, E_2—Equilibration bulbs	t_1, t_2 —Menisci tubes
F —Inlet funnel	T_1, T_2 —Thermometers

could be observed through the microscope designated *Mic.* The device designated *Cell* through which the capillary tube passes is essentially a tube of brass provided with glass ends and filled with Canada balsam.

The letter J_1 designates a jacket enclosing the meniscus tube t_1, provided with an inlet tube I_1 and an outlet tube O_1, through which liquid at any de-

sired temperature can be passed for the purpose of regulating the temperature of the water or other liquid in the meniscus tube t_1. The letters J_2, I_2, O_2 have a similar significance with respect to the meniscus tube t_2. The letters T_1, T_2 designate thermometers which serve to indicate the temperatures of the liquids in the menisci tubes t_1, t_2.

The manometer is mounted on a slate frame which is supported in a vertical plane perpendicular to the axis of the magnet by a suitable cast-iron structure, the latter being bolted to the cement base upon which the magnet rests.

The method of operation of the balance is exemplified by the procedure followed when pure water is under experimentation. While the temperatures of the water in the menisci tubes t_1, t_2 are maintained at the standard temperature T_0, the positions of the menisci m_1, m_2 are varied until a balance is obtained as estimated by the lack of motion, upon throwing on and off the magnetic fields, of the suspended particles in the capillary tube, observed through the microscope *Mic*. The two magnetic fields acting upon the menisci m_1, m_2 are then the same, H_0, say. These positions of the menisci are called their zero-positions. Upon changing the temperature of the water in the meniscus tube t_1, the balance is destroyed; a new balance is obtained upon moving the meniscus m_2 (by varying the currents through coil 1 and coil 2) through a distance D, say, into a slightly stronger or weaker field H, say, as required. During this procedure the meniscus m_1 is kept in its fixed zero-position. The distance D through which the meniscus m_2 is moved in order to effect a balance is measured by the micrometer telescope focussed upon it.

The field H relative to H_0 is derived from a calibration curve, obtained by substituting for the water in the left-branch dilute solutions of nickel chloride at the temperature T_0 and of different known concentrations.[3]

Sensitivity of Balance

In calculating the sensitivity of the balance, we suppose that the water columns in the menisci tubes have the same cross sections, a; that the mercury columns in the bulbs E_1, E_2, have the same cross sections b; and that the water column in the capillary tube *Cap* has a cross section c. Furthermore, we suppose that the menisci tubes are each inclined downwards at an angle θ to a horizontal plane.

Assuming an initial state of equilibrium, if we let Δl denote the apparent displacement, observed in the microscope *Mic*, of a suspended particle in the capillary tube *Cap* due to a difference of pressure Δp on the menisci m_1, m_2, then the sensitivity S, say, of the balance will be proportional to $\Delta l/\Delta p$. A simple calculation shows that:

$$S = \frac{\alpha}{g}\,\frac{a}{c}\left[\rho_m \frac{a}{b} - \rho_w\left(\frac{a}{b} + \sin\theta\right)\right]^{-1} M, \tag{1}$$

[3] The method does not require a knowledge of the absolute values of H and H_0; in our experiments these values were probably in the neighborhood of 18,000 c.g.s. units.

where α is the factor of proportionality, g the acceleration due to gravity, ρ_m, ρ_w the densities of mercury and water, respectively, and M the magnifying power of the microscope. It can also easily be shown that the condition for stable equilibrium is:

$$\sin\theta < (a/b)(\rho_m/\rho_w - 1).$$

For the special case in which the menisci tubes are horizontal we have sin $\theta=0$, and hence:

$$S = \alpha(b/c)(\rho_m - \rho_w)^{-1}M. \tag{2}$$

For the balance used in our experiments: $\theta=0$, and $a=0.070$, $b=34.0$, $c=0.0064$, $M=400$, $\rho_m=13$, $\rho_w=1$, approximately, in c.g.s. units. The proportionality factor α could be determined without great trouble if desired.

The sensitivity of the balance used by us is such that changes in the susceptibility of water as small as one ten-thousandth part can easily be detected.

We estimate, with the aid of Eq. (2), that the sensitivity of our balance could easily be increased one thousand times but, owing to vibrational disturbances, this would not be feasible.

Theory of the Method

Let κ, κ_0 designate volume susceptibilities of water at the temperatures T, T_0. When balance obtains:

$$\tfrac{1}{2}\kappa H_0^2 = \tfrac{1}{2}\kappa_0 H^2.$$

If χ, χ_0 denote specific susceptibilities and ρ, ρ_0 densities of water at the temperatures T, T_0, then $\kappa=\rho\chi$ and $\kappa_0=\rho_0\chi_0$; and hence:

$$\chi/\chi_0 = (\rho_0/\rho)(H^2/H_0^2). \tag{3}$$

We now recall that H_0 represents strength of the magnetic field at the meniscus m_1 in its zero-position, while H represents the strength of the magnetic field acting on the meniscus m_2 when it has been displaced from its zero-position by the amount D, say, necessary to obtain the balance. When the quantity $\rho_0 H^2/H_0^2$ as a function of D is known, formula (3) can be used to calculate the ratio χ/χ_0, the density ρ being taken from a table for water. A calibration curve giving this quantity as a function of D is obtained as follows:—

A water solution of nickel chloride is prepared which is neutral at the standard temperature T_0 (23.5°C). From this neutral solution several diamagnetic solutions are made, each of which is prepared by adding to a mass m of the neutral solution a mass μ of water, so that the total mass of the diamagnetic solution is $m+\mu$. If χ_n denote the specific susceptibility of such a diamagnetic solution at the standard temperature T_0 and χ_0 that of pure water, then by Wiedemann's law:

$$(m + \mu)\chi_n = \mu\chi_0.$$

Hence:

$$\chi_n/\chi_0 = 1/(1 + \delta), \text{ where: } \delta = m/\mu. \tag{4}$$

If such a diamagnetic solution be introduced in the left branch of the balance with its meniscus m_1 in the field H_0, and if the right branch contain water with its meniscus m_2 in a field H which is such as to give a balance when the two liquids are at the standard temperature T_0, then it is evident from Eq. (3) that:

$$\chi_n/\chi_0 = (\rho_0/\rho_\delta)(H^2/H_0^2), \tag{5}$$

where ρ_δ denotes the density of the diamagnetic solution at the standard temperature T_0. Hence from Eqs. (4) and (5):

$$\frac{\rho_0 H^2}{H_0^2} = \frac{\rho_\delta}{1+\delta}. \tag{6}$$

Now, supposing the values of δ and ρ_δ to be known, if D denote the necessary displacement of the meniscus m_2 from its zero-position in order to obtain a balance, and if the values of D for several diamagnetic nickel-chloride solutions are known by experiment, a calibration curve can be constructed with the quantity $\rho_0 H^2/H_0^2$ plotted against D.

From the calibration curve the values of the quantity $\rho_0 H/H_0^2$ can be taken for use in Eq. (1), after the value of D has been found for the case in which water at temperature T is balanced against water at the standard temperature T_0.

Calibration of the Balance

The data used in the construction of a typical calibration curve are given in Table I. The quantity δ represents the ratio of a mass m of neutral solution to the mass of water μ added to it in forming the diamagnetic solutions numbered 1, 2, $\cdots$ 6; ρ_δ represents the density of a diamagnetic solution at the standard temperature T_0 (23.5°C); and D represents the displacement of the meniscus m_2 from its zero-position, expressed in terms of head divisions of the micrometer telescope focussed upon it, in order to produce a balance of a diamagnetic solution against water at the standard temperature T_0.

Table I.

Solution number	δ	ρ_δ	D	$\rho_\delta/(1+\delta)$
1	0	0.99742	0	0.99742
2	0.003749	0.99750	65	0.99377
3	0.007516	0.99758	119	0.99014
4	0.011241	0.99767	175	0.98658
5	0.014999	0.99775	236	0.98301
6	0.018767	0.99783	316	0.97945
7	0.026858	0.99800	413	0.97190
8	0.031305	0.99806	484	0.96776

A calibration curve constructed with the aid of these data is shown in Fig. 3. It is the one used in the construction of curve 2 shown in Fig. 4.

Results

In Fig. 4 there are shown two curves, one labelled curve 1 and the other curve 2. In the case of each curve the ratio of the specific susceptibility of

water at temperature T to that at 20°C, is plotted against the temperature, the temperature 20°C being chosen instead of 23.5°C as the standard temperature in order to facilitate comparisons with the curves of Fig. 1.

The figures associated with the observation points on each curve indicate the corresponding observation times reckoned in minutes from the time at which the zero adjustment of the manometric balance was made. The significance of these annotations will presently become apparent.

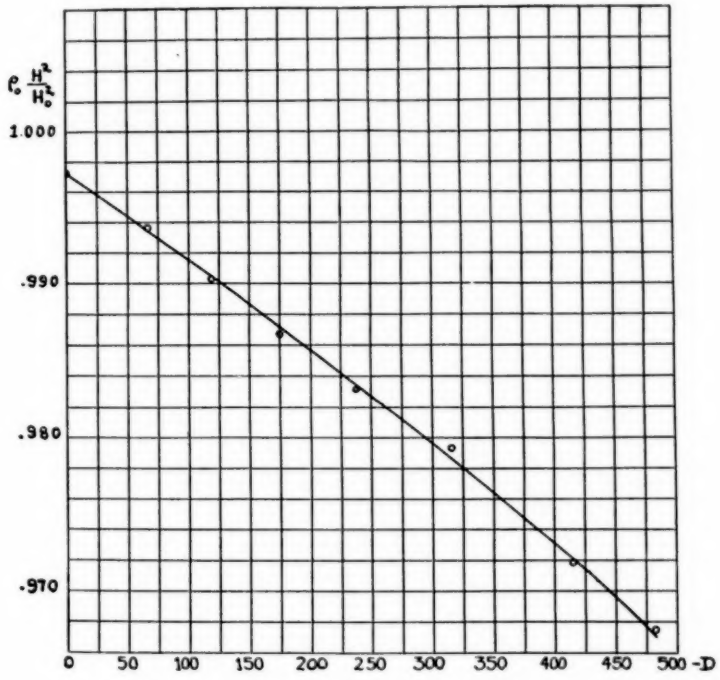

Fig. 3. Calibration curve.

The two curves have certain characteristic features in common, notably the correspondence of maxima and minima points. They differ essentially, however, in that curve 1 indicates that at higher temperatures the diamagnetism of water is *less* than at our standard temperature 23.5°C, while curve 2 indicates that it is *greater*. Each curve was satisfactorily checked by an independent run under corresponding conditions.

The results represented by curve 1 might be cited in support of those found by Cabrera and Duperier (1925), while the results represented by curve 2 might be cited in support of those found by Piccard and Johner (1930); in fact, for temperatures up to 40°C the agreement of curve 2 with the corresponding curve of Piccard and Johner (see Fig. 1) is rather good.

Since the sensitivity of the manometric balance is such as to permit easy detection of changes in relative susceptibility of the order 10^{-4}, the differences between curve 1 and curve 2 must be looked for elsewhere than in the errors of observation.

Various experiments led us finally to the conclusion that these differences have their origin in differences in the procedures followed in preparing the samples of water used in the two sets of experiments.

The water used in both sets of experiments was distilled in the apparatus of the Department of Chemistry, Columbia University. That used in the first set was afterwards boiled vigorously for about 15 minutes in a Pyrex container just before the experiments whose results are represented by curve 1 were begun. The water used in the second set of experiments was similarly prepared, except that after boiling it was sealed in its container after the air

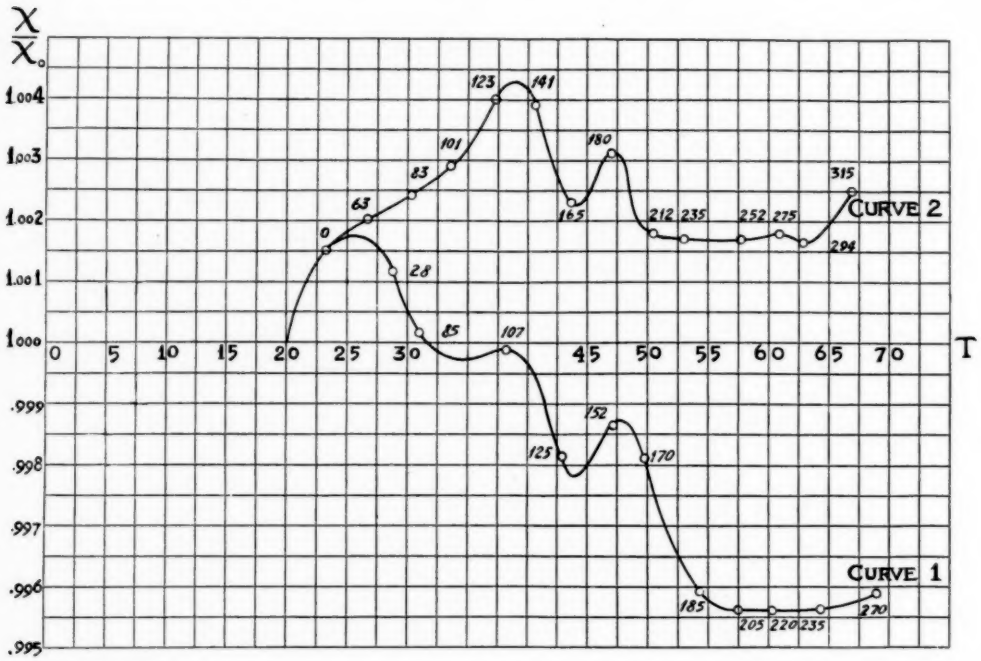

Fig. 4.

therein had been displaced by helium gas and then left to stand for 3 days before using. Throughout each set of experiments the water was kept in contact with helium gas with no air present.

The calibration curve used in the construction of curve 1 was obtained by balancing diamagnetic nickel chloride solutions which had stood for several days in contact with helium gas against recently boiled water at the standard temperature 23.5°C, and the calibration curve used in the construction of curve 2 was obtained in the same way, except that the water used had stood for several days in contact with helium gas.

We are now of the opinion that curve 2 approximates fairly closely a true equilibrium curve, but further rather lengthy experiments will have to be carried out before this opinion can be fully substantiated.

The observations upon which curve 2 was constructed are recorded in the

first three columns of Table II, captioned respectively T, $H \cdot D$, and $T \cdot E$; the first column contains the values of the temperatures at which the observations were made expressed on the centigrade scale; the second column contains the values of the displacements of the meniscus m_2 from its zero position expressed in terms of head divisions on the micrometer telescope focussed upon it; the third column contains the values of the times elapsed expressed in minutes reckoned from the time at which zero adjustment of the manometric balance was made. In the fourth column are found the values in c.g.s. measure of the quantity which captions it, taken from a calibration curve whose derivation is explained above. The fifth column contains the values for the densities of water at the corresponding temperatures. In the sixth column

TABLE II.

T	$H \cdot D$	$T \cdot E$	$\rho_0 H^2/H_0^2$	ρ	χ/χ_0
23.50	0	0	0.99742	0.99742	1.0000
26.80	6	63	0.99710	0.99660	1.0005
30.45	18	83	0.99640	0.99554	1.0008
33.90	28	101	0.99579	0.99443	1.0013
37.45	30	123	0.99565	0.99318	1.0024
40.60	51	141	0.99440	0.99201	1.0024
43.85	98	165	0.99145	0.99070	1.0007
46.90	106	180	0.99100	0.98944	1.0015
50.50	145	212	0.98860	0.98784	1.0007
53.50	176	235	0.98670	0.98646	1.0002
57.60	210	252	0.98480	0.98455	1.0002
61.00	238	275	0.98300	0.98272	1.0002
63.00	260	294	0.98180	0.98167	1.0001
66.70	280	315	0.98060	0.97966	1.0009

As regards the numbers in the last column of this table, we estimate that, as far as our actual observations are concerned, they may be in error one way or the other by 1 or 2 units in their last places.

are found the ratios of the specific susceptibilities of water at temperatures T to its specific susceptibility at the temperature 23.5°C.

The curve shown in Fig. 5 represents the results of a cyclic run on water which, after boiling, was left for several days in contact with helium gas. The figures associated with the observation points have the same significance as with curve 1 and curve 2, Fig. 4.

An entirely reliable interpretation of the anomalies in the results represented by the curves in Fig. 4 and Fig. 5 cannot, we believe, be given at present. We are confident, however, that the apparently anomalous behavior of water as indicated by these curves cannot be ascribed to errors of observation or to peculiarities of the apparatus; for the susceptibility-temperature curves for benzene and for toluene show no such anomalies.

Questions arise, of course, as to whether the curves for water represent reliable values for the diamagnetism of water or values vitiated by the action (catalytic, perhaps) of unknown impurities or, possibly, by some unsuspected action of a magnetic field upon the surface tension of water, although action of this sort has been fruitlessly sought by various investigators.

If, however, it be granted that the results represented by the curves in Fig. 4 and Fig. 5 are trustworthy, they might, we believe, be explained on the assumption that polymerization changes in water produced by variation in temperature required for their completion a considerable time; but such an assumption is difficult to justify on theoretical grounds.

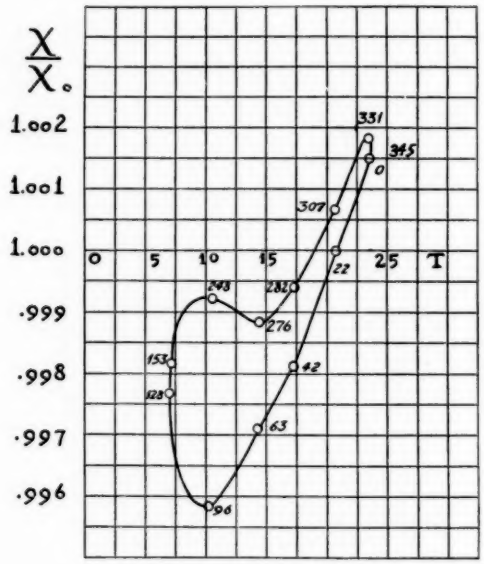

Fig. 5. Cyclic run for water.

A more exhaustive investigation, suggested by the results of our preliminary investigation, will be undertaken in the near future.

We wish to express our appreciation of the very helpful collaboration of Mr. Donald Woodbridge during the later stages of the present investigation.

Some Properties of Homogeneously Distorted Cubic Ferromagnetic Lattices

By FRANCIS BITTER
Westinghouse Research Laboratories, East Pittsburgh, Pennsylvania

(Received September 9, 1932)

The work of Becker and Kersten is amplified in that, starting with a convenient expression for the energy of a magnetically saturated and homogeneously distorted cubic ferromagnetic lattice, the problem is treated with especial reference to the crystallographic symmetry, rather than with the assumption of an isotropic medium, as was done by the above named authors. Application is made of the foregoing to the magnetostriction and magnetization of samples of iron, nickel, and their alloys under tension and compression. The agreement with experiment is qualitatively satisfactory. Further experimental data are needed for a quantitative check. Finally, there is a brief discussion of the effect of magnetization on elastic properties and of hysteresis, and a few important problems are listed.

IN TWO very interesting papers by Becker,[1] and Becker and Kersten,[2] the magnetic properties of distorted lattices are discussed. These authors assume an expression for the energy of the lattice that is a linear function of the tensor components representing the distortion, and a quadratic function of the direction cosines of the direction of magnetization. In applying this expression, however, they use an approximation which eliminates the symmetry of the crystal present in the original expression for the energy. It is the purpose of this paper to carry out the various calculations without making such simplifying approximations.

ASSUMPTIONS

Although the models of Ewing and Honda have been very useful in the development of ideas about ferromagnetism, recent advances indicate that it is time to examine them critically. It seems desirable, to a certain extent, to get away from such unobservable quantities as the individual magnetic moments of the various atoms in a crystal. Indeed, since wave mechanics has taught us to treat the electric charge surrounding an atom as a continuum, it is only logical to treat the magnetization of a solid as a property of the electric density which occupies the entire space surrounding the nuclei. This indicates that we have to deal, not with an aggregate of dipoles, but with a vector field. We may expect to derive the laws governing the behavior of this vector field from general quantum-mechanical principles, but since the attempts so far made have not been entirely successful, it may be worth trying to formulate them independently, with reference to experimental results only. The first of these laws relates to saturation phenomena. It gives the energy of

[1] R. Becker, Zeits. f. Physik **62**, 253 (1930).
[2] R. Becker and M. Kersten, Zeits. f. Physik **64**, 660 (1930).

a saturated ferromagnetic lattice as a function of the direction of magnetization. This part of the problem has been attacked from an atomic point of view by Heisenberg,[3] who discusses the existence of magnetization of the type under discussion, and Bloch and Gentile[4] who take up the orientation in the crystal lattice. An attempt to establish a corrective term applicable to distorted lattices forms the body of this paper. In addition to these laws governing the orientation of the vector I, we need to know how I changes in magnitude. The most generally accepted suggestion is that I does not change in magnitude at all, if we measure it in sufficiently small volumes, but is always equal to I_w, the Weiss spontaneous magnetization. These small volumes must, nevertheless, contain a large number of atoms. In other words, a crystal is divided into small regions whose directions of magnetization are determined by a probability function. This model surely contains some truth, but has not been very useful in explaining the detail of demagnetization, perhaps because other phenomena, such as a periodic reversal of the direction of magnetization,[5] for instance, obscure its implications. An interesting alternative possibility is to assume that in this problem, as in the case of other vector fields, two separate treatments are called for, corresponding to geometrical optics on the one hand and wave optics on the other. In fact, in view of the general orderliness of nature on a small scale, as contrasted with the general disorder found on a large scale, one might almost suspect that all polarization and diffusion vector fields, when examined in detail, would reveal a wave structure rather than random fluctuations. However that may be, experimental evidence has recently been found, which shows that the magnetization of a single crystal is not uniform, that inhomogeneities exist, and are arranged according to well-defined geometrical patterns.[6] Therefore on purely empirical grounds we may expect a wave equation to govern the intensity of magnetization, that is, one whose solutions are some sort of oscillating functions. The existence of such an equation will then somehow have to be reconciled to the existence of spontaneous magnetization as postulated by Weiss and Heisenberg.

The above discussion has been introduced in order to emphasize two points. (1) The magnetic properties of a saturated lattice are representable by a function derivable from symmetry considerations and containing a few constants which it is the business of atomic theory to interpret. (2) Whenever other than saturated lattices are discussed, further assumptions must be made. The simplest and most convenient for our purposes are given below.

We shall assume that when the energy of a saturated lattice is less for magnetization along some one direction than for any other direction, then the lattice will actually be magnetically saturated in this one direction of minimum energy. Further, when the energy of a saturated lattice is less for magnetization in n specified directions than in any other directions, then the

[3] W. Heisenberg, Zeits. f. Physik **49**, 619 (1928).
[4] F. Bloch and G. Gentile, Zeits. f. Physik **70**, 395 (1931).
[5] P. S. Epstein, Phys. Rev. **41**, 91 (1932).
[6] F. Bitter, Phys. Rev. **38**, 1903 (1931); **41**, 507 (1932).

lattice behaves as if a fraction $1/n$ of its total volume were magnetized to saturation in each of the n directions. The justification for these assumptions is that they are very simple to handle, and that to a first approximation they have been found to represent certain facts very well,[7] and seem to be adequate here also. As a rule, however, they fall down when applied to problems in which two or more directions have almost equal energies, or when hysteresis is important.

We shall further assume that the energy E_θ' of a *perfect* cubic lattice insofar as it depends on the direction of magnetization may be written

$$E_\theta' = E_1' + E_2' + E_3 \tag{1}$$

$$E_1' = \text{const.} + c' \sum{}'\alpha_i^2\alpha_j^2 \tag{2}$$

$$E_2' = \text{const.} + K_1 \sum B_{ii}\alpha_i^2 + K_2 \sum{}' B_{ij}\alpha_i\alpha_j \tag{3}$$

$$E_3 = -\boldsymbol{I}_w \cdot \boldsymbol{H}. \tag{4}$$

Here E_1' refers to the undistorted cubic lattice, and results from the spin-orbit coupling.[4] The tensor components B_{ij} give the position x', y', z' of a point after distortion in terms of its coordinates before the distortion.

$$x' = (B_{ii} + 1)x + B_{ij}y + B_{ik}z, \text{ etc.} \tag{5}$$

The quantities α_i are the direction cosines of the magnetization along the i, j, k axes which are assumed parallel to the tetragonal axes of the crystal. E_3 is the energy component due to the external field H. The summations extend over all values of i, j, k, the primed summation indicating $i \neq j$, etc. The constants include all terms independent of α_i, etc.

These equations are inconvenient because they refer to an ideal cubic lattice which is not experimentally available. In order to correct this we must calculate the equilibrium configuration of the lattice under no external forces, and use this as our starting point.

Lattice under no External Forces

Let us write $B_{ij} = A_{ij} + C_{ij}$, where the quantitites B_{ij} refer to total distortions measured from the original cubic form of the lattice, C_{ij} are the distortions produced in the lattice by internal forces, and A_{ij} are the distortions produced by external forces alone, measured from the equilibrium configuration of the lattice. We can write

$$E_2' = \text{const.} + K_1 \sum A_{ii}\alpha_i^2 + K_2 \sum{}' A_{ij}\alpha_i\alpha_j + K_1 \sum C_{ii}\alpha_i^2 + K_2 \sum{}' C_{ij}\alpha_i\alpha_j.$$

In addition we put for the elastic energy of distortion[8]

[7] A review is contained in F. Bitter, Phys. Rev. **39**, 337, 371 (1932).

[8] This is the expression used by Becker[1] and is correct for isotropic media. In general, three elastic constants are required to describe cubic crystals. The energy is (Love, *Math. Theory of Elasticity*, page 158)

$$E_4 = (c_{11}/2)\sum C_{ii}^2 + (c_{12}/2)\sum{}' C_{ii}C_{jj} + c_{44}\sum{}' C_{ij}^2$$

which reduces to the above for $2c_{44} = c_{11} - c_{12}$. The use of this complete expression does not alter the form of Eqs. (7) or (11), but does alter the relationships 10 and 12 to

$$c = c' + K_1^2/2(c_{11} - c_{12}) - K_2^2/4c_{44};\ \chi_1 = -K_1/(c_{11} - c_{12});\ \chi_2 = -K_2/2c_{44}.$$

$$E_4 = \tfrac{1}{2}\lambda[\sum C_{ii}]^2 + G\sum C_{ij}^2,$$

G being the modulus of shear, or rigidity, and $(\lambda+2G/3)$ the modulus of compression of the (non-magnetic) cubic lattice. The quantities C_{ij} are then so determined that in the absence of external forces ($A_{ij}=0$)

$$(\partial/\partial C_{ij})(E_2' + E_4) = 0.$$

Carrying this out, we obtain

$$\sum C_{ii} = \text{const.}$$
$$C_{ii} = \text{const.} - (K_1/2G)\alpha_i^2$$
$$C_{ij} = \text{const.} - (K_2/2G)\alpha_i\alpha_j$$

and, remembering that

$$\sum \alpha_i^4 = [\sum \alpha_i^2]^2 - \sum{}' \alpha_i^2\alpha_j^2$$

we obtain

$$E_4 = \text{const.} + [(K_2^2 - K_1^2)/4G]\sum{}' \alpha_i^2\alpha_j^2$$
$$E_2' = f(A_{ij}) + [(K_1^2 - K_2^2)/2G]\sum{}' \alpha_i^2\alpha_j^2.$$

Consequently, putting $E_\theta = E_\theta' + E_4$ and lumping all the terms independent of the direction of magnetization into a single constant, we obtain

$$E_\theta = E_1 + E_2 + E_3 + \text{const.} \tag{6}$$

where

$$E_1 = c\sum{}' \alpha_i^2\alpha_j^2 \tag{7}$$
$$E_2 = K_1\sum A_{ii}\alpha_i^2 + K_2\sum{}' A_{ij}\alpha_i\alpha_j \tag{8}$$
$$E_3 = \boldsymbol{I}_w \cdot \boldsymbol{H} \tag{9}$$
$$c = c' + (K_1^2 - K_2^2)/4G \tag{10}$$

where E_1 is the energy of the lattice including magnetostrictive strains, and where the A_{ij} are measured from that configuration of the lattice in which it is in equilibrium with itself. Further, the magnetostriction given by the tensor C_{ij} is more conveniently expressed by the formula for the change in length per unit length in the direction β_i, β_j, β_k

$$\delta l/l = \chi_0 + \chi_1\sum \alpha_i^2\beta_i^2 + \chi_2\sum{}' \alpha_i\alpha_j\beta_i\beta_j \tag{11}$$

which can be derived by noticing that

$$\delta l/l = \sum C_{ii}\beta_i^2 + \sum{}' C_{ij}\beta_i\beta_j + \text{const.}$$

and substituting the values of C_{ij} found above. On doing this, one obtains Eq. (11) with

$$\chi_1 = -K_1/2G;\ \chi_2 = -K_2/2G. \tag{12}$$

The expression for $\delta l/l$ gives the difference in length between the final magnetically saturated state and the initial cubic state. Since this initial condition

cannot be realized experimentally, we must choose some other cubic condition as our starting point and correct the above expression by choosing χ_0 to fit experimental observations, instead of using for it that function of λ, G, etc., which results from the foregoing calculation. It is convenient to use as our reference configuration one with no applied field H, in which the sample is completely demagnetized. For the present we need not specify further what this demagnetized condition is. It should be noticed that formula (11) may be checked without any special assumptions regarding χ_0 by measuring the difference in magnetostriction between various directions of magnetization and observation. χ_0 will then drop out.

Insofar as the foregoing considerations are correct, Eqs. (6) to (12) should describe the behavior of saturated crystals. There appear five constants, I_w, c', K_1, K_2, and G which are to be interpreted by quantum theory. This has been attempted for the first two only.

Evaluation of E_2

In the following we shall not be concerned with the elastic properties of crystals, but confine ourselves to the description of strains, and moreover to extensions with transverse contractions. The tensor components have been calculated for the following cases.

Extension parallel to [100] axis

$$A_{ii} = A;\ A_{jj} = A_{kk} = -\mu A;\ A_{ij} = A_{jk} \cdots = 0.$$

Extension parallel to [110] axis

$$A_{ii} = A_{jj} = [(1-\mu)/2]A;\ A_{kk} = -\mu A;$$
$$A_{ij} = A_{ji} = [(1+\mu)/2]A;\ A_{jk} = A_{ik} = 0.$$

Extension parallel to [111] axis

$$A_{ii} = A_{jj} = A_{kk} = [(1-2\mu)/3]A;\ A_{ij} = A_{jk} = \cdots = [(1+\mu)/3]A.$$

A measures the extension, and μ determines the extent of the accompanying change in volume. In the ensuing formulae additive constants are neglected.

E_2 for extension parallel to [100] axis

Substituting the values found above into Eq. (8) and putting $\alpha_i = \cos\theta$; $\alpha_j = \sin\theta \sin\phi$; $\alpha_k = \sin\theta \cos\phi$ one obtains

$$E_2 = [(1+\mu)/2]K_1 A \cos 2\theta, \tag{13}$$

indicating that the energy is independent of the orientation of I_w in the plane normal to the extension, and is a maximum in the direction of extension if $K_1 > 0$.

E_2 for extension parallel to [110] axis

Substituting the appropriate values of A_{ij} into Eq. (8) and putting $\alpha_i = \sin\theta \sin\phi$; $\alpha_j = \sin\theta \cos\phi$; $\alpha_k = \cos\theta$ we obtain

$$E_2 = K_1A[(1-\mu)/2]\,[\sin^2\theta - \mu\cos^2\theta] + K_2A(1+\mu)\sin^2\theta\sin\phi\cos\phi. \quad (14)$$

Putting $\theta=\pi/2$, this gives for the (001) plane, which contains the direction of extension

$$E_2 = [(1+\mu)/2]K_2A\sin 2\phi$$

which expression has a maximum for $\phi=\pi/4$, or in the direction of extension, if $K_2>0$. However, by putting $\phi=\pi/4$, this gives for the $(1\bar{1}0)$ plane which also contains the direction of extension,

$$E_2 = -[(1+\mu)/4](K_1+K_2)A\cos 2\theta$$

or for the (110) plane perpendicular to the direction of extension, for which $\phi=-\pi/4$

$$E_2 = -[(1+\mu)/4](K_1-K_2)A\cos 2\theta$$

which shows that the energy is not independent of the orientation of I_w in the plane normal to the extension unless $K_1=K_2$. Further, E_2 will have its maximum or minimum value in the direction of extension as long as K_1+K_2 has the same sign as K_2. But if K_1+K_2 has the opposite sign of K_2, then both maximum and minimum of E_2 will lie in a plane perpendicular to the extension. This latter case is of considerable importance in describing the Villari reversal in iron, as discussed further on.

E_2 for extension parallel to [111] axis

Substituting the appropriate values of A_{ij} into Eq. (8), and writing for the angle θ between the direction α_i, α_j, α_k and the [111] axis whose direction cosines are $3^{-1/2}$,

$$\cos\theta = 3^{-1/2}(\alpha_i+\alpha_j+\alpha_k)$$

we obtain

$$E_2 = [(1+\mu)/2]K_2A\cos 2\theta,$$

an expression similar to that for extension along the tetragonal axes, except that K_2 replaces K_1.

Magnetostriction

The formula given in Eq. (11) expresses a complicated relationship between the parallel and transverse components of magnetostriction in their dependence on the direction of magnetization in the crystal. Existing data are not sufficiently reliable for a satisfactory quantitative check, but are perhaps sufficient for a rough estimate of χ_1 and χ_2 for iron and nickel. From Eq. (11) we find the following values of $\delta l/l$. We shall evaluate these con-

Table I. *Table of theoretical magnetostrictions.*

Case	Direction of magnetization	Direction of observation	$\delta l/l$
a	[100] axis; $\alpha_i=1$, $\alpha_j=0$, $\alpha_k=0$	$\beta_i=1$, $\beta_j=0$, $\beta_k=0$	$\chi_0+\chi_1$
b	" " " "	$\beta_i=0$, $\beta_j=1$, $\beta_k=0$	χ_0
c	" " " "	$\beta_i=0$, $\beta_j=2^{-1/2}$, $\beta_j=2^{-1/2}$	χ_0
d	[110] axis; $\alpha_i=2^{-1/2}$, $\alpha_j=2^{-1/2}$, $\alpha_k=0$	$\beta_i=2^{-1/2}$, $\beta_j=2^{-1/2}$, $\beta_k=0$	$\chi_0+\frac{1}{2}(\chi_1+\chi_2)$
e	" " " "	$\beta_i=2^{-1/2}$, $\beta_j=-2^{-1/2}$, $\beta_k=0$	$\chi_0+\frac{1}{2}(\chi_1-\chi_2)$
f	" " " "	$\beta_i=0$, $\beta_j=0$, $\beta_k=1$	χ_0
g	[111] axis; $\alpha_i=3^{-1/2}$, $\alpha_j=3^{-1/2}$ $\alpha_k=3^{-1/2}$	$\beta_i=3^{-1/2}$, $\beta_j=3^{-1/2}$, $\beta_k=3^{-1/2}$	$\chi_0+\frac{1}{3}(\chi_1+2\chi_2)$
h	" " " "	$\beta_i=2^{-1/2}$, $\beta_j=-2^{-1/2}$, $\beta_k=0$	$\chi_0+\frac{1}{3}(\chi_1-\chi_2)$

stants for iron and nickel, assuming that in the experiment the zero reading corresponds to the length for perfect demagnetization. The observations on iron are taken from Honda and Masiyama,[9] and those on nickel from Masiyama.[10] The observations are tabulated in Table II.

TABLE II. *Comparison of theoretical and experimental magnetostrictions.*

Case	Theoretical value	Experimental value $\times 10^6$ Iron	Nickel
a	$\chi_0+\chi_1$	17.1 15.3	−54.4 −50.7
b	χ_0	−15.7	21.1
c	χ_0	−15.4	24.0
d	$\chi_0+\frac{1}{2}(\chi_1+\chi_2)$	−7.2 −2.7	−31.3 −33.9
e	$\chi_0+\frac{1}{2}(\chi_1-\chi_2)$	14.0	14.5
f	χ_0	−9.1	18.3
g	$\chi_0+\frac{1}{3}(\chi_1+2\chi_2)$	−12.9	−27.1
h	$\chi_0+\frac{1}{3}(\chi_1-\chi_2)$	20.6	7.2

In order to fit these values we have chosen the constants shown in Table III.

TABLE III. *Magnetostriction constants* $\times 10^6$.

	Iron	Nickel
χ_0	−15.5	21.0
χ_1	32.0	−73.5
χ_2	−12.3	−23.5

These values fit the observations in Table II fairly well, except case *h* in iron, which becomes 0 instead of 20.6, and case *e* in nickel, which becomes −4 instead of 14.5. A better all-around fit might be attempted, but this is hardly worth while, since the observations were made on disks cut perpendicular to tetragonal and digonal axes in which the demagnetization is probably structurally different. The constants as evaluated in Table III are therefore only roughly reliable.

As to the dependence of the volume on the direction of magnetization, we have[11] $\delta v/v=\sum C_{ii}=$constant, a relation which holds independently of the choice of constants K_1 and K_2.

In order to calculate the change in magnetostriction produced by tension we shall make use of the assumption regarding the nature of demagnetization —the material behaves as if a fraction $1/n$ of the total volume is magnetized in each of the n directions of easy magnetization. This assumption requires that the observed longitudinal magnetostriction, or the total change in length from a demagnetized state to saturation can be written:

[9] K. Honda and Y. Mashiyama, Sci. Rep., Tohoku Imp. Univ. **15**, 755 (1926).

[10] Y. Masiyama, Sci. Rep., Tohoku Imp. Univ. **17**, 945 (1928).

[11] ΣC_{ii} is invariant to a rotation of axes, and is therefore equal to the sum of the principal axes of the tensor ellipsoid.

For iron

$$\frac{\delta l}{l}\Big]\begin{pmatrix}\alpha_i, & \alpha_j, & \alpha_k\\ \beta_i, & \beta_j, & \beta_k\end{pmatrix} - \frac{1}{3}\frac{\delta l}{l}\Big]\begin{pmatrix}1, & 0, & 0\\ \beta_i, & \beta_j, & \beta_k\end{pmatrix} - \frac{1}{3}\frac{\delta l}{l}\Big]\begin{pmatrix}0, & 1, & 0\\ \beta_i, & \beta_j & \beta_k\end{pmatrix}$$
$$- \frac{1}{3}\frac{\partial l}{l}\Big]\begin{pmatrix}0, & 0, & 1\\ \beta_i, & \beta_j, & \beta_k\end{pmatrix}.$$

For nickel

$$\frac{\delta l}{l}\Big]\begin{pmatrix}\alpha_i, & \alpha_j, & \alpha_k\\ \beta_i, & \beta_j, & \beta_k\end{pmatrix} - \frac{1}{4}\frac{\delta l}{l}\Big]\begin{pmatrix}3^{-1/2}, & 3^{-1/2}, & 3^{-1/2}\\ \beta_i, & \beta_j, & \beta_k\end{pmatrix} - \frac{1}{4}\frac{\delta l}{l}\Big]\begin{pmatrix}-3^{-1/3}, & 3^{-1/2}, & 3^{-1/2}\\ \beta_i, & \beta_j, & \beta_k\end{pmatrix}$$
$$- \frac{1}{4}\frac{\delta l}{l}\Big]\begin{pmatrix}3^{-1/2}, & -3^{-1/2}, & 3^{-1/2}\\ \beta_i, & \beta_j, & \beta_k\end{pmatrix} - \frac{1}{4}\frac{\delta l}{l}\Big]\begin{pmatrix}3^{-1/2}, & 3^{-1/2}, & -3^{-1/2}\\ \beta_i, & \beta_j, & \beta_k\end{pmatrix}$$

where the quantities in brackets indicate the directions of magnetization and observation, respectively. Both of these expressions reduce to

$$-\chi_1/3 + \chi_1 \sum \alpha_i^2\beta_i^2 + \chi_2 \sum{}' \alpha_i\alpha_j\beta_i\beta_j,$$

which is equivalent to our original expression (11) provided $\chi_0 = -\chi_1/3$. The values in Table III are not quite consistent with this result, so that we may expect discrepancies when making use of the above assumption concerning demagnetization.

We proceed to discuss the longitudinal magnetostriction in crystals under tension and compression in the direction of magnetization. This tension or compression, whenever it is referred to in this article, means tension or compression so large that E_1 may be neglected in Eq. (6). The procedure is here outlined, by way of illustration, for nickel under tension along a trigonal axis. Tension along a trigonal axis in nickel makes the energy a minimum for magnetization in the plane perpendicular to the tension. Therefore the magnetostriction under tension will be that observed without tension plus the change due to the new configuration for demagnetization, which change is given by

$$-\frac{\delta l}{l}\Big]\begin{pmatrix}2^{-1/2}, & -2^{-1/2}, & 0\\ 3^{-1/2}, & 3^{-1/2}, & 3^{-1/2}\end{pmatrix} = -\left[\chi_0 + \tfrac{1}{3}(\chi_1 - \chi_2)\right]$$

or for the total magnetostriction under tension

$$\chi_0 + \tfrac{1}{3}(\chi_1 + 2\chi_2) - \left[\chi_0 + \tfrac{1}{3}(\chi_1 - \chi_2)\right] = \chi_2.$$

In this case, as in all others, the magnetostriction under tension does not involve χ_0, and is therefore independent of our special assumptions about demagnetization. Various other cases have been calculated and are tabulated in Table IV. Here χ_0 has been put equal to $-\chi_1/3$ to show in which cases the relation

$$\frac{\delta l}{l}\Big]_{\text{tension}} = \frac{3}{2}\frac{\delta l}{l}\Big]_{\text{no tension}}$$

which was found by Becker for nickel, holds. In Table IV the values of $\delta l/l$ only are affected by the special choice of χ_0.

TABLE IV. *Longitudinal magnetostriction in crystals with and without tension or compression in the direction of magnetization, assuming a special mechanism for demagnetization which requires that* $\chi_0 = -\chi_1/3$.

Material	K_1	K_2	K_1+K_2	Direction of magnetization	$\delta l/l$	$\delta l/l$ with tension	$\delta l/l$ with compression
Fe	−	+	−	[100]	$2\chi_1/3$	0	χ_1
				[110]	$\frac{1}{2}(\chi_1/3+\chi_2)$	χ_2	$\frac{1}{2}(\chi_1+\chi_2)$
				[111]	$2\chi_2/3$	χ_2	0
Ni	+	+	+	[100]	$2\chi_1/3$	χ_1	0
				[110]	$\frac{1}{2}(\chi_1/3+\chi_2)$	$\frac{1}{2}(\chi_1+\chi_2)$	0
				[111]	$2\chi_2/3$	χ_2	0
80% Ni 20% Fe	?	0	?	[111]	0	0	0
45% Ni 55% Fe	?	−	?	[111]	$2\chi_2/3$	0	?

The sign of K_2 for the alloys containing 80 percent Ni and 45 percent Ni is taken from data by Buckley and McKeehan.[12] Further, McKeehan and Cioffi[13] found that the magnetostriction of a wire of the 80 percent Ni alloy with and without tension is zero, while Honda and Shimizu[14] found that for a wire of the alloy containing 45 percent Ni the magnetostriction under tension is zero. In nickel and iron wires, the last named authors find the magnetostriction with and without tension as shown in Table V.

TABLE V. *Magnetostriction of wires.*

Without tension		With tension
	in iron	
-4×10^{-6}		$<-9\times10^{-6}$
	in nickel	
-30×10^{-6}		$\sim-42\times10^{-6}$

All these results are in general agreement with the predictions of Table IV provided we assume the iron wires to be fibered with a digonal axis parallel to the wire axis, and all the other wires to be fibered with a trigonal axis parallel to the wire axis.

The calculation of magnetostriction under tension as a function of H is of course quite possible in accordance with the above. We shall here be content with pointing out that both for iron and nickel wires under sufficient tension, I is proportional to H up to saturation, and the magnetostriction is proportional to I^2. This is of especial interest for iron, in that it predicts the disappearance of the change in sign in the magnetostriction which has often been observed in wires[14] and single crystals[15] magnetized in a [110] direction. The

[12] O. E. Buckley and L. W. McKeehan, Phys. Rev. **26,** 261 (1925).
[13] L. W. McKeehan and P. P. Cioffi, Phys. Rev. **28,** 146 (1926).
[14] K. Honda and S. Shimizu, Phil. Mag. **4,** 338 (1902).
[15] W. L. Webster, Proc. Roy. Soc. **A109,** 570 (1925).

change in sign, or Villari reversal, is discussed from a theoretical point of view by Heisenberg[16] and Akulov.[17] Its disappearance has been observed by Honda and Shimizu.[14]

MAGNETIZATION[18]

The magnetization curves for crystals under tension may be calculated with the help of Eq. (6) by finding the minima of E_θ. If tension produces a maximum in the direction of magnetization, the material will be more difficult to magnetize under tension, and conversely. Since E_θ has a maximum in the direction of extension for extension in nickel along the tetragonal, digonal and trigonal axes, and in iron along the trigonal axes, these conditions will give rise to properties similar to those found in nickel wires, and discussed at length by Becker and Kersten.[19] On the other hand, iron under tension along a tetragonal axis has a minimum of E_θ in the direction of extension. The four minima at right angles to the direction of extension have been bulged out. In other words, suppose an iron crystal is placed with its tetragonal axes parallel to the axes of a cartesian system of coordinates. E_θ has a minimum along the $\pm x$, $\pm y$, and $\pm z$ axes due to the fact that $C>0$ in Eq. (7). Extension along the z axis changes E_θ so that it has a minimum in the $\pm z$ directions but a maximum in any direction in the x-y plane. In order to see the effect of extension on magnetization let us assume a small field in the direction of the $+z$ axis. We shall here give up the simple assumption that this small field produces saturation, and assume instead merely that there is a slightly greater probability of finding a volume element magnetized in the $+z$ direction than in any other direction. If, now, we apply tension along the z axis, we effectively dump the contents of the minima along the $\pm x$ and $\pm y$ axes into the minima along the $\pm z$ axis, which, because of the small magnetic field in the $+z$ direction, will fall more into the $+z$ than $-z$ direction, and so increase the magnetization. Iron under tension along a digonal axis is more complicated. Let us assume that extension is along the [110] axis in the model just discussed. This extension will produce maxima of E_θ along the $\pm z$ axes, and minima along the $[1\bar{1}0]$ directions, as may be seen by substituting the values for K_1 and K_2 as given by Table III and Eq. (12) into Eq. (14). A small field in the [110] direction will make the minima of E_θ in the x and y directions less than the minima in the $-x$, $-y$, and $\pm z$ directions. If tension is gradually applied along the [110] axis, the minima in the $\pm z$ directions are first emptied, producing an increase in magnetization. Further extension shifts the minima along the x and y directions into the $(1\bar{1}0)$ directions, producing a decrease in magnetization. This is in accordance with the observations of Honda and Terada[20] and others. In general, if a substance is easier

[16] W. Heisenberg, Zeits. f. Physik **69**, 287 (1931).

[17] N. Akulov, Zeits. f. Physik **69**, 78 (1931).

[18] A further discussion of magnetization with illustrations of the function E_θ will be published in a further paper.

[19] See references 1 and 2, and M. Kersten, Zeits. f. Physik **76**, 505 (1932).

[20] K. Honda and T. Terada, Jour. Col. Sci., Tokyo **21**, Art. 7 (1906).

to magnetize under tension, it is more difficult to magnetize under linear compression. This, however, is not true of iron along a [110] axis. Changing from extension to compression changes the sign of A in Eqs. (13) through (15), and consequently reverses the positions of the maxima and minima of E_θ. But iron under tension along a [110] axis has both maxima and minima of E_θ at right angles to the extension. Compression will reverse these, and so will not produce a minimum in the direction of compression.

Elastic Properties

Since the energy of distortion E_2 as given in Eq. (9) is a linear function of the distortion, we may say that the atomic interactions responsible for E_2 give rise to forces that are independent of the distortion, and dependent only on the direction of magnetization. Consequently, in order to discover any change in the elastic properties of iron due to a change in magnetization from a [100] axis to a [010] axis, for instance, it would be necessary to use methods that were capable of detecting the change in elastic properties due to the application of a constant force.[21]

Finally, it follows from Eq. (12) that the modulus of shear G may be written

$$G = -K_1/2\chi_1 = -K_2/2\chi_2.$$

Since χ_1 or χ_2 can be determined by measurements on magnetostriction, and K_1 or K_2 by measurements on the change in magnetization or magnetostriction under tension, it follows that we can determine G, an elastic constant, by purely magnetic measurements.[8]

Hysteresis

Whether or not homogeneous strains are important in determining hysteresis depends entirely on the mechanism by which magnetization changes from one direction, say A, to another B. If this is essentially a rotation, so that the nature of E_θ between A and B actually enters into the problem, then homogeneous distortions certainly will be important. Such a condition is to be expected in rotating fields. It may very well be, on the other hand, that the values of E_θ between A and B are in some cases quite irrelevant. In such cases homogeneous strains would not be important.[22]

Problems

The following problems appear to be among the most interesting and important ones confronting students of ferromagnetism today: (1) The inter-

[21] If the direction of magnetization depends on distortion the elastic behavior will be modified in a complicated way which will be discussed elsewhere.

[22] F. Bloch discusses a mechanism for such changes in direction of magnetization, Zeits. f. Physik **74**, 295 (1932).

pretation of the constants c, K_1, and K_2 in Eqs. (7) and (8). (2) The effect of alloying on these constants, both from an experimental and theoretical point of view. (3) The establishing of Eq. (8) for the energy of distortion and its derivative Eq. (11) for magnetostriction on a firm experimental basis. (4) A determination of the law stating how magnetization changes from one direction to another, together with the related but perhaps more difficult problem of describing demagnetization.

Hall e.m.f. and Intensity of Magnetization

By E. M. Pugh and T. W. Lippert
Carnegie Institute of Technology

(Received October 3, 1932)

Previous experiments have indicated that the Hall e.m.f. depends on intensity of magnetization rather than upon applied field or magnetic induction. Additional evidence is offered, the most important being that provided by a material in which H and B-H are of the same order of magnitude.

IT HAS been shown by one of us[1] that in certain ferromagnetic materials the Hall e.m.f. E is a linear single-valued function of the intensity of magnetization B-H, but is neither a linear nor single-valued function of either the induction B or the applied field H.

The nature of the apparatus used at that time was such that it was possible to obtain accurate results on only two substances, namely, K.S. magnet steel and high carbon steel, and only after they had been hardened by proper heat treatment.

Whether the above rule is general or is merely characteristic of the two materials tested, should be thoroughly investigated on account of its theoretical importance. This is especially true since these two substances had somewhat similar magnetic properties. It was therefore decided so to modify and improve the apparatus that accurate measurements of E, B and H could be made on a great variety of materials.

Apparatus

In the old apparatus[1] the method of measuring the Hall e.m.f. with a Kohlrausch slide wire made the sensitivity proportional to the resistance of the test bar, forstalling the testing of low resistance bars. The Kohlrausch slide wire was replaced with a Wolff potentiometer which, together with decided improvements in the storage battery current supply, reduced the uncertainty in the e.m.f. measurements on all materials to $\pm 10^{-8}$ volts—less than half the uncertainty previously obtained in high-resistance materials.

The magnetic measurements were also considerably improved by the use of a high-sensitivity galvanometer shunted with a very low resistance which gave it excellent fluxmeter characteristics. Such a well-damped fluxmeter is essential for the accurate measurements of the slow magnetic changes occurring in the bars.

Procedure

The bar under test was first heat treated in an atmosphere of hydrogen, and then placed in the apparatus where it was measured by the step-by-step method described in the former paper.[1] The quantities E, B, and H were ob-

[1] E. M. Pugh, Phys. Rev. **36**, 1503 (1930).

tained over the virgin curve and over several succeeding hysteresis loops. These same quantities were then measured over the normal magnetization curve by the method of reversals.

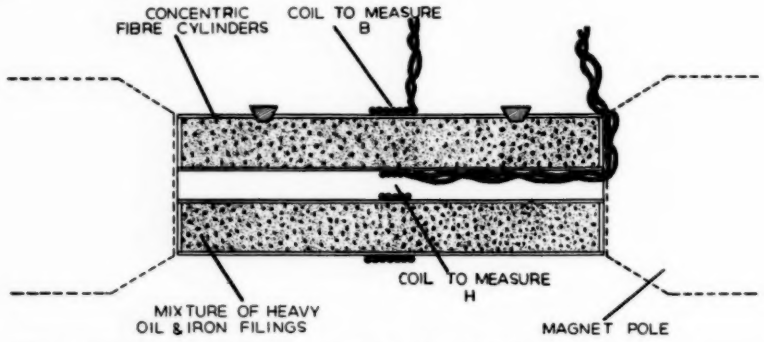

Fig. 1. Variable permeability cylinder to find value of H for samples of low permeability.

The following materials were tested after they had been carefully annealed and also after they had been quenched from a suitably high temperature,—electrolytic iron, high carbon steel, K.S. magnet steel, an iron-cobalt

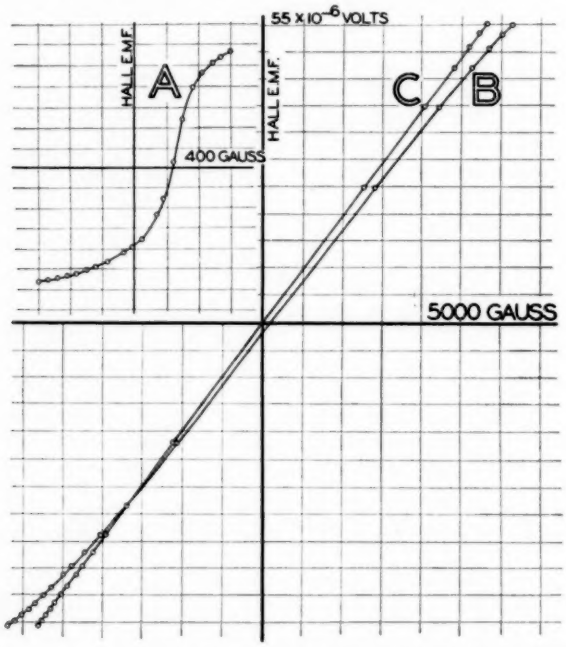

Fig. 2. Hall e.m.f. E in annealed K.S. magnet steel taken along the ascending branch of the first hysteresis loop. Plotted (A) against H, (B) against B, (C) against B-H. Current density 40 amperes per cm².

alloy (Fe 50 percent, Co 50 percent), and an iron-nickel alloy (Fe 70 percent, Ni 30 percent). The iron-nickel alloy is only slightly magnetic at room temperature, having a maximum permeability between 3 and 4. It loses its ferromagnetic properties at about 140°C.

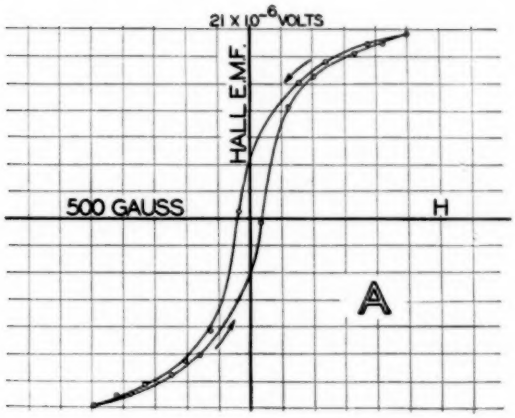

Fig. 3A.

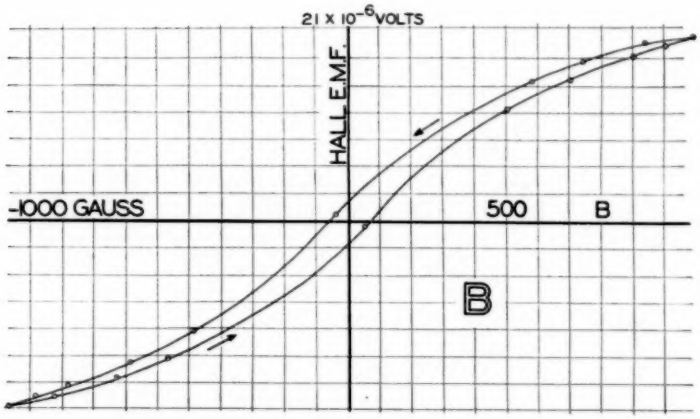

Fig. 3B.

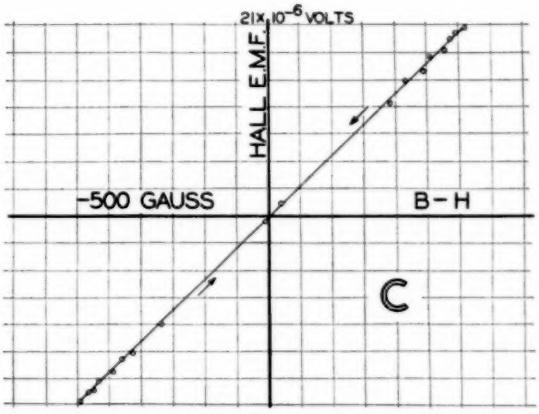

Fig. 3C.

Fig. 3. Hall e.m.f. in quenched iron-nickel alloy (Fe 70 percent, Ni 30 percent). (*A*) and (*B*) show the multiple-valued character of the curves with H or B as abcissae; (*C*) shows the single-valued character of E with B-H as abcissae. Current density 40 amp. per cm².

The tests on this slightly magnetic bar were far more conclusive than on any other specimen because in it the quantities H and B-H were of the same order of magnitude whereas in the other bars H was never more than 5 percent of B-H.

The saddle coil method[1] of measuring H was inapplicable to this slightly magnetic alloy and was discarded. Instead H was measured by substituting in place of the bar two concentric cylinders (Fig. 1) between the pole pieces of the electromagnet. The space between the cylinders was filled with a mixture of heavy oil and iron filings in such a proportion that the additional flux due to the iron filings was the same as the additional flux previously due to the test bar. Under these conditions the search coil around the inner cylinder enclosing air only measured the desired value of H.

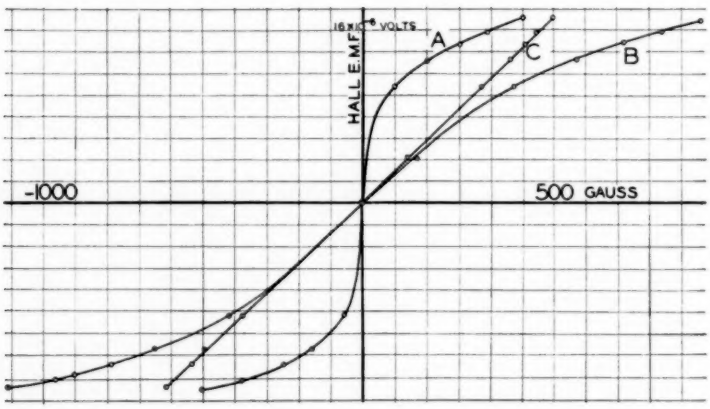

Fig. 4. Hall e.m.f. in baked iron-nickel alloy taken along the normal magnetization curve, where greatest accuracy is obtainable. Current density 40 amp. per cm². (A) and (B) show definite curvature of E with H or B as abcissae; (C) shows the linear character of E with B-H as abcissae.

Results

Figs. 2, 3 and 4 are good examples of the results obtained. Fig. 2 shows the results obtained on the ascending branch of the first hysteresis loop following the annealing of K.S. magnet steel. While the intensity of magnetization was different on the different successive hysteresis loops, no change was found in the ratio of E to B-H. *In each material tested the ratio $E/(B\text{-}H)$ remained constant, dependent on temperature and previous heat treatment only, for all of the magnetic changes to which it was subjected.*

The best results were obtained with the iron-nickel alloy (Figs. 3 and 4) which, because of its low permeability, furnished a very exacting test of this relationship. It is here obvious that the graph of E is curved and multiple valued (Figs. 3A and 3B) when plotted against either H or B but is straight and single valued against B-H, Fig. 3C. The greatest accuracy is attained in taking a normal magnetization curve because the method of reversals eliminates the cumulative errors of the step-by-step method. Fig. 4 shows the Hall

e.m.f. curve taken along the normal magnetization curve of the iron-nickel alloy.

It was not possible to make measurements over a large range of temperatures with the apparatus but the variation of the ratio $E/(B\text{-}H)$ in electrolytic iron and in the iron-nickel alloy was investigated over the range available (Fig. 5). In this region the ratio $E/(B\text{-}H)$ varies linearly with temperature whereas both E/B and E/H plotted against temperature give curves.

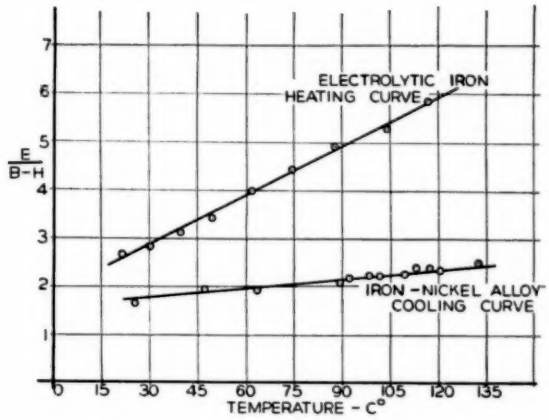

Fig. 5. Variation of ratio $E/(B\text{-}H)$ with temperature in electrolytic iron and in the iron-nickel alloy.

These and previous results furnish convincing evidence that the Hall e.m.f. should be considered as a function of the intensity of magnetization alone.

The authors wish to thank Professor Honda of Japan for the K.S. magnet steel and Dr. Elmen of the Bell Telephone Laboratories for other alloys used in this work.

Mono-Crystal Barkhausen Effects in Rotating Fields

By FRED J. BECK, JR.* AND L. W. MCKEEHAN
Sloane Physics Laboratory, Yale University

(Received October 10, 1932)

The directions of Barkhausen effects in a single crystal disk of silicon steel, held stationary in a magnetic field rotating slowly in the plane of the disk, have been determined. Search coils at right angles picked up impulses proportional to selected rectangular components of the changes in magnetization. Measurements on an oscillographic record were made at two values of magnetization, 190 and 100. Values of the angle ϕ between the change in magnetization ΔI and the corresponding variation in the applied field, $(dH/dt)\Delta t$ were determined for various positions of the applied field relative to the crystallographic axes. The normal to the disk made angles of 30°, 60°, 90° with these axes. For these low values of magnetization the effects are mainly transverse with respect to H (and therefore nearly parallel to dH/dt) and are more nearly transverse for the greater value of magnetization. The average value of ϕ is about 20° (ΔI lagging dH/dt) for the lower value of I and is less than 5° for the higher value. The average magnetization apparently lags the applied field and makes a small angle with it. The direction and frequency of effects seemed unaffected by changing the direction of H in the plane of the disk, so that no dependence upon the crystallographic directions of I, H or dH/dt have been established.

INTRODUCTION

A GREAT deal of experimental evidence relating to discontinuous changes in magnetization has been presented since the discovery of the Barkhausen effect.[1] Data have been obtained concerning the effect in various materials, the size of the volume element, or rather the magnitude of the change in magnetic moment, the relation between mechanical strain and effect and the relation between the effect and the slope of the magnetization curve or hysteresis loop. Various methods have been employed for the detection of the discontinuities principal among which are, the measurement of the noise from a telephone receiver, the measurement of the average current output from an amplifier by means of a galvanometer, and the measurement of the instantaneous current output from an amplifier by means of an oscillograph. All but the most recent studies have concerned themselves wholly with the changes in magnetization which take place in the direction of the applied field. Recently Bozorth and Dillinger[2] and Bozorth[3] have studied in addition the change in magnetization occurring in a direction at right angles to the applied field. It is recognized that a knowledge of this so-called transverse effect may give additional information as to the nature of processes occurring in the elementary domains.

* Part of a dissertation presented for the degree of Doctor of Philosophy at Yale University.

[1] H. Barkhausen, Phys. Zeits. **20**, 401 (1919).

[2] R. M. Bozorth, and J. F. Dillinger, Phys. Rev. [2] **38**, 192 (1931); **41**, 345 (1932).

[3] R. M. Bozorth, Phys. Rev. [2] **39**, 353 (1932).

In the present investigation a single crystal of silicon steel was employed as a test specimen. An apparatus was devised so that an indication of the longitudinal and transverse components of the change in magnetization arising from one and the same discontinuity could be obtained. As a means of causing the effect a uniformly rotating field was employed, the specimen being held stationary. It was felt that an investigation along these lines would give some insight as to the transverse effect, relate the direction of the change in magnetization with the position of the exciting field and disclose any dependence of the direction of the change in magnetization upon the crystallographic directions of $\boldsymbol{I}$, $\boldsymbol{H}$ and $d\boldsymbol{H}/dt$. It seemed likely that a better indication of the actual phenomena taking place could be had by obtaining the ratio of the change in magnetization along the field and at right angles to the field corresponding to each individual discontinuity and then averaging this ratio, rather than considering the ratio of the average longitudinal component to the average transverse component.

The Apparatus

The apparatus devised to give the information desired consists essentially of the main exciting field and the search coils, the amplifiers, and the oscillograph. Fig. 1 illustrates the essential features of the effect producing me-

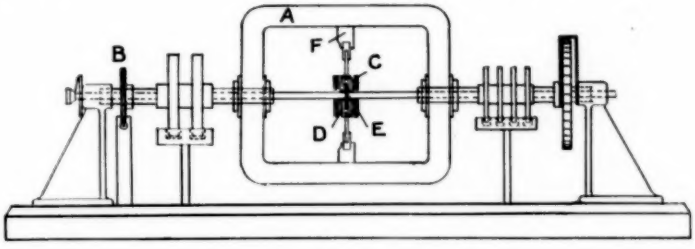

Fig. 1. Side view of mechanism.

chanism. Here A is the field-producing coil consisting of 65 turns of 9 A. W. gauge (diameter 0.289 cm) double cotton covered wire. The winding is excited from a storage battery source of supply and produces a field of strength 4.8 gauss per ampere directed in the plane of the crystal. The main field is electrically driven through reduction pulleys and the worm and wheel B. Throughout the course of the investigation the rate of rotation of the field was 1 revolution in 5.63 minutes. This low rate was found to be necessary in order to secure sufficient resolution between successive discontinuities. To pick up two mutually perpendicular components of magnetization due to a single discontinuity it was necessary to employ two search coils mounted at right angles to each other. These coils are indicated in the diagram as C and D, referred to herein as the outer and inner coils, respectively. The outer coil consists of 12,000 turns of 44 A. W. gauge (diameter 0.0051 cm) enameled wire wound in two sections. The inner coil consists of 11,000 turns of 44 A. W. gauge enameled wire also wound in two sections. The sections of each individual coil are connected in series so that the induced e.m.f.'s will be ad-

ditive. The coils were wound on specially constructed Bakelite forms so arranged that the inner coil could be slipped out of the outer coil and the crystal disk E inserted. The coil holder F maintains the coils with 90° between their axes and permits shifting of the arrangement relative to the field coil.

In order to obtain measurable impulses it was necessary to amplify the outputs from each search coil. Fig. 2 is a wiring diagram of the amplifiers employed. It was found advisable to use an output transformer in the last

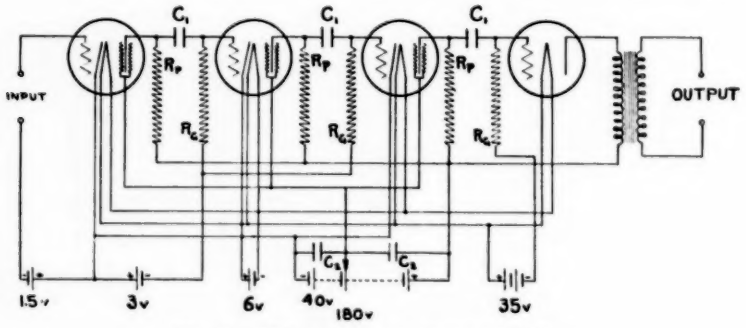

Fig. 2. Wiring diagram of one amplifier.

stage to increase the output current to a value which would actuate the oscillograph. The value of the coupling resistances, coupling condensers and by pass condensers are given below in Table I. Considerable difficulty was met

TABLE I.

	1st	2nd	3rd	4th
R_g	—	50,000	750,000	250,000
R_p	25,000	100,000	50,000	—
C_1	—	0.1	0.1	0.1
C_2=4 mfd				

with in securing the high amplification necessary, consistent with good stability. In order to eliminate feed back, extreme care was taken in the wiring of the amplifiers. Each individual stage of both amplifiers was separately shielded. The input leads from the search coils and the output leads to the oscillograph were also separately shielded. Further, to eliminate disturbances of an electromagnetic origin, the entire apparatus was placed in a large copper box. The search coils and main field were, in addition, separately shielded. The effect of sound vibration was almost wholly eliminated by using non-microphonic tubes and by suspending the amplifiers from rubber tubing which served to damp out the vibrations.

The oscillograph used was a G. E. Type PM-12-A 1 two element instrument. The sensitivity of the elements was 0.7 m.a. per millimeter.

The specimen employed in the experiments was a disk one inch (2.54 cm) in diameter and 0.018 inch (0.0457 cm) thick cut from a single crystal of silicon steel grown by W. E. Ruder of the General Electric Laboratories. Precautions were taken in the cutting to minimize the effect of strain as much as possible. The analysis of the steel used is as follows:

C	Mn	P	S	Si
0.05	0.15	0.038	0.026	3.24.

X-ray analyses showed the specimen to be a single crystal and determined the direction of the cubic axes relative to an indicating mark ruled on the crystal. These directions are indicated in the diagram of Fig. 3.

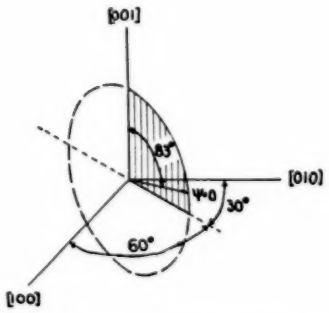

Fig. 3. Relation of cubic crystal axes to plane of disk and fiducial line thereon.

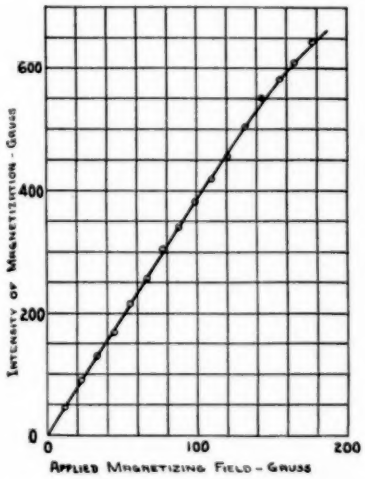

Fig. 4. Relation between magnetization and applied magnetizing field.

A curve showing the relation between the field strength of the main field and the intensity of magnetization is plotted as Fig. 4. The curve was obtained by suspending the disk by means of a fiber in a uniform magnetic field. The disk was then set into oscillation and the period of the system determined at various field strengths. Measurements of the effect were made at two values of I, 190 and 100, corresponding to a main field current of 10 amperes and 5 amperes, respectively.

Method of Procedure

In taking observations the crystal was placed in position in the apparatus so that the indicating mark on it was perpendicular to the base of the apparatus. The main field was then excited from a storage battery source of supply. With the amplifiers in operation the field was slowly rotated at a uniform rate. The rotation of the field caused the appearance of Barkhausen discontinuities, the effect of which could be viewed or photographed by means of the oscillograph. The crystal position was maintained fixed during the course of the measurements. The positions of the field are designated by the angle ψ which is the angle between the field vector and the mark on the crystal. The positions of the search coils relative to the field are designated by means of the angle θ which is the angle between the field vector and the axis of the inner coil.

With the field is a given position, e.g., $\psi = 0$ and the search coils at the position $\theta = 0$, a photograph is taken of the discontinuities affecting each coil. With the field in the same position, i.e., $\psi = 0$ photographs are taken for values of θ from $\theta = 0°$ to $\theta = 90°$ at 10° intervals. The above process is repeated for values of ψ from $\psi = 0$ to $\psi = 180°$. Photographs have been taken in the manner outlined above for a main field current of 10 amperes corresponding to an intensity of magnetization of 190 gauss. Another run was taken at a field current of 5 amperes corresponding to an induction of 100 gauss. Here the search coils were always maintained at a position $\theta = 45°$ with respect to the field.

The change in magnetization taking place when a discontinuity occurs is proportional to the area under the corresponding curve traced out by the oscillograph. The areas corresponding to each discontinuity were obtained by considering the impulse to be triangular in shape and measuring the base and altitude of the triangle. From these measurements the ratio of the change in magnetization in the outer coil to the change in magnetization in the inner coil can be obtained for the various values of ψ and θ. Curves of this ratio plotted as a function of θ are then obtained corresponding to various values of ψ. In order that these curves have any significance it is necessary that the over-all amplification of both the outer and inner coil circuits be the same in magnitude. The amplifiers employed were matched as closely as possible and the outer coil wound with more turns than the inner coil in order to compensate for the relatively smaller efficiency of the outer coil. Adjustment of the over-all amplification of both circuits was then made by comparing the ratio of the impulses at $\theta = 0°$ and $\theta = 90°$. If the over-all amplification is f_o for the outer coil circuit and f_i for the inner coil circuit we have

$$f_i/f_o = [(A_i/A_o)_{90}/(A_o/A_i)_0]^{1/2}.$$

Here $(A_o/A_i)_0$ is the ratio of the impulses in the outer and inner coil circuits at $\theta = 0°$ and $(A_o/A_i)_{90}$ is the same ratio at $\theta = 90°$.

From the data obtained in the manner outlined above the ratio of the change in magnetization along the field and perpendicular to the field may be determined. From this information the angle ϕ which the change in magnetization makes with $(d\boldsymbol{H}/dt)$ may be determined. These data can be averaged for the various positions of the field and a curve of average ϕ plotted as a function of ψ.

Results and Discussion

The results of the investigation are contained in curves of which Fig. 5 is typical and in the curves of Fig. 6. In Fig. 6, curve 1 is for a field current of 10 amperes while curve 2 is for a field current of 5 amperes.

The data indicate that changes in magnetization sometimes occur which give a component in a direction opposite to the applied field. This result is in apparent contradiction with expectation in that it seemingly involves a change in magnetization for which there is an increase of the potential energy. However, Bozorth[3] points out that in all probability the volume element

undergoing a change is exceedingly small, approximating 10^{-9} cm³. It seems reasonable to suppose that the actuating field causing a Barkhausen discontinuity is the field in the immediate vicinity of the volume element which subsequently undergoes a change. This field is the resultant of the externally applied field and the field due to all other surrounding elements. With this

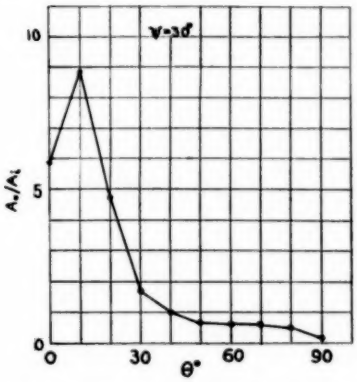

Fig. 5. Relation between ratio (A_o/A_i) of impulses in outer and inner search coils to the search coil setting θ for a single value of ψ. Magnetizing current 10 amperes; A_o/A_i has been corrected for inequality of amplifiers.

supposition the discontinuity may give a longitudinal component in an opposite direction to the applied field and still give a component in the direction of the actuating field in its immediate vicinity. From the curves of average ϕ-*vs.*-ψ we see that the average change in magnetization involves a transverse component which has a direction always in the direction of the incre-

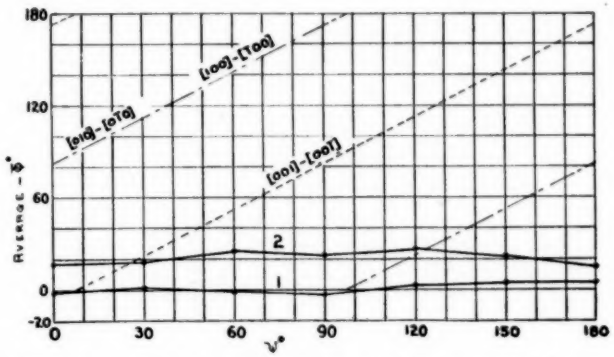

Fig. 6. Relation between mean ϕ and ψ for two magnetizing currents. Curve marked 1 for 10 amperes, curve marked 2 for 5 amperes.

ment of the applied field. Changes in magnetization involving a transverse impulse opposite to this would give values of ϕ greater than 90°. One is led to the conclusion from these results that the average direction of magnetization always lags the direction of the applied field. The data indicate that, for these low values of magnetization and for the particular crystal in question, the change in magnetization has a large component transverse to the

applied field. The average angle ϕ appears to decrease as the field strength is increased. This apparently indicates that the angle between the average magnetization and the applied field is small at large values of magnetization. When saturation is reached the average intensity of magnetization should be directed along the applied field.

It will be interesting to consider the data in light of the possible modes of change in magnetization as indicated by the recent theoretical considerations of Akulov.[4] On the basis of energies involved Akulov concludes that the changes in magnetization which occur are most probable when these changes occur between pairs of the six [100] directions in a crystal. The theory further indicates that two possible modes of change must be considered in attempting to explain experimental results. The first is the so-called *Umklappungprozess* in which the magnetization vector of a small single magnetized region reverses its direction but retains its absolute value unchanged. A change of this type is that in which the change is from the [100] direction to the [$\bar{1}$00] direction. The second mode of change is the so-called *Drehprozess* in which the magnetization vector turns through 90° but again suffers no change in absolute value. An example of this type would be a change from the [100] direction to the [010] direction. The first type of change involves smaller energies than the second and occurs for lower values of magnetization. At the low values of magnetization at which our experiment was performed it is more probable that changes of the first type would occur. Changes of this type are illustrated by the diagonal lines of Fig. 6. As is seen, there occur regions in the interval $\psi=0$ to $\psi=180°$ for which the expected impulses are of the longitudinal type. The actually observed curves indicate that impulses occur which are transverse in character.

If one considers the distortion of the lattice due to mechanical strains as the guiding factor a similar variation of ϕ with ψ would result as was found in connection with Akulov's theory. On Becker's theory[5] one would have to conclude from the experimental data that the distorted regions travel with the applied field in order to account for the small deviations in the average angle ϕ between $\psi=0$ and $\psi=180°$. This is contrary to Becker's postulate that the strains are nearly independent of the condition of magnetization.

[4] N. S. Akulov, Zeits. f. Physik **67**, 794 (1931).
[5] R. Becker, Zeits. f. Physik **62**, 253 (1930).

The Velocity of Sound in an Absorptive Gas

By D. G. BOURGIN
Dept. of Mathematics, University of Illinois

(Received June 13, 1932)

The theory of velocity propagation in a gas as conditioned by internal energy exchanges is considered in detail for the simplest case in which the "lags" may be different—namely, the model with three sets of states. This "second order" theory is required for the interpretation of experimental results where the wave period is of the order of the lag for some states. Assuming the first vibration state of CO_2 to have the largest lag in accordance with Kneser's interpretation of his recent experiments, the necessary approximations are given explicitly and the results are directly applicable to CO_2. The apparent lag as measured in sound velocity experiments is not the simple stationary state mean "collision life" nor the mean life of the energy quantum except under special conditions and then for only one of the states. The velocity increment in the "resonance" region is given more accurately in terms of transition probabilities and is not described completely by the specific heats as might be expected from the "first order" theory. Contrary to the indications of the simple theory with an empirical constant the external energy is always merely the translation term. The status of the assumed lag assignment in CO_2 is discussed in the light of the results and underlying theory of this paper.

IN TWO earlier papers[1] the author has presented a theory of the propagation of sound in a gas and gas mixtures which deals directly with the fundamental kinetic and atomic qualities of the system. The problem of a gas whose rate of adjustment to fluctuation in translational energy is the same for all internal states was taken up as a special case, or first approximation, under this theory. It was pointed out that this special case corresponded to the macroscopic theory of Herzfeld and Rice.[2] Recently O. Kneser[3] in discussing his important experimental results has used essentially this macroscopic theory and has tried to utilize the ideas of transition probabilities, etc., in connection with it. Such a procedure is artificial and seems limited to "first order" approximations—any more thorough investigation must proceed on some such lines as those pursued in I and II and the present paper.

Because of the highly suggestive nature of Kneser's data and the increasing interest in the field of supersonics, it was felt desirable to refine the pertinent formulae in the same measure as the increase in experimental technique. In the interest of the general reader that part of the theory of I and II germane to the present discussion is briefly reviewed in section I. In section II the problem of a gas model with three internal states is taken up in some detail and the calculations are developed with special reference to Kneser's[4] research on CO_2.

[1] D. G. Bourgin, Nature **122,** 133 (1928); Phil. Mag. **7,** 821 (1929); Phys. Rev. **34,** 521 (1929). (These last will be referred to as I and II, respectively.)

[2] K. F. Herzfeld and F. O. Rice, Phys. Rev. **31,** 691 (1928).

[3] O. Kneser, Ann. d. Physik **11,** 761, 779 (1931).

[4] Kneser's remark in a footnote that the writer's developments "nicht zu experimentalle

Section I

The principle of detailed balancing yields at equilibrium[5]

$$(\Delta N_i)_T = 0 = \{N_i^2(\bar{f}_{ij} - f_{ij}) + NN_i f_{ij}\} - \{N_j^2(\bar{f}_{ji} - f_{ji}) + NN_j f_{ji}\}. \quad (1.00)$$

If we disturb equilibrium

$$\Delta N_i = -\sum \delta N\{N_i f_{ij} - N_j f_{ji}\} + \delta N_i\{2N_i(\bar{f}_{ij} - f_{ij}) + Nf_{ij}\}$$
$$- \delta N_j\{2N_i(f_{ji} - f_{ji}) + Nf_{ji}\} + N_i^2\{\delta(\bar{f}_{ij} + f_{ij})\} + NN_i\delta f_{ij} + . \quad (1.01)$$

We introduce

$$R_{ij} = [2N_i(\bar{f}_{ij} - f_{ij}) + Nf_{ij}]/N. \quad (1.02)$$

Suppose the effective temperature for the state i is $\omega_i\delta T + T_0$, i.e., the number of molecules in state i may be considered to be that corresponding to this temperature at equilibrium, then the change in N_i due to increase of the temperature of this state to $\omega_i\delta T$ is

$$\delta N_i = (\delta NN_i + N\dot{N}_i\omega_i\delta K)/N \quad (1.03)$$

where $K=(3/2)kT$ and $\dot{N}_i = dN_i/dK$ and the first term corresponds to a density increase.

We now observe that if $\omega_r \equiv 1$ then the ΔN_i of Eq. (1.01) is the difference between the number of molecules leaving state i at temperatures T_0 and $T_0+\delta T$ because of collisions. Since for each fixed temperature $(\Delta N_i)_T = 0$, therefore ΔN_i for $\omega_r \equiv 1$.

If the first term of Eq. (1.03) were alone active we should have (neglecting the effect of variation of N on f_{ij} for the moment)

$$(\Delta N_i)_T, f = (\delta N/N)[(\Delta N_i)_T] = 0. \quad (1.011)$$

Accordingly we may neglect all terms in Eq. (1.01) with δN. Collecting the remaining terms and bearing in mind

$$(\Delta N_i)_{\omega_i=1} = 0 = \sum_j N(\delta N_i R_{ij} - \delta N_j R_{ji})$$
$$+ (NN_i - N_i^2)\delta f_{ji} + N_i^2\delta f_{ij} - \cdots . \quad (1.012)$$

We may therefore replace the sum of the terms in δf (where δf_{ij} involves δN and δK) by

$$- N[\delta N_i R_{ij} - \delta N_j R_{ji}]_{N,\omega_r=1}.$$

Prüfung dürften" must be ascribed to insufficient acquaintance with the contents of I and II. In fact on adopting the expression for ω given in I, p. 831 footnote, the resulting formula for V^2, cf. Eq. (2.02) and reference 6 of this paper, is (except for one important point of difference taken up in section II) Kneser's main equation. Even the present paper which provides a more solid basis for interpretation of Kneser's experiments is again only a special case of I.

[5] If $N^2\gamma/2$ be the number of collisions per unit time in a gas at temperature T then the number involving $N_i - N_i$ meetings is $N_i^2\gamma/2$ (where N_i is the number of molecules per unit volume in state i). The number involving $N_i - N_j$ meetings is $N_i(N-N_i)\gamma$. If $\bar{f}_{ij}^1$ and f_{ij}^1 are the probabilities of $i \to j$ transition correlated with each type of collision and if $\bar{f}_{ij} = f_{ij}^1\gamma/2$ and $f_{ij} = f_{ij}^1\gamma$, then there results Eq. (1.00).

Eq. (1.01) becomes

$$\Delta N_i = -\left\{N \sum_j \dot{N}_i R_{ij}(\omega_i - 1) - \dot{N}_j R_{ji}(\omega_j - 1)\right\} \delta K. \qquad (1.013)$$

The change of energy due to collision is defined as

$$\Delta K = -\sum \Delta N_i \epsilon_i. \qquad (1.04)$$

The equation of continuity is

$$\partial N/\partial t = -(\partial/\partial x) N v \qquad (1.05)$$

where v equals the x component of the mass velocity.

Also

$$(\partial \dot{N}_i/\partial t) = -(\partial/\partial x) N_i v + \Delta N_i \qquad (1.06)$$

$$(\partial/\partial t) m N v = -(2/3)(\partial K/\partial x) N \qquad (1.07)$$

$$(\partial K/\partial t) N = -(5/3)(\partial/\partial x) K N v + \Delta K. \qquad (1.08)$$

Assume a plane wave in the gas then

$$\delta N = |\delta N| e^{-j(\nu t - x/\lambda)}$$

where ν is frequency and λ is wave-length, and $j = (-1)^{\frac{1}{2}}$

$$\delta T = |\delta T| e^{-j(\nu t - x/\lambda)}$$

$$\delta v = |v| e^{-j(\nu t - x/\lambda)}.$$

In the undisturbed gas clearly v is 0.

For small amplitude waves v is so small that $v\delta N$ and $v\delta T$ may be neglected. From Eq. (1.05) we have

$$j\nu |\delta N| = jN |v| /\lambda. \qquad (1.051)$$

From Eq. (1.06) we get, on referring to Eq. (1.02),

$$j\nu \{\dot{N}_i \omega_i \delta K + |\delta N| N_i/N\} = j\nu N_i/\lambda + \Delta N_i. \qquad (1.061)$$

Eq. (1.061) yields

$$j\nu \dot{N}_i \omega_i = -N \sum_j \dot{N}_i R_{ij}(\omega_i - 1) - \dot{N}_j(\omega_j - 1). \qquad (1.062)$$

These are a set of n non-homogeneous equations in the n quantities ω_i with a unique solution for, because of the presence of $j\nu$ on the diagonal, the determinant will not vanish, i.e., the coefficient of the ii term is $j\nu N_i + N\Sigma_j N_i R_{ij}$ and is the only term in the ith row containing ν.

The elimination of the moduli of K, N and v, leads to one of the key formulae of I and II, namely:

$$j\nu \left[\frac{3mV^2 - 10K/3}{3mV^2 - 2K}\right] = \sum_i (\omega_i - 1)(\Delta K)_i \qquad (1.10)$$

where $(\Delta K)_i$ is $N_i A_i \epsilon_i$ V is the complex velocity of sound, and

$$A_i = \sum_j (\dot{N}_i R_{ij} - \dot{N}_j R_{ji})/\dot{N}_i. \tag{1.11}$$

Section II

Before taking up the second order calculation which is the primary object of this paper it seems appropriate to make some preliminary remarks having a direct bearing on Kneser's paper. First we exhibit in slightly more detail than given in I the special case

$$\omega \equiv \underset{i}{\omega_i}.$$

It follows immediately from Eq. (1.062) that

$$\omega \equiv NA_i/j\nu + NA_i. \tag{2.00}$$

We remark that, with E the internal energy,

$$\begin{aligned} \sum_i \dot{N}_i \epsilon_i &= dE/dK \\ &= NC_i/(3/2)k \end{aligned} \tag{2.01}$$

where C_i is the internal specific heat pro molecule.

Thus

$$V^2 = \frac{K}{3m}\left[\frac{(5/2)k + C_i + j\nu(5k/2)A_iN}{(3/2)k + C_i + j\nu(3k/2)A_iN}\right]. \tag{2.02}$$

This is essentially the equation derived in I expressed in experimentally meaningful terms.[6] It is the same as Kneser's except in the one respect that the external energy (Kneser's notation C_a) is here given explicitly as $3k/2$ while it is left undetermined in Kneser's formula and is indeed finally given a value greater than that corresponding to the translational energy.

It will be shown in this paper, however, that it is physically inaccurate to assume that the external energy differs from $3/2k$—the apparent departure is due to the deficiency of the simple $\omega \equiv \omega_i$ theory. In order to avoid repetition the $\omega \equiv \omega_i$, or Herzfeld-Rice, Kneser theory will be referred to under the properly descriptive head, first order theory, to distinguish it from the second order theory of this section.

Kneser has shown by straightforward, detailed computations that the dispersion formula used by him as well as that of Lorentz and Herzfeld-Rice, yields an inflection point with respect to log ν. Since Eq. (2.02) is, with the exception mentioned, the precise analogue of Kneser's formula, it is clear that properties of this sort hold for Eq. (2.02) also. However, the existence of an inflection point is immediately evident without calculation for a wide class of formulae including the extremely general case taken up in I on the basis of the most simple considerations. One observes merely that for all natural dispersion formulae $r.p.V^2$ is a function of ν^2 finite together with its first derivatives at the end points of the interval $0 \leqq \nu \leqq \infty$ and continuously differ-

[6] The only difference is that Eq. (2.02) involves the full expression for ω whereas I employs the first terms only of the series expansion.

entiable twice on this range. Rolle's theorem is all else that is needed (for with these restrictions $r.p.dV^2/d\nu=0$ for $\nu=0$ and $\nu=\infty$).

For a very general case $r.p.V^2$ is a rational function of ν^2 with poles not on the real axis. Since the poles of the derivatives of a rational function are at the same points as the poles of the function and all the derivatives of V^2 are rational functions, it follows that this satisfies the conditions stated. For exhibiting the data, it may be convenient to introduce $z=f(\nu)$ which, generally, will be some simple[7] functional relation. Accordingly the conditions just stated in terms of ν are as easily applied with z.

It is worth while to point out that if $n-1$ states have the same ω then $\omega_n=\omega$ also. Hence one cannot talk about a two state gas model having different ω values.[8] The proof is immediate and involves the assumption that v is very small.

From Eq. (1.061) we derive:

$$j\nu\sum_i \dot{N}_i\omega_i = \sum_i(\Delta N_i) = \Delta N. \tag{2.03}$$

Manifestly, ΔN the change in N due to collisions is 0. We observe next that

$$\sum_i \dot{N}_i = dN/dK = 0. \tag{2.04}$$

Therefore if $\omega_i=\omega$ for $i=n, \cdots$ n, we have

$$\dot{N}_1\omega_1 = -\omega\sum_2^n \dot{N}_i$$

$$= \omega\dot{N}_i$$

or

$$\omega_1 = \omega.$$

Accordingly the next simplest gas model consists of three states (or classes of states) correlated with different ω values.

In order to maintain symmetry, Eqs. (2.03) and (2.04) are not used in what follows now.

Eq. (1.061) yields:

$$\begin{aligned} \dot{N}_i(j\nu + Ns_1)\omega_1 - N\dot{N}_2R_{21}\omega_2 - N\dot{N}_3R_{31}\omega_3 &= N\dot{N}_1A_1 \\ . \quad + \dot{N}_2(j\nu + Ns_2)\omega_2 - \quad . \quad &= N\dot{N}_2A_2 \\ . \qquad . \qquad . \quad &= N\dot{N}_3A_3 \end{aligned} \tag{2.031}$$

where $s_i=\Sigma_j R_{ij}$. The constant term in the determinant of the equations vanishes and there results

$$\omega_i = \frac{j\nu NA_i + N^2S}{(j\nu)^2 + j\nu N\sum s_i + N^2S} \tag{2.05}$$

[7] It is therefore of perfunctory interest only to state sufficient conditions on $z=f(\nu)$ to insure finite inflection points in z and dependent on the parameters of $V(\nu)$ when there are inflection points in ν.

[8] This is not clear in some recent papers.

and accordingly

$$\omega_i - 1 = -\frac{j\nu[j\nu - N(A_i - \sum s_i)]}{(j\nu)^2 + j\nu N \sum s_i + N^2 S} \tag{2.051}$$

where

$$2S = \sum_i^3 \sum_j^3 s_i s_j - R_{ij}R_{ji},\ i \neq j.$$

Eq. (2.051) allows of direct physical interpretation. $NA_i\dot{N}_i\delta K$ expresses the change in N_i due to collisions in unit time. The difference in value of N_i for T_0 and $T_0+\delta T$ is $\dot{N}_i\delta K$. Hence the fictitious time required at constant rate to attain the new equilibrium value would be the ratio of these two quantities or $(A_iN)^{-1}$. This is the "static" lag.[9] Since increase of the *K.E.* changes N_i and ΔN_i in the same direction it follows from Eq. (1.013) that $A_i>0$. Although for the first order theory the important low-frequency term for ω_i-1 is just this static lag the corresponding lag term in the second order theory is $N(A_i-\Sigma s_j)/N^2S$. The important point to notice is that the order of the states according to lags is the same as that given by this last formula. This follows from the fact that $\Sigma s_j > A_i$. While in some instances, because of the approximation that may be made, the lag for state i is closely the mean life of the ith quantum of energy, nevertheless the strict value of this latter life[10] is, of course, $(s_iN)^{-1}$.

In order to make close contact with Kneser's experimental work let us make assumption *A*

$$(a)\quad A_2, A_3 \gg A_1 \qquad (b)\quad \epsilon_1 \gg \epsilon_2, \epsilon_3.$$

Furthermore we assume that $(c)\dot{N}_2R_{21}+\dot{N}_3R_{31}/\dot{N}_1$ is negligible. The implication of this last condition will perhaps be better apprehended by writing

$$\dot{N}_2R_{21} + \dot{N}_3R_{31} \sim (N_1\dot{N}_2/N_2)R_{12} + (N_1\dot{N}_3/N_3)R_{13}. \tag{2.06}$$

From

$$N_i = Ne^{-\epsilon_i/kT}/\sum_j e^{-\epsilon_j/kT} \tag{2.07}$$

(where possible degeneracy has been remoted by the familiar artifice of a small electrostatic field) one finds $N_1\dot{N}_2/\dot{N}_1N_2=(\bar{\epsilon}-\epsilon_2)/(\bar{\epsilon}-\epsilon_1)$ with $\bar{\epsilon}$ the average internal energy (c) at temperature T_0. Assumption (c) is satisfied if

[9] As pointed out in II, the $j\nu$ term is the in the "phase" term and hence the word lag is here used with a different connotation from that employed in II where it characterizes the $(\nu)^2$ term. We remark also that it is the combination A_iN, and likewise s_iN and N^2S that is independent of N. In the notation of I our present A_i is $A_i/\dot{N}_i$ and $B=\sum_i \dot{N}_iA_i\epsilon_i$. For the $\omega\equiv\omega_i$ case, $(AN)^{-1}$ corresponds to $2\beta/3B$ of I.

[10] The impression seems to persist that radiation "lives" generally are of the order of the atomic ones, namely, 10^{-8} to 10^{-10} seconds and that the collision lives are much longer. (Cf. Kneser, p. 779, ibid. and Henry, Nature, Feb. 6, 1932), Actually the radiation "lives" will most likely be the longest. In the case of HCl for instance, both theory and experiment indicate a life for the first vibration state as long as 10^{-2} seconds. D. G. Bourgin, Phys. Rev. **29**, 794 (1927) and Phys. Rev. **32**, 237 (1928).

$$\left| \bar{\epsilon} - \frac{\epsilon_2}{\epsilon_3} \right| \ll | \bar{\epsilon} - \epsilon_1 | \tag{2.08}$$

which carries with it $N_1 < N_2$, N_3. With these assumptions $S = s_1(s_2 + s_3)$, $A_1 = s_1$ and as may easily be verified,

$$\omega_1 - 1 = -j\nu/j\nu + Ns_1. \tag{2.052}$$

We remark now that

$$N \sum_i \left(A_i - \sum_j s_j \right) (\Delta K)_i = NS \sum_i \dot{N}_i \epsilon_i.$$

Hence on substituting Eq. (2.051) in Eq. (1.10) and using A one finds:

$$V^2 = \frac{2K}{3m} \left[1 + \frac{\frac{2}{3}}{1 + \left\{ \sum_i \dot{N}_i A_i \epsilon_i j\nu + NS\dot{N}_i \epsilon_i/(j\nu)^2 + j\nu N \sum s_i + N^2 S \right\}} \right] \tag{2.09}$$

for determining the inflection point we need only the second term in the bracket. The real part is expressible as

$$\frac{\nu^4 + \nu^2 \{ N^2 [\sum s_i (\sum s_i + \sum \dot{N}_i A_i \epsilon_i / N) - S - S[1 + (C_i/(3k/2)] + N^4 S^2 (1 + C_i/(3k/2)}{\nu^4 + N^2 \nu^2 [(\sum s_i + \sum N_i \dot{A}_i \epsilon_i / N)^2 - 2S[1 + (C_i/(3k/2)] + N^4 S^2 (1 + C_i(3k/2))^2} \tag{2.091}$$

For comparison with Kneser's result we find the inflection point with reference to $\log \nu = z$. To a fair approximation[11] the abscissa of the lowest inflection point is:

$$\nu_0 = \frac{Ns_1(3k/2 + C_i)}{(3/2)k - (4s_1/s_2 + s_3)((3k/2) + C_i)}. \tag{2.10}$$

The first order theory yields in this notation:

$$\nu_0 = [Ns_1(3k/2 + C_i)]/(3/2)k. \tag{2.101}$$

The subsequent discussion uses V^2 with the sense of the real part of the squared velocity and the subscripts $0, \mu$ distinguish between the low and the intermediate frequency velocities. Our immediate concern is the magnitude of the increment $V_\mu^2 - V_0^2 = \Delta V^2$ through the resonance region. Kneser obtains numerical agreement with his experimental data by assuming that the external energy is not simply the translational energy but includes[12] the rotational energy as well while the total specific heat remains unaltered. This statement is not correct physically. In fact for the "first approximation" theory involved in Kneser's formulae, one may reason on altogether general grounds as follows. Under assumption A it is clear that at high frequencies

[11] In this approximation the next higher order terms are retained till the end.

[12] It is again to be pointed out that we are assuming tentatively with Kneser that the vibration states are the large lag states but the substance of the discussion is independent of this special circumstance.

the vibrational transitions will play a negligible role because of their large lags. Hence one would expect as an approach to the truth that the apparent total specific heat would omit these terms though C_a as always remains the translational energy. Kneser's mistake arises from the fact that his presentation of the simple theory is not really descriptive in that first the shorter lag states are neglected and then the resulting formula is analyzed with respect to behavior in a range where just these states are dominant.

On going to the second approximation it develops that the statements just made are in need of modification and it is evident how a more precise estimate of ΔV^2 is to be arrived at; namely, one needs to determine the value of V_μ^2 for $s_2^2, s_3^2 > (\nu/N)^2 \gg s_1^2$. We shall use Eq. (2.091) for this purpose. Neglecting ν^4 terms restricts the validity of this equation to the low-frequency region. For high frequencies the constant term in the quotient may be omitted and there is obtained thus a sort of asymptotic approximation. In both these extreme cases V^2 (real) is a quotient of monomials in ν^2 in formal analogy with the first approximation problem. The low-frequency equation corresponds to Eq. (2.02) with the important difference that the coefficient of ν^2 is no longer C_a. V_μ^2 lies in the intermediate region of validity of both subsidiary equations. Unless $1 \gg s_1/s_i$ $i=2, 3$ a good approximation will not[13] be obtained if either the constant or ν^4 terms are neglected. However, in the interest of analytic simplicity we shall consider the ν^2 term as alone being of consequence.

This implies

$$S^2/(s_2 + s_3)\nu^2 \doteq 0$$

$$\omega_i - 1 \doteq + (- j\nu + N(A_i - \textstyle\sum_j s_j)/j^\nu + N \sum_j s_j) \quad i = 2, 3. \quad (2.11)$$

If, besides, terms in S are dropped then

$$V_\mu^2 = \frac{2K}{3m}\left[1 + \frac{k}{(3k/2 + \sum A_i \epsilon_i dN_i/dT/N(s_2 + s_3)}\right]. \quad (2.092)$$

The first order approximation discussed above indicated a relationship of the form

$$V_\mu^2 = \frac{2K}{3m}\left[1 + \frac{k}{3k/2 + C_i - \left(\dfrac{d N_1}{dT}\, \epsilon_1/N\right)}\right]. \quad (2.021)$$

Eq. (2.092) and Eq. (2.021) differ except under special supplementary conditions. (For instance if $(dN_1/dT)A_1\epsilon_1/s_2+s_3$ is negligible then we should require the special relation $A_1=A_2=s_2+s_3$.)

We now turn to the question of deriving transition probabilities information from sound velocity and absorption experiments. All our approximations in this paper have been on the assumption that the vibrational energy has, associated, the larger lag. The assumption is, however, not altogether certain even in the case of CO_2. The correct argument for such an assignment as a

[13] This remark is to be kept in mind in any comparison of Eq. (2.091) with the experimental data.

working hypothesis is the agreement of Eq. (2.021) with Kneser's experimental data. The fortunate coincidence that his assumption leads to the same numerical value here is explained by the fact that there are only two terms of importance in C_i (the two rotational states are lumped in the symbol $C_R = k$). With additional terms in C_i the Kneser postulate yields a result at variance with Eq. (2.021). In order to maintain the agreement one should be led to the bizarre conclusion that all the internal energies, save the one vibrational term, are included in the external energy. More explicitly, for the model considered in this paper Eq. (2.02) yields the rigorous value

$$V_\mu^2 = (1+k/(3/2)k)2K/3m.$$

Kneser's procedure amounts to arbitrarily replacing the $(3/2)k$ term by $(3/2)k+C_R$. This modified V_μ^2 has just the value given by Eq. (2.021) as is evident on observing that the vibrational energy denoted by

$$C_S = dN_1/dT\,\epsilon_1/N \quad \text{and} \quad C_i = C_R + C_S.$$

For confirmation[14] it is necessary now to use the more accurate Eq. (2.092) and then the analogous second order formula that would result from the supposition that the low energy states[15] (2, 3) have the large lags.[16] The assumption that all rotation states have one type of lag and all vibrational states another may be wide of the truth, in which case a theory is required in which both rotational and rotation-vibrational states exist characterized by the same lag value. Such modifications in the hypothesis may be taken account of by suitably varying the approximations in a treatment like the present one. Then too it may be remarked that the data points in Kneser's figure do not continue into the critical intermediate region, and besides, the experimental accuracy is least here. It seems desirable to supplement and extend the experimental results to higher frequencies by varying the CO_2 percentage in a mixture with a non-masking gas.[17]

[14] Conversely if the lag assignment be adopted the experimental data yield estimates of the A_i and C_i combinations occurring in Eqs. (2.10) and (2.092).

[15] Kneser's use of the ratio of the squared velocities in CO_2 and Ar may be expected to minimize viscosity, conductivity, etc., corrections.

[16] Without going into details here, Kneser's attempted "a posteriori" justification for expecting larger lags for the vibration state is inadequate in the writer's opinion if only for the reason of the lack of satisfactoriness in the present day treatments of the circumstances of energy transfer in collision.

[17] The theory of gas mixtures may be developed along lines similar to that presented in this paper. Cf. the footnote in a forthcoming publication of the writer in the Jour. Acoust. Soc. where an error in Eq. (1.2) of II is corrected. The work in II is what I have called here a first order theory—incidentally Eq. (7) of II is the theoretical basis for computing humidity effects, etc., and provides the validation for Reid's empirical formula. Reid, Phys. Rev. 35, 814 (1930). A form of Eq. (7) more convenient to use is

$$\frac{\delta V}{V} = \tfrac{1}{2}\overline{\sum}_\omega \frac{\delta N_\omega}{N}\left[\frac{C_{n\omega}}{\overline{C_n}} - \frac{C_{v\omega}}{\overline{C_v}} - \frac{m_\omega}{\overline{m}}\right]$$

where the notation is self-explanatory.

The second order treatment of the absorption may be made to parallel the development of this section by taking the imaginary part of V^2 in Eq. (2.09) and very likely other than lag influences may probably be neglected if the ratio with a rare gas is taken (in accordance with Kneser's suggestion).

An experimental study of the temperature effect seems likely to yield important evidence—the theoretical aspect is clearly outlined, namely, the dependence of R_{ij} (and $\dot{N}_j$) on T in connection with the variation in collision frequency and average collision energy. In a way this provides a means for isolating the effects of various groups of states; for instance, the inequalities of (cf. Eq. (2.08)) c valid for sufficiently low temperatures but may actually be reversed if the gas be raised to a very high temperature.

In order to make a close contact with Kneser's experimental work let us make assumption A

$$(a)\ A_2, A_3 \gg A_1; \quad (b)\ \epsilon_1 \gg \epsilon_2, \epsilon_3.$$

Furthermore we assume that (C) $\dot{N}_2R_{21}+\dot{N}_3R_{31}/\dot{N}_1$ is negligible. The conditions implied in this last assumption are indicated clearly on writing

$$\dot{N}_2R_{21} + \dot{N}_3R_{31} = N_1\dot{N}_2R_{12}/N_2 + \dot{N}_1N_3R_{13}/N_3. \tag{2.06}$$

From

$$N_i = Ne^{-\epsilon_i/kT}/\sum_j e^{-\epsilon_i/kT} \tag{2.07}$$

one finds

$$N_1\dot{N}_2/\dot{N}_1N_2 = (\bar{\epsilon} - \epsilon_2)/(\bar{\epsilon} - \epsilon_1) \tag{2.08}$$

with $\bar{\epsilon}$ the average internal energy at temperature T_0.

LETTERS TO THE EDITOR

Prompt publication of brief reports of important discoveries in physics may be secured by addressing them to this department. Closing dates for this department are, for the first issue of the month, the twenty-eighth of the preceding month; for the second issue, the thirteenth of the month. The Board of Editors does not hold itself responsible for the opinions expressed by the correspondents.

The Tropism of Crystals

A crystal is generally described in terms of the positions of its constituent atoms. These are regarded as points, and consequently the energy of the crystal is expressed in terms of the positional coordinates of the atoms. This model may be amplified by giving up the assumption that the atoms are points, or spherically symmetrical centers of force, and by introducing angular coordinates to specify the orientation of each atom. In the language of the quantum theory, the state of an atom or molecule is specified by a variety of quantum numbers that may be interpreted geometrically as specifying an orientation. The orientation of an atom in empty space is, of course, quite arbitrary, as its energy is independent of orientation. In a crystal lattice this is no longer true. Because of the anisotropy of the atomic arrangements in a crystal, certain orientations of the atoms will be energetically preferable to others. We have, thus, besides the anisotropy of the crystallographic planes themselves, other directional properties associated with the various vectors specifying atomic states. If, for instance, all the electronic spins are coupled, we have what might be called spintropism, or *s*-tropism. Likewise, coupled orbits would give rise to *l*-tropism, etc.

To illustrate the significance of the above, let us consider two special cases. The first is that of a cubic lattice in which each atom has a magnetic moment resulting from the electronic spins. The spins are so coupled to each other that the energy is least when neighboring spins are parallel. The crystal exhibits spontaneous magnetization. The spins are further so coupled to the lattice (or to orbits fixed in the lattice) that, if α_i, α_j, α_k represent the direction cosines of the spins with respect to the tetragonal axes of the crystal, the energy of the crystal depends on the orientation of the spins according to the formula

$$c\sum_{i,j,k}{}'\alpha_i^2\alpha_j^2.$$

If the crystal is distorted by external forces, the energy is increased, first, by the work done against the elastic forces, and secondly, by an amount depending on the orientation of the spins

$$k_1\sum_{i,j,k}A_{ii}\alpha_i^2+k_2\sum_{i,j,k}{}'A_{ij}\alpha_i\alpha_j$$

where A_{ij}, etc., are the components of the tensor describing the distortion, and finally, if the crystal is subjected to the action of a magnetic field, there is a further term in the energy $-(\boldsymbol{I}\cdot\boldsymbol{H})$.

If the distortion A_{ij}, etc., and the field H are given, it is possible to calculate the energy of the crystal for any orientation of the spins. If this energy has a single minimum, we assume that this minimum gives the direction of actual magnetization, and hence uniquely determines the actual energy of the crystal. If the energy has minima for more than one orientation of the spins, the direction of actual magnetization is not uniquely determined. Changes in the relative position of two or more minima will in general give rise to irreversible changes in the orientation of the spins, and therefore to a dissipation of energy, or hysteresis. This procedure, based on the work of N. Akulov and R. Becker, is shown, in a paper appearing in this journal, to describe the properties of ferromagnetic crystals fairly well.

The second model we shall assume identical with the first, except that the spins are so coupled that the energy is least when the spins cancel each other in pairs. Although there is no resultant magnetization, one may still refer to an orientation of the spins, given again by the quantities α_i, α_j, α_k. The orientation of the spins is in this case unaffected by a magnetic field. In general, we may refer to that condition of a crystal in which at least one

aspect of its constituent atoms is unchanged throughout a group of atoms as spontaneous alignment, just as we speak of spontaneous magnetization in a ferromagnetic crystal. A crystal showing spintropism as above would be very similar to a ferromagnetic crystal except in its reaction to a magnetic field. What, then, is peculiar about a ferromagnetic crystal in the absence of a magnetic field? We shall consider here only mechanical and thermal properties. There are others, such as electrical, optical, etc. Four such peculiarities are listed below. These peculiarities may be thought of as defining certain kinds of tropism in crystals of which spintropism is one. Ferromagnetism is then a special kind of spintropism.

(1) There is a critical temperature, or "Curie point," above which ferromagnetism, or more generally spintropism, etc., disappears. In general, a substance may have more than one such critical temperature.

(2) Just as there is a magneto-caloric effect, or reversible change of temperature with magnetization, there should be a reversible change of temperature accompanying elastic distortion, having a maximum at the critical temperature.

(3) There should also exist an elastic hysteresis, or dissipation of energy resulting from elastic distortion. This is caused by irreversible changes in spin orientation. These irreversible processes should occur only when the distortion produces the above-mentioned ambiguity of two or more energetically possible spin orientations. Magnetic hysteresis is most pronounced in distorted or hardened materials, and becomes very slight in single crystals at ordinary temperatures. The same should be true of elastic hysteresis. If a single crystal is rotated in a magnetic field, hysteresis is particularly pronounced in the neighborhood of certain orientations of the crystal in the field. Similarly, if a single crystal is rolled between plates exerting a compressive force, elastic hysteresis should also be more pronounced in the neighborhood of certain orientations of the crystal.

(4) When distortion produces only a single possible orientation of the spins, the elastic properties are uniquely defined. They differ from those of normal cubic crystals because of the dissymmetry introduced by the spin interactions, or because of the energy expression above involving both the distortion and the spin orientation. In other words, the spin interactions produce strains in the crystal. In the case of ferromagnetic crystals we call these strains magnetostrictive strains. Since any tropism of the kind here under discussion will tend to distort a crystal, we may refer to this distortion as tropostriction. In distorting a cubic crystal, we do work not only against the cubically symmetrical elastic forces, but also against the tropostrictive forces which vary as the direction of spontaneous alignment in the crystal varies. In a paper that is to appear shortly, the effect of spontaneous alignment on the elastic properties of cubic crystals will be investigated mathematically.

Do any crystals aside from ferromagnetic crystals, show tropism of the kind discussed in this note? Many peculiarities, such as elastic hysteresis, unexplained critical temperatures,[1] etc., have been observed, but until the subject is quantitatively formulated and checked it is not possible to determine to what extent such ideas as the above may be useful in explaining the behavior of actual materials. It seems likely, however, that there is something to orient in most crystals. Few atoms are spherically symmetrical, and such spherical symmetry would probably be destroyed by the interatomic forces and fields in a crystal. It is, therefore, to be expected that at sufficiently low temperatures the atoms in a crystal will either be spontaneously aligned, or if the atomic interaction is such that neighboring atoms are not parallel, the crystal will exhibit a complicated tropism and probably periodic structural peculiarities.

F. BITTER

Research Laboratories,
Westinghouse Electric & Mfg. Co.,
East Pittsburgh, Pennsylvania,
October 25, 1932.

[1] Is the transition to the supra-conducting state perhaps the lowest of these critical points below which all the constituents of a crystal are spontaneously aligned and the atomic planes have lost their "thermal roughness"?

X-Ray Reflections from a Quartz Piezoelectric Oscillator in a Bragg Spectrograph

Recently G. W. Fox and P. H. Carr[1] found that the intensity of Laue spots, obtained by passing an x-ray beam through quartz, were increased when the quartz plate was oscillating electrically. However, in a later paper[2] Fox and Cork failed to obtain any changes in intensity of oscillating quartz lines produced by a Bragg spectrograph. C. S. Barrett and C. E. Howe[3] suggested that this failure to get increased intensity was probably due to the existence of an imperfect surface layer in which the extinction had already been reduced to a minimum by the preparation of the crystal. The mode of oscillation of the quartz plate used by Fox and Cork[2] was such that there existed a node of pressure at the surface of the plate from which the x-ray beam was reflected. Hence, even if elastic deformations of the atomic plane spacings were taking place, no widening of the line obtained could be expected from this experiment.

From experiments performed in this laboratory a widening and an increase in intensity for lines reflected from oscillating quartz were obtained. The quartz crystal used in the experiments was prepared in the following manner. Let EE^1 (Fig. 1) represent the electric

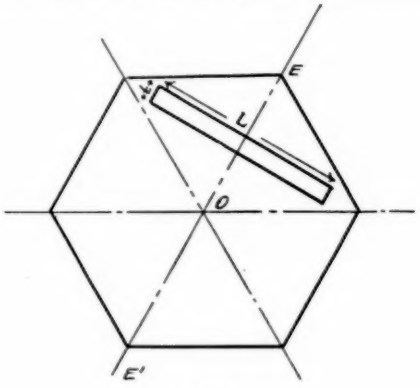

Fig. 1.

axis of a quartz crystal, and let the optic axis pass through O perpendicular to the plane of the paper. The specimen was cut from the crystal as is shown in Fig. 1 with the following dimensions: $L=100$ mm, $t=2$ mm, $w=6$ mm. The dimension L is mutually perpendicular to the electric axis EE^1 and to the optic axis which is perpendicular to the plane of the drawing. The dimension t is parallel to the axis EE^1 and perpendicular to the optic axis. The dimension w (not shown in Fig. 1) is parallel to the optic axis and perpendicular to the electric axis EE^1.

The oscillating quartz plate was placed in a Bragg spectrograph between two brass plates which were connected in parallel with the condenser of a resonating circuit. The crystal-to-film distance of the spectrograph was 20 cm. The top brass plate had a window cut so as to allow the x-ray beam to fall on the surface of the quartz which had dimensions 100×6 mm. The crystal was made to oscillate in such a manner that there existed a loop of motion at each end and a node of motion in the center; consequently there was a loop of pressure in the center, and nodes of pressure at the ends. The x-ray beam was reflected from the center of the oscillator. The crystal oscillated at a frequency of 27,400 cycles per second, which result agreed with the calculated value. The source of power was the output of an audio-oscillator connected to an amplifier and inductively coupled with the resonating circuit containing the quartz plate. A shield enabled only half of the film to be exposed at a time. One side of the film was exposed with the crystal not oscillating and the other half with the crystal oscillating. The crystal was kept oscillating at such an amplitude that dL/L was 0.0003 in the L direction. This quantity was measured by means of a calibrated eye piece. The doublet used in the experiment was the $K\alpha_1$ and $K\alpha_2$ lines of molybdenum obtained by the sixth order reflection from the (1 1 0) set of planes. The crystal was rocked through an angle of 5° during the exposures. It was necessary to expose each side of the film for 40 hours. A careful watch was kept on the power in-put of the x-ray tube so that accurate intensity comparisons might be made.

The curves shown in Fig. 2 were obtained by examining the photographic record with a microphotometer. The film was passed over a photoelectric cell in steps of 0.02 mm each by means of a ruling machine mechanism. A slit of light 0.02 mm wide and 0.05 inches long was placed above the film in such a position as to be directly over the photoelectric cell. This cell was connected to the grid of a vacuum tube which composed one arm of a Wynn Williams bridge. The deflections of the galvanometer were proportional to the amount of light

[1] Fox and Carr, Phys. Rev. **37**, 1622 (1931).
[2] Fox and Cork, Phys. Rev. **38**, 1420 (1931).
[3] C. E. Howe, Phys. Rev. **39**, 889 (1932).

falling on the cell.

Curve A (Fig. 2) was the curve obtained for the oscillating lines, while curve B was the curve obtained for the non-oscillating lines. At half maximum amplitudes the width of the oscillating $K\alpha_1$ line was found to be 0.600 mm, while the width of the non-oscillating $K\alpha_1$ line was found to be 0.540 mm. The values for the widths of the $K\alpha_2$ lines were practically the same at half amplitudes as those of the $K\alpha_1$ lines. If we take the area under the loops as proportional to the intensity of the lines, we find that the $K\alpha_1$ oscillating line is about 1.5 times as intense as the $K\alpha_1$ non-oscillating line, and that the $K\alpha_2$ oscillating line is about 1.5 times as intense as the $K\alpha_2$ non-oscillating line.

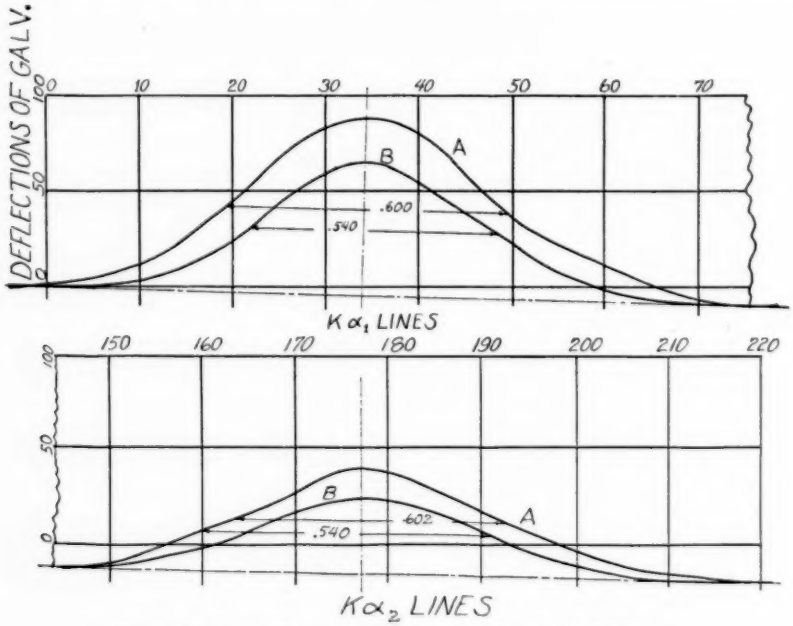

Fig. 2. Settings of ruling machine. One setting = 0.02 mm.

It is interesting to note that if we take $\Delta D/D$ to be $\frac{1}{4}$ the magnitude of dL/L where $\Delta D/D$ is to represent the elastic deformations of the plane spacings for the (1 1 0) set which is at right angles to the elastic deformations of magnitude dL/L; and substitute the value in the relation: $dS = 2r(\Delta D/D)$ tan θ, where r is the crystal-to-film distance, and θ is in our case 60.3°, we have for dS the following: $dS = 0.0525$ mm. The oscillating lines were found to be 0.060 mm wider at half maximum amplitudes than the non-oscillating lines.

It is not at present known whether this effect obtained is due to extinction reduction solely or whether it is a combination of extinction reduction and elastic deformations of the plane spacings. Experiments are now in progress in which an attempt will be made to take Bragg reflections from quartz plates which are deformed mechanically and in a homogeneous fashion. A detailed account of the experiments performed in this laboratory and further conclusions will be given at an early date.

M. Y. Colby
Sidon Harris

Physical Laboratories,
University of Texas,
November 8, 1932.

Determination of e/m for an Electron by a New Deflection Method

In spite of the many measurements which have been made of the specific charge of the electron, there is still some uncertainty especially in connection with the value obtained from free electron measurements. Although two recent measurements[1,2] on free electrons

[1] C. T. Perry and E. L. Chaffee, Phys. Rev. **36**, 904 (1930).

[2] F. Kirchner, Ann. d. Physik [5] **8**, 975 (1931) and [5] **12**, 503 (1932).

in which linear acceleration was used have yielded "low" values of e/m in fair agreement with the spectroscopic value $(1.761 \pm 0.001) \times 10^7$ *em* units, there remains the fact that the apparently very precise work of Wolf[3] using a deflection method gave a high value $(1.7689 \pm 0.0018) \times 10^7$ *em* units. Hence, it is important that a new deflection determination be made with an accuracy sufficient to determine if the discrepancy is real or due to some unknown sources of error. Secondly, an accurate value of e/m is needed in the very important method that has been developed by Bond[4] and Birge[5] of obtaining the most probable values of the physical constants e, h, e/m and α. Not only does the value of e/m influence the values obtained for the other constants but also the major portion of the uncertainty of the results is due to the uncertainty in e/m.

The new deflection method being used was conceived by Professor Ernest O. Lawrence and was most kindly offered to the author as a means of obtaining the results mentioned above. The success of this new determination was made possible by the important advantages of this method over previous ones. The method is essentially as follows. An evacuated brass box B contains six slits labeled A, S and D which are on a circle of radius r. The slits S and the outer slits at A and D are integral parts of the box, while the inner slits at A and D are separate from it and are connected to the output of a radio-frequency oscillator. The box is connected to the grounded side of the output. During the half of each cycle in which the box is positive, electrons are accelerated across the slits at A and leave the outer slit with velocities ranging from zero to that corresponding to the peak voltage of the oscillator. These electrons are bent in circles of various radii by a magnetic field having a direction into the plane of the sketch and produced by a pair of Helmholtz coils. For any given magnetic field H, electrons having a velocity v given by the radial force equation $mv^2/r = Hev$ (*em* units) will be bent around through the slits S and arrive at D where they will experience a further acceleration or deceleration depending on the time of arrival relative to the radio-frequency cycle. If a magnetic field is chosen with a related electron velocity such that the time required for the electrons to travel from A to D is one period, then the electrons in traversing the slits at D experience a deceleration exactly equal to the acceleration they received at A and consequently are stopped and fail to reach the collector C. For any other magnetic field a simple analysis shows that half of the electrons passing through the slits S will reach the collector. Hence e/m is determined by the conditions existing when the current to the collector is zero (in reality when it is a minimum). The electron velocity necessary to travel from A to D in one cycle is given by $v = r\theta/T$, where T is the period of the oscillator and θ the angle subtended by the path; or since the frequency $\nu = 1/T$ the velocity is given by $v = r\theta\nu$. Eliminating the velocity by combining this equation with that given above for the radial forces gives the relation

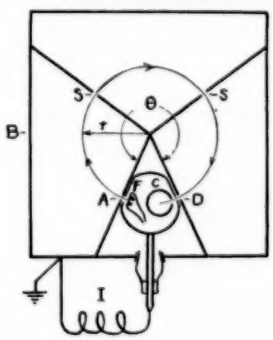

Fig. 1.

for obtaining e/m, namely $e/m = \theta\nu/H$ *em* units. Here θ is in radians and H is in gauss.

A most important advantage of this method over other free electron methods is that no accelerating voltage need be measured since it is not necessary to know the electron voltage. This feature combined with a modification in the method not described above (due to space limitations) *practically eliminates all errors due to contact potentials* except those due to stray electric fields in the deflecting regions of the box. Due to the construction the latter are necessarily small. Further, the observational precision which the method gives is very good. For example, fifty magnetic field readings (the frequency being held constant) were of such constancy that the observational probable error in e/m was only one part in 100,000.

[3] Fritz Wolf, Ann. d. Physik [4] **83**, 849 (1927).

[4] W. N. Bond, Phil. Mag. **10**, 994 (1930) and **12**, 632 (1931).

[5] R. T. Birge, Phys. Rev. **40**, 228 (1932).

The present results, although still of a preliminary nature, are of an accuracy comparable with present published values. Observations have been taken at two frequencies since constancy of results with change in frequency is of primary importance. With a change in frequency of about 30 percent two frequency runs made up of about 90 observations each gave results differing by only two parts in 10,000. The weighted value of e/m obtained from these two groups of observations with the calculated probable error is $e/m_0=(1.7592\pm0.0006)\times10^7$ *em* units. The major part of this probable error is due to allowance for possible errors in the magnetic field measurement. However, to allow for still other possible errors in the experiment the present result may be stated as $e/m_0=(1.7592\pm0.0015)\times10^7$ *em* units. This result is somewhat lower but not in disagreement with the accepted spectroscopic value. It is in good agreement with Kirchner's results.[2] A more detailed description of the method and results will be published soon.

The writer is indebted to Professor Ernest O. Lawrence not only for the method, as mentioned above, but also for many helpful discussions during the development of the method.

FRANK G. DUNNINGTON
University of California,
November 12, 1932.

The Value of e/m

During the past two years there have appeared four direct determinations of e/m, each of high accuracy. These results are:[1] (1) C. T. Perry and E. L. Chaffee,[2] $e/m=1.761\pm0.001$, from electrostatic acceleration of free electrons. (2) F. Kirchner,[3] $e/m=1.7585\pm0.0012$ and 1.7590 ± 0.0015, from two different investigations, by the same method as (1). The weighted average is 1.7587 ± 0.0009, with the probable error based on internal consistency. The probable error from external consistency is, by chance, only ±0.00016. (3) J. S. Campbell and W. V. Houston,[4] $e/m=1.7579\pm0.0025$, from Zeeman effect measurements. (4) F. G. Dunnington,[5] $e/m=1.7592\pm0.0015$, from magnetic deflection of free electrons.

The weighted average of these four results, based on three radically different methods, is $e/m=1.75953\pm0.00043$, from external consistency, or ±0.00059 from internal consistency. This is a very satisfactory agreement and tends to indicate that the probable error assumed by each investigator is a reasonable estimate. In each case, however, this assumed error is essentially a personal estimate by the investigator, and includes an arbitrary allowance for possible systematic errors of various kinds. Each of the four investigations seems, from superficial examination, to be of essentially the same accuracy. With this new assumption one obtains for the (unweighted) average, $e/m=1.75920\pm0.00044$. This happens to be identical with Dunnington's value. I think that $(1.759\pm0.001)\times10^7$ *em* units may be taken as a conservative estimate of the present most probable direct evaluation of e/m.

I should like to take this occasion to call attention to a numerical error in my recent paper[6] on certain general constants. On page 257 the correct value of $e_{3/4}$, resulting from $h_{4/3}=6.5431\pm0.0042$, is 4.7721 ± 0.0023, and not 4.7738 ± 0.0041 as given. This makes the results of solutions k and l incorrect. The correct results of solution k are $h=6.5432\pm0.0083$, $e=4.7683\pm0.0038$, $e/m=1.7611\pm0.0011$, $1/\alpha=137.310\pm0.048$. Solution l is based on $e/m=1.759\pm0.001$, as now adopted for the best direct value. The resulting values of e, h, etc., in solution l, corrected for the above error, may accordingly be considered the present most probable values. These corrected results are,

$-h=(6.5420\pm0.0083)\times10^{-27}$ erg·sec.,
$e=(4.7668\pm0.0038)\times10^{-10}$ *es* units,
$e/m=(1.7592\pm0.0011)\times10^7$ *em* units,
$1/\alpha=137.374\pm0.048$.

RAYMOND T. BIRGE
University of California,
November 12, 1932.

[1] This list does not include a very recent value by G. G. Kretschmar (Chicago, November, 1932 meeting of the American Physical Society) of 1.7555 ± 0.0026, since his method requires a knowledge of other fundamental constants.

[2] C. T. Perry and E. L. Chaffee, Phys. Rev. **36**, 904 (1930).

[3] F. Kirchner, Ann. d. Physik **12**, 503 (1932).

[4] J. S. Campbell and W. V. Houston, Phys. Rev. **38**, 581 (1931).

[5] F. G. Dunnington, Phys. Rev. **42**, 739 (1932).

[6] R. T. Birge, Phys. Rev. **40**, 228 and 319 (1932).

Structure of Atomic Nuclei
Errata

(Phys. Rev. **41**, 370 (1932))

I have noticed certain errata in my letter to the Physical Review **41**, 370 (1932). They are as follows:

P. 370, column 1, line 10 should read "consists of 2 $(2l+1)$ protons and 2 $(2l+1)$ neutrons" instead of "consists of $2l+1$ protons and $2l+1$ neutrons."

P. 371, column 2, line 8 should read "neutrons to be . . . ." instead of "electrons to be . . . ."

JAMES H. BARTLETT, JR.

University of Illinois,
November 9, 1932.

BOOK REVIEWS

Molekulstruktur. Edited by P. Debye. Pp. 197+vii. Figs. 44, Tables 5. S. Hirzel, Leipzig, 1931. Price 10 R.M.

The real benefit from the annual Leipzig lectures is to be had by sitting around the table in the cafe of the Ipabad in Leipzig in between talks. The publisher makes no attempt to collect the discussion which is the most valuable feature of such a scientific gathering. The lectures themselves are usually limited to matters already published and well known to workers in the general field. In some cases new material presented is likely to require immediate modification. But the reader is left to guess what happened after the lectures.

The present series is devoted to chemistry. The speakers are, however, all physicists. K. L. Wolf presents interesting experimental results on the free rotation of the carbon bond. In the second talk R. Mecke provides a masterly exposition of the problems of the spectroscopy of polyatomic molecules. He calls attention to some important regularities in the behavior of simple chemical compounds which are not discussed at all in the fashionable quantum theories of valence. He also shows how these matters can be treated with some success from a classical point of view. Next is a description by F. Rassetti of his experiments on Raman effect in gases and solids. It seems rather strange that he should here repeat his suggestion that the lines he found in calcite and fluorite are due to scattering with large ($\sim$7000 cm^{-1}) frequency shifts. No comment is made of the very convincing explanation furnished by R. Tomaschek (Nature, **128**, 495 (1931)) that these lines are due to known fluorescence of common impurities in these minerals.

G. Placzek has a useful paper on his very important method of treating the Smekal-Raman effect. This effect is of interest chiefly in the study of molecular structure and it is therefore appropriate instead of describing it by the roundabout method of general dispersion theory to treat it as an interaction between the electron motions and the motions of the nuclei. Placzek's presentation is not complete but he furnishes references and an extensive table of tensor components.

H. Spooner and R. de L. Kronig have papers on dissociation—especially predissociation. Their discussions are perhaps carefully stated but do not advance the subject beyond innumerable papers which have discussed it in the past. They do not even refer to the experimental results which V. Henri announces in his talk and leave the subject of polyatomic molecules entirely untouched. Henri finds the phenomenon of predissociation to be very widespread among polyatomic molecules which usually have several regions of predissociation. A most remarkable observation which he reports is that the predissociation limit shifts toward longer wave-lengths as the temperature of the absorbing gas is increased.

G. Herzberg contributes the last talk. It is an unusually clear and concise presentation of the newer methods of discussing the electronic structure and valence characteristics of molecules. Herzberg as well as Mullikan and Hund has contributed much to this subject. The methods advocated are still approximate but have important advantages over that due to Heitler and London. The unsatisfactoriness of the latter has been brought out on many hands, especially during the past two years. It is one great advantage of the newer methods that they lead to their wrong results without any stupendous amount of calculating.

R. M. LANGER
California Institute of Technology

The Theory of Electric and Magnetic Susceptibilities. J. H. VAN VLECK. Pp. 384+xi, Figs. 15. Clarendon Press, Oxford. Price $7.50.

In this book Van Vleck has given with his own characteristic thoroughness and care for details, an excellent survey of the quantum theory of electric and magnetic susceptibilities. In a certain respect the purpose of the book is the same as that of Stoner, which was written in

1926, namely to correlate and explain the great amount of experimental results from the standpoint of the quantum theory. But Van Vleck had the great advantage that he could use the quantum mechanics. Especially in magnetism, since the classical work of Curie, Langevin and Weiss, there has been a great accumulation of experimental material, but I think one may say that a real advance in the understanding first came with the penetration of the ideas and methods of the new mechanics, partly without doubt because of the clarification it brought in the theory of line and band spectra. In dielectrics the advance since Debye is perhaps less striking. The quantum mechanics has, however, here removed, by restoring the classical factor $\frac{1}{3}$, several difficulties, which the application of the old quantum theory had brought.

Chapter I gives the classical foundations. It shows carefully how the macroscopic field equation of Maxwell can be obtained by averaging the microscopic equations of the electron theory. It is perhaps a pity, that the author has not gone into the criticism of the usual expression (34) of the local field, from which the Lorentz-Lorenz formula follows. To the reviewer the validity seems doubtful, especially for polar substances. This point is of interest because of the recent measurements of ϵ for gases at high pressures. Chapter II gives a very complete classical derivation of the Langevin-Debye formula for dielectrics. The reviewer objects though to calling the ordinary simple derivation a rudimentary proof. It follows strictly from the general Boltzmann theorem:

$$dN_1/dN_2=(dN_1/dN_2)_{T\to\infty}e^{-V/kT}$$

for the ratio dN_1/dN_2 of the numbers in two elements of the q-space. Of special interest in this chapter is the derivation in §13 for quite general molecular models in close analogy with the quantum mechanical derivation of chapter VII. Chapter III gives then a discussion of the experimental material. Though there is here some overlapping with the book of Debye, the remarks of Van Vleck on the "atomic polarization" are very interesting.

All this was perhaps more or less known. But in chapter IV Van Vleck gives a very striking discussion of the classical theory of magnetism. He throws the proper light and puts the proper stress on the main result of the Leidener thesis of Miss van Leeuwen, namely, that in classical statistics we get strictly always *zero* susceptibility. The well-known result, that the translatory motion of free electrons in a metal gives no diamagnetism with classical statistics, is a special case of the theorem of Miss van Leeuwen. Perhaps the author could have stressed still more the very artificial assumptions one must make in the classical theory to obtain para- or diamagnetism. The assumptions required are: (1) that each molecule has an electronic motion (or current) which is so shielded that the collisions have no effect on it; (2) that when the gas is formed, each molecule is born with the same value for the angular momentum of that electronic motion. Assuming this, one can derive quite generally the Langevin-Pauli formulas for the para- and diamagnetism. Miss van Leeuwen has given several examples; in her terminology, there must exist besides the energy (or function of Routh) other "interesting" additive integrals of the motion.

In chapter V the many difficulties and paradoxes of the old quantum theory with regard especially to electric susceptibilities (i.e., the Glaser effect) are very clearly discussed. And so we are led to the quantum mechanical chapters. Chapter VI gives all that is necessary from the general theory; in addition to the perturbation theory, it contains a very useful treatment of the angular momentum matrices and of the anomalous Zeeman effect. In Chapter VII we are then given the general quantum mechanical derivation of the Langevin-Debye formula, which is due to Van Vleck himself. It is hardly necessary to stress its importance. Besides containing all earlier derivations for special models it has shown clearly the essential assumptions, which are necessary and sufficient. By a witty application of the theorem of spectroscopic stability the author rehabilitates the classical factor $\frac{1}{3}$. Also because of this theorem all the difficulties of the old quantum theory (i.e., with regard to "weak" and "strong" quantization) disappear. Essential in the derivation, and I think already for qualitative discussions of importance, is the distinction between the (compared to kT) high- and low-frequency non-diagonal matrix elements of the magnetic moment. The first contribute to the temperature independent part of χ; the second, because of the second order Zeeman and Stark effects, which are so often forgotten, *together* with the diagonal elements give the term inversely proportional to T. That it is *not* the diagonal elements alone is perhaps simplest seen in the example of NH_3. The two

lowest levels, considering only the vibrational states, corresponding to the symmetric and antisymmetric wave functions of the N-nucleus, have no diagonal element of the electric moment at all. The observed temperature dependence of ϵ is here due only to the second order Stark effect.

The chapters VIII, IX and X give the applications. Chapter VIII discusses the diamagnetic susceptibilities of atoms and monatomic ions; chapter IX the paramagnetism of free atoms and especially of the rare earth ions. The success of Hund's prediction of the magneton numbers had already shown here that these ions even in the solid salts can be considered as being nearly free. Europium and samarium were the only two apparent exceptions. Van Vleck (with Miss A. Frank) has been able to explain these cases also by taking into account the finite multiplet width *and* the second order Zeeman effect. Also the temperature dependence of χ then agrees beautifully with experiment. Chapter X gives the application to the paramagnetic gases, especially O_2 and NO. The experimental confirmation of Van Vleck's prediction of χ as a function of T in the case of NO is one of the most beautiful successes of his theory.

In chapter XI a new idea enters, namely the crystal field. The author shows how this is able to quench the orbital magnetic moment, and he gives in this way an explanation of the Bose-Stoner hypothesis, which had thrown the first light on the difficult question of the magneton numbers of the iron group. How successful this idea is, Van Vleck and his students have since then shown. It explains beautifully the Curie-Weiss law and its deviations (see Penney and Schlapp, Phys. Rev. **41,** July 15, 1932). The book closes with a short and clear discussion of the Heisenberg theory of ferromagnetism (chapter XII) and of some related optical phenomena (chapter XIII).

I hope that this review, which, although rather long, could touch only the main points, has given sufficient impression of the rich contents of the book. Because it is written completely from the theoretical standpoint, a beginner will not find it always easy. But for one who has already sufficient background and who wants to acquire a thorough knowledge of the subject, Van Vleck's book is indispensable. I am sure that it will be the starting point for many investigations.

G. E. UHLENBECK
University of Michigan

The Adsorption of Gases by Solids. A general discussion held by the Faraday Society, January, 1932. Pp. 320+iv. Gurney and Jackson, London 1932. Figs. 109. Price, 15/–.

In his introduction to the general meeting of the Faraday Society at Oxford, Professor H. S. Taylor stated that "it is eminently fitting at a time when so much attention is being paid to the fundamental contributions of Faraday to electrical science that the society which bears his name should also devote some thought and discussion to a field of knowledge in which Faraday displayed the same qualities of genius and pre-vision that have given him so preeminent a position among the leaders of scientific thought." With this motivating idea Professor Taylor initiated this important meeting of the Faraday Society at which forty papers were presented and later published as this volume.

Three section meetings were held and at each of these a definite subject was chosen for discussion. The section subjects together with the authors of the introductory papers were as follows: Section I. Experimental methods. Introductory paper by Eric K. Rideal. Section II. Kinetics and energetics of gas adsorption. Introductory paper by Professor Herbert Freundlich. Section III. Theories of the adsorption of gases. Introductory paper by Professor M. Polanyi.

Leading investigators throughout the world presented papers and entered into the discussions which followed. Most of the modern work on the adsorption of gases was covered and many important points of view were given in the general discussion which followed the presentation of the papers. This general discussion fills about forty pages of the book and follows the last paper presented. To those interested in the adsorption of gases by solids, this volume constitutes an important summary of the work in progress, as well as giving the modern point of

view with regard to the theories on the subject. There are a few typographical errors which do not seriously harm the usefulness of the book.

L. H. REYERSON
University of Minnesota

Les Principes de la Mécanique Quantique. P. A. M. DIRAC. Translated by A. Proca and J. Ullmo. Pp. 314+viii. Les Presses Universitaires de France, Paris, 1931. Price 95 Fr.

As is indicated by its title this book is a literal translation of Dirac's work into French, except for the addition of an appendix by Proca on Poisson bracket expressions in classical analytical dynamics. As the English original has been reviewed previously in this journal (Phys. Rev. **37,** 97 (1931)) further comment seems unnecessary except that one might have expected some indication in the very last pages of the book that Dirac no longer supports his original interpretation of the negative energy states of relativistic electron theory, (e.g., Proc. Roy. Soc. **A133,** 60 (1931)). However, those who succeed in getting through to the last page will undoubtedly also succeed in correcting this for themselves.

E. L. HILL
University of Minnesota

Gmelin's Handbuch der anorganischen Chemie 8 Auflage, Herausgegeben von der Deutschen Chemischen Gesellschaft. System Nummer 59, Eisen, Teil A, Lieferung 4. Pp. 260, Figs. 180. Verlag Chemie G.m.b.H. Berlin, 1932, R.M. 41; (subscription price R.M. 35.50).

The volume preceding the present one was published in 1930 and has been reviewed in these columns. Volume 4 of the series on the technology of iron deals with the manufacture, properties, and testing of wrought, bar, cast, and pig iron, of open hearth and Bessemer steel and of slags. One of the outstanding features is the truly international bibliography at the end of each chapter. The great practical importance of iron and steel justifies the extensive technological treatment of the subject in the Gmelin series.

I. M. KOLTHOFF
University of Minnesota

CURRENT LITERATURE OF PHYSICS

Extracts from the Tables of Contents of Some of our Contemporaries

NATURE

VOL. 130, NO. 3286 — OCTOBER 22, 1932

Letters to the Editor:

Possible Existence of Multiply Charged Particles of Mass One. By **M. Delbrück** 626
Atmospheric Conditions and the Kennelly-Heaviside Layer. By **R. C. Colwell** 627
Further Doublets of As V. By **A. S. Rao** 630

NATURE

VOL. 130, NO. 3287 — OCTOBER 29, 1932

Letters to the Editor:

Bead-Corona on Raio Antenna. By **Balth. van der Pol** 662
Influence of Impurities on the Transformation Point of Liquid Allotropic Modifications. By **Stanistaw Dobinski** 662
Proof of Stability of Poiseuille's Flow. By **Th. Sexl** 663

NATURE

VOL. 130, NO. 3289 — NOVEMBER 12, 1932

Letters to the Editor:

Heat Distribution in a Uniform Bar. By **D. K. McCleery** 737
Radiations from Radium *D* and *E*. By **J. A. Gray** 738
Mercury Traps. By **L. Marton** 739
Dispersion of Sound in Several Gases, and its Relation to the Frequency of Molecular Collisions. By **William T. Richards and James A. Reid** 739
Spectrum of Trebly Ionized Lead. By **Jai Kishen** 739
Structure of Line Spectra in Crystals. By **R. Tomaschek** 740
Anomalous Behavior of Methane in the Raman Effect. By **S. Bhagavantam** 740

ZEITSCHRIFT FÜR PHYSIK

VOL. 78, NOS. 7 AND 8 — OCTOBER 12, 1932

Nature of the Spontaneous Current Accompanying the Illumination of Different Detector Substances. By **F. Waibel** 423
Quantitative Investigations on Frictional Electricity. By **E. Hess** 430
Image of a Surface Element in a Reversing Optical System. By **H. Boegehold and M. Herzberger** 445
Isoplanatic Image Formation by a Centered Optical System. By **E. Lihotzky** 452
Ionizing Effect of Metastable Neon Atoms Formed by Resonance Radiation. By **F. M. Penning** 454
Relaxation Time of Heat-Treated Copper and Aluminum Wires. By **Dankwart Schenk** 470
Dissociation of Hydrogen Molecules by Collison with Optically Excited Xenon Atoms. By **Henry R. Calvert** 479
Bands of Silicon Chloride in the Near Ultraviolet. By **A. C. Datta** 486
Charge Measurements on Selenium Particles at High Gas Pressures. By **E. Wasser** 492
Influence of Lattice Forces on the $K\alpha$-Line of Carbon. By **M. Renninger** 510
Band Spectrum of Chromium Oxide. By **Chandrasekhar Ghosh** 521
Reflection of Fast Electrons from Single Crystals. By **Heinz Raether** 527
Dirac's New Field Theory. By **S. Schubin** 539
Series in the Complex Spectrum of Singly Ionized Mercury. By **T. S. Subbaraya** 541
Some Orienting Questions in the Quantum Mechanics. By **P. Ehrnefest** 555

Simple Method for the Determination of the First Piezo-Modulus of Quartz from Measurements on a Quartz Resonator. By **Angelika Székely** 560

ZEITSCHRIFT FÜR PHYSIK

VOL. 78, NOS. 9 AND 10 — OCTOBER 18, 1932

Visible Part of the Aurora Spectrum. By **L. Vegard** 567
Intensity Relations in the *L*-Region of the Rare Earths. By **G. v. Hevesy and E. Alexander** 576
Logical Justification of the Wentzel-Brillouin Calculation of Eigen Values. By **E. Fues** 580
Influence of Collisions on the Decay of Sodium Resonance Radiation. By **F. Duschinsky** 586
Gradient in the Positive Column in Mercury Vapor. By **W. Elenbaas** 603
Absorption of Carbon Tetrachloride in the Infrared. By **Clemens Schaefer and Rudolf Kern** 609
Note on the Electrical Conductivity of Deformed Sodium Chloride Crystals. By **Z. Gyulai** 630
General Field Theory. By **J. A. Schouten and D. van Dantzig** 639
Measurements of Fluctuations of Cosmic Rays. By **W. Messerschmidt** 668
Quantitative Evaluation of the Matteucci Effect. By **Hans Ostermann and Fritz v. Schmoller** 690
Induction Effect at the Ends of a Twisted Ferromagnetic Wire in Relation to the Theory of the Magnetization Curve. By **Wilhelm Schütz** 697
Simple Registering Infrared Spectrometer. By **Carl Leiss** 704

DIE NATURWISSENSCHAFTEN

VOL. 20, NO. 43 — OCTOBER 21, 1932

Ion Spectrum of Atmosphere. By **K. Kähler** 783

Short Original Communications:

Peculiar Reaction of N_2O Adsorbed on Carbon. By **Lothar Meyer** 791
Non-conducting Modifications of Metals. By **J. Kramer and H. Zahn** 792
Determination of Numbers of Isotopes. By **E. Gapon and D. Iwanenko** 792

DIE NATURWISSENSCHAFTEN

VOL. 20, NO. 44 — OCTOBER 28, 1932

(No articles of interest to physicists.)

DIE NATURWISSENSCHAFTEN

VOL. 20, NO. 45 — NOVEMBER 4, 1932

Quantum Mechanics and the Fundamental Problems of Biology and Psychology. By **P. Jordan** 815

Short Original Communications:

Production of Atomic Hydrogen for Use in Preparing Organic Chemicals. By **Hans Kroepelin and Erwin Vogel** 821

PHYSIKALISCHE ZEITSCHRIFT

VOL. 33, NO. 20 — OCTOBER 15, 1932

Original Communications:

Influence of Temperature on the Scattering of X-Rays by Gas Molecules. By **R. W. James** 737
New X-Ray Interference Method for Multicrystals, Especially Rolled and Fibrous Material (Object between Two Slits). By **H. Seemann** 755
Spontaneous Magnetization and Thermo-Remanence in Ferromagnetic Single Crystals. By **J. Koenigsberger** 763
Calculation of the Molecular Weight of a Polar Colloid from the Dispersion Curve of its Water Solution. By **B. M. Bloch and J. Errera** 767
Use of Monochromatic Radiation in X-Ray Scattering by Gases. By **W. van der Grinten** 769
Device for the Introduction of Photographic Plates into a High Vacuum. By **E. G. Andresen** 771
Realization of Homogeneous Magnetic Fields. By **A. Bühl and F. Coeterier** 773

Relativity Correction to the Maxwellian Distribution of Velocities. By **A. Busemann**.. 775
Atomic Disintegration with Hydrogen Canal Rays. By **F. Kirchner**..... 777
Selenium or Selenide Rectifier? By **W. S. Gripenberg**..... 778

PHYSIKALISCHE ZEITSCHRIFT

VOL. 33, NO. 21 NOVEMBER 1, 1932

Significance of Some Experiments on Supraconductivity. By **M. v. Laue**..... 793
Striking of a Gas Discharge. By **W. Rogowski**..... 797
Energetics of Gas Discharges. By **Max Steenbeck**..... 809
Two Kinds of Negative Characteristics for Self-Sustaining Gas Discharges. By **F. M. Penning**..... 816
Energy Balance in the Positive Column in Sodium Vapor. By **M. J. Druyvesteyn**..... 822
Diffusion Velocity of Suspended Dust Particles in Electrofilters. By **G. Mierdel**..... 823
Application of the Selenium Contact-Layer Photocell to Physical Measurements. By **Ludwig Bergmann**..... 824
Formation of Double Molecules in Gases under the Influence of Electric Fields. By **H. Senftleben**..... 826
Electrical Conductivity of Mercury at High Temperatures and Pressures. By **Werner Braunbek**..... 830
Contribution to the Equivalence Principle of Optical Representation. By **Cl. Münster**.. 831
Rotation-Vibration Spectrum of Water Vapor. By **R. Mecke and W. Baumann**..... 833
Quartz Clock for Time and Frequency Measurements of Very High Accuracy. By **A. Scheibe and U. Adelsberger**..... 835
Refraction Experiments with Slow Electrons. By **A. Bühl**..... 842
Moving Striae in the Positive Column of Inert Gases. By **W. Pupp**..... 844

ANNALEN DER PHYSIK

VOL. 14, SERIES 5, NO. 7

Line Emission and Absorption of Chromium Phosphors. II. By **Otto Deutschbein**..... 729
Natural Sensitivity Limits of Measuring Instruments. III. The Practical Realization of the Sensitivity Limit of a Galvanometer. By **Gustaf Ising**..... 755
Statistical Method for Precise Vapor Pressure Measurements at High Temperatures and its Application to the Establishment of the 100° Point of the Temperature Scale. By **Helmut Moser**..... 790
Influence of a Superposed Magnetic Field on the Dielectric Behavior of some Solid and Fluid Gaseous Substances. By **Richard Schmid**..... 809
Emission of Glowing Platinum in Gases Especially in Iodine Vapor and Chlorine. By **Edgar Müller**..... 831
Correction to the Paper "Absorption Spectra of Carbon Dioxide, Carbon Monoxide and Water Vapor in the Region 600–900A." By **H. J. Henning**..... 856

ANNALEN DER PHYSIK

VOL. 14, SERIES 5, NO. 8

Electron Emission of Metals under the Influence of X-Rays. By **Hans Küstner**..... 857
Electrical Currents from Hot Cathodes in Gases and Vapors at Atmospheric Pressure. By **Martin Ruhnke**..... 881
Stability of Couette Streaming. By **H. Schlichting**..... 905
Investigation of Vapor Pressure of Sodium. By **Erwin Thiele**..... 937
Explanation of Short-Wave Echoes of Aurora and of Magnetic Disturbances. By **Hans Dostal**..... 971

ANNALEN DER PHYSIK

VOL. 15, SERIES 5, NO. 1

Theory of the Frahm Time-of-Vibration Indicator. By **W. Meyer**..... 1
Magnetic Behavior of Isotropic Ferromagnetic Media. By **Richard Gans**..... 28
Investigation of Magnetostriction and the Magnetization of Single Crystals of the Iron-Nickel Series. By **Fritz Lichtenberger**..... 45

Turmaline Resonator for Short and Ultra-Short Waves. By **V. Petrzilka**..... 72
Investigation of the Absorption Spectrum of Nitrogen Dioxide. By **Alfred Herrmann**.. 89
Increase of Thermo-Forces of Oxides by the Use of Oxide Mixtures. By **Franz Fischer, Karl Dehn and Heinz Sustmann**..... 109
Reply to Hallens Remark on my Paper "Electrical Characteristic Vibrations of Rodlike Conductors." By **Karl F. Lindman**..... 127

COMPTES RENDUS

VOL. 195, No. 13 — SEPTEMBER 26, 1932

(No articles of interest to physicists.)

COMPTES RENDUS

VOL. 195, No. 14 — OCTOBER 3, 1932

Hydrodynamical Interpretation of the Periodicity of Sun Spots. By **D. Riabouchinski**.. 574
Magnetic Moment and Moment of Rotation of the Electron. By **Louis de Broglie**..... 577
Intensity of the Components of Hyperfine Structure of the More Intense Rays in the Visible Spectrum of HgI. Hyperfine Structure of the Term $(Hg^{199})7\,^3D_2$. By **J. Gilles** 579

COMPTES RENDUS

VOL. 195, No. 15 — OCTOBER 10, 1932

Identity of Two Bodies having the Same Newtonian Potential in a Common Internal Region. By **Pierre Dive**..... 597
Application of the Electrical Method to a Problem Concerning an Airplane Wing of Finite Extent. By **J. Pérès and L. Malavard**..... 599
Some Statistical Properties of the Cepheids. By **Li Hen**..... 601
New Micromanipulator. By **P. de Fonbrune**..... 603
Study of Cosmic Rays at High Altitudes. By **A. Piccard and M. Cosyns**..... 604
Registration of Atmospheric Electric Disturbances. By **F. Link**..... 619

LE JOURNAL DE PHYSIQUE

VOL. III, SERIES VII, No. 9 — SEPTEMBER, 1932

Perturbation Problems and Self-Consistent Fields. By **L. Brillouin**..... 373
Passage of Photon Rays through Atoms. By **V. Posejpal**..... 390
Magnetic Multiplets, their Mechanism and their Experimental Verification. By **R. Forrer and J. Martak**..... 408

JOURNAL OF THE FRANKLIN INSTITUTE

VOL. 214, No. 5 — NOVEMBER, 1932

Electron Diffusion, Electron Attachment, and the Ageing of Negative Ions in Commercial Nitrogen at Atmospheric Pressure. By **John Zeleny**..... 513
Absorption of Radiation Originating from a Beam of Electrons in Helium: A Note on the Electron Excitation Function for the Sharp Series of Orthohelium. By **Louis R. Maxwell**..... 533
Ionization of the Atmosphere and its Biological Effects. By **Lewis R. Koller**..... 543
Fine Structure in X-Ray Absorption Spectra. By **J. D. Hanawalt**..... 569

BUREAU OF STANDARDS JOURNAL OF RESEARCH

VOL. 9, No. 6 — DECEMBER, 1932

Isolation of the Three Xylenes from an Oklahoma Petroleum. By **Joseph D. White and F. W. Rose, Jr.**..... 501
Characteristic Equations of Vacuum and Gas-Filled Tungsten-Filament Lamps. By **L. E. Barbrow and J. Franklin Meyer**..... 502
Calorimetric Determination of the Intrinsic Energy of Gases as a Function of the Pressure. Data on Oxygen and its Mixtures with Carbon Dioxide to 40 Atmospheres at 28°C. By **Frederick D. Rossini and Mikkel Frandsen**..... 503
Shear Tests of Reinforced Brick Masonry Beams. By **D. E. Parsons, A. H. Stang and J. W. McBurney**..... 504

Measurement of Low-Voltage X-Ray Intensities. By **Lauriston S. Taylor and C. F. Stoneburner** 505
Multi-range Potentiometer and its Application to the Measurement of Small Temperature Differences. By **H. B. Brooks and A. W. Spinks** 506
Density of Some Soda-Lime-Silica Glasses as a Function of the Composition. By **F. W. Glaze, J. C. Young and A. N. Finn** 507
Coiled Filament Resistance Thermometers. By **C. H. Meyers** 508
Deflection of Cosmic Rays by a Magnetic Field. By **L. F. Curtiss** 509
System: CaO–B_2O_3. By **Elmer T. Carlson** 510
Metal-Connected Glass Electrode. By **M. R. Thompson** 511

JOURNAL OF RHEOLOGY

VOL. 3, NO. 4 OCTOBER, 1932
Contribution to the Study of Viscous Friction and the Application to the Theory of Lubrication. By **Pierre Mercier** 391
Contribution to the Study of the Flow of Viscous Liquids. By **C. Camichel and Collaborators** 413
Structural Properties of Anisotropic Solutions of Soap as Determined by a New Centrifugal Falling Ball Method. By **James W. McBain and Otto O. Watts** 437
Viscosity Problems in Igneous Rocks. By **Robert Balk** 461
Further Study of Association by the Fluidity Method. By **Eugene C. Bingham and Harold L. DeTurck** 479
Method for Determining Diffusion Constants of Colloids which Show Mechanical Birefringence. By **Paul Boeder** 494
Mechanics of Plastic Deformation: The Flow of Duralumin through Orifices. By **S. I. Goubkin** 501

THE JOURNAL OF THE ACOUSTICAL SOCIETY OF AMERICA

VOL. 4, NO. 2 OCTOBER, 1932
Brief Survey of Supersonics. By **J. C. Hubbard** 99
Quasi-Standing Waves in a Dispersive Gas. By **D. G. Bourgin** 108
Acoustics of Large Auditoriums. By **Samuel Lifshitz** 112
Acoustic Pick-Up for Philadelphia Orchestra Broadcasts. By **J. P. Maxfield** 122
On the Accuracy of the Aural Method of Measuring Noises. By **Jûichi Obata and Sakae Morita** 129
Position Finding by Under-Water Sound Signals. By **B. R. Hubbard** 138
Theory of Acoustic Filtration in Solid Rods. By **R. B. Lindsay and F. E. White** 155

PHYSICS

VOL. 3, NO. 5 NOVEMBER, 1932
Magnetostriction Oscillator Producing Intense Audible Sound and Some Effects Obtained. By **Newton Gaines** 209
Three Superfluous Systems of Electromagnetic Units. By **George A. Campbell** 230
Vacuum Apparatus for Measuring Thermal Expansion at Elevated Temperatures, with Measurements on Platinum, Gold, Magnesium and Zinc. By **J. B. Austin** 240